Universidade de Aveiro 2009

Departamento de Engenharia Civil

Luís Pedro Esteves

Internal curing in cement-based materials

Universidade de Aveiro 2009

Departamento de Engenharia Civil

Luís Pedro Esteves

Internal curing in cement-based materials

Dissertação apresentada à Universidade de Aveiro para cumprimento dos requisitos necessários à obtenção do grau de Doutor em Engenharia Civil, realizada sob a orientação científica do Dr. Paulo Barreto Cachim, Professor Associado do Departamento de Engenharia Civil da Universidade de Aveiro e do Dr. Victor Miguel C. de Sousa Ferreira, Professor Associado do Departamento de Engenharia Civil da Universidade de Aveiro.

Beside other problematic, it was often astonishing to run after thoughts. As an ancient philosophy doctor pointed out:

“The greater the attempt that is made to study the nature or behaviour of a photon or a particle, the greater will be the uncertainty or error of the measurements.”

Heisenberg summarised this in his uncertainty principle, the concept being demonstrated by means of idealized “*thought*” experiments.

If it is permitted for me to say, I would add:

(…), provided that it can not be seen or felt.

O júri

PRESIDENTE: **Reitora** da Universidade de Aveiro

VOGAIS: Doutor **Ole Mejhede Jensen**, Professor Catedrático da Technical University of Denmark.
Doutor **Klaas van Breugel**, Professor Catedrático da Delft University of Technology.
Doutor **Aníbal Guimarães da Costa**, Professor Catedrático da Universidade de Aveiro.
Doutor **José Luís Barroso de Aguiar**, Professor Associado com Agregação da Universidade do Minho.
Doutor **Paulo Barreto Cachim**, Professor Associado da Universidade de Aveiro (Orientador).
Doutor **Victor Miguel Carneiro de Sousa Ferreira**, Professor Associado da Universidade de Aveiro (Co-Orientador).

Acknowledgments

This thesis is written to fulfil the requirements for the Portuguese degree of Doctor of Philosophy in Civil Engineering at Aveiro University. It is focused on the internal curing of cement-based materials, with concern on the study of autogenous phenomena and volume change at early-age.

The experimental work was developed in approximately three years, comprising material testing at Aveiro University under the supervision by Paulo Cachim and Victor Ferreira, which is greatly acknowledged, and a short-term experimental framework at the main concrete laboratory of the electrical power plant at EDP, which was kindly granted by Armando Camelo. The assistance during the material testing by the technical staff at EDP is greatly acknowledged.

Approximately one third of the Ph.D. work was conducted as guest researcher at Technical University of Denmark. This was made possible by Ole Mejlhede Jensen. No conference participations were possible during this period, due to professional obligations at Porto Engineering Institute, where I do lecture since April 2004, in the Civil Engineering Department.

Two standard journal publications and one contribution for edited book have emerged from the preliminary results developed in the first year of the PhD work[1-3]. Other publications are expected in 2009, as a result of the findings presented in this document and from work that will follow. Particularly, in section 3.4, the simulation of the absorption kinetics in augmented reality and the graphical representation of polymer particles were performed in conjunction with Gonçalo Henriques. The author wishes to acknowledge his assistance in this work.

A fairly chaotic strategy was taken during the last two and a half years of intensive work to explain the observations presented in the following chapters. It seemed that it was more important to pursuit fundamental research rather than running empirical or applied research to add-up text about history of cement and concrete research. It is then fair to say that inductive thinking was preferred at some point, rather then the deductive mode of thinking.

"The findings may be a little chaotic, as cement!"

keywords

Internal curing, high performance concrete, autogenous deformation, superabsorbent polymers, fine aggregate particles

abstract

The development of high performance concrete in the early 80 revealed that this particular branch of cement-based materials is highly sensible to curing problems. It is well known the consequences of autogenous phenomena in high performance systems, namely the early-age cracking. This is seen as the major limitation on the further development of new materials with superior durability. Recent developments have returned internal curing methods as mean to mitigate such phenomena, where this thesis finds it space in time.

Internal curing of cement-based materials by superabsorbent polymers is further analysed, with emphasis on the consequences of the volume-changes in plain Portland and SF-modified cement based systems at early age. Some limitations in the use of superabsorbent polymers are encountered, being concluded that the physical and chemical nature of superabsorbent polymers may significantly affect the efficiency of internal curing. In addition, the mechanisms of internal curing are discussed in more depth, from where it transpires that beyond the mechanisms with physical or chemical ground, significant mechanical effects do exist.

Several techniques are used in the course of the investigation, which aimed, beside the characterisation of certain material properties, to pursue the open questions left by the international community, in respect with the fundamental mechanisms that may explain the autogenous phenomena. Examples of that are the hydration studies at a microscopic scale, rather than macroscopic.

Furthermore, a new technique of internal curing is proposed, which is based on the use of very fine aggregate particles, as mean of partial mitigation of autogenous shrinkage. So far, this technique has not been reported in the research community as mean of mitigation, but the extent of internal curing that may potentially be obtained from this concept encounters several limitations. The significance of this technique in preventing microcracking is yet to be proved, but it is concluded that fine aggregate particles may be beneficial in reducing the restraint effects, and thus, reducing the potential for cracking events.

The combined use of superabsorbent and fine aggregate particles may have as a consequence the development of concrete with nanocracking, rather than micro, during a period where the “culture” in the concrete technology is putting considerable effort in getting more intimate with the durability aspects of cement-based materials.

keywords

Cura interna, betão de elevado desempenho, deformação autogénea, polímeros super absorventes, agregados finos

Portuguese summary

O desenvolvimento de betões de elevado desempenho, durante o início da década de 80, revelou que este tipo particular de materiais com base em cimento é susceptível a problemas de cura. São bem conhecidos os efeitos dos fenómenos autogéneos em sistemas de elevado desempenho com base em cimento, nomeadamente a fissuração em idade jovem. Esta é, aliás vista como a maior limitação no desenvolvimento de novos materiais com durabilidade superior. Desenvolvimentos recentes de métodos de cura interna provaram ser uma boa estratégia de mitigação dos efeitos da auto-dissecação destes sistemas, onde a presente tese ganha o seu espaço no tempo.

Este estudo centra-se essencialmente em sistemas de elevado desempenho com base em cimento com cura interna através de partículas superabsorventes, dando particular importância à alteração de volume em idade jovem. Da análise mais aprofundada deste método, resultam algumas limitações na sua aplicabilidade, especialmente em sistemas modificados com sílica de fumo. Conclui-se que a natureza física e química dos polímeros superabsorventes pode afectar significativamente a eficiência da cura interna. Em adição, os mecanismos de cura interna são discutidos mais profundamente, sendo que para além dos mecanismos baseados em fenómenos físicos e químicos, parecem existir efeitos mecânicos significativos.

Várias técnicas foram utilizadas durante o decorrer desta investigação, com o objectivo, para além da caracterização de certas propriedades dos materiais, de perseguir as questões deixadas em aberto pela comunidade internacional, relativamente aos mecanismos que fundamentam a explicação dos fenómenos autogéneos. Como exemplo, são apresentados os estudos sobre hidratação dos sistemas para avaliação do problema numa escala microscópica, em vez de macroscópica.

Uma nova técnica de cura interna emerge da investigação, baseada na utilização de agregados finos como veiculo para mitigar parcialmente a retracção autogénea. Até aqui, esta técnica não encontra par em investigação anterior, mas a extensão da cura interna ou a eficácia na mitigação baseada neste conceito encontra algumas limitações. A significância desta técnica em prevenir a micro fissuração é um aspecto que está ainda em aberto, mas pode concluir-se que os agregados finos podem ser benéficos na redução dos efeitos da restrição localizada no sistema, reduzindo o risco de micro fissuração.

A utilização combinada de partículas finas de agregado e polímeros super absorventes pode ter como consequência betão sem microfissuração, ou pelo menos com nanofissuração.

CONTENTS

1. Introduction

This section presents the goals and specific objectives of this thesis. In addition, the scope is addressed, sustaining the importance of internal curing in high performance concrete. In the following, an approach on the terminology is made, where autogenous phenomena and internal curing is defined.

1.1. Scope

High performance concrete

High performance concrete, falling into the category of the so-called modern concrete, is essentially characterised by a cement matrix with low water/cement ratio (w/c), often including mineral additions like silica fume and the use of admixtures as superplasticizers[4]. Curing is the critical period of fresh cement in the hardening process, in which concrete develops its fundamental characteristics under specific conditions[5]. A proper curing essentially consists in the permanent availability of internal moisture to sustain the hydration reactions at moderate temperatures, and in absence of external forces at early ages. High performance concrete is particularly sensible to curing problems and may undergo considerable early-age deformations and microcracking development throughout the system[6, 5]. The dense microstructure of modern concrete rapidly develops capillary discontinuity in the still younger porous network and thus, the access of external water turns out unviable to assure continuous saturation of the total bulk volume[7].

Early-age cracking: "the Achilles heel of high performance concrete"

Cracking is usually not wanted in concrete, since it results in loss of durability, affects aesthetics and results in loss of strength. Early-age cracking is a complex phenomenon influenced by numerous parameters, and it can occur in HPC from two different sources: external or internally in bulk cement paste. While external sources refer to system restraints to intrinsic deformation, e.g. friction between the material and the formwork or restraint due to cast-in reinforcement bars, internal microcracking is mostly related to volume changes at early-age resulting as a consequence of cement hydration, e.g. chemical shrinkage and self-desiccation. When the system is open to external conditions, early-age deformation may also have base in the water loss from the system and resultant plastic and drying shrinkage will govern the volume changes. It is well known that these phenomena may lead to various types of crack patterns [8]. The problem of shrinkage cracking within the plastic state of the cement matrix is mostly related with the rate of the water loss[9]. Accordingly, the rate of water loss is governed by environmental conditions such as the curing temperature, the relative humidity and wind velocity. These may be active, solely or combined, on elements with high exposed surface area, such as floor units or bridge decks. The system may experience cracking if the bleeding rate, referring to the rate of water movement from the bulk towards the surface is lower than the rate of water loss. In addition, the mix design may also have a significant effect in restraining or enhancing water evaporation, through water fixation by physical links between water molecules and the particles that compose the system. Thus, a primary concern in preventing plastic shrinkage cracking is to understand the underlying mechanisms brought out from the physical characteristics of the system[10]. In principle, the use of higher powder content, e.g. mineral additions, may help in partially preventing plastic shrinkage. In either case, the mitigation of plastic shrinkage cracking is therefore a function of the efficiency in preventing the evaporation of water from the surface, which is equivalent to maintain the internal

moisture gradient in negligible values. As soon as an open system develops a degree of rigidity, cracking may develop due to subsequent drying. The mechanisms of drying shrinkage, thoroughly discussed in previous research are equally valid to explain autogenous shrinkage, with the exception of the water loss parameter (see section 2.2.3). As noted by Aitcin[11], plastic and drying shrinkage can be prevented by proper curing of concrete, but self-desiccation shrinkage is non avoidable by traditional forms of curing processes. Cracking sensitivity is higher in high performance and high strength concrete, mostly due to autogenous deformation, which essentially results from the physical nature of these particular systems (low w/c ratio and mineral addition). To understand cracking, one needs to understand the driving force. As mentioned by Bentur[12], in the forthcoming note of RILEM TC 181-EAS, which focused particularly in early-age cracking: "*An understanding of these mechanisms is of particular significance, since the cracking seems sometime to be a random and irreproducible event. Resolving the nature of these mechanisms and their quantification can provide the tools for rational design to prevent, or at least mitigate, this kind of cracking.*" Anton Bentur is referring to cracking due to autogenous deformation.

Autogenous deformation

Autogenous shrinkage was only recently recognised by the concrete society as a significant source of damage in high performance cement-based materials[13]. In fact, several authors have neglected the relevance of autogenous deformation within the early-age volume changes. One example is given by Jensen[14], transcribing the opinion expressed by Collepardi in the early 1980: *"…autogenous shrinkage, which is in the order of 100 μm/m, is significantly smaller than drying shrinkage, which may amount 1000 μm/m. In any case, apart from the negligible importance of autogenous shrinkage if compared to drying shrinkage, in practice the later would include the former, if the former actually existed."* This view, shared by other authors within the concrete society at this time[15], was in principle correct, according to the existing practical experience. In fact, no measure of autogenous deformation would be reasonably possible, since no measurement system for this early-age unrestrained contraction existed. Over more than a decade since, scientific community have put considerable effort in the development of several methods to evaluate autogenous shrinkage, but despite the growing interest in the subject, no consensus was reached over the standard test method, until recently (see section 2.2.5).

Internal curing

The idea of internal curing of concrete is registered long gone within concrete research community[16]. It is interesting to note that the existence of internal curing in concrete may have been underlying through history only in terms of wording. In fact, as registered by T. A. Holm[17], the application of lightweight aggregate concrete is dated back to the time of the first Great War, in the construction of concrete ships. In addition, concrete with internal curing may also have evolved from the concept of self-curing concrete, which is based on the introduction of a chemical admixture that is able to reduce water evaporation by a retaining function. According to Dhir[18], the addition of a self-cure chemical based on a water-soluble polymeric glycol lead to improved durability of concrete cured in air. However, the performance of such admixture does not attain the efficiency of the water film curing[19]. The use of water retaining agents should not be seen has internal curing, since it is conceptually based in the internal sealing rather than internal curing, the later consisting in a water curing agent capable of enhancing cement hydration maintaining optimal curing conditions. Moreover, the selection of a specific curing method is highly dependent on the

actual design constraints. In either case, there are many examples that require other form of curing procedures rather than the traditional or external curing methods, e.g. high strength concrete applied in submerged pipe systems within oil platforms structures. In high performance concrete, capillary discontinuity may significantly delay and even limit the water movement throughout the system. This makes the use of water pounding or other external curing methods inefficient in assuring the continuous internal moisture of the material. In this case, the use of internal curing methods may be required to counteract autogenous deformation. As there is only little experience on the practical use of internal curing methods to improve early-age properties of high performance concrete, the subject constitutes per se a great challenge to technicians and industrials at the present time.

1.2. Terminology

Internal curing and autogenous deformation terminology

Terminology presented in this thesis is adopted from the definitions proposed by RILEM TC 196-ICC, aggregating terms and definitions previously accepted within RILEM TC_EAS report by Japan Concrete Institute committee JCI in this subject.

Definitions

1) Curing: maintaining a satisfactory moisture content and temperature after concrete is placed, aiming the improvement of concrete properties by promoting cement hydration and also minimize shrinkage. Curing methods include water and sealed curing, external and internal curing.
2) Internal curing: incorporation of a component, which serves as curing agent, to the concrete mixture. Internal curing may be classified into two categories: internal water curing (or water entrainment) and internal sealing.
3) Self-desiccation: is the reduction in the internal relative humidity of a sealed system when empty pores are generated. This occurs while chemical shrinkage takes place, when the paste matrix has developed a self-supportive skeleton, and the chemical shrinkage is larger than autogenous shrinkage.
4) Chemical shrinkage: is the internal-microscopic volume reduction, which is the result of the fact that the absolute volume of the hydration products is smaller than that of the reacting constituents (cement and water).
5) Autogenous shrinkage: is the external-macroscopic (bulk) dimensional reduction (volume or linear) of the cementitious system, which occurs under sealed isothermal and unrestrained conditions.

Comments on definitions

Definition 1):
Several standardisation parties, including the ACI committee 308[8], add-up *time* as a fundamental parameter when approaching the definition for curing, viz. *curing period*. This is not reflected in the RILEM definition. However, the adequate time to prescribe any curing method may be reductive since it would embrace any cement-based system. Even being ambiguous, the term adequate time should be used.

Definition 2):
Internal water curing is preferable when curing high performance concrete, since internal sealing is unable to prevent self-desiccation. The methods of water entrainment depend on the internal curing agent, which includes water entrainment by superabsorbent polymer and pre-saturated lightweight aggregates. The water curing agents serve as an internal water reservoir, which is gradually released as hydration proceeds and water is consumed.

Definition 5):
The term shrinkage is usually connected to a reduction in volume or dimension. This term is in fact changed to *deformation*, since the later includes both expansion and shrinkage, which is also possible to obtain in autogenous measurements. However, and as pointed by Ole M. Jensen, the term *deformation* seems thoroughly oriented to mechanical behaviour of matter. In addition, it also involves stress as a consequence. This is not the case, if the system is not restrained. In the author opinion, this term should be changed to *strain*. Thus, it corresponds to the linear strain behaviour of cement and it can be positive or negative.

1.3. Objectives

The main goal of this thesis is to comprehend the basic and fundamental aspects underlying internal curing of cement-based materials, with particular interest by autogenous phenomena and RH-change. This is a major task, by observing the possible individual or combined processes that are required to understand, which are simultaneously time-dependent and inter-dependent, as shown in Figure 1.1.

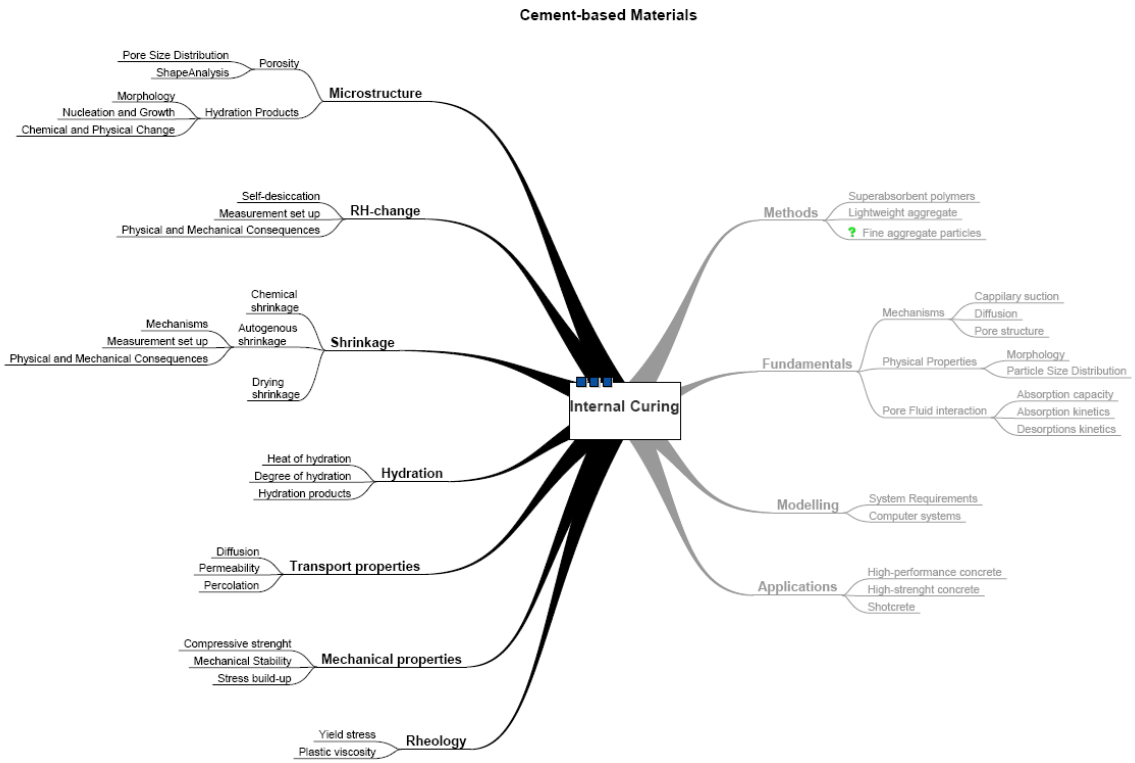

Figure 1.1.

On mapping the main aspects of cement-based materials in respect with autogenous phenomena, internal curing and material properties.

Thus, a simple static approach on each process will not be able to give a proper answer of the dynamic phenomena. Priority should be given to the study of the underlying properties of cement-based materials at early-age, rather than more technical or macroscopic properties solely based on the mechanical properties of cement-based materials. This is done with one purpose: to understand mechanisms that may provide base-knowledge to prevent, if possible, microcracking and thus, aiming concrete durability.

The specific tasks are directly related with the methods of internal curing, which may be sub-divided in two main branches: the use of superabsorbent polymers and the use of fine aggregate particles, as mean for partial/full prevention of autogenous deformation. These categories constitute the main structure of the experimental part of the thesis.

Part I: Cement Paste

Autogenous deformation of white Portland cement paste is measured in a digital dilatometer at room temperature, with the objective of understanding the basic perception on the effect of material parameters on autogenous deformation. In addition, the nature of superabsorbent, both physical and chemical, should be analysed in terms of their ability to mitigate autogenous deformation, since any reference to this important aspect is found in the literature.

Hydration of cement-silica systems is monitored by several techniques with insight in the physical and chemical changes occurring simultaneously with autogenous deformation. The purpose of this investigation is to gain a deeper perspective of the individual influence of purely chemical-based phenomena and the thermodynamics involving low water and low porosity systems.

Furthermore, fundamental research is required to perceive the influence of the particle size of the superabsorbent polymers on autogenous deformation. Although the optimum size of superabsorbent is suggested in previous research, a systematic approach on the kinetics of absorption may open new perspectives in a wide range of concrete applications. A model that may control the absorption kinetics should be brought out from the investigation. This should be useful in predicting the performance of a water-entrained system, in respect with the fresh and hardened properties of the composite material. Moreover, the mechanisms of internal curing are poorly documented. Thus, another specific task is to find out if the existing ideas about the functioning of the superabsorbent polymers, referring to the water movement within desorption and extent of curing time are correct.

Part II: Cement-silica-quartz systems

Fine aggregate particles incorporated in cement-silica systems is analysed as source of internal curing. A new model is brought out to explain the physical properties of cement paste "internally cured" by fine aggregate particles, by re-interpretation of Powers model of hydration of cement paste: cement-quartz model. Packing theory is applied to characterize interfacial transition zone (ITZ) regions and the volume of internal water available for further hydration. This is found to partially counteract self-desiccation and reduce the deformation of the system. However, this idea requires further research, since silica fume addition in amount higher than 10% may severely limit the proposed phenomena. Moreover, it is possible that the findings may have as a consequence the idea of non-cracking high performance concrete or at the most, concrete with nanocracking.

2. Theoretical

This section is dedicated to cement hydration and paste microstructure. Cement-silica system is analyzed in respect with autogenous deformation and discussion is made on the mechanisms of self-desiccation, autogenous deformation and relation with the hydration stages and early-age properties of cement paste. In addition, the measurement techniques are reviewed and discussed. Furthermore, discussion is made on the internal curing methods as mitigation strategy of autogenous deformation.

2.1. Physical properties of cement paste

Many of the important properties of concrete can be attributed to the peculiar nature of the hydration products of Portland cement. Although the chemical constitution of all structural units is not fully known, the development of each phase with water under specific conditions gives ground to the development of mechanical and physical properties of these units[20].

2.1.1. Hydration and Microstructure

Two of the most comprehensive books on chemistry of cement hydration may be found in references[21, 22], where more fundamental theory involving the chemical reactions between each structural unit, water and interaction between clinker compounds is discussed. According to Jennings[23], cement hydration starts at water contact and it can be divided in three stages: early period, transition period and late period:

Early period: the contact of cement particles with water generates immediately dissolution and reaction of *calcium aluminate*, the C_3A phase, with gypsum and water. The last prevents flash set of the major structural units, namely the C_3S and C_2S phases. The resultant product is *ettringite* or in cement chemistry notation $C_3A(C\$)_3H_{32}$. Hydration is then at dormant period, which can take several hours, depending on the type of cement and which admixtures are introduced.

Middle period: the hydration rate increases while reaction takes place at the surface of the principal structural units: *tricalcium silicate*, C_3S, and *dicalcium silicate*, C_2S, generating amorphous calcium silicate hydrates, CSH and crystalline *calcium hydroxide*, CH. Aluminate phases are also converted in monosulphate, C4A$H12 at later stages. This period is physically characterized by the formation of connections between growing phases, which bridge together to form the initially saturated pore structure.

Late period: Hydration rate decreases, while dense hydration points form an outer-layer, reducing diffusion of ions, and thus, reducing the energy from the reaction of anhydrous cement to form new products.

The hydration stages are accompanied by changes in state, morphology and volume of the structural units. In concrete petrography, this could be named the change from crystal structure to amorphous or ill-crystallised, meaning that the unit cells are lost to give place to gel that is not well organized as crystals.

The microstructure of cement paste is built in the first hours of hydration. An example is shown in Figure 2.1.

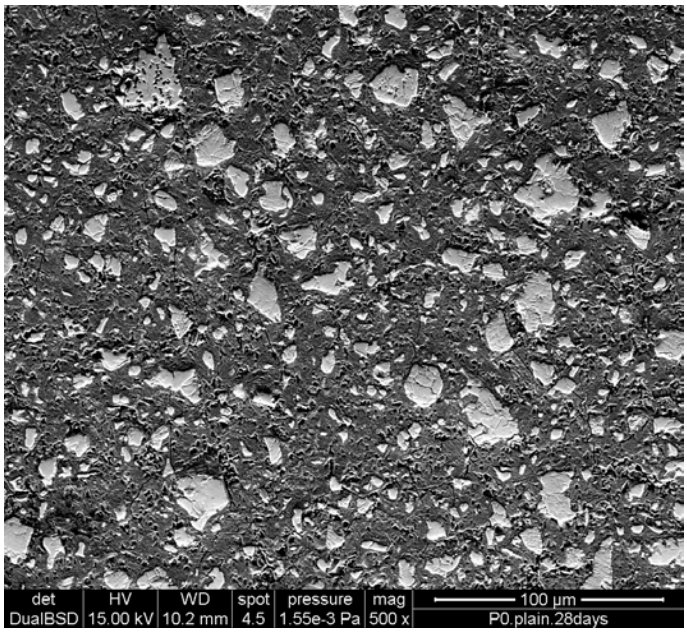

Figure 2.1.

Mature microstructure of plain cement paste with w/c=0.30 at 28 days. The white area represents non-hydrated cement grains, whilst the gray part is related with hydrated cement gel. The image was taken by ESEM and refers to a polished section of the sample.

Depending on the intrinsic components or structural units, water and cement react in a disordered pattern. This means that the microstructure of cement paste is highly heterogeneous and may result in an "infinite" number of different morphologically-based structural units, referring for example the different types of hydrated cement gel resultant from the hydration of the silicate phases at different stages[23]. Therefore, it is common to characterize hydration of cement-based materials by the degree of reaction between cement compounds and water. This may be done either directly or indirectly, at macroscopic or microscopic scale, by a number of techniques, which include the measurement of the heat of hydration, combined SEM and image analysis or simply through the measurement of non-evaporable water (see section 2.1.3). An important consequence of the cement hydration is the formation of pores, which is dealt in the following.

2.1.2. Paste Porosity

Cement paste is considered a porous material at the hardened state. T.C. Powers[20] defined pores in cement paste as the space occupied by evaporable water, typified in two orders of magnitude: gel pores and capillary pores. A more fundamental and general classification is proposed by Dubinin[24], which was later adopted by the International Union of Pure and Applied Chemistry[25], as presented in Table 2.1.

Table 2.1 – Classification of pores according to their width[25].

Pore type	Width [Å[a]]
Micropores	Less than ~20 Å
Mesopores	Between ~20 and ~500 Å
Macropores	More than ~500 Å

Note

[a] $1Å=10^{-10}m=0.1nm$

In cement-based materials, different classifications frequently appear in the literature[26]. For example, Bažant and Wittman[27] defined the capillary pores being greater than 1000 Å. Larger

than the capillary pores, there are air pores or air voids, which, being greater than 10 μm, is in one order of magnitude in relation with the maximum value proposed for capillary pores. Air pores are well connected within the capillary system, which is initially defined by the water to cement ratio of the system. The classification of the range of porosity is not relevant *per se*, but the physical implications brought by the pore size distribution and surface area are fundamental features in relation with both mechanical behaviour and the volumetric stability of the system.

While the dormant period is not finished, the capillary system is fully saturated. During the transition from viscous-elastic to solid state, the capillaries tend to be filled with solids produced between the water and the constituents of cement. As hydration proceeds and solid skeleton is formed, capillary pores are being emptied. In systems with high water to cement ratio, these channels are easily connected throughout the paste volume in time, since there is enough space initially created by the water phase. On the other hand, if the water to cement ratio is lower than 0.36, hydration products will, at very early age, partially occupy the capillary porosity, potentially breaking the connectivity of the percolation system and thus, limiting free access to water sources or even the movement of matter, referring to diffusion of species. In addition to difficulties to the water movement, there is also little space to accommodate the reaction products. Some consequences arise from this purely geometrical constrain: water movement within the capillaries may pass from a percolation to a diffusion process, introducing difficulties to access water from both internal and external sources. In fact, porosity of high performance cement-based materials may not include capillary porosity and open porosity at very early age.

2.1.3. State of water in hardened paste

Water exists in cement paste and it is responsible for fundamental fresh and hardened properties in concrete. In a bi-component system of water and cement, water fixation and the state of water is still in discussion, but the main categories are still attributed to the study of Powers and Brownyard[20]. These categories are divided in the following types:

(1) Water of constitution – refers to water of crystallization or chemically combined, forming part of the solid matter in the hardened paste (OH groups).
(2) Adsorbed water – refer to water physically bond by surface forces or by van der Waals forces.
(3) Capillary water – free water in the system or that occupies the space beyond the range of surface-forces of the solid-phase.

This classification is of little practical use, for as yet no way has been devised for separating the total water content in such divisions. By other hand, this approach permits to define evaporable (type (2) and (3)) and non-evaporable water (type (1)), with respect to the relative volatilities exhibited by different portions of water in the system. The non-evaporable water is an indirect way of determining the hydration degree, which is defined as the amount of cement reacted by weight of original cement. The infinite value of this ratio is equivalent to the complete hydration and it represents about 0.23 of chemically bound water for a mature Portland cement paste[20]. It is also noted that in sealed systems, the full water set introduced at the mixing time cannot still be identified. In reality, the value of 0.23 is used in a macroscopic scale. From a chemical point of view, the water plays the role of medium for dissolution of the major compounds. The pure water is automatically transformed in pore fluid upon water contact, as salts are being dissolved. The

knowledge about the pore fluid[28, 29] is of great importance since it may significantly influence the hydration and internal relative humidity of the system[30].

2.1.4. Silica Fume and cement-silica systems

Silica fume, also referred as microsilica or condensed silica fume is a by-product of the manufacture of silicon and ferrosilicon alloys from high purity quartz and coal in a submerged-arc electric furnace. The gaseous SiO_2 oxidizes and condensate in extremely fine spherical particles of amorphous silica.

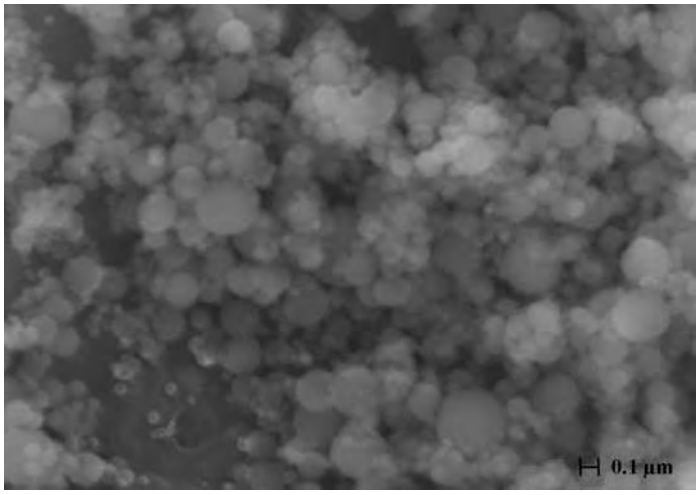

Figure 2.2.

Scanning electron micrograph of silica fume particles. Silica fume consists of sub-micron amorphous SiO_2. Is used in concrete since 1980 and is considered as the "queen" of the mineral additions in the formulation of high strength and high performance concrete.

The principal effects of silica fume on the microstructure of cement paste are due to the pozzolanic reaction with calcium hydroxide produced by the hydration of Portland cement, and to the filler-effect, since the relative size of particles is considerably small in respect with cement grains, and thus can improve material packing. The average size of silica fume particles may be as low as 0.1 micrometers, which is about fifty times less, in terms of order of size, the medium grain size of typical Portland cement. Therefore, the porosity of cement pastes with silica fume is greatly diminished, although changes in the pore size distribution are also reported in the literature[31, 32]. In addition, the use of silica fume was proved valuable to improve workability and avoid bleeding in fresh cement-based materials[15].

Silica fume has found wide use in producing high performance concrete in the last two decades. This is mostly related with the strength potential of systems with silica fume, which is due to densification of the interfacial transition zone between aggregate and paste[33], as documented by scanning electron microscopy measurements in references[34, 35].

A drawback was encountered in respect to the use of silica fume in cement-based materials, which is related to the reactivity with calcium hydroxide: the high chemical shrinkage, about 0.22 ml per 100 grams reacted silica[30, 36]. Silica fume modified cement pastes show much higher self-desiccation and self-desiccation shrinkage than Portland cement pastes[37]. Pallière et al[38] registered several consequences of the use of silica fume related with autogenous phenomena, when accessing durability of high performance concrete.

2.2. Volume changes and autogenous phenomena

2.2.1. Overview

Volume changes refer to any disturbance in the volumetric equilibrium of cement-based materials in time. There are numerous aspects in the "life" of matter that can be of importance in respect with their volumetric stability, starting with the physical characteristics of cement paste, as determined by the composition of cement and water content. Several phenomena can cause volume change in a porous material in both fresh and hardened states: thermal change, hydration or other chemical reactions, freeze-thawing cycles, and internal relative humidity change.

Autogenous phenomena have been subject of scientific research since the early 1980 and deal essentially with the volume change that arises upon hydration and subsequent drop in the internal moisture of the system. The raise of interest for this particular aspect of cement-based materials is in large extent, connected with the development of high strength/ high performance concrete. After more than a century of research on cement-based materials, there is still an open discussion upon the mechanisms leading to the macroscopic shrinkage of low water and low porosity cementitious systems. While there is an agreement that RH change is strongly related to autogenous deformation, there are also numerous open questions that continue unsolved. For example, the uncertainty of the real build-up stress related with the development of early-age mechanical properties and early-age creep may have a considerable influence in the actual mechanical performance. It is important to relate the physical changes versus the real stresses operating internally, and to understand how the measurement techniques developed so far to study these phenomena may be applied to comprehend such relation.

In the following, the mechanisms that may be on the base of autogenous deformation are reviewed and discussed. The purpose is only to make as clear as possible the basic principles underlying the phenomena, without pretence of rigor or completeness.

2.2.2. Chemical shrinkage and Self-desiccation

Chemical shrinkage, also named of Le Chatelier contraction, takes place during hydration of the cementitious system and is defined as the volume reduction of the resultant hydration products in respect to the initial volume of cement plus water. The measurement of chemical shrinkage may be done through gravimetric and volumetric methods, and depends mainly on the unhindered suction of water into the structuring cement paste[39]. Thus, the measurement is done on unsealed specimens, which remains saturated during the whole time profile of the test procedure. Inversely, autogenous measurements, or bulk shrinkage, are performed under sealed conditions, without any excess water surrounding the specimen. Here relies on of the major differences between chemical and autogenous shrinkage. The amount of chemical shrinkage and bulk shrinkage may be equal as long as the cement paste has not set[39], where after the magnitude between both shrinkages result quite different (see Figure 2.3). According to Tazawa et al[40], most of the chemical shrinkage turns into air voids within hardened cement paste, while autogenous shrinkage consists in a very small part of chemical shrinkage. However, autogenous shrinkage is considerably large when compared to drying shrinkage, the latter being usually expressed in microstrain (μm/m).

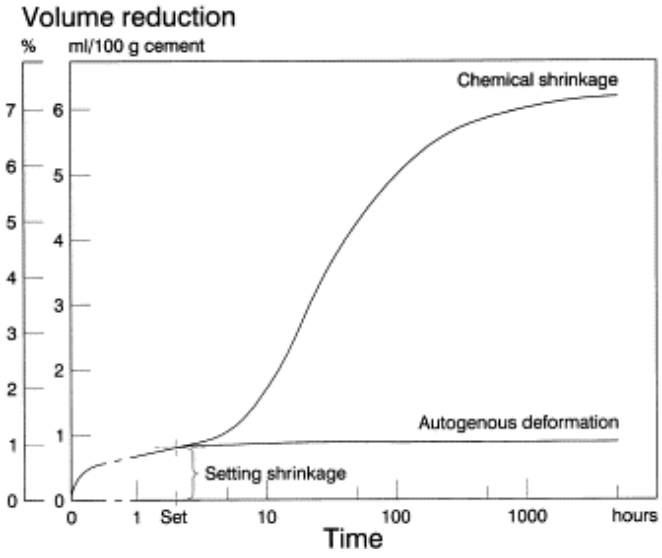

Figure 2.3.

Schematic development of volume changes, which take place in a sealed cement paste system. Before set chemical shrinkage and autogenous deformation may be identical. This volume reduction is referred to as setting shrinkage, and may amount to about 1% of the total shrinkage. After set the chemical shrinkage may be 50 times larger than the autogenous deformation on a volume basis[6].

It is a well known fact that the hydration reactions of sealed cement paste with low w/c ratio may cause self-desiccation. Implications of this phenomenon are found in earlier works by Powers and Brownyard[20]. At a fluid state the chemical shrinkage may be converted into an external volume change[41]. When the system percolates and the solid skeleton is formed, the system stiffness increases and gas bubbles start to nucleate, growing in the macropores. Further, when hydration ceases, the system is accompanied by a drop in the internal RH, corresponding to a volume-shrinkage of the paste matrix. These phenomena is probably caused by chemical reactions taking up physically adsorbed water from the precipitated cement gel[42, 14], the change of thickness of the adsorbate creating an internal pressure within the pores. At this stage of hydration, the stiffness of the paste is so low and the viscous behaviour so pronounced that only a slight stress formation results in a large deformation[14, 41].

2.2.3. Autogenous Deformation: Discussion of the Underlying Mechanisms

Autogenous strain is a volume change that occurs in hardening cement paste and arises due to self-desiccation. C.G. Lynam[43] was perhaps the first to define the shrinkage arising from self-desiccation in sealed curing conditions, viz. autogenous shrinkage.

In the solid matter as hydrating cement paste, changes in the volumetric stability produced by any kind of mechanism may result in: changes in the specific volume of the material composed by solid parts and pores, or changes in the solid parts which may be compressed or dilated with resultant change in the porosity without change of the specific volume, or both changes occurring simultaneously[44]. For an open system under given external forces, the internal equilibrium between forces of cohesion and dispersion define the volume of space required by the solid matter. However, within a close system in isothermal conditions, external forces and thermal effects will be assumed negligible in the following discussion.

The four mechanisms commonly admitted to explain the volume changes in a cement-based system are reviewed and discussed with emphasis on the dominant mechanisms within the autogenous phenomena. Moreover, a fifth mechanism, where fewer attention is given in the literature is analysed, which is based on the microstructure of low water and low porosity systems.

Surface Tension

Surface tension is for long referred as a source of volume instability of porous materials. When a molecule approaches the surface distance of a solid, which may be less than the range of molecular forces (10^{-7} cm), a force towards the centre appears, giving rise to the formation of an adsorbed water film, if the equilibrium vapour pressure is in excess in respect with the surface[45]. Accordingly, when a molecular layer is removed, changes in the surface tension lead to compression of the body, expressed by the shortening in the molecular distance of the solid matter. The surface tension is primarily dependent from the boundary conditions, being greatest for surfaces in vacuum and cancels when the surface is in contact with the same material[44]. Thus, surface tension is a function of the vapour pressure existing in the interaction medium which acts on the gel particles through one or more adsorbed water layers.

As referred by Shuttleworth[46], surface tension was first described in liquids by Young in terms of molecular forces. Accordingly, the surface tension is the tangential stress, in force per unit length in the surface layer, which must be balanced either by external forces or by volume stresses in the body. Surface tension (γ) is related to surface energy (F), which is defined as the work necessary to form unit area by a process of division, as expressed by eq. (2.1), where A is the surface area of a crystal.

$$\gamma = F + A \cdot \frac{dF}{dA} \tag{2.1}$$

It is shown that in a one-component liquid, surface tension and surface free energy are numerically equal. However, as pointed out by Gibbs, the previous argument is not true for solid surfaces, in this case the surface tension being three times greater than the surface energy[46]. Wittmann[45] found a value of 1370 erg/cm^2 for the surface energy in a 28th day mature paste with w/c=0.45. Based on the value of 1750 erg/cm^2, reported by Polzer[47] for a cement paste with w/c=0.30, it is apparent that the surface tension is affected by the water to cement ratio, which is physically equivalent to say that as the bulk density of the hydrated gel solid increases, it may be subjected to higher pressure upon changes in the relative vapour pressure.

The relation between the change in the surface energy and the volume change expressed by the length change ($\frac{\Delta l}{l}$) is given by Bangham equation:

$$\frac{\Delta l}{l} = \lambda \cdot (F_0 - F) \tag{2.2}$$

In eq. (2.2), λ is a constant of proportionality, (F_0-F) being the surface energy variation. Bangham and Fakhoury[48] have validated the previous expression in their experiments on the swelling of charcoal, by means of an extensometer. Setzer[49], making use of the adsorption isotherm, was able to derive the material properties of surface area and pore size distribution, as base input to calculate the surface free energy. By computing data from the work by Feldman[50], it is found that eq. (2.2) is fulfilled in the RH-change between 2 and 38%, where after a significant deviation with the measured volume change is observed. The expansive behaviour in the upper range of the vapour pressure is attributed to the expansion of the porous body as a whole. In fact, although the surface

free energy changes monotonically with the equilibrium vapour pressure, it is highly dependent of the magnitude of the space where it operates. Thus, in regions where space is limited to the formation of multilayer adsorbed film, which may be defined as microporosity, there must be other forces governing, from where the mechanism of surface tension is no longer valid to describe the swelling or shrinkage of the macroscopic body, if considered individually.

Furthermore, Lura et. al[51] suggest that the mechanism of surface tension may not play a relevant role in autogenous deformation. This claim is linked to the fact of that the relative importance of the surface tension should be higher within the lower range of the relative humidity (up to 50%), whereas the RH-change evolved from self-desiccation in a cement paste will not drop below 75%, as observed by Jensen[52]. However, the addition of shrinkage reducing admixture (SRA), primarily developed to reduce drying shrinkage, may also partially resolve the autogenous deformation, up to 20 or 30%[53-55]. In addition, Bentz et. al[53] have found a value of 0.0325 N/m for the surface tension of a solution with 6% of SRA, whereas for distilled water the surface tension is of 0.0765 N/m, as measured by means of a Du Noüy tensiometer. Since SRA is believed to act directly on the surface tension of liquids, it follows that the surface tension should be considered as a relevant mechanism when evaluating autogenous deformation, which is acting solely or in combination with other mechanisms on the volume change of the system, the later being described in the following sections. To consider this is to assume that the absolute value of the internal relative humidity may include regions that somehow show deficiency in pressure, there is, that are subjected to the effects of surface forces, even in the upper range of relative humidity. In other words, there may be existing microscopic relative humidity change.

Disjoining pressure

The force produced by adsorbed water in places of hindered adsorption, defined as the narrow distance between solid gel surfaces, is so-called disjoining pressure. Powers[44] estimate that the average surface to surface distance in the densest structure, referring to the maximum density achievable in a plain cement paste, may be of about 15 Å. Moreover, it is suggested that more than half of opposite surfaces fall within the range of van der Waals attraction across interparticle space. Thus, it seems feasible to assume that there may be adsorbed water subjected to higher pressure in respect with adsorbed water at more open capillary surfaces.

There are contradicting ideas about the role and relevance of disjoining pressure on the volume changes in cement-based materials. Beltzung and Wittman[56] suggest that disjoining forces dominate the macroscopic swelling of a nanoporous material in the range of RH>50%. In their experiments on the observation of disjoining force by surface separation of two quartz spheres, any discontinuity in the displacement versus RH-change which supports the existence of dominant attractive forces, e.g. capillary condensate and capillary tension, is registered. This fact is also illustrated by Splittgerber[57] and Ferraris[58].
However, the radius formed by the annulus of capillary condensed liquid is not comparable with the existing radii present in the meniscus within the solid gel particles, characteristic of the cement paste. By considering the set up that is in the base of the previous conclusions, it comes apparent that the tension formed at the capillary condensate can be of neglected magnitude, by taking the Young-Laplace equation under consideration (see following section). According to the work by Völkl et al[59] on the examination of the surface area by small angle x-ray scattering in hardening cement paste, it is found that the surface area decreases rapidly down to 40% RH during

desorption, resulting a significant hysteresis in the sorption isotherm. Again, this is explained by disjoining forces operating in narrow pores. Taking as base the data in reference[60] on the crystallization of pore water within the low temperature cooling of hardened cement paste, this being about 40 ºC negative, it is predicted that capillary condensation may be operating from 50% RH upwards. However, as pointed by Hagymassy et al[42], the hysteresis between absorption and desorption differ fundamentally due to the time for equilibrium (or absorption versus desorption rate), and given the adequate time, very small or no hysteresis loops would be obtained, the time being greater in low porosity systems. It is also interesting to note in proceeding work by Odler et al[61] that low porosity pastes show a great number of ink-bottle pores and one-halph to three quarters of surface area calculated by BET method, is located in micropores. Thus, the disjoining pressure may be limited by capillary condensation occurring in microporosity, which is a function of the pore size and shape distribution. However, this fundamental purely physical knowledge cannot be easily foreseen by current means of instrumentation.

Furthermore, the disjoining pressure seems to be related with the presence of alkali in the system. Beltzung and Wittman[56] found a relevant effect of this aspect in measurements of surface force, the presence of alkali being determinant in increasing the autogenous deformation. This observation is consistent with theoretical framework by Pashley[62]. In two series of experiments, a mortar system consisting in a w/c ratio of 0.40 and an aggregate to cement ratio of 1.44, was alkali-enriched by adding sodium or potassium hydroxide into the mixing water. Within an enrichment factor of 2, it is registered an increase of 500 microstrain, in the ultimate exogenous deformation, which was taken at 200 days. Moreover, it is suggested that the presence of alkali cations in higher concentrations lead to the reduction in the solubility of calcium hydroxide. Since it is thought that the latter may act as shrinkage compensating sites, the reduction of this phase in the system due to poor solubility could explain the increase in strain by the disappearance of restraining elements.

Capillary tension

Capillary tension, schematically represented in Figure 2.4, is seen as a major mechanism primarily influencing the volume changes at high RH-range. There may be found different approaches when analysing this mechanism as a base model to describe autogenous deformation[63, 51].

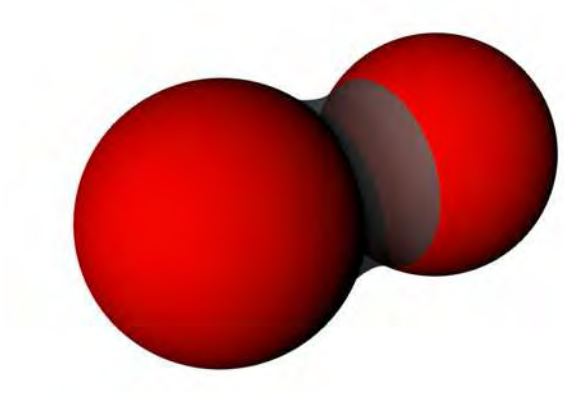

Figure 2.4.

Meniscus developing between two solid spheres due to capillary tension.

The postulate is given by Young-Laplace equation, which relates the tension (or difference in pressure, ΔP_c) formed in the liquid-vapour interface with the surface tension of the water and the principal radii (r_i) of the water surface.

$$\Delta P_c = \gamma \cdot \left(\frac{1}{r_1} + \frac{1}{r_2} \right) \cdot \cos\theta \tag{2.3}$$

If the surface of the water is spherical, eq. (2.3) reduces to:

$$\Delta P_c = \frac{2\gamma}{r} \cdot \cos\theta \tag{2.4}$$

If the surface of the curvature is that of a droplet, ΔP_c is the hydrostatic pressure in the droplet in excess of atmospheric pressure, leading to a positive radius, but if a meniscus is considered, then the radius is negative, which implies that ΔP_c is the deficiency of pressure in the water in the capillary relatively to the atmospheric pressure, and thus, may be referred as hydrostatic tension. As shown by Kelvin, given the condition of the relative vapour pressure p/p_s and assuming the gaseous phase to behave as a perfect gas, the capillary tension may be derived from eq. (2.5), R being the ideal gas constant, T the absolute temperature, M the molar volume of water and V_w is the specific volume of bulk water.

$$\Delta P_c = \frac{RT}{MV_w} \cdot \ln\left(\frac{p}{p_s} \right) \tag{2.5}$$

It follows that for a given vapour pressure, a correspondent radius may be found to apply at the all meniscus forming throughout the system.

According to Fisher[64], bridges of capillary condensed liquid may produce strong dominating adhesion forces between particles at vapour atmosphere, but there is a limit in the applicability of macroscopic thermodynamics to microscopic menisci. It is found that the Kelvin and Laplace equations may apply for meniscus radii down to 5 nm in the case of capillary condensed water. This is further verified in experiments by means of surface force apparatus in reference[65]. Thus, by combining Kelvin and Laplace equations, it may be deduced that capillary tension may be operating in the range of RH down to 86% if such minimum radius exists.

Several authors suggest that capillary action may be the unique underlying mechanism operating in the upper-range of RH change[63]. According to Powers[44], the area fraction where disjoining pressure is operating should be extended due to the appearance of capillary action. It is shown that the area factor within the upper-range of RH change can apparently be unity for cement pastes that are being dried for the first time. T.C. Hansen[66] further developed the theory of capillary action on drying shrinkage of cement pastes. As the paste dries out and water leaves the larger capillary voids, tension builds up in the remaining water giving rise to an elastic compression of the solid gel structure and an overall volume change. By considering all voids being spheres with different radii, he was able to demonstrate that capillary tension in all water-filled capillaries with radii less than the Kelvin radius is equal. Further, by making use of Lamé equations to describe the stress building up in a shell encapsulating a void, a relation for the volume change due to capillary action is proposed.

However, as pointed out by Churaev et al[67], capillary action should be only valid in curved surfaces, where adsorbed water films cannot be stable. Thus, in a cylindrical pore capillary condensation occurs due to capillary instability of curved wetting films on a capillary surface when film thickness grows or reduces[68].

In the case of slit pores, coalescence of wetting films formed on opposite slit surfaces proceeds under the action of attractive dispersion forces. It is concluded that the hysteresis in the isotherm within upper ranges of RH, even near saturation may arise also due to the effect of wetting film coalescence in thin pores. It follows that, beside the knowledge of the pore size distribution, the morphological characterization of porosity may be determinant to disclose the regions of applicability of the previous theoretical predictions.

Expansive mechanisms

As notice by Le Chatelier as early as in the year of 1900, a cement paste may show macroscopic expansion when is subjected to immerse curing. It should be emphasized that this is particularly true for cement-based systems with open porosity during the course of the hydration process. In fact, if the capillary porosity forms a well connected percolation network, free access of water may be supplied from external sources, even though chemical shrinkage is occurring between the reactants. Several researchers reported this apparent swelling, by observing the rupture of the glass tubes used in the experiments of chemical shrinkage. The previous discussion forms the basic argumentation in the swelling theory, where sorption of water within the solid phase may govern[69]. However, other mechanisms, based on the crystal growth theory, are pointed out to explain the expansive behaviour of Portland cement[70, 71]. These are essentially based on the formation of crystalline materials within the hydration reaction of cement clinker compounds, referring to *calcium hydroxide*, CH and to *ettringite*, $C_6A\overline{S}_3H_{32}$, the later being one of the major AFt phases in hydrated cement-based materials. P.K. Metha and Klein[72], reported an expansion of 107% in the volume of solids resultant from the formation of *ettringite*, despite a reduction of 8% in the absolute volume. Other workers have also found a similar behaviour in studies on pure expansive substances[73].

While the recognition of the expansion through *ettringite* growth is commonly accepted, the specific physical and chemical changes are still issues that are not in clear agreement. For example, the crystal structure of *ettringite* is identified as needle-like and gel-like, or, for the chemical process, dissolution and through-solution. The crystal nature of each phase is an important parameter, since it may influence the surface energy that is actually interacting with the envelope, i.e. pore walls, and subsequently inducing expansion. The more colloidal nature of crystals will likely induce higher pressure into the CSH structure, while the more acicular nature will induce only punctual stresses, which may not be sufficient to cause substantial expansion.

M. Ish-Shalom and Arnon Bentur[74] have performed intensive studies in this respect, finding that ettringite in Type I (white) cement pastes precipitated as crystals. Growth of these in confined sites caused expansion.[70]

The thermodynamics of the crystallisation pressure are known for long. For a crystal growing from solution, as in the case of salts present in pore solution of cement pastes, the chemical potential difference between the crystal and the liquid may be given by:

$$\Delta u = RT \cdot \ln \frac{a}{a_0} \tag{2.6}$$

In eq. (2.6), R is the ideal gas constant and a is the activity of the solution, a_0 being the activity of the solution in equilibrium with a large crystal. Carl W. Correns[75] proposed the following formula to describe the relation between the crystallisation pressure exerted by a crystal growing in a supersaturated solution.

$$P \cdot V_{solid} = RT \cdot \ln \frac{c}{c_s} \tag{2.7}$$

Here, P stands for the pressure of crystallisation (or difference of pressure in the crystal and the pressure in the liquid phase), c is the actual concentration in the liquid, c_s the concentration at saturation, V_{solid} referring to the molar volume of the crystalline substance. When the solution is supersaturated, corresponding to the validity of $c>c_s$, the hydrostatic pressure needed to be applied on the crystal to suppress the growth is given by eq. (2.7). If a twofold supersaturation is considered to exist in the liquid phase, the pressure needed to suppress growth would ascend to approximately 30 MPa in a system at 20 ºC. In comparison, as noted by Lura[41], if the term c/c_s equals 100, which is equivalent to assume the condition of saturation, a pressure of 16 MPa is found. If the morphology of the crystal is known, the force acting on the pore network may be derived. Whether this force is high enough to push the solid network outwards, inducing a macroscopic expansion, it depends to great extent on the mechanical state of the solid matter, referring to the degree of deformability of the amorphous gel solid. Nevertheless, a pressure of the previous magnitude overpasses by large the tensile strength of any plain cement paste.

According to George W. Scherer[76], the stresses generated on the pore walls depend, in addition to the supersaturation of the species in solution, on the pore size and surface energy at the interface pore wall-crystal, and in the case of acicular crystals, it should be added the mechanical properties of the crystal, referring to the yield stress and the buckling strength of the crystal. It is further suggested that small spherical crystal is in equilibrium with a higher concentration than a large flat crystal, resulting that higher pressure may be expected in smaller pores at the same degree of saturation. Thus, in low water and low porosity systems, the crystal growth may induce higher pressures within the cement matrix.

In either case, it should be noted that water availability seems determinant to support such expansive behaviour. It is commonly accepted that expansion based on the formation of *ettringite* requires a considerable amount of water. As reported by P.K. Metha[71], the swelling of wet cured specimens is much higher than the expansion behaviour of the body within a dry condition, where significant expansion is not seen. In the case of low water systems cured in autogenous conditions, the referred expansive mechanisms may be only relevant during the very early stages of hydration. In fact, the different structural units present in the cement paste may be competing for water molecules. Thus, the absence of moisture may significantly affect both the rate and extent of crystal growth. Moreover, the space available for the growth of such crystals may also play an important role on the global movement of the solid body, which exhibits different rigidity over the course of hydration.

As referred by Jason Weiss[77], expansive agents, inter-grounded with clinker mineral were widely used as shrinking compensating admixtures for more than three decades to control drying shrinkage phenomena. One of the difficulties attributed to the efficiency of this approach in the practice is associated with controlling the chemical reactions occurring in the system which is subjected to environmental changes. Only one contribution about the use of expansive agents for controlling autogenous deformation is found in the literature, referring to the work by Hori et al[78]. Accordingly, in mortars with high fluidity, it is observed that by the addition of moderate amounts of both lime-free rich gypsum-anhydrite based or calcium sulfoaluminate as expansive agents, autogenous shrinkage may be offset. In addition to the difficulties in controlling the expansion rate, Bentz and Jensen[79] suggest other limitation, which is related with the discrete nature of crystal growth, that being a highly localised phenomena, may not be operating within the whole network, in respect to self-desiccation, which is generally uniform throughout the system via the water link.

However, as stated by Sellevold et al[80], the *ettringite* formation, although widely discussed as a potential swelling mechanism, may not have yet been proven by experiments and thus there may be other underlying swelling mechanisms related to chemical reactions. In addition, it is suggested that potential swelling may be due to internal bleeding occurring in the system, the internal water being locally held at aggregate particles. This would however be true, if the aggregate particles are porous enough to incorporate part of the mixing water. However, and as refuted by Lura[41], in the presence of external bleeding, the paste would remain in a saturated condition prior to the re-absorption of the external bleeding water into the system, and thus self-desiccation would not develop.

Self-restraining mechanism

Given the mechanisms of shrinkage and expansion due to changes in the relative humidity, it may be another mechanism that has not been taken in great account by the research community. This is mostly due to the fact that the assumptions giving ground to the former mechanisms do not take into consideration the microstructural changes of the cement grains upon hydration. Let the system be composed by two components, one of solid material and other by viscous gel, the latter comprising the solid gel and water. It is well known that in low water and low porosity systems, hydration of cement particles cannot be completed. Therefore, the resultant system needs to consider at least two solid parts: non-hydrated particles and hydrated solid gel plus water. To this respect, it is fundamental to know the connection between two structurally different solid parts. Non-hydrated cement particles show a density which is significantly different from that of the solid gel. Therefore, the former volume is not able to shorten or expand its atomic distance, since it remains basically uncompressible crystalline material during hydration. For a system with water to cement ratio of 0.30, the total fraction of this phase may ascend to 30 or 50%, the exact amount being governed by the hydration degree of the paste, which is function of time, particle size distribution of cement grains and the use of admixtures. The interaction between solid gel structure and solid particles may be on the base of self-restraining action exerted by the solid matter. Thus, the movement of such fraction is physically restricted by gravitational forces and may induce a degree of restrain in the viscous-elastic paste, viz hydration products, as for example aggregate do. This leads us to the knowledge of nucleation and growth of species on the surfaces of cement grains[81, 82].

Dale P. Bentz et al[83] have analysed the effect of the particles size distribution of cement grains in the autogenous shrinkage of cement pastes. It is observed that the coarser cement grains, rather than undergoing self-desiccation shrinkage after initial setting, they instead exhibit an initial expansion, as the effects of self-desiccation are initially overwhelmed by those of *ettringite* formation. However, slower hydration rates may also apply to *ettringite* formation. It follows that other possible explanation for the observed phenomena is that of the restraint effect being exerted by larger clinker particles, which may govern the shrinkage behaviour of such systems.

Non-hydrated cement particles are not the unique crystalline phase in the hydrating cement paste. It was suggested by Powers[20] that the disappearance of crystals formed in the hydration of cement, e.g. calcium hydroxide, might be responsible for unrestraining the system subjected to carbonation. Jensen and Hansen[37] also support this idea, adding that, in systems with silica fume addition, the consumption of $Ca(OH)_2$ crystals may be related with the free deformation of the system by removal of restraining elements. In addition, Setzer and Roy[84] suggest that the main factor in restraining the bulk chemical shrinkage is the overall rigidity of the system. It follows that for the same degree of hydration, the total contact points between reaction products will be higher in lower water to cement ratio cement pastes, from where results higher degree of restrain in the system. Lawrence et al[85] have increased the size of $Ca(OH)_2$ crystals in calcium silicate mortars by hydrating the system at 5 ºC, resulting reduced drying shrinkage in the system. The same fundaments are suggested in the work by de Haas et al[86] for explaining the difference in the degree of shrinkage between cement pastes with high w/c versus low w/c due to changes in the size and morphology of *ettringite*, being greatest in the later case. In this thesis, an approach is tried to further comprehend the restraining mechanisms.

2.2.4. Modelling Autogenous Deformation

There can be found different approaches in the literature to model autogenous deformation of cement-based systems. Jensen and Hansen[87] used the model suggested by T. Knudsen[88], the so-called Dispersion Model, to parameterize shrinkage data. It is concluded that superimposing two linear kinetics, the model curve almost exactly reproduces the measured self-desiccation shrinkage at very early-age. Further research performed by the same authors reveals a close relation between autogenous RH change and autogenous deformation.

Hua et al[63] uses a different strategy to describe macroscopic shrinkage in close systems, viz. autogenous deformation. Accordingly, the capillary depression should equal the intrusion pressure as measured by mercury intrusion porosimetry, MIP, as expressed by eq. (2.8), where γ_w is the surface tension of the interface water/ water vapour, γ_{Hg} is the surface tension of the interface mercury/ vacuum, and θ_i is the contact angle between each liquid and the solid walls.

$$p_c\left(\Delta V_{t_0}\right) = \frac{\gamma_w \cos\theta}{\gamma_{Hg} \cos\theta_{Hg}} \cdot p_{Hg}\left(\Delta V_{t_0}\right) \tag{2.8}$$

It follows that the time dependent function $p_c(t)$ may be obtained by a series of MIP tests at subsequent stages of hydration, the ΔV_{t_0} being equivalent to the volume change due to chemical shrinkage, as determined by direct measurements or via degree of hydration. In order to calculate the autogenous shrinkage, the paste was considered to be a continuum medium with aging viscous-

elastic behaviour characterised by an empirical creep function $J_{(t,t')}$, which was related to the compressive stress $\Sigma^{S}_{(t')}$ acting in the pore walls by the following equation:

$$\varepsilon_{(t)} = \int_{t_0}^{t} (1-2\nu) \cdot J_{(t,t')} \cdot d\Sigma^{S}_{(t')} \tag{2.9}$$

As noted by Charron et al[89], according to experiments by Hua et al[63] performed in a system with w/c ratio of 0.42, the deformation induced by capillary depression may explain about 90% of the measured deformation. This approach is however seen with criticism by Lura[41]. This is due to the fact that the drying of the paste prior the MIP evaluation may induce volume change by altering the pore structure of the cement paste. In fact, as shown by Diamond[90, 91], the MIP technique has several limitations in the accurate characterisation of the pore system, due to existence of ink-bottle pores, being described by a large capillary pore with thin access radius. Thus, since the intrusion of such pores by mercury should hold high intrusion pressures, it follows that this kind of pores will be identified as microporosity instead of macroporosity.

A different strategy with basis in the capillary tension is tried by Lura[51], by taking the knowledge of the macroscopic RH-change as base input to compute the Kelvin radius and tensile stress in the pore fluid. The model assumptions rely on cylindrical pores and perfect wetting. The relation between the stress in the pore fluid, as given by the combination of the Kelvin and Young-Laplace equations and the macroscopic linear strain ε_{LIN} is determined according the equation proposed by Bentz et al[92]:

$$\varepsilon_{LIN} = \frac{S \cdot \Delta P_c}{3} \cdot \left(\frac{1}{K_p} - \frac{1}{K_s} \right) \tag{2.10}$$

In eq. (2.10), S is the saturation fraction, ΔP_c is the stress in the pore fluid and K_i are the bulk modulus of whole porous body, e.g. cement paste and the bulk modulus of the solid material. The saturation fraction is calculated by the volumetric model developed by Powers[20], and corresponds to the ratio between the evaporable water and the total pore volume of the paste. The calculated deformations are shown substantially smaller than the measured data points, but it is again seen a close agreement between RH-change and autogenous deformation within the first 24 hours. It is concluded that self-desiccation shrinkage based solely in the capillary tension approach can explain only part of the measured shrinkage in cement paste[41].

Furthermore, computer modelling applied at microscopic scale in cement-based materials may prove valuable to describe the macroscopic behaviour of cement systems. Some approaches were made to describe autogenous deformation by means of computer modelling. A common base to the development of such computer codes is the study of the nature in the hydration of cement particles. The first of the existing examples may be found in the work by van Breugel[93, 94]. The application of the computer model HYMUSTRUCT to characterize autogenous deformation was performed by Koenders and van Breugel[95], taking as theoretical ground the surface tension approach, as supported by Bangham and Hiller equations.

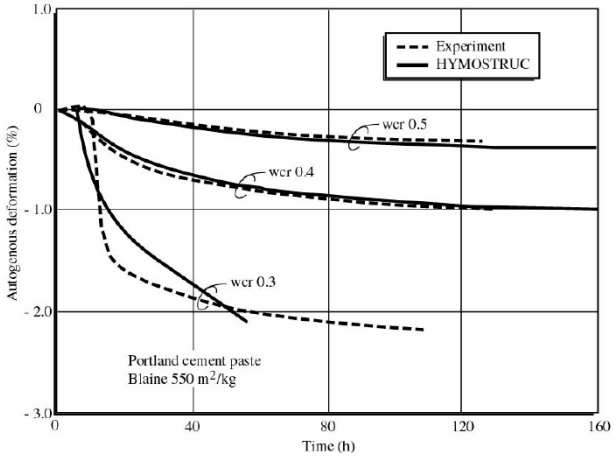

Figure 2.5.

Measured and predicted autogenous shrinkage of cement paste[95].

Although there is merit in approaching the experimental and the model prediction in the upper range of w/c ratio in cement pastes, there is an obviously misfit in the case of lower w/c ratios, as shown in Figure 2.5.

A distinct approach of microscopic modelling is found in the work of Bentz and Garboczi[96-98]. Although remarkable model accuracy is found in applying the CEMHY3D to predict the chemical shrinkage and other related properties of cement pastes, no application of this model to describe autogenous deformation, in addition to the experiments with porous glass[92] is found so far.

A third major microstructure-based computer model is proposed by Meakawa and co-workers[99], the so-called DuCON program. As referred by Zhutovsky[100], Ishida et al[101] described autogenous shrinkage based on the capillary action. In this approach, the pore structure is a model parameter, three difference pore clusters being identified as interlayer (p_l) pores, gel pores (p_g) and capillary pores (p_c). The pore distribution is calculated according to eq. (2.11), B_i being the distribution parameters representing the peak porosity distribution on logarithmic scale and r the pore radius. The interlayer space was deduced from the model by Feldman and Sereda[50].

$$p(r) = p_l + p_g \cdot \left(1 - e^{-B_g r}\right) + p_c \cdot \left(1 - e^{-B_c r}\right) \tag{2.11}$$

The linear shrinkage is calculated directly from the capillary stress in the pore water according to the Young-Laplace equation, affected by an area factor parameter, which represents the regions where capillary water are still operative. A purely elastic relation between stress and strain is assumed. However, the prediction overestimates the measured deformation on mortar systems, as seen in reference[89].

According to Jensen[6], the difficulty in the calculation of RH-change is connected with the empirical ground and subsequent deductive modelling that give only isolated estimates of the real changes, being inadequate for quantitative description of autogenous RH-change. It is further recognised: *"This approach seems fruitless, due to the complexity of the underlying relations and due to a lack of theoretical basis. For autogenous deformation, modelling of this type is even more difficult."*

Leaving aside the less optimistic, though real reasoning related with the difficulties in explaining the autogenous phenomena, consensus is found in some general ideas: that the w/c ratio lowering and silica fume addition promotes self-desiccation and autogenous shrinkage, the autogenous RH-change is not able to proceed below approximately 75% and that cracking may develop in restrained systems undergoing autogenous deformation.

2.2.5. Measuring Techniques

The discussion about which test set up should be used to minimise measurement artefacts and conduce to truthful results to explain a certain phenomena is always on the agenda of any research group. Different methods can be found to measure autogenous strains in cement-based materials. The first discussion about this subject may be centred in the question of linear displacement measurements *versus* volumetric measurements of paste and mortar formulas. The background and particular set up differences of each technique can be found elsewhere in the literature[102-105, 41], but it is important to retain that the volumetric approach frequently lead to higher shrinkage values than the linear approach[106, 107]. An example of the large scatter between both techniques is shown in Figure 2.6.

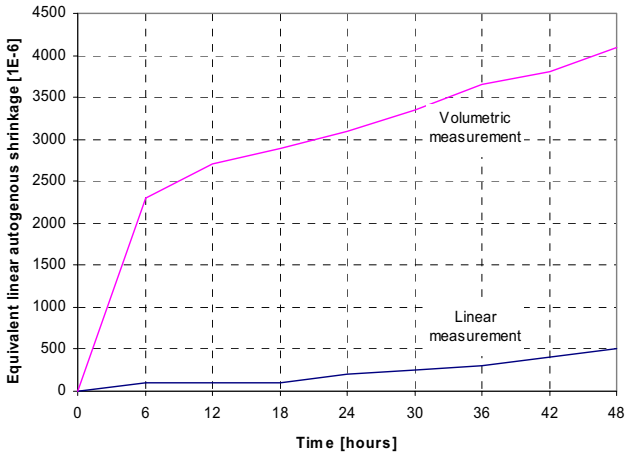

Figure 2.6.

Comparison between linear (horizontal position) and volumetric measurements of autogenous deformation[106].

This figure refers to a cement paste with w/c ratio of 0.26.

Volumetric shrinkage was converted in equivalent linear shrinkage.

(published in 1999)

The sources of error identified to support these observations are related with[106-109]: a) friction between the hardening cement paste and the mould during linear measurement, b) influence of the membrane pressure on hardened cement paste and water penetration during volumetric measurement, c) bleeding.

Although the volumetric measurement permits the recording of the volume change immediately after mixing-pouring procedure and within the plastic stage, Hammer et al.[108] pointed out that the rubber bags (condoms) used in the volumetric measurements could not prevent full waterproof to the system. Pietro Lura and Ole M. Jensen[110] discuss that the water penetration in the condoms used in the volumetric method introduce a change in the immersed weight overriding the buoyancy change due to deformation of the paste, which may be one order of magnitude lower. In addition, is suggested that the mechanism of osmosis can effectively contribute to water penetration since the plastic stage, leading to further water transport into de cement paste[110]. Recent work from G. Sant et al[111] show that through careful experimentation and interpretation, the results of these tests can be perfectly correlated with one another, and thus complementary information may be

obtained. This agreement includes the procedure recommended in ASTM C157 or C494, by superimposing the strain measurement taken from this protocol with the linear autogenous data on to a 24 hours shift. As already pointed out by Aitcin[112], the standard methods for measuring drying shrinkage are not suitable to the measurement of shrinkage that occurs at early-age, thus in high performance concrete. This is not surprising since this ASTM standard test recommends the start of the recording of strains 24 hours after mixing time, and therefore the test protocol miss the capture of the substantial part of the autogenous deformation. Despite the dispute on the better measurement technique that seemed, at some point, to rule the course of the study on autogenous deformation, it is noted that the linear technique gained more acceptability by the research community in the recent years, being at present under consideration for standardisation by the ASTM C09.68 volume change subcommittee. In addition, the Portuguese Laboratory for Civil Engineering LNEC, has recently (2007) adopted the measurement technique based on the linear technique as proposed by Jensen and Hansen[104].

One of the major issues in the autogenous deformation measurement systems rely on the definition of the transition from viscous-elastic to solid state of the hydrating cement paste, e.g. “time zero”. Setting time, as measured by VICAT needle, is usually taken as the time for zeroing the strain. However, if time zero is taken before the time where the system has gained a degree of rigidity, the excess measured deformation will be meaningless in respect with the perception of the risk of cracking. On the other hand, if the “beginning of time” is conversely later, the autogenous deformation may be underestimated, and also the risk of cracking. In concrete mixtures with very low water to binder ratio or silica fume addition, it is registered by Liu Jia-ping et al[113] that meniscus depression appear substantially earlier than initial setting, which implies that the time zero determined by penetration resistance is underestimating the real self-desiccation shrinkage. Some set up enhancements may be done to improve this point. For example, the monitoring of acoustic emissions or electrical conductivity in hydrating cement pastes during the first hours may give a closer indication of this transition[114, 115]. In addition, the development of heat of hydration or temperature increase can also be used with the same purpose. The latter was adopted in this thesis, since it also gives an indication of the chemical reaction of Portland cement. Still, there are considerable doubts about the state of matter at the period of setting. Where and how far the system can absorb deformations without cracking is a question that needs further research.

Other aspect collecting high interest within research community, by analysing the number of publications in the subject, is the bleeding effect on the measured autogenous deformation. This problem is registered in both techniques by several workers. E.J. Sellevold and Ø. Bjontegaard[80] suggest a method to avoid bleeding, consisting in the continuous rotation of the sample prior to setting. However, this procedure may significantly alter the microstructure of the system, especially referring to the entrapped air content, as discussed by Justes[105]. The previous technique was also used in the linear technique by Jensen[30] and Lura[41]. Q. Tian and O.M. Jensen[116] present a recent study on the evaluation of bleeding in both vertical and horizontal concrete dilatometers. It is concluded that for a bleeding system, the two positions within the linear method (vertical and horizontal) can lead to opposite results, e.g., for a bleeding mixture the strain in concrete is seen as expansion in the horizontal direction, while in the vertical direction is seen as shrinkage. This observation is coincident with the previous work by Setter[84] and Hammer[117], as referred by P. Lura[41], and it may be explained due to the absence of settlement phenomena in the horizontal position. On the other hand, it is seen that both vertical and horizontal linear measurement techniques agree for non-bleeding samples[116].

When evaluating strains in concrete, the volumetric approach may present more disadvantages. For example, the rubber envelope that surrounds the specimen can be damaged by the aggregate particles during the pouring procedure. Thus, the linear technique may prove to be more efficient in the determination of early-age deformations in concrete samples. There is a variety of concrete dilatometers that were use to measure autogenous deformation. Strictly speaking, the concrete dilatometers only vary in size in respect with the paste dilatometers, and consist in the same principle, but it is still in the discussion agenda the question of vertical *versus* horizontal measurements and their intrinsic artefacts. For example, the settlement in the vertical position may be difficult to avoid when the system does not stand self-supporting capacity. This may be especially relevant in the case of self-compacting concrete, in connection with the rheology properties of the system. Furthermore, it should be pointed out that the size of the specimen should be carefully selected to minimize thermal effects. In the course of autogenous measurements, it is assumed that isothermal conditions are attained. As hydration takes place, the size of the specimen may influence the rate of heat diffusion and introduce confusion in the real deformation of the system. The coefficient of thermal expansion (CTE) should be accurately characterised with this respect, but it is well known fact that this property is particularly difficult to measure at early-age[118]. On going research in fibber optic-based systems may offer valuable information in order to solve this dilemma, as suggested by Dale Bentz[119].

Despite all the efforts in controlling autogenous phenomena, the actual panorama, as presented in the last RILEM conference especially dedicated to volume changes in cement-based materials, and citing the author[120]: "*Very good reproducibility for nominally identical mixes was demonstrated with this rig. A Round Robin test, carried out within the Brite EuRam-project "IPACS", involving six European laboratories (NTNU/SINTEF included), testing nominally identical mixes, showed however a large scatter."*

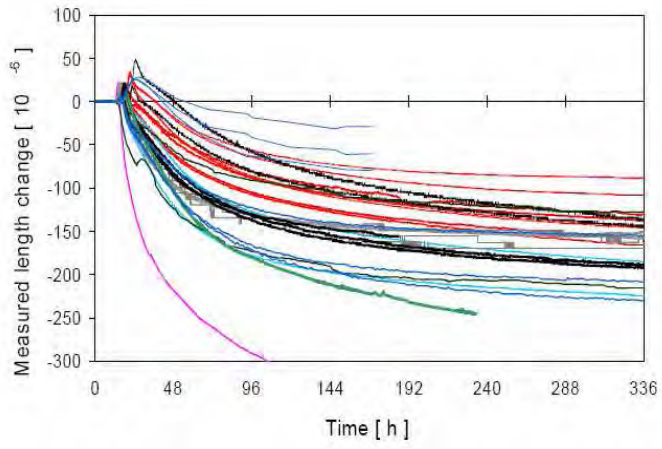

Figure 2.7.

TC195 DTD RR Dilation Rig tests. Measured length change between of start of expansion period and 333 hours. Negative values are contraction. Raw data[120].

The results refer to linear measurements after setting. The setting time was imposed at 7 hours, time where the deformations were zeroed.

(published in 2006)

2.2.6. Mitigation: Internal curing?

Internal curing consists in providing curing water to the bulk cement paste during hydration by means of internal curing agents acting as water reservoirs[121]. The main strategies to mitigate autogenous deformation in cement-based materials known so far are based in the use of lightweight aggregate (LWA)[122], and superabsorbent polymers (SAP)[123, 124]. The basic principle of both internal curing agents is to offset the empty space created by chemical reactions in the cement

paste, by additional hydration products evolved from the existing internal curing water and non-hydrated cement.

The use of LWA in concrete as mean of internal curing of HPC may have been initially proposed by R.E. Philleo[125]. A good review on the background of this technique is given in reference[41]. The idea was later followed by S. Weber and H.W. Reinhardt[122]. The pre-saturated lightweight expanded clay aggregate replacing a volume fraction of the normal aggregate could reduce the early-age deformations occurring in concrete. Because the LWA aggregate is physically more porous than normal aggregate (up to 50% of intrinsic porosity), it can uptake water relatively fast within its open porosity. The efficiency of this approach, which may be extended to any internal curing agent, will depend to large extent on the water kinetics between the curing agent and the absorbate and also from the desorption process that follows the initial hydration. For LWA, P. Lura[41] estimate 50% saturation by weight of LWA at 30 minutes, but that the full absorption profile can take many days (up to one month). M.H. Zhang and O.E. Gjørv[126] measured lower absorption rates, which suggests that it may be difficult to control the saturation level of this high heterogeneous material. This may lead for example to difficulties in controlling consistency within concrete applications. In addition, the strength and elasticity of the composite material may be significantly reduced[124]. However, with a good and constant control of the physical properties of LWA, together with a tight control of the water interaction, the use of this internal curing agent in high performance concrete may develop. It is reported by Dale P. Bentz that the industry of LWA concrete in U.S. is very active at the moment, as the use of high performance concrete is growing substantially.

Research on internal curing by LWA evolved from the use of coarse lightweight aggregate towards fine lightweight aggregate with narrow diameter size, as a replacement fraction of equivalent fine aggregate[122, 127]. Thus, the highest effectiveness would be achieved if the aggregates are in a small size range and are well dispersed in the concrete. S. Zhutovsky et al[128] obtained satisfactory results with pumice aggregate particles in the diameter range of 2.36 and 4.75 mm, used as partial replacement of normal fine aggregate particles in a concrete with a water to binder ratio of 0.25 and 12% silica fume addition. The autogenous shrinkage is fully mitigated and even an initial expansion is observed. No considerable detrimental effects on strength are found. The concept of efficiency factor is brought out to calculate the required amount of water to counteract autogenous shrinkage. This concept is based on previous work by D.P. Bentz and K.A. Snyder[129], designated by protected paste volume in concrete in extension to internal curing. In turn this approach is adapted from the more conventional application of the protected volume fraction to characterise air void systems in air-entrained concrete. The computer simulations performed in the hard-soft shell 3D concrete model[98], with internal curing by fine LWA particles show that the particle size influences the effectiveness of water movement towards the surrounding paste. From this modelling approach, it is concluded that the double of paste is at the distance of 100 μm from the fine LWA surface, by varying the particle size distribution of fine LWA according to the upper and lower limits defined in ASTM C33[130]. M. Geiker[131] support the idea of maximum travelling distances between 100 to 200 μm. However, the use of lower w/c ratio and silica fume in the system may result in shortening the effective distance in respect to the water movement in cement-based materials when percolation threshold is achieved[132]. As observed by Christensen et al[133] and also El-Enein et al[134], porosity in cement-silica systems is significantly lower from that of plain cement systems, when subjected to electrical conductivity measurements. Thus, the use of higher quantities of silica fume may result in an earlier and more severe

discontinuity of the percolation system, where diffusion of ions and solution may be harshly diminished.

A relatively recent strategy is proposed to mitigate autogenous deformation and is designated by water-entrainment of cement-based materials by superabsorbent polymers[123]. This invention is attributed to Per F. Hansen and Ole M. Jensen, and is object of patented work[135]. The basic principle of internal curing by superabsorbent polymers does not differ from that of the use of LWA particles to internally cure concrete. Superabsorbent polymers are hydrogels capable of taking into their cross-linked structure considerable amounts of water without collapsing. Detailed information about these modern polymer-based materials can be found elsewhere in the literature[136]. Their use in cement-based materials were initially focused on maintaining a high level of internal moisture in order to prevent self-desiccation and thus, with the purpose of mitigating autogenous deformation. The use of superabsorbent polymers has shown to be highly effective on this purpose, as observed in a number of scientific publications[137, 124, 138]. On the other hand, one of the consequences of the use of superabsorbent polymers in cement-based materials is the formation of water-filled macro pore inclusions. Little was done in respect with this aspect: state and volume change of macro pore inclusions during hydration and internal curing of cement pastes. SAP porosity may affect strength properties of the composite material (paste, mortar or concrete), as registered in previous research work[124, 139-141]. However, contradicting results exist when analysing strength of water-entrained mortar systems by superabsorbent polymers, where strength gain is observed[138]. Similar behaviour regarding the strength properties is found when comparing water-entrained and non-water-entrained specimens in non-autogenous curing regimes.

The modelling approach to prescribe the necessary amount of SAP to mitigate autogenous deformation in cement-based materials was carried by Jensen and Hansen[123]. Based on Powers model[20], the water requirement to internal curing should correspond the chemical shrinkage of the system for a given maximum degree of hydration. The extension of this approach to include silica fume addition in relation with internal curing is proposed by P. Lura[41]. However, one of the assumptions made in the later work may encounter some criticism: the assumption of that silica fume reactivity is equal to that of Portland cement.

The mechanisms of internal curing by superabsorbent polymers are poorly understood. O.M. Jensen and P.F. Hansen[124] support the idea of that the initial expansion observed after setting is due to re-absorption of water by the hydrated gel. This perspective originates in the observations of more ancient research work[15, 20], by submerging a cement paste sample in water, viz. water curing method. However, the water state during cement hydration or the desorption kinetics of the water existing in the superabsorbent polymers are questions that require further investigation, as no observation of water movement in water-entrained systems was yet foreseen.

Summing up, the controversial around the strength properties in systems with internal curing is not yet clarified, especially from the perspective of the user. Particle size distribution of superabsorbent polymers may play an important role in the cement paste properties and thus, knowledge about this aspect requires investigation. It should be noted that strength is only one parameter in evaluation in relation with internal curing. If durability aspects are brought in to evaluation, the previous argumentation may be questioned. For example, if thaw-freeze resistance is required in the concrete structure, SAP porosity may be used to equilibrate the crystallization pressure of water

present in the microstructure. Internal curing agents may be used with this purpose, in detrimental of the potential gain in strength, but with increased performance during service and extended life of the material.

One of the doubts that still persist is that of the ability of the internal curing agents to prevent microcracking within the build-up stress in the pore network. It is well established that the autogenous strain is mitigated. In respect with the early-age cracking, this may be not straightforward.

In this thesis, a new concept of internal curing is brought out from the research work. This new strategy consists in very fine aggregate particles and takes advantage of the high surface area relation arising from the use of fine aggregate particle-diameter. The theoretical approach and experimental observations are given in chapter 4.

2.3. Closing remarks

In the present chapter, it was been outlined the motive and background for the work that follows. The mechanisms of self-desiccation and internal curing in high performance cement-based materials require further research work, as yet is not sufficiently clear how the internal curing water is transferred to the cement paste during the viscous-to-solid transition. However, it does not seem questionable that self-desiccation is the driving force for stress build-up in the absence of any curing agent, processing throughout the bulk cement paste in composite low water and low porosity cement-based materials, and thus, in the presence of any restraining elements, may result in generalized microcracking.

The key aspects on the state of knowledge related with the underlying mechanisms to explain such phenomena were identified. Some aspects are in part properly solved by previous work, but it should be point out that there are still missing many pieces in the forever puzzling world of cement. Thus, many open questions need further understanding, emphasizing the modelling and comprehension of such complex phenomena. Where and how far the stress generated may be confined under the developing tensile strength within hardening is not of easy perception. To understand this key-aspect is to provide the cement-based systems the possibility of existing without microcracking, during unprecedented large periods of time.

3. Internal Curing by Superabsorbent Polymers

3.1. AD measurements at room temperature: from the basics to mitigation

This study is focused on autogenous deformation (AD) in cement-silica systems at room temperature. AD measurements were performed manually in a digital dilatometer. The effect of silica fume addition and water to cement ratio on AD is analysed within a period of 28 days. It is concluded that both silica fume addition and lower water to cement ratio has a drastic effect on the development of autogenous strains at early-age. In addition, different chemical-based superabsorbent polymers were used with the purpose of gaining insight on the influence of the physical and chemical nature of the polymer on the mitigation efficiency of autogenous deformation, being concluded that different superabsorbent polymers act differently while counteracting the autogenous strain. Moreover, sodium-acrylate-based polymers showed that an upper threshold value for internal curing of cement-silica paste exists. Furthermore, the long-term pore structure and hydration degree performed to the same mixtures indicate that the water-entrained cement-silica pastes may sustain further the hydration of cement, while changing the pore structure. The relation between the pore structure and hydration degree of water-entrained cement based materials is tried and discussed.

3.1.1. Theoretical introduction

Self-desiccation is related with the early-age shrinkage caused by chemical reactions of the cementitious materials where lack of sufficient water to support hydration is of fundamental importance [6, 142]. The subject of the effect of silica fume addition on AD as a partial replacement of Portland cement is not fully understood. In the literature, normal amounts of silica fume in the range of 5 to 10% by the weight of cement are used to access AD of cement-silica systems [15]. Alias, this rate of cement substitution fits the value suggested in the specific regulations for the use of this mineral addition in cement-based materials [143]. It is well established that increasing dosages of silica fume lead to higher values of autogenous strain in cement-based materials. In ultra-high strength concrete, the replacement of cement by silica fume can be easily higher than 20%. Thus, increasing dosages of silica fume up to 30% may result in higher potential to cracking phenomena. A primary objective of the present study is to access the influence of low w/c ratio and of higher dosages of silica fume on autogenous deformation in cement-silica systems.

Furthermore, internal curing by means of superabsorbent polymers were proved an efficient strategy to counteract autogenous deformation [124]. Yet, no study on the effect of the nature of superabsorbent polymers, either physical or chemical, on autogenous deformation, is found. Thus, a different physical or chemical structure of superabsorbent polymers may lead to undesirable results, as very few or little practical experience can be found with this new internal curing technique. Therefore, two different superabsorbent polymers were used in the experimental framework to access their efficiency on mitigating autogenous deformation. In addition, the pore network arising from the superabsorbent polymers was characterized and relation with the long term hydration degree was tried.

3.1.2. Materials

A low-alkali Danish white Portland cement with Blaine fineness 420 m2/kg was used in the mixtures. The density of the cement is 3150 kg/m3. The Bogue-calculated phase composition (in

wt.%) is: C_3S: 66.1, C_2S: 21.2, C_3A: 4.3, C_4AF: 1.1, $C\bar{S}$: 3.5, free CaO: 1.96, Na_2O eq.: 0.17. Silica fume (SF) was added as a dry powder at a rate of 15 to 30 wt.% of cement. The specific surface of the silica fume is 17.5 m^2/g (determined through BET method). The chemical composition (in wt.-%) is: SiO_2: 94.1, Fe_2O_3: 1.00, Al_2O_3: 0.13, MgO: 0.71, SO_3: 0.43, and Na_2O eq.: 1.09. A naphthalene-based dry powder superplasticizer (SP) was added at a rate of 1.0 wt.-% of cement. Slight variations in the SP were required to avoid excessive bleeding or lack of cohesion.

Two different superabsorbent polymers (SAP) were used in the mixtures. Images from both polymers at dry and swollen state, as acquired by optical microscope are shown in Figure 3.1 and Figure 3.2.

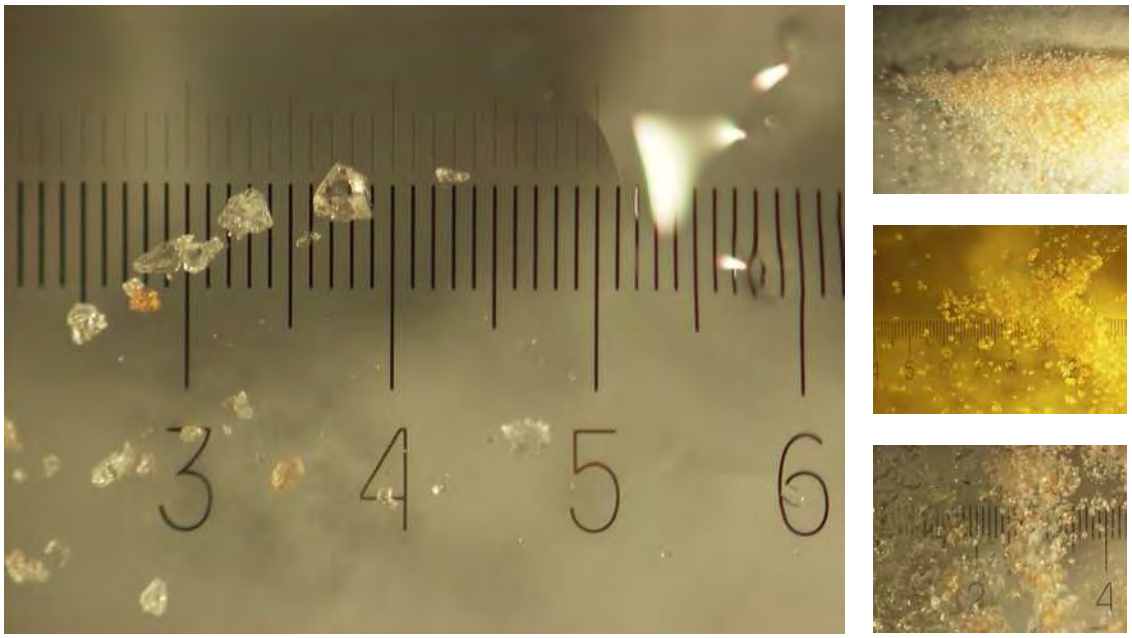

Figure 3.1.

SAP type A. Observed particle size is in the range of 0 to 300 µm. The average size is about 200 µm. The dry state of this polymer resembles fine aggregate particles with random angularity. The swollen state is characterized by a gel, whereby no morphological information may be perceived. Numbers refer to mm.

Both superabsorbent polymers are a suspension-polymerized covalently cross-linked acrylamide/acrylic acid copolymer. SAP A is an industrial by-product, sodium-acrylate based, in the form of crushed material, similar to quartz aggregate particles in shape. SAP B consists in microscopic spheres with particle size ranging between 0 and 250 µm. The density was evaluated in 1400 kg/m^3. Superabsorbent polymer was added in dry state at a rate of 0.2, 0.4 and 0.6 wt.-% of cement.

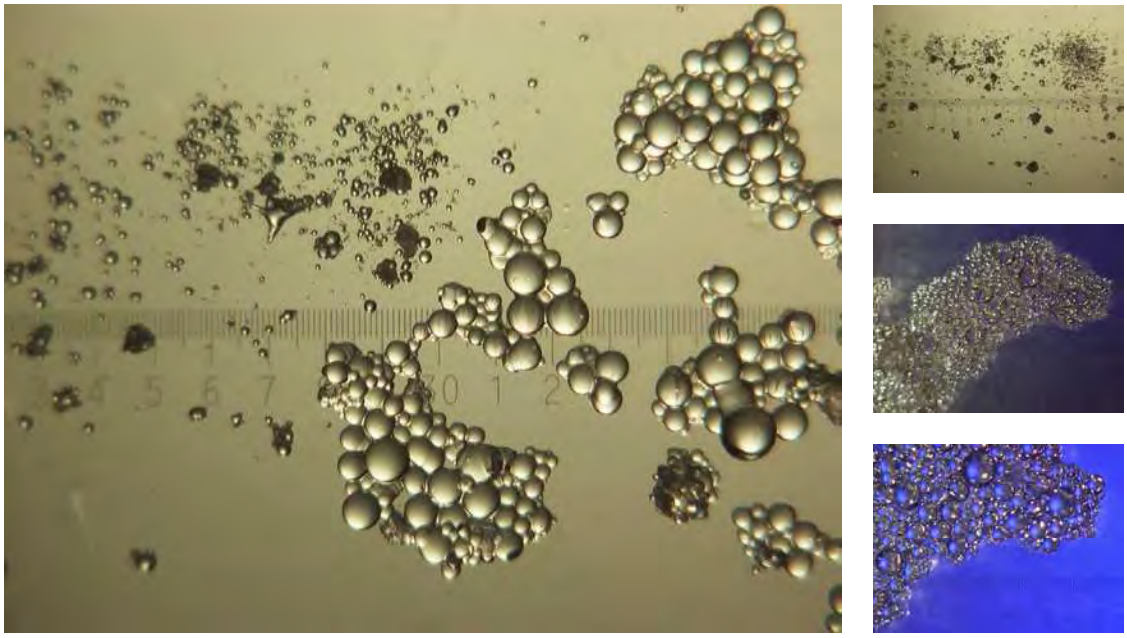

Figure 3.2.

SAP type B. Observed particle size is in the range of 0 to 250 µm. The average size seems to be at 150 µm. The dry state is characterized by spherical shape particles. The swollen state (right hand side of the main image) is characterized by independent particles with considerable attraction by water-links. Numbers refer to mm.

The size of the swollen SAP particles in the cement pastes and mortars is two to three times larger due to pore fluid absorption. Internal curing was performed according to eq. (3.1):

$$(w/c)_e = K \cdot (SAP/c) \tag{3.1}$$

Where $(w/c)_e$ is the additional (entrained) ratio between water and cement to be added to the system, (SAP/c) is the weight ratio of SAP at dry state and cement, and K is the absorption capacity of the superabsorbent polymer. The following absorption capacity was used in the water-entrained systems, as taken from references [124, 144]:

$$\begin{cases} K_{SAP\_A} = 30.0 & \text{g/gram of dry polymer} \\ K_{SAP\_B} = 12.5 & \text{g/gram of dry polymer} \end{cases} \tag{3.2}$$

3.1.3. Methods

Cement pastes were mixed in 5-1 epicycle mixer. All the components were mixed in dry state, and added demineralised water during the first 2 minutes at low speed (speed level 1). The mortar was left stand for 1 minute and again mixed for 2 minutes at high speed (speed level 2).

Autogenous deformation measurements

AD measurements were performed in the digital dilatometer. Detailed specifications of this set up are given in the literature[145]. Though, the main characteristics are addressed here in the following. The set up consists in a measurement bench built in steel to support the corrugated

tubes, which were especially design for this measurement system, and a linear displacement device, Mitutoyo ID-C series, with a resolution of 0.001 mm (see Figure 3.3).

Figure 3.3.

Digital dilatometer for measuring autogenous deformation in paste and mortar systems. The full set up, including the measurement device and accessories is shown in the picture: corrugated tubes and Teflon plugs, the reference bar and the remote control of the digital displacement device [145].

Specimens are cast individually, by pouring the fresh cement paste into the low density polyethylene corrugate tubes. While pouring, continuous vibration is applied on the specimen in a paste vibrating-table. Despite all the preventions in this procedure, few uncontrolled amount of air bubbles do form throughout the sample. After the pouring procedure, the tube is sealed with Teflon plugs assuring autogenous conditions. The first measurement for each mixture started at final setting, which is calculated in compliance with ASMT C 191 [146]. This is done in parallel samples casted into conical ring moulds and protected from moisture loss by covering the top surface with an acrylic glass plate. This ensures that setting is simulated at the same closed conditions as the specimens in the corrugated tubes. All samples were kept in a temperature controlled room at 20 degrees Celsius during one month. For mass control, individual cylindrical samples were casted in smaller cylindrical tubes, the initial mass being obtained at final set. After the measurement period, samples were weighted again for water loss control. Results indicate that the corrugated tubes can assure adequate sealing during one month at moderate environments. The length of the corrugated tubes was calculated according eq. (3.3).

$$L(t) = L_{ref} + R(t) - 2 \cdot L_{plug} \tag{3.3}$$

Where L_{ref} represents the length of reference bar (415mm), $R(t)$ is the reading of gage with sample in the dilatometer and L_{plug} is the length of one end-plug (19mm). Autogenous strain of the sample at the time t, expressed as μm/m is calculated by eq. (3.4), where $L(t_{fs})$ is the length at the time of final set, when the first measurement is performed.

$$\varepsilon_{autogenous} = \frac{L(t) - L(t_{fs})}{L(t_{fs})} \cdot 10^6 \text{ [µm/m]} \quad (3.4)$$

Optical microscopy and image analysis

Optical microscope was used in the water-entrained samples to study SAP-pore structure in hardened state. Specimens were taken from the AD samples after AD measurements were finished. The sample preparation consisted in fine polishing the surfaces with two abrasive diamante-discs. The diamante mesh of each disc was respectively #500 and #1000. This level of polishing ensures a good quality of the image within the microscope resolution that is needed for this purpose (SAP pore structure between 0.01 and 1 mm). The images were then analysed in the software package IMAGE-J, developed at the Research Services Branch of the National Institute of Mental Health. Detailed information about this software package is available elsewhere. The data collection procedure involved two samples from the same batch in each system. Image processing consisted in applying a threshold filter to each image which was prior transformed into gray scale. Holes or pores appear in black when subjected to raising light[26]. Quantitative analysis was then performed to the binary images by calibrating the pixel resolution with the area size of the image taken from the microscope. Different properties could be analysed by this procedure: SAP pore distribution in hardened pastes and the maximum distance from between SAP surfaces.

Hydration Degree by Non-evaporable water

Degree of hydration was calculated by the determination of non-evaporable water according to procedure described at reference[147]. Small samples of about 3 to 5 grams were prepared for each mixture. After each sealed curing period, specimens were vacuum dried during 1 hour to stop hydration. After the first weight measurement, samples were oven dried at 105 degrees Celsius for the next 24 hours, and weighted again for adsorbed water and evaporable water content. After the second measurement, samples were crushed and grinded to powder for loss of ignition determination at 1050 degrees Celsius during 1 hour. This was done in a furnace during approximately 4 hours at increasing temperature according to the temperature-time profile presented in Figure 3.4.

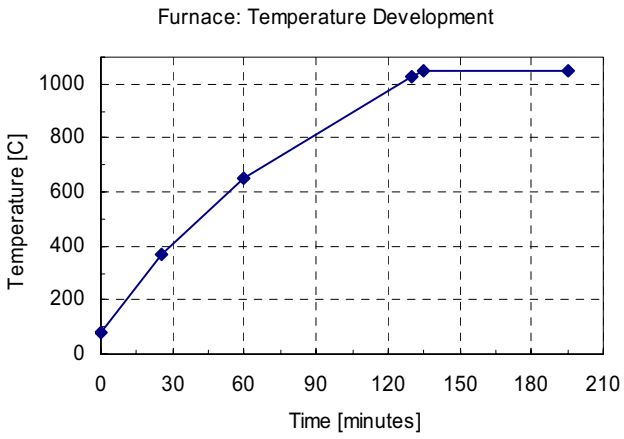

Figure 3.4.

Furnace temperature development in time and digital control.

Specimens were weighted immediately after temperature equilibrium was achieved at room temperature (see Figure 3.5). The non-evaporable water, which is defined as the increase in loss of ignition due to hydration, in grams per gram of original cement is then derived from eq. (3.5).

$$\frac{W_n}{c} = \frac{W_1}{W_2}(1-L)-1 \tag{3.5}$$

Where $\frac{W_n}{c}$ represents the ratio of non-evaporable water in grams per gram of cement reacted, W_1 is the weight of dry sample in grams, W_2 is the weight of ignited sample in grams and L is the ignition loss of original cement in grams per gram of cement reacted. Hydration degree α was derived by normalizing the non-evaporable water with the ultimate value (0.23), as taken from the literature [148].

Figure 3.5.

Specimens after loss of ignition at 1050 ºC. Temperature equilibrium was performed in desiccators with silica gel.

3.1.4. Results and discussion

Effect of silica fume and water to cement ratio on AD

Figure 3.6 shows the measurement of AD of cement pastes with varying water to cement ratios during 2 weeks hydration in sealed conditions. As expected, the lowering of water in the system promotes the self-desiccation of the cementitious system, from where results an increased effect on autogenous deformation. The naphthalene-based superplasticizer retarded setting time and thus the kinetics of hydration, resulting in some degree of uncertainty when comparing different systems at macroscopic scale. The presence of lower water in the system indicates faster setting, even for pastes with the introduction of SP. It is noted an initial expansion for all mixtures with exception of the mixture with w/c of 0.2. This may be explained by the occurrence of bleeding, unavoidable for plain cement pastes with water to cement ratio above 0.35. It is also concluded that the deformation greatly increases with decreasing water to cement ratio in the range of 0.2 to 0.4.

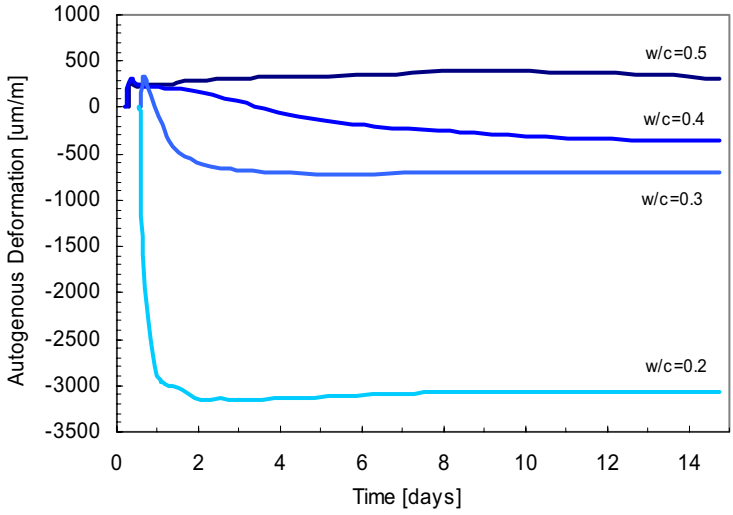

Figure 3.6

Autogenous deformation of cement pastes with increasing steps of the water to cement ratio. It was observed bleeding for all mixtures.

The registered AD in the first case (w/c=0.2) was 3000 μs, comparable to systems with silica fume addition (see Figure 3.7.). The presence of more 10% of water in the system corresponds to a decrease of about 80% of the autogenous shrinkage in respect with the previous system. The strain rate clearly differs among the studied systems. It is interesting to note that shrinkage is registered even for the mixture with 40% of water by weight, after a short expansion. The strain rates vary accordingly to the decrease of the water content. In the mixture with 20% of water, the registered strain rate after setting is about 170 μs per hour. This rate is abruptly hampered within the first 24 hours. This behaviour is not altered within the first month in sealed conditions. A smother transition is observed in the system with w/c of 0.3. After the initial expansion, the measured strain rate is 25 μs per hour up to 1.5 days, where follows the levelling of strain. This behaviour is consistent with early research work developed in this topic [149].

Plot of AD measurements of cement pastes with increasing steps of silica fume addition is presented in Figure 3.7. Silica fume addition resulted in dramatic increase of early-age shrinkage, as observed by the drop of the curves. By comparing the cement-silica paste with the equivalent cement paste (0%SF), it is concluded that silica fume addition results in a deformation increase with factor of 4, in respect to the equivalent cement paste. Surprisingly, the higher dosage of silica fume at 30% does not seem to have detrimental effect on the early-age deformation. Inversely, the double of the silica fume content shows a beneficial effect on the early-age deformation up to the age of 7 days. This may be due to the limitation in the combined reaction of silica fume with calcium hydroxide. In fact, the chemical properties of cement may govern the extent to which silica fume can influence autogenous deformation in sealed and unrestraint cement-silica based systems. It is possible that the mechanism governing the strain is related with the production of calcium hydroxide. Further investigation is required to have a deeper comprehension of this aspect: cement-silica ratio versus hydration kinetics of main clinker compounds. Previous research was done on the effect of silica fume addition in autogenous deformation. O.M. Jensen and P.F. Hansen [37] have studied the effect of silica fume addition of cement paste with water to cement ratio of 0.35. In this work, deformations up to 1500 μm/m are registered for 10% of silica fume addition.

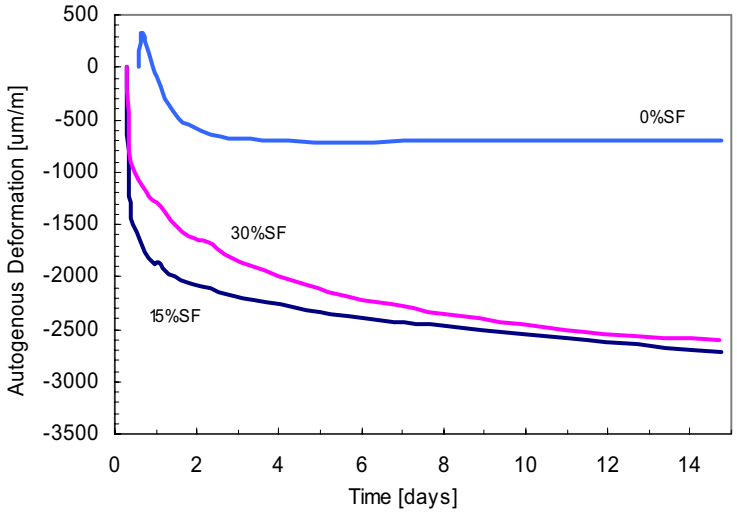

Figure 3.7.

Autogenous deformation of cement-silica paste for increasing steps of silica fume addition. Basic w/c is 0.3.

The higher values of autogenous shrinkage in low water cement-silica systems with higher content of silica fume are therefore consistent with the previous research work. Though, the drop of the curve seems to be more serious for low water content and higher amount of silica in the system. Thus, hydration rates may play an important role on the strain rates of the composite systems of cement and silica fume. Break on the curve in Figure 3.7 occurs before the first 24 hours, and may be related with the onset of pozzolanic reaction of the silica fume[87], or with an enhancement of the chemical reaction by clinker minerals. In either case, more fundamental research seems needed to characterise the hydration of cement-silica systems.

Effect of different chemical-based superabsorbent polymers on the mitigation of AD

Different types of superabsorbent polymers were analyzed at increasing amounts in cement-silica systems. For each type of superabsorbent, plots of autogenous deformation and time were developed, as presented in the following figures. Figure 3.8 show the effect of the amount of polymer type A in the autogenous strain. The optimal dosage seems to be at 0.4% (wt. of cement), corresponding to extra curing water of 0.075. Contrarily to what was expected, higher dosage of water-entrained within this polymer-type did not further reduce the deformation at early-age. Inversely, AD increased substantially autogenous deformation: from 500 to 800 μs. The higher value of shrinkage for 0.6% of polymer type A requires further research to explain what might have happened. A possible explanation is that this type of polymer may present limitations on the absorption kinetics. In addition, the combination forces with liquid molecules, motivated by stronger links between the sodium-acrylate-based polymer and water may also influence the interaction of the polymer with the surrounding paste. Thus, the hydration kinetics might also be affected from this point of view. If the osmotic pressure that ensures that the water is adsorbed at the cross linked structure of the superabsorbent is somehow affected, the absorption capacity of the polymer may change. Fredric L. Buchholz [136] developed experimental work on the dependence of the swelling capacity by different concentrations of sodium chlorine. It is noted that the swelling capacity varies within an inverse linear relation with the salt concentration on the liquid phase: by increasing the salt concentration the swelling capacity of the gel decreases in similar proportion. This is explained by different chemical gradients forming within the gel and liquid, thus, different osmotic pressures.

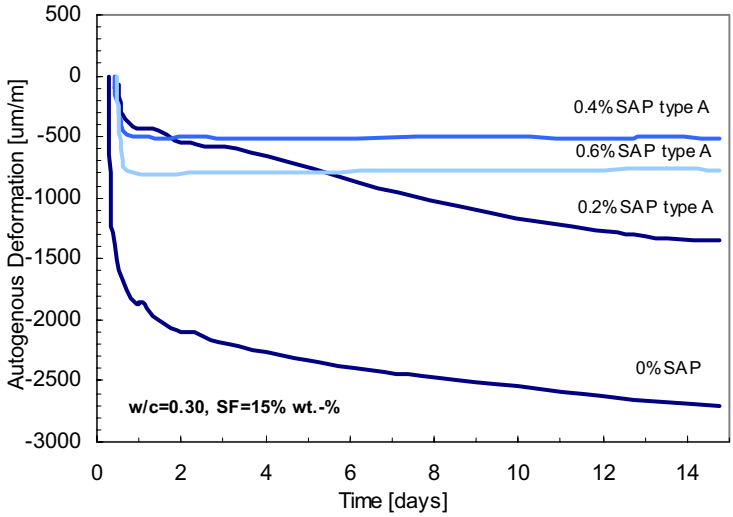

Figure 3.8.

Autogenous deformation of water-entrained cement pastes by superabsorbent polymer type A.

Basic w/c is 0.3. Water entrainment was performed according to eq. (3.1). (K=30 ml/g).

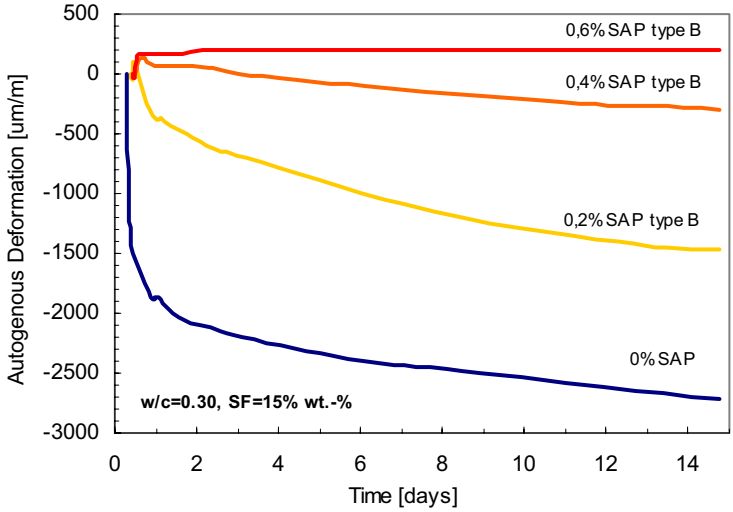

Figure 3.9.

Autogenous deformation of water-entrained cement pastes by superabsorbent polymer type B.

Basic w/c is 0.3. Water entrainment was performed according to eq. (3.1). (K=12.5 ml/g).

Polymer B exhibited a more consistent behaviour in relation with polymer A, when the amount of SAP and respective internal curing water was increased. Optimal dosage should be around 0.4% for a deformation lower than 500 μs at the age of 15 days, at a silica fume content of 15%. In the case of polymer B, the pastes show even a slight expansion, suggesting that both superabsorbent polymers may act differently with the surrounding paste. Thus, water movement from the superabsorbent seems to be controlled by different mechanisms. By analysing the slopes for mixtures with 0.2% of SAP, a common observation can be drowned between both polymers. Immediately after setting, the drop of the curve is already more smooth, in comparison with the equivalent cement-silica paste. Until the age of 2 days, samples could maintain a low deformation. From this point, deformation increase continuously up to 1500 μs. This may be related with the limited amount of water available for internal curing of cement-silica paste. Despite of this, the shrinkage reduction capacity, as measured by linear autogenous deformation technique, even with lower amounts of water entrained, was remarkable. The measured deformation at 2 days is about 500 μs versus 2000 μs in the equivalent cement paste. It is also observed that both superabsorbent polymers show different strain behaviour within dosages above 0.2%, as notice in the rate of autogenous deformation after the initial 24 hours. Polymer type A presents a zero deformation rate

with time for mixtures with internal curing water of 0.12 and 0.17. Polymer type B induces a continuous deformation rate to the system in the case of the mixture with 0.4% and a zero deformation rate for the mixture with 0.6%. In the later, the internal curing water of 0.10 is preceded by expansion, while, in the case of polymer type A, with similar internal curing water, only shrinkage is registered. It is concluded that different superabsorbent polymers result in different kinetic behaviour while curing cement-silica systems.

3.1.5. Hydration degree versus SAP porosity

The optical microscope may prove of value in controlling the hardened properties of water-entrained cement-based materials, especially those related with macro porosity. The image analysis performed to water-entrained specimens was compared with the equivalent non-entrained system in order to evaluate the SAP pore network, according to the initial amount of SAP introduced in the system. About 10 frames were used in the quantitative analysis. Typical 2D images taken from each system are given in Figure 3.10.

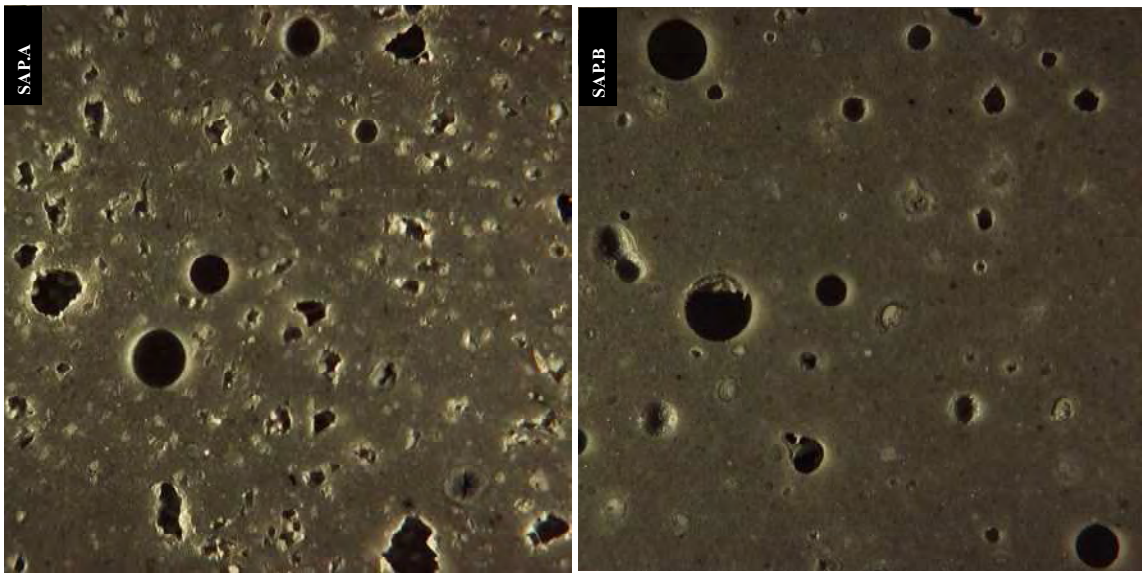

Figure 3.10.

2D sections of water-entrained samples with 1 year. On the left, superabsorbent type A in quantity of 0.4% by weight of cement. The right image refers to a water-entrained paste with superabsorbent type B in amount of 0.4% by weight of cement. Length to height ratio is unitary and corresponds to 5.50 mm.

It is apparent that different superabsorbent polymers create different pore structures in water-entrained cement-based materials. The spherical pores observed in the image in the left indicate that higher number of air pores may form in the presence of the superabsorbent type A. This was observed in a number of frames. On the other hand, it seems that the introduction of SAP.A results in a pore network with lower pore diameters in relation with SAP.B. The maximum measured pore sizes fall in the pore-range between 500 and 600 μm, respectively for SAP.A and SAP.B. These sizes occur at a small frequency throughout the sample, but represent a significant part of the total pore volume. The quantitative analysis performed to both systems is summarized in Table 3.1. The results of pore volume in hardened state for SAP type B are consistent with the initial composition. By increasing the amount of superabsorbent polymer, the pore volume in the hardened state increases accordingly. This clearly shows that both types of superabsorbent are stable in the

swollen state during mixing. The same analysis performed to SAP type A confirms the observation of a lower SAP pore volume in relation with SAP.B. This suggests that additional curing is occurring in the presence of SAP.A. However, it is noted that the colour of the paste is slightly different between the two mixtures. Since the intensity of light is kept constant during the tests, the darker gray in the right-image indicates that the bulk paste may have higher density, assuming that the degree of moisture in the paste is not the dominant factor at this age.

Table 3.1. Quantitative analysis of SAP pore structure in the fresh and hardened state

Mixture	Volume fraction					
	Initial state			Hardened state		
	Binder	Water	SAP plus water	SAP.cavity pore volume fraction	Standard deviation SD	Variance COV
	[vol.-%]					
Plain_SF15%	0.57	0.42	0.00	0.13	0.06	43%
SAP type A 0.2%	0,53	0,40	0,06	0.37	0.06	16%
SAP type A 0.4%	0,50	0,37	0,12	4.20	0.53	13%
SAP type A 0.6%	0,47	0,35	0,17	4.93	0.87	18%
SAP type B 0.2%	0,54	0,41	0,03	1.80	0.34	19%
SAP type B 0.4%	0,53	0,39	0,07	5.00	1.02	20%
SAP type B 0.6%	0,51	0,38	0,10	5.65	1.61	28%

The results of HD tests taken by non-evaporable water content in the water-entrained mixtures and the correspondent cement-silica paste are shown in Table 3.2. Although the coefficient of variation in turn of the average-value is as high as 10%, it is seen that the internal curing by superabsorbent polymers leads to higher hydration degree in respect with the cement-silica paste. Previous research performed to similar mixtures give reproducibility and repeatability to the short term measurements[138]. However, the analysis of the long-term results reveals that this method may present limitations in the real calculation of the effective water that is being used to form new products. In 3 systems, the long term hydration degree is lower than the HD at 28th day in sealed curing condition.

Table 3.2. Hydration degree

Mixture	Short term. HD [28 days]			Long term HD [360 days]		
	Average	Standard deviation SD	Variance COV	Average	Standard deviation SD	Variance COV
Plain_SF15%	0,59	0,00	0,8%	0,56	0,06	10,4%
SAP type A 0.2%	0,74	0,02	3,1%	0,63	0,02	3,7%
SAP type A 0.4%	-	-	-	0,66	0,02	3,1%
SAP type A 0.6%	-	-	-	0,65	0,04	5,5%
SAP type B 0,2%	-	-	-	0,57	0,04	7,6%
SAP type B 0,4%	0,72	0,00	0,7%	0,61	0,05	7,8%
SAP type B 0,6%	-	-	-	0,65	0,01	1,9%

A possible explanation is that the water-entrained specimens may physically keep part of the water towards a higher temperature in relation to the 110 degrees Celsius, which is conventionally taken as the temperature from which physical and chemical bound water may be differentiated. This assumption is rather arbitrary and may induce wrong interpretations of the water state in composite materials beyond the pure clinker cement materials. On the other hand, the non-entrained pastes also show a slight reduction in the long term HD. The sample storing at a reduced moisture level (50%RH) may be a reason for this phenomenon. If a moisture gradient was created between the bulk and the environment, then it is possible the water reacted may be partially removed by drying.

In either case, the results show that the hydration degree grows accordingly with the increase in the quantity of superabsorbent polymer and correspondent internal curing water for SAP.B. The same conclusion does not apply to SAP type A. By increasing the amount of SAP.A from 0.4 to 0.6%, a similar degree of hydration is found. This observation indicates that there is a limitation in the amount of internal curing that can be introduced in high performance systems with this type of polymer. Other possible explanation is that the water-entrainment procedure in the case of polymer SAP.A is overestimating the absorption coefficient, from where results a different w/c ratio at the bulk paste. In addition, this may explain the lower SAP pore volume found in the samples with SAP type A with equivalent internal curing water, in respect with SAP.B. Nevertheless, the results are revealing the non-linear behaviour between SAP.A dosage, autogenous deformation, and hydration degree. Further research on the absorption kinetics and stability of this particular hydrogel seems fundamental.

Because SAP pores exist in the hardened state, the hydration degree may be related with the decrease in porosity taken from the final to the initial state. The difference between initial and final porosity may be plotted against the normalized ratio of HD, taken as the ratio between the HD of water entrained systems and the HD of non-entrained cement paste. This difference expresses the volume change of the superabsorbent during hydration, which should be equivalent to the effective degree of hydration that the system achieved due to internal curing in relation with the basic system. Figure 3.11 resumes the previous discussion.

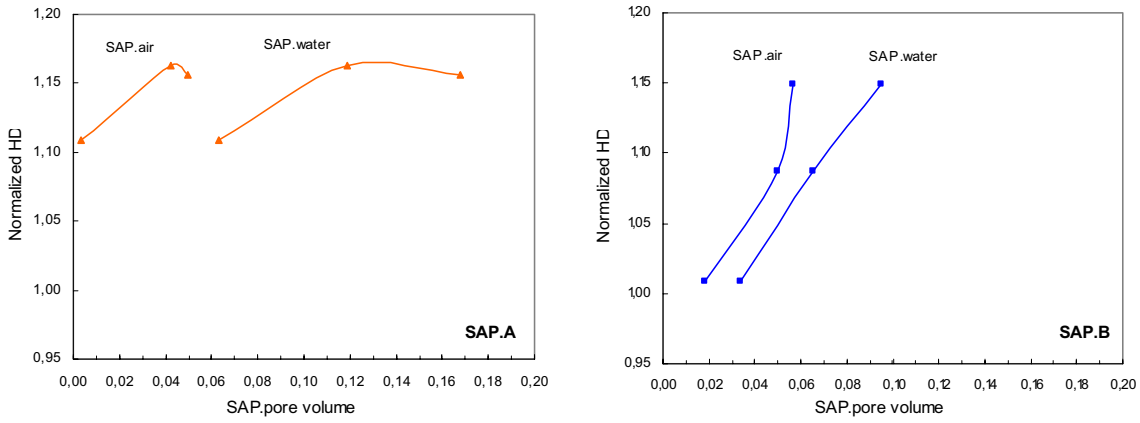

Figure 3.11.

Relation between the normalized HD and SAP pore volume. SAP water was taken directly from the formulation, assuming the prediction given by the absorption coefficient of each superabsorbent. SAP air pore volume is taken from Table 3.1, by assuming that the area fraction is equivalent to the volume fraction.

3.1.6. Conclusions

More fundamental investigation is needed to characterize hydration of cement with silica fume addition. From the analysis of the previous experimental results concerning cement-silica systems in autogenous conditions, the following conclusions can be drawn:

1. In the first 28 days, hydration degree of water-entrained cement paste by superabsorbent polymers (SAP) was considerable higher than in the plain cement paste, further sustaining cement hydration. Efficiency of superabsorbent in respect with enhancing hydration of clinker compounds is higher at later ages, accentuated after 2 weeks sealed curing.
2. The addition of silica fume clearly affects the autogenous strain in high performance cement-based materials. Higher contents of silica fume in the system may have an early-age beneficial effect on autogenous deformation, which may be explained by the limitation of the pozzolanic action, being governed by the formation of calcium hydroxide from the chemical reactions of Portland cement. The threshold value should be between 15 and 30% for a SF-modified paste with w/c ratio of 0.30.
3. Plain cement pastes with water to cement ratio below 0.36 experience significant early-age shrinkage, especially in the range of 0.2 and 0.3. Self-desiccation seems to be the source of the observed deformation. Bleeding occurring in the mixtures may be masking the total deformation occurring at the bulk paste in some cases. The bleeding occurs due to presence of superplasticizer within the low water to cement ratio mixtures.
4. The expansive mechanism of bleeding requires further research. It is argued if the known detrimental effects on the strength and other hardened properties occurring due to bleeding may be preferred in respect with the deformation occurring in its absence.
5. The physical and chemical nature of the superabsorbent polymers significantly influences the mitigation efficiency of autogenous deformation in low water and low porosity cement-based materials. The polymer-pore fluid interaction is of major importance, since it controls the kinetics of sorption and desorption. This might be one of the reasons for the results obtained with polymer type A.
6. It is also concluded that superabsorbent polymers have a strong effect on the porosity of cement-based materials. The macro porosity induced in water-entrained cement-based materials may be kept to a minimum, to prevent significant strength loss. On the other hand, this may constitute the base for the use of superabsorbent polymers in other applications rather than high strength materials.

3.2. On the hydration of water-entrained cement-silica systems: Combined SEM, XRD and Thermal Analysis on cement pastes

This section is focused on the hydration of SF-modified cement-based materials with low water to cement ratio and low porosity. Hydration of the clinker compounds was followed by X-Ray diffraction (XRD), differential thermal analysis (DTA) and thermogravimetry (TG) in a plain cement paste, a SF-modified cement paste and a water-entrained SF-modified cement paste with superabsorbent polymers. In addition, the microstructure of the systems was accessed by means of SEM in order to support the findings taken from the previous methods. It is found that TG/DTA technique is preferable in respect with XRD or SEM, in order to determine the CH phase developing in the system and thus to give better indication of the pozzolanic reaction. The results from XRD analysis suggest that the calcium hydroxide may be poorly crystalline in low water and low porosity systems, even in the absence of silica fume. It is also concluded that pozzolanic activity at a moderate rate of silica to cement, in the present case being of 15% wt.-cement, is not able to fully convert the calcium hydroxide into calcium silicate hydrate during the first month of hydration in sealed conditions.

3.2.1. Theoretical

Hydration of combined Portland cement with silica fume is a topic of intensive research work. Due to the complexity of the multi-phase reactions between clinker compounds and water, the studies on hydration were often restricted to the analysis of pure substances in controlled environments[150, 151].

The phase development of Portland cement compounds may be studied by combined TG and DTA/DSC analysis[152, 153]. While the latter gives information about phase transformations by energy change with a reference standard, the first can be used to estimate hydration degree and isolate the specific quantities of CH species in the system. Studies on the differentiation of adsorbed and chemical combined water are also documented in the literature. TG/DTA profiles were used in addition to study the pozzolanic activity of mineral additions such as silica fume, fly ash and slag[154, 155]. However, these tests are usually performed in cement-based materials with relatively high water to cement ratio. The existence of insufficient water to fully hydrate the cement compounds leads to relevant uncertainties in respect with the “performance” of the silica fume addition in low water to cement ratio cement pastes. Is a sealed system cured enough for any given quantity of pure SiO_2 in the system? Is the contribution of silica fume to form additional calcium silicate hydrates efficient at any given low-water content? In practice, silica fume content is restricted to strictly low amounts, typically within 5 to 10% per gram of cement. It is stated in a number of scientific documents that above this dosage, few benefits are to be expected[15]. Thus, if all CH phase is converted in CSH hydrate, the alkaline environment would be lost, as the result of the decrease of the PH value, which is attributed to the presence of CH species[29]. On the other hand, in the case of high strength and high performance concrete, the formulation often includes higher silica to cement ratios, either to enhance pore refinement or for strengthening of the Interfacial Transition Zone (ITZ) regions[156]. Thus, the ingress of hazard substances is limited by extremely fine pore connectivity with improved durability of the material.

Furthermore, XRD technique was also used to track the development of individual clinker compounds in time. This is done by monitoring the consumption of the mineral phases as they loose their crystal nature upon hydration. For standard cement-based systems (w/c=0.50), Parrot et

al[157] have found good correlation between XRD and the non-evaporable water measurements, an indirect way to describe the degree of hydration of the system.

TG/DTA methods may be more reliable, especially in the case where small phases are present in the system and to distinguish between products with similar XRD patterns[152]. Thus, combined XRD/TG/DTA analysis may prove valuable in the comprehension of hydration phenomena. The analysis of various techniques to characterise hydration of high performance cement-based materials with mineral additions is one of the objectives of this study.

It is well known that the mineral additions show different kinetics, the nature and the particle size being of major importance in both rate and extent of secondary reactions. It follows that the pozzolanic reaction is primarily dependent from the formation of calcium hydroxide, and secondly, from the microstructure of the system, in particular from the pore network system, both being time-dependent. Ono et al[158] have conducted studies on the evaluation of the pozzolanic activity in cement pastes with silica fume addition. In a low water system with w/c=0.23 and at moderate rate of silica fume addition (10%), it is found that 50% of the CH is consumed during the first month.

However, as reported by ACI committee 234[159], the exact constituents of Portland cement and silica fume that determine the extent of pozzolanic reaction have not been well defined, although it is generally recognised that higher purity silica promotes the secondary reaction in blended systems.

In sum, if the full hydration is not attainable due to lack of water, the development of the main phases will be restricted, resulting lower pozzolanic activity by the silica fume and lower extension of the primary reactions in Portland cement hydration. The main objective of this study is to comprehend the nature of the hydration in SF-modified systems, by following the pozzolanic activity of silica fume addition in low water and low porosity systems. Since silica fume reacts with $Ca(OH)_2$, it is possible to derive the onset of pozzolanic activity by thermal analysis of the CH-phase de-hydration. By comparing the system with a plain cement paste, it may be possible to model the pozzolanic activity of silica fume for a given water to cement ratio. In addition, the effect of the addition of superabsorbent polymers on the hydration of SF-modified systems, which is poorly documented so far, is further analysed by the same means of instrumentation as for SF-modified systems. Although it is accepted that the introduction of internal curing water via superabsorbent leads to increase amount of hydrated phases, no study on the differentiation of the hydrates or on the microstructure of water-entrained cement pastes may be found. Furthermore, a method based on thermogravimetry is proposed to follow the release of water from the water-curing agent, in the present case, superabsorbent polymers added to the SF-modified system.

3.2.2. Materials

A Danish white Portland cement Type I, with a nominal strength of 52.5, was used in the study. The density was 3150 kg/m^3 with a specific surface of 3150 m^2/kg as measured by Blaine. The phase composition as determined by Bogue procedure is presented in Table 3.3.

Table 3.3: Cement phase composition by Bogue method

Cement type	C_3S	C_2S	C_3A	C_4AF	CS	CaO	Na_2O eq.:
	[wt. %]						
CEM I 52.5_DK	66.1	21.2	4.3	1.1	3.5	1.96	0.17

Silica fume (SF), was added as a dry powder at a rate of 15% of the wt. of cement. The specific surface of the silica fume is of 17.5 m^2/g, as measured by BET method. The chemical composition is the following, in wt.-%: SiO_2: 94.1, Fe_2O_3: 1.00, Al_2O_3: 0.13, MgO: 0.71, SO_3: 0.43, and Na_2O eq.: 1.09. A naphthalene-based superplasticizer was added at a rate of 1% of the wt. of cement.

Three systems are analyzed here: a plain cement paste (system P0), a cement-silica paste (system P1) and a water-entrained cement-silica paste (system P2). The basic water to cement ratio is 0.30 in all mixtures. The water-entrained system included superabsorbent polymers at a rate of 0.4%, as function of the wt. of cement, and an additional water to cement ratio of 0.05, following the equation for water-entrained cement-based materials proposed by Jensen[124]. The specimens are kept in sealed conditions at constant temperature of 20 ˚C until each curing age is achieved.

3.2.3. Methods

X-Ray Diffraction

The powder spectra were collected in a Philips Bragg-Brentano diffractometer equipped with a gas proportional detector at environmental conditions by using CuK_α radiation (λ=1.54 Å). Scanning was performed twice in different samples of the same age for each system in the range of 10 to 80 2-θº at 5 seconds in steps of 0.02 º2θ. The sample was crushed to powder and mixed with *Corundum* (Al_2O_3), which is used as internal standard. The grounded powders were loaded into a sample holder by pressing with a frosted glass side to minimise preferred orientation, which followed the collection of the diffraction pattern. The tests were performed at curing ages of: "0" (anhydrous), 1, 3, 7 and 28 days.

A previous calibration was performed to adjust the internal standard weight factor. The crystallinity of Al_2O_3, referring to the degree of structural order of the solid matter, is higher than the clinker compounds, as shown in the calibration plot (see Figure 3.12). Therefore, in order to equilibrate the peak intensities of the clinker compounds and internal standard, the selected weight ratio for the internal standard was 20% per gram of cement (anhydrous or hydrated).

Phase abundance is related to the intensity peak of each constituent[160]. For the sake of simplicity, the constitutive equation of each compound was related by individual peaks characterising each phase in the primary standard, hence:

$$\frac{m_i}{m_{Al_2O_3}} = k_i \cdot \frac{I_i}{I_{Al_2O_3}} \tag{3.6}$$

Where m_i is the mass of each phase, k_i is the coefficient taken for each linear regression of each phase and I_i is the intensity in CPS counts of the characteristic peak of each phase.

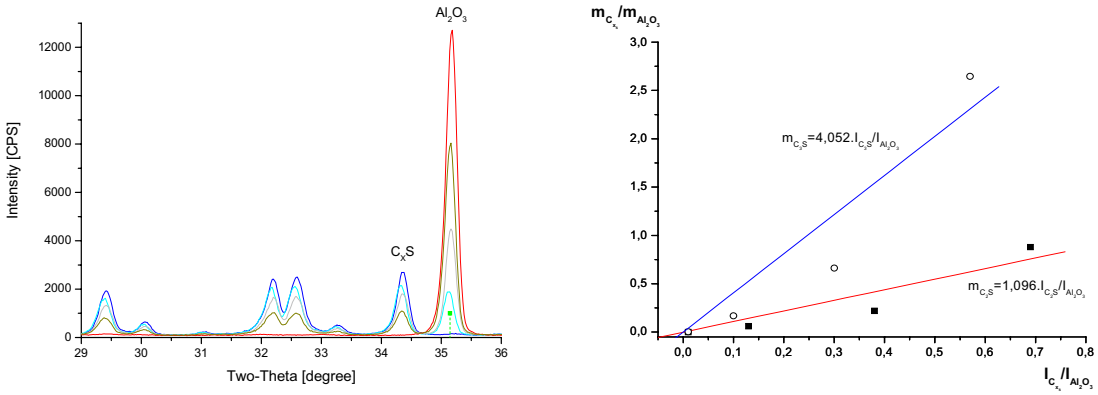

Figure 3.12. Calibration profile of the primary standard with Al_2O_3 as internal standard.

There may be considerable sources of error in this measurement technique. Adding to the standard deviation of the mean value found in each set of measurements, which was about 200 to 500, referring to CPS counts (internal standard characteristic peak at 35.14), the linear regression analysis of the data resulted in an uncertainty of more than 10%. H.G. Midgley[161] reported a coefficient of variation of 4%, by using the same principle, but he used pure substances within a sharp crystallite size. In addition, the Bogue values were used as weight reference in the calibration procedure. It is well know that this procedure can lead to a relevant degree of uncertainty[162, 163].

Differential Thermal Analysis and Thermogravimetry

TG/DTA profiles were obtained with samples from the same batches than XRD specimens in a Setaram Labsys DTA-TG/DSC. A total amount of 50 to 100 milligrams of sample is heated at 10 ºC/min up to 1050 degrees Celsius. The tests were performed in argon atmosphere at 1.5 bars. Alumina crucibles were used in the experiments. From the energy exchange with Corundum (Al_2O_3), used as internal reference, the phase transformations were recorded. The heat transfer was monitored by a thermocouple Pt/Rh with 10% Platinum. In the calculation of the calcium hydroxide content, a separate test was performed with pure $Ca(OH)_2$ to check the enthalpy of this compound. Hence, the amount of $Ca(OH)_2$ in the system was then derived from eq. (3.7).

$$Ca(OH)_2\left[wt.\%\right] = k \cdot A_{Pk^{450}} \tag{3.7}$$

Where *Ca(OH)₂* is the wt.-% of calcium hydroxide in the sample, *k* is the calibration constant of the pure compound and $A_{Pk^{450}}$ is the peak area taken from the DTA profile in µvolts. A *k*-value of 8.01×10^{-4} is found in the measurement of pure $Ca(OH)_2$, which is slightly lower than the value 8.23×10^{-4}, as found in the literature[161]. The TG method does not require any calibration procedure since the mass can be directly derived from the stoichiometry of the $Ca(OH)_2$ de-hydroxylation, hence:

$$Ca(OH)_2 \xrightarrow{450°C} CaO + H_2O \tag{3.8}$$

From the molar ratio between reactants and products of the chemical reaction, a coefficient of 4,706 is found, which may be directly applied to derive the wt.-% of the $Ca(OH)_2$ phase in the system.

Scanning electron microscope

SEM may be useful to describe the microstructure of cement-based materials, being used for a wide number of purposes, e.g. pore size distribution, geometry analysis, hydration products, degree of hydration, and other properties. The main purpose of using SEM in the present case was to characterise hydration products at early age, with focus in the morphology of phases and thus, to empower the interpretation of the results taken by the previous techniques. Therefore, the systems were studied in the first 24 hours and at 28 days. The images were acquired with several detectors in crushed and polished samples. In the later case, referring to polished samples, a backscattered electron detector was preferentially used, because it enables to differentiate hydrated from non-hydrated phases. Within the interaction of primary electrons with the nucleus of the atoms, the number of backscattered electrons increases for increasing atomic number within the elements under the backscattering, being read as a grey scale image.

The quality of the images taken by SEM is in large extent dependent from the sample preparation procedure. In the present study, samples were casted into cylindrical plastic tubes with diameter of 12 mm, from where slices were obtained. The slices were then immerged in a bath of high purity ethanol for 24 hours, in order to stop hydration by exchange of the ethanol with the free water in the sample. Prior to the impregnation procedure, the samples were vacuum-dried during additional 24 hours and then let in a desiccator with silica gel over night. In the following, samples were marked and inserted into cylindrical containers to initiate the impregnation with epoxy resin. The samples are inserted in the impregnation chamber, which is submitted to a vapour pressure of about 1 mbar during 30 min. A two-component low viscosity epoxy-based chemical is fed slowly into the sample containers submerging the samples. The system is then let to cure at atmospheric pressure and 20 ºC during 24 hours preceding the grinding/polishing stage. The grinding and polishing of the surface was performed in a fully automated Struers-ABRAMIN tabletop machine equipped with a microprocessor controller, operating at a pressure of 10 N. The samples were fixed in the sample holder with capacity for 6 samples, being previously levelled in a Uniforce Struers, in order to reduce the grinding time. The procedure consisted in a three-step grinding and a two-step polishing. Abrasive particles are used in successively finer steps to remove material from the surface, until the required result is reached. Between each step, the sample holder is emerged in ethanol for ultrasonic rinsing, to assure that ultrafine material detached from the surface during grinding or polishing is not being transferred between steps. The specifications for the grinding/polishing procedure applied in each sample are given in Table 3.4.

Table 3.4: Sample Preparation for SEM analysis

Stage	Step	Medium	Time
Grinding	MD-Piano #80	Water	½ min
	MD-Piano #600	Water	2 min
	MD-Piano #1200	Water	2 min (+2)
Polishing	MD-DAC	Suspension 3	2 min
	MD-NAP	Suspension 5	2 min

The polishing stage was performed with cloths in a wet medium by using DiaPro polycrystalline diamond suspensions. The final step was done with 1 µm diamonds on a NAP cloth for 2 minutes. Between each step, the quality of the surface was controlled in a light microscope. This ensures that the step time was adequate to remove progressive finer scratches from grinding and that surface is adequately exposed or epoxy coating-free. Figure 3.13 presents a graphical resume of the procedure.

Figure 3.13.

Sample preparation for SEM analysis.

3.2.4. Results

X-Ray Diffraction Analysis

Figure 3.14 shows the X-ray diffraction pattern of anhydrous cement, which was used in the experiments.

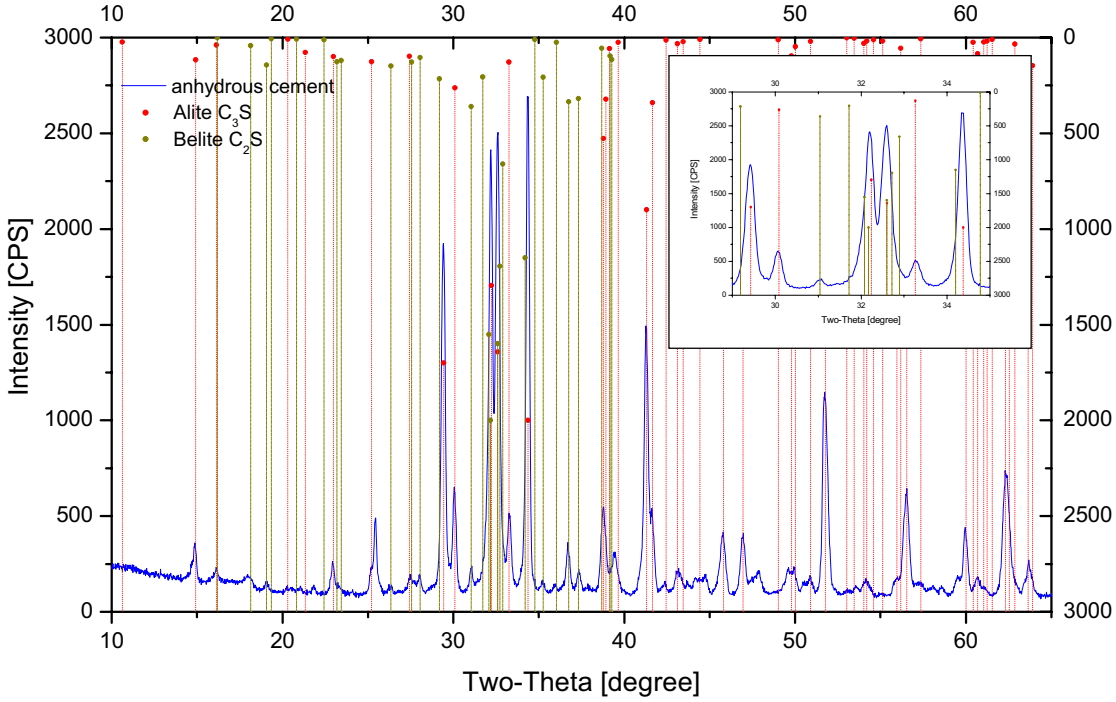

Figure 3.14.

X-ray diffraction profile of cement powder. C_3S and C_2S control files are shown in dash-lines and symbols. It can be noted the peak superposition of the main compounds of type I Portland cement.

It can be noted the existence of a considerable number of representative peaks, where C_3S and C_2S phases overlaps within the two-theta degree between 30 and 35 two-theta degrees. This induces a high degree of complexity to quantitatively describe each phase individually.

The quantities of each phase are quite difficult to obtain from the data taken, since the crystalline indexes of the each phase are not known. This might introduce a high degree of error on the specific quantities, especially on the quantification of the crystalline phase forming with the hydration of the silicate phases, e.g. calcium hydroxide. On the other hand, it is possible to think in a semi-quantitative analysis of the clinker mineral hydration, by following the evolution of each phase assuming that the individual amounts at the initial state (anhydrous cement), are equivalent to the quantities as determined by the Bogue procedure. Figure 3.15 shows the X-ray diffraction analysis of hydrating cement paste during 28 days in sealed conditions. It can be noted the evolution (consumption) of both C_3S and C_2S as hydration proceeds.

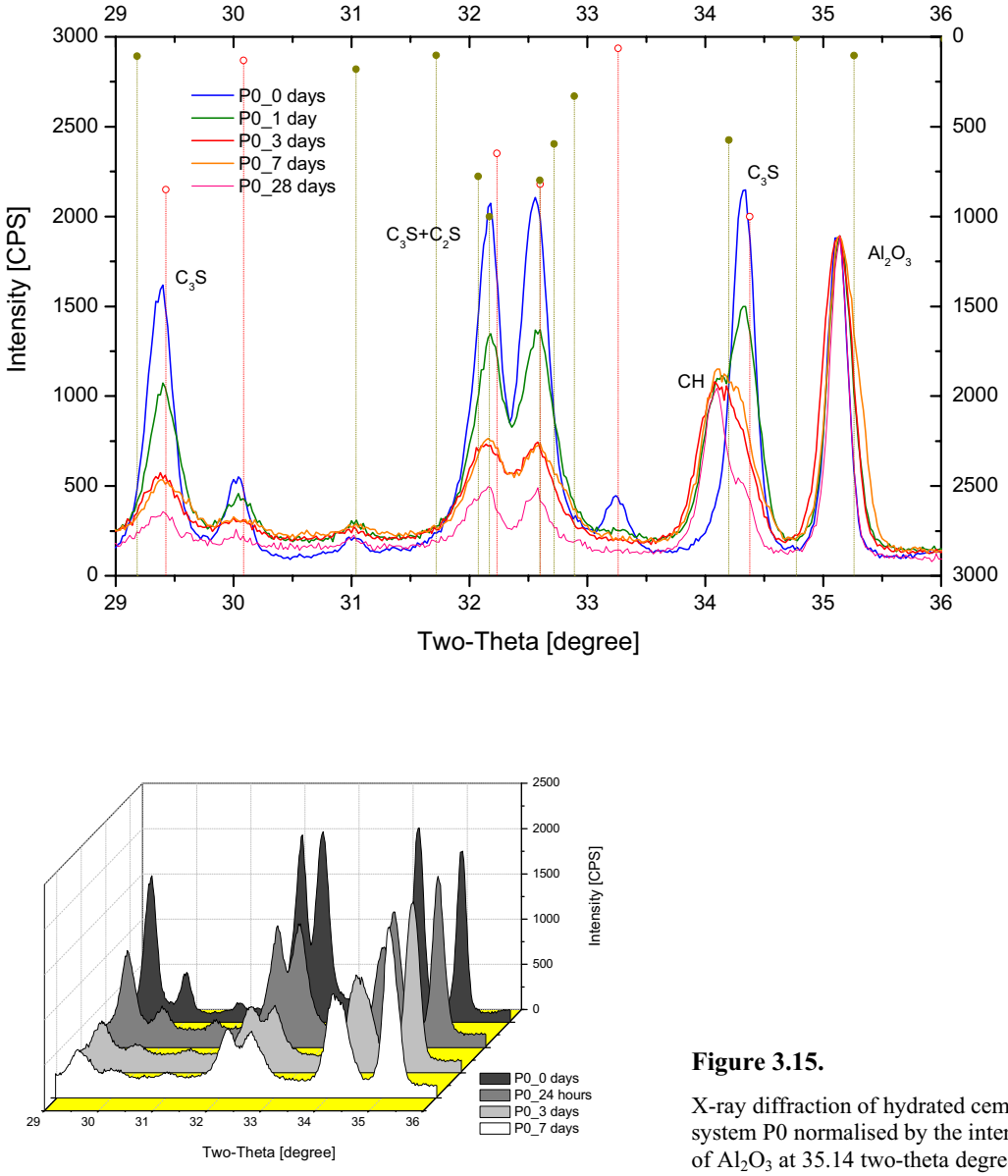

Figure 3.15.

X-ray diffraction of hydrated cement paste, system P0 normalised by the intensity peak of Al_2O_3 at 35.14 two-theta degree.

The evolution of the two main cement compounds is hampered between the first 24 hours and 3 days sealed curing, as observed by the XRD-profile from the third and seventh day. The characterising peak of C_3S is not representative of the consumption of this phase, since another peak is formed at 34.16 two-theta degree, which is related to *calcium hydroxide* formation. Therefore, is more convenient to choose the C_3S characteristic peak at 29.36 two-theta degree for monitoring the hydration of this phase. The mineral consumption versus degree of hydration of each of the major compounds of Portland cement is shown in Figure 3.16.

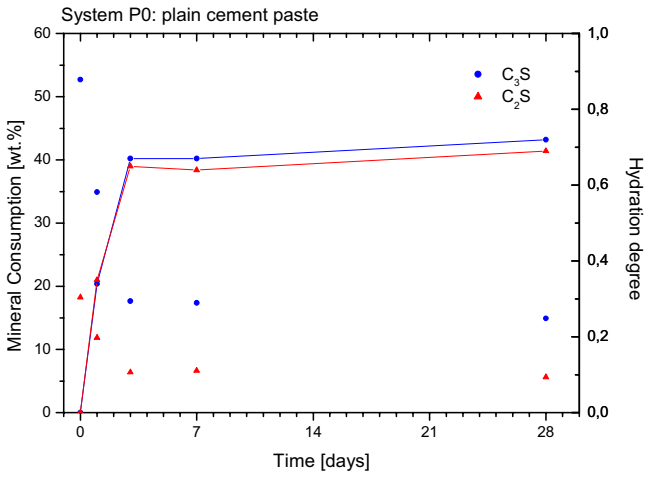

Figure 3.16.

Hydration of silicate phases in system P0-plain cement paste. The dots represent the mineral consumption and are scaled at the left. The line plus dots represent the hydration degree of each silicate phase and are scaled at the right.

According to data, the silicate phases reacted similarly within the first 3 days in sealed conditions. About 0.6% of each C_3S and C_2S is consumed per hour within this period. This rate is reduced to 0.006%/hour after the third day and up to the 28th day. A remark should be made about this point. The development of heat in the primary reaction between cement and water is often characterised by a peak occurring within the first 24 hours, as shown in isothermal calorimetry performed to the same system (see section 3.3). The time interval between 1 and 3 days discloses an interesting observation. The hydration of more than 20% of silicates in the form of C_3S or C_2S occurs without significant heat liberation. The rate of heat liberation measured in the same mixture in the same time frame is negligible in face with the total amount of heat produced during the first day or until later ages, indicating that a part of the hydration of clinker minerals may not be denoted by isothermal calorimetry.

The same procedure was applied to the cement-silica system, from where resulted the plot shown in Figure 3.17. The hydration development follows a similar trend as in the plain cement paste mixture. However, the consumption of the silicate phases occurs in higher extent, which results in a higher degree of hydration at the 28th day. This is not surprising due to the presence of silica fume, which may be promoting the hydration of Portland cement. Moreover, the consumption rates clearly differ within the time frame between the first 24 hours and the third day in sealed curing (closed system). This suggests that the system is restricted earlier to further hydrate, the rates being of 1.26%/hour during the first 24 hours and 0.12 %/hour from the later point up to the third day. By comparing the reaction rates of both systems, it is concluded that the silica fume addition accelerates the reaction rate up to the double during the first 24 hours. This is particularly important, since it sustain the idea that the silica fume addition in low porosity systems clearly enhances the kinetics at the early age hydration of Portland cement. This view was first supported

in work by Cheng-yi and Feldman[164], although an opposite view may still be found in more recent contributions.

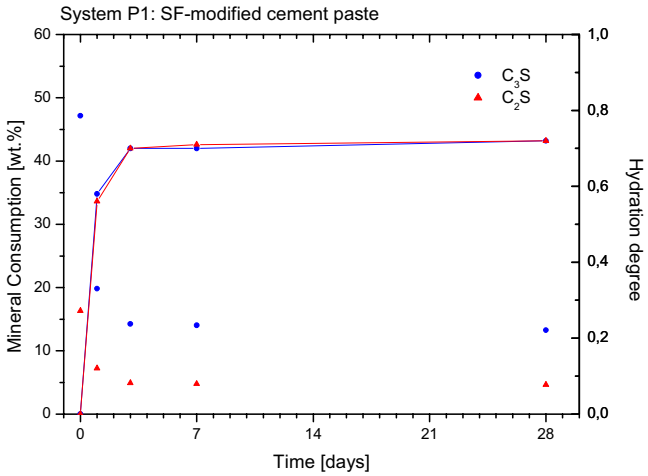

Figure 3.17.

Hydration of silicate phases in system P1-cement-silica paste. The dots represent the mineral consumption and are scaled at the left. The line plus dots represent the hydration degree of each silicate phase and are scaled at the right.

The development of calcium silicate hydrates within hydration of water-entrained cement-silica system is shown in Figure 3.18. It may be observed a higher amount of hydrated silicate phase in this system, especially in the case of the low calcium silicate. It is also apparent that the rate of hydration is enhanced in the first 24 hours, the final hydration degree being higher in respect to the SF-modified cement paste.

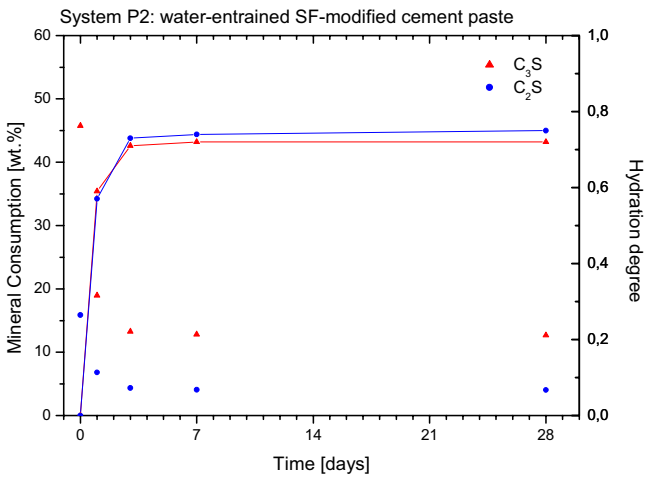

Figure 3.18.

Hydration of silicate phases in system P2-water-entreined cement-silica paste. The dots represent the mineral consumption and are scaled at the left. The line plus dots represent the hydration degree of each silicate phase and are scaled at the right.

Although, generality speaking, the results of XRD are consistent with the analyses made by TG/DTA/SEM, further argumentation will not be made here due to the uncertainty degree found in the study of hydration by this technique, especially in estimating the amount of calcium hydroxide formed within the primary reaction. The results were by far lower than the registered values of this phase by TG/DTA, suggesting that is either possible to think that a phase change occurred during the measurement or that a poorly defined crystal nature is formed in low water systems. As an example, the measured amount of CH phase at 28 days is of 10% for the plain cement paste, less

than a half of the amount found by TG or DTA technique. The same inconsistency is reported by Escalante et al[165].

TG/ DTA thermal analysis

The results from the TG/DTA tests performed to the system P0 (plain cement paste) are shown in Figure 3.19.

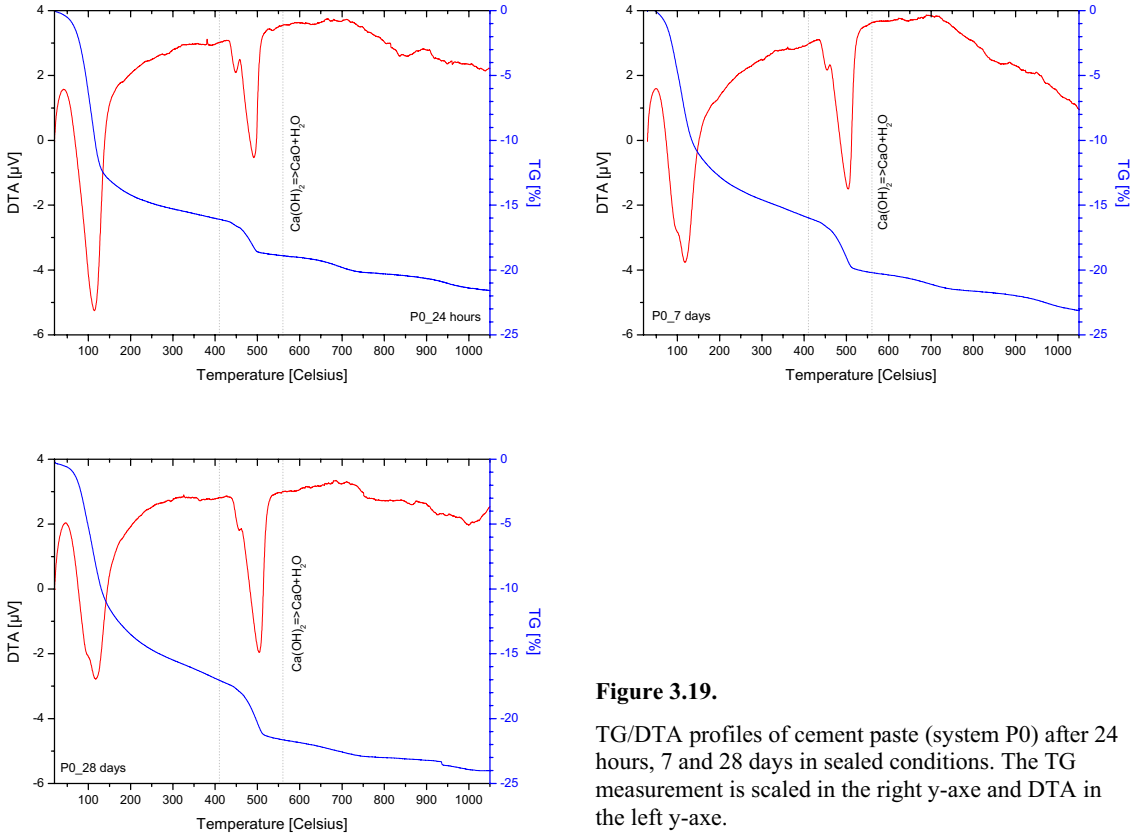

Figure 3.19.

TG/DTA profiles of cement paste (system P0) after 24 hours, 7 and 28 days in sealed conditions. The TG measurement is scaled in the right y-axe and DTA in the left y-axe.

The DTA profiles show the typical reactions occurring in the cement-based paste when subjected to temperature increase (from room temperature up to 1050 ºC). The first endothermic peak is attributed to the de-hydroxylation of CSH phase, corresponding to the mass loss on the TG profile up to 150 ºC. The main weight loss in this stage is due to the loss of weakly bind water on gel solid, which is physically adsorbed, taken at about 110 ºC. The second major peak is also endothermic and corresponds to the de-hydration of calcium hydroxide, resulting new loss of mass starting at about 410 ºC. In addition, it is noted a smaller endothermic peak, occurring at the same temperature level, which will be dealt further on this document. It is not found any other representative peak in the DTA profile, although curves present minor instability around the 800 ºC, which may be related to a minor uncontrolled carbonation of the sample.

As expected, the absolute weight loss occurring in the samples grows with the curing age. The value at the 28th day is 24% by weight. This is an indirect indication about the degree of reaction of

the main clinker compounds. The evolution of the second peak also supports that further hydration took place, as the CH phase is one of the by-products of silicate reaction with water.

Figure 3.20 show the TG/DTA thermal analysis of the cement-silica paste. The plot of the 24 hours for this system denotes a higher first peak in respect with the plain cement paste. The total weight loss is lower than the value measured for the plain cement paste, indicating that the system hydrated to smaller extent. This result is in disagreement with the XRD pattern found at the same age for this system. However, the second peak, related with the CH formation, seems slightly smaller in respect with the same peak measured for the plain cement paste.

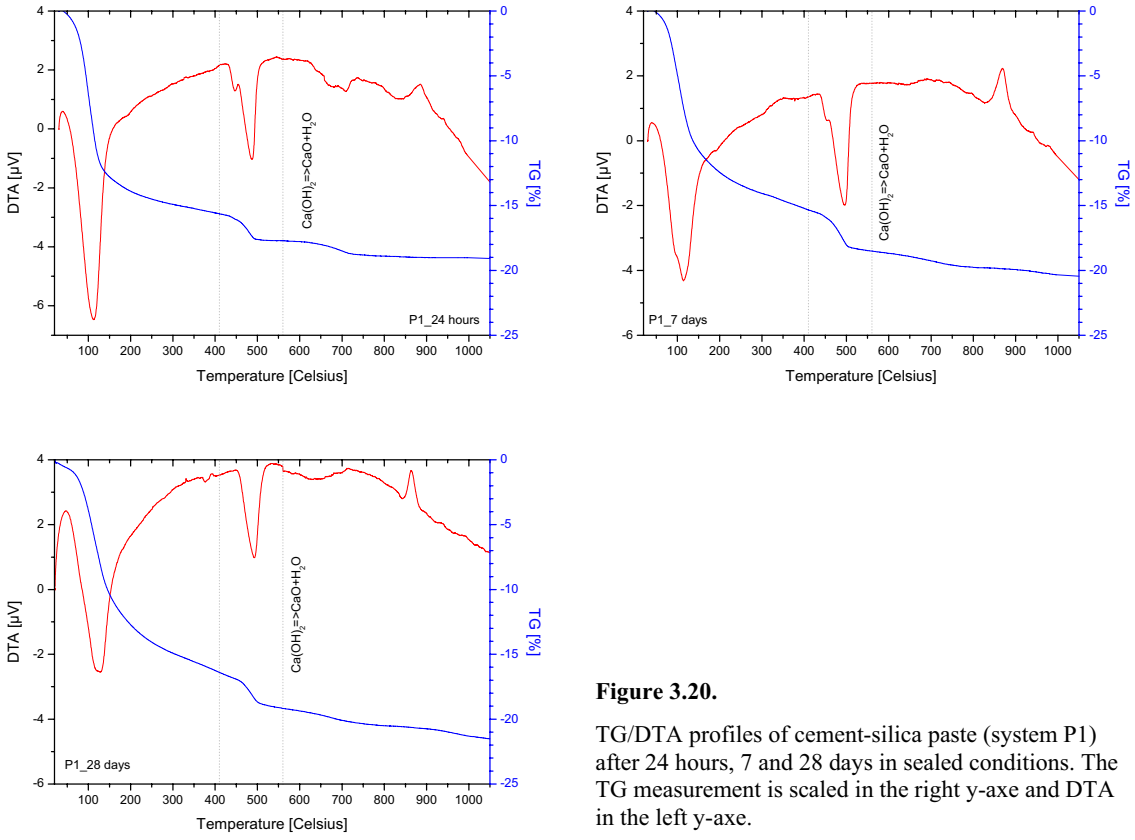

Figure 3.20.

TG/DTA profiles of cement-silica paste (system P1) after 24 hours, 7 and 28 days in sealed conditions. The TG measurement is scaled in the right y-axe and DTA in the left y-axe.

As the temperature increases towards 1000 degrees Celsius, a new exothermic peak is observed on the DTA profile, without a significant mass change. The reactions occurring at this temperature level may be related to the formation of new silicate compounds, brought out by crystallization of certain types of CSH within a specific molar ratio between the main elements present on the system, SiO_2 and CaO[166]. This occurs at a specific temperature of 900 degrees Celsius. The evolution of this peak with time suggests that the reaction is time-dependent, as function of the decrease in $Ca(OH)_2$ content. This observation may be related with the pozzolanic activity of silica fume and will be dealt further on this document.

$Ca(OH)_2$ de-hydroxylation

Calcium Hydroxide reacts with pure silica fume to further create CSH (amorphous/ poorly crystalline) phase. This secondary reaction is reported since early research work[166, 150]. The evolution of calcium hydroxide in the studied systems is shown in Figure 3.21.

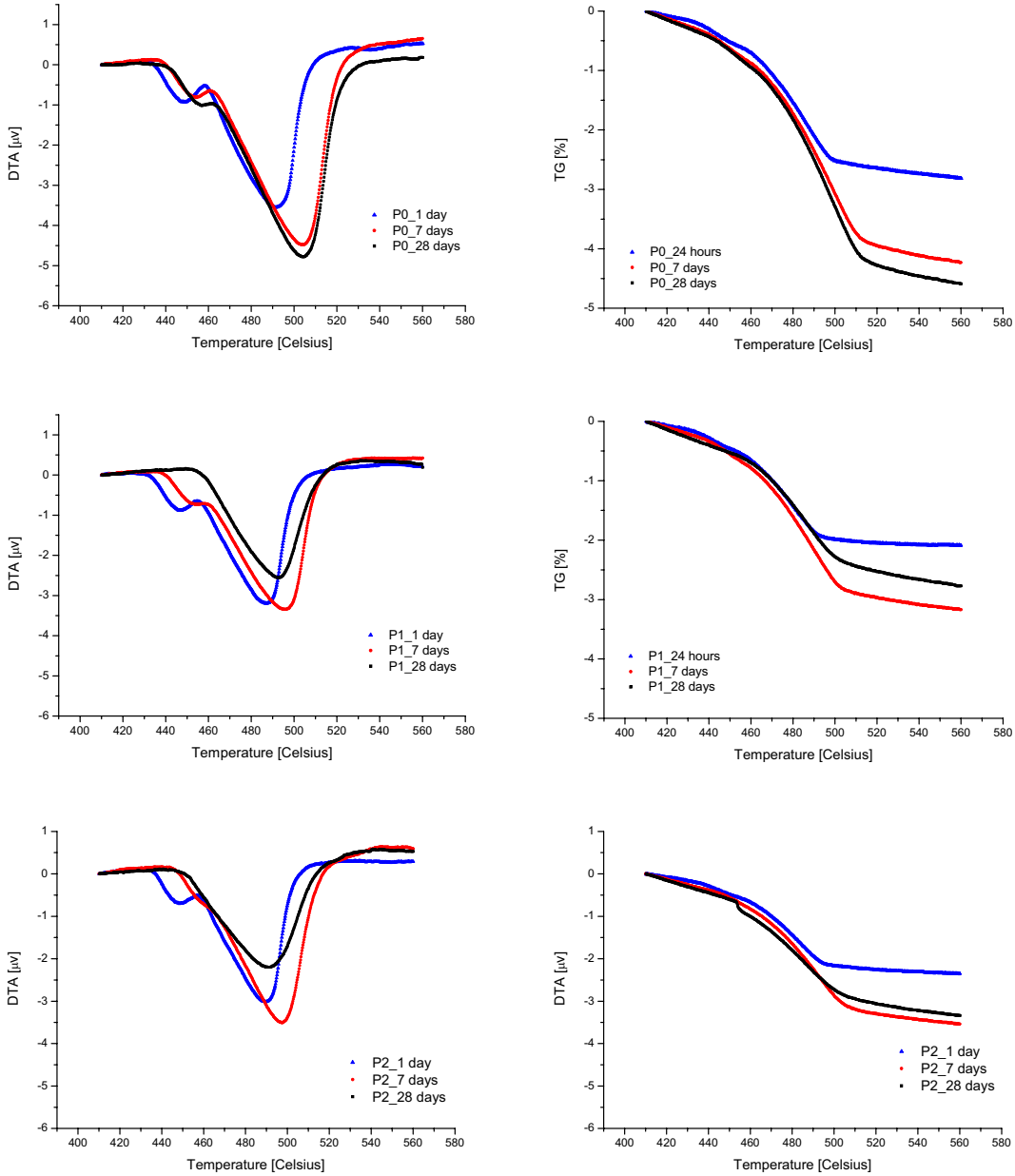

Figure 3.21.

TG/DTA profiles of cement pastes after 24 hours, 7 and 28 days in sealed conditions. The data was normalized at the temperature of 410 degrees Celsius.

The analysis of the peak areas in the DTA profiles indicate the growth of CH phase during sealed hydration. As the hydration proceeds, the peak position is translated towards higher temperature, suggesting that different enthalpies may exist for the crystallites and the phase abundance of this substance is increasing. This aspect may be related to the continuous growth of the cement compounds, which is traduced in higher energy needed for the activation of the chemical process. As noted by H.G. Midgley[161], the grain size affects the peak position of pure calcium hydroxide. The TG measurements are consistent with DTA results. The rate of CH production is maintained until the third-day sealed curing in both systems, accompanying the rate of hydration found for the CSH phases. In the case of the plain cement paste, it is registered a marked increase of $Ca(OH)_2$ species during the first week, from where no significant evolution is seen. Between seventh and the twentieth-eight day, there is a decrease in the observed species in the SF-modified systems, which indicates activity of silica fume in a secondary reaction. In particular, the initial curves of 24 hours up to 7 days in sealed hydration show representative peaks of two endothermic reactions, occurring at 460 and 490 degrees Celsius. The later was previously attributed to the de-hydroxylation of calcium hydroxide. The evolution of this peak is influenced by a weak endothermic peak, which is increasingly broader as hydration progresses. Tough, this endotherm seems to occur without significant mass loss. Thus, endotherms without mass loss are usually related with state-change phenomena. This observation was not been reported in the literature, as far as *my* knowledge can foreseen. Thus, some hypothesis may be drawn. At first glance, the first peak might have been related with poorly built connections between the fine silica fume nucleuses positioned at the surface of the $Ca(OH)_2$ crystals. This is not an option, since the event occurs in both pastes (system P0 and P1). In addition, the system is tested in argon atmosphere, which eliminates a second hypothesis, which is related with the possible de-carbonation of the hydrated compounds, the substances leaving the global system should be produced within the system components. Thus, a third possibility would be of that related with the presence naphthalene-based superplasticizer, which includes $C_{10}H_8$. Since no weight loss is thought to be associated with this reaction, it is assume that the mass change in the sample evolve only from the de-hydroxylation of $Ca(OH)_2$.

The production of calcium hydroxide in the studied systems is shown in Figure 3.22. The area calculated in the DTA-profile was taken by de-convolution between both peaks through a *Lorentz* multi-peak function, and thus, is excluding the small endothermic peak. A good correlation factor is found in both TG and DTA techniques. In the first three days of sealed curing, the variation of CH content between the systems is not significant, the registered values ranging between 15 and 17%. Thereafter, the behaviour between the plain cement paste and the systems with silica fume is opposite: the effect of silica fume is evident in reducing the amount of $Ca(OH)_2$. Although higher amount of calcium hydroxide is found in water-entrained paste, it is interesting to note that the addition of superabsorbent does not substantially influence the rate of depletion of calcium hydroxide. This is an indication of that the microstructure is not significantly altered in terms of diffusivity of the paste.

The inversion in the growth tendency of the amount of $Ca(OH)_2$ occurs within the first 3-days of sealed curing. However, this should not be seen as a complete depletion of this phase. As seen in the plain cement paste, the rate-production of crystalline CH is severely diminished after the third day as well. This may suggest that the rate of pozzolanic activity surpasses the rate-production of CH in the system. Another interesting finding is that the difference in the amount of calcium hydroxide in the systems does not vary more than about 5% at the end of 28 days, being slightly

lower in the case of the water-entrained system. If the results are normalised by weight of cement, the differences almost disappear, remaining only the inverse tendency in the rate-production of CH phase.

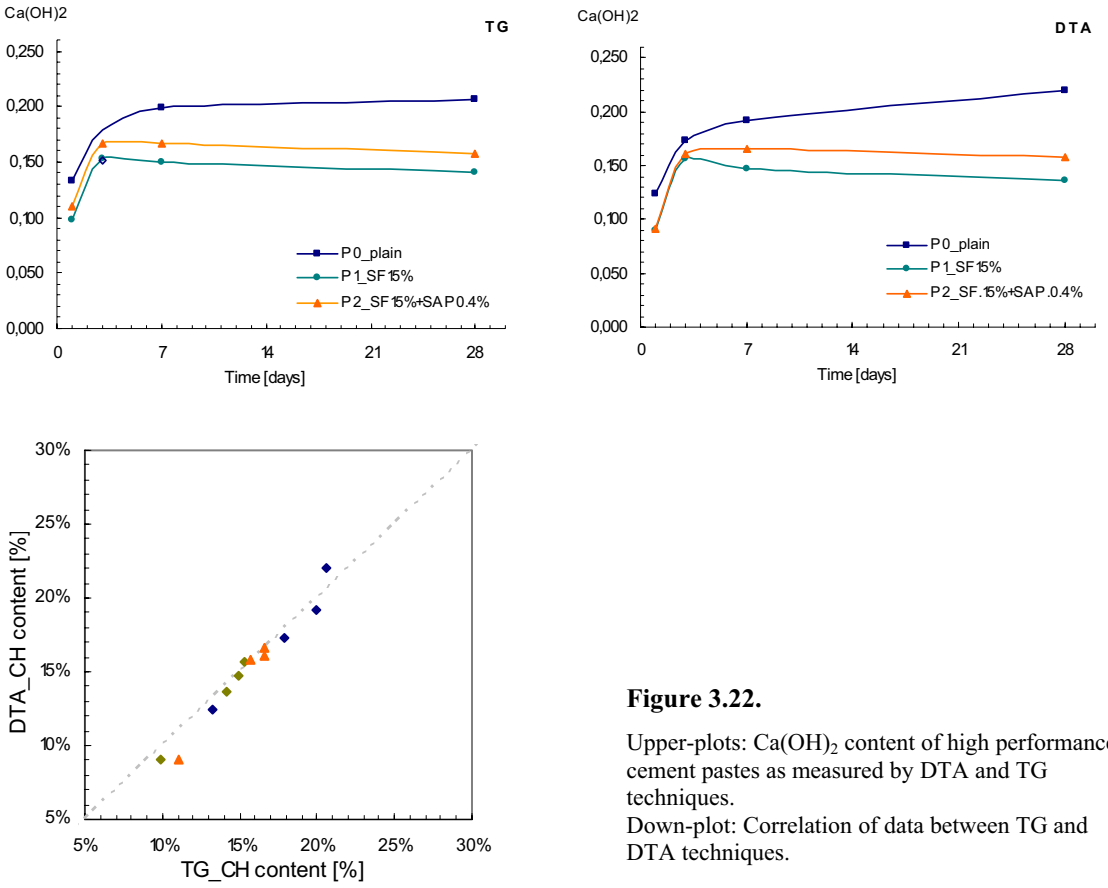

Figure 3.22.

Upper-plots: $Ca(OH)_2$ content of high performance cement pastes as measured by DTA and TG techniques.
Down-plot: Correlation of data between TG and DTA techniques.

Crystallisation of SiO_2-CaO following CSH de-hydroxylation

In the section dedicated to DTA analysis, it was suggested a degree of crystallization between Ca and Si to explain the exothermic peak denoted at the end of the DTA-profile (at about 900 degrees Celsius). It is observed that this peak is growing with the curing age.

H.F.W. Taylor[22] supported the idea of that of different types of CSH co-existing in cement-based systems. In his work, it is proposed that the type of CSH may be differentiated by the C/S ratio. Accordingly, a higher C/S shall be preferably found in a cement-based reaction and a low C/S ratio in the secondary reactions, viz. pozzolan-based reaction[150].

Figure 3.23 shows the evolution of $CaO\text{-}Si_2O$ crystallization with time in the SF-modified cement paste, as obtained by baseline-subtraction of the DTA-profiles shown previously. The area of peak measured at 24 hours hydration is considerably lower in respect with the measured values at the subsequent testing ages, the peak position shifting by 20 Celsius with curing age. This may be explained by different crystallite sizes within the sample preparation procedure or the growth

nature of this phase related with the state of equilibrium of the structural units within the amorphous phase that leads to higher delay in the heat response by the reactants when subjected to the heat ramp, or a combination of both, the late assumption being more probable.

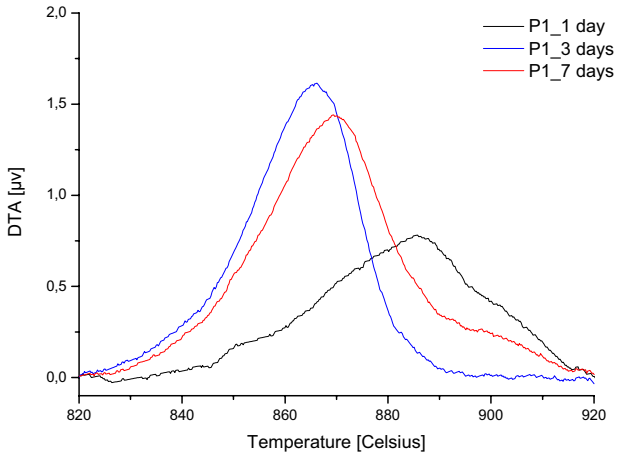

Figure 3.23.

Crystallization of calcium and silica to form crystalline C_2S from the CSH-type I phase at about 900 degrees Celsius.

The assumption of crystallisation occurring upon decomposition of the CSH-type I at the DTA peak at 900 was further confirmed by XRD testing on the burned sample. It is registered higher amount of *larnite* within a highly amorphous material, in respect with the non-burned sample at the same curing age.

It should be mentioned that the source reactants of the reaction may be found within two events occurring when the sample is subjected to the temperature ramp. The first event is related with the de-hydroxylation of calcium hydroxide into free calcium oxide, which is known to be highly reactive since it shows poor stability. It follows that the free CaO may react with remaining SiO_2, which have not been dissolved or reacted at the instant *t*. A second possibility is connected with the de-hydration of CSH to form physically-bound CS. It is known that the crystallization in the C-S system requires a given energy and a specific C/S ratio, to which corresponds a different nature of crystalline C_xS, as defined by *x*. Since the type of CSH formed in the secondary reaction may be poor in *calcium*, the energy and time, viz. power needed to decompose the system C-S-H is lower, in respect with calcium-rich CSH structures. According to the ratio between both reactants, the product may be more or less rich is calcium, in the present case, it seems that the major product forming is *larnite*, as shown by XRD analysis. In comparison, El-Enein et al[166] suggested Wollastonite ($CaSiO_3$) forming at 900 ºC. This is seen in pure lime-silica pastes.

Scanning electron microscopy

The microstructure of the systems was analysed in the three systems over fracture and polished surfaces. It is found high homogeneity of phases at the microscopic level. However, the observation of the samples at the nanometer scale discloses fine crystalline material within the amorphous CSH. In the first set of images, referring to Figure 3.24 and Figure 3.25, sub-microscopic fractured surface of SF-modified paste and water-entrained SF-modified cement paste is shown. The occurrence of crystalline heterogeneities is seen mainly in entrapped air voids or in large capillary space, where precipitation of crystals is favoured.

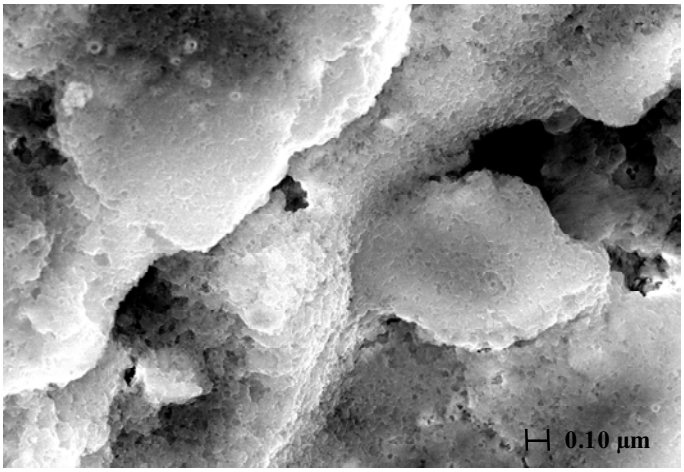

a)

Spatial network of cement gel involving cores of non-hydrated clinker minerals. Curing age is 24 hours.

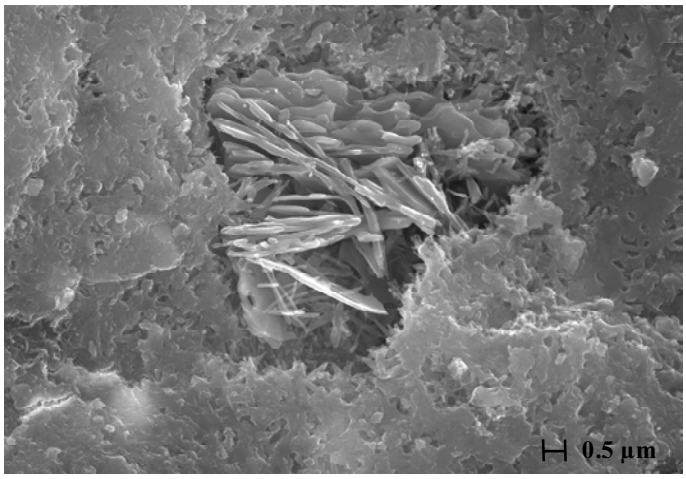

b)

Fine fold-like crystals filling an air void enclosed by hydrated solid gel. It is seen that the crystal grows in a large space, forming a low density region, in respect with the surrounding CSH. Curing age is 24 hours.

Figure 3.24

Crushed surface of SF-modified cement paste with w/c=0.30 and s/c=0.15. The system is highly homogeneous material gel.

It is interesting to note that the growth of crystalline phases may occur in three different locations: in the pore network structure within other hydration products, in trapped air-voids left upon mixing or in SAP pores upon empty of the SAP-water, the latter being only possible in the case of water-entrained systems. Figure 3.25 (b) shows a typical macro-inclusion left by a particle of superabsorbent polymer, in this case the resultant macro-inclusion having 300 µm in diameter. The diameter of SAP-particles may be of considerable size, lying at three to four orders of magnitude from the average size of a capillary pore. However, a water-entrained system may have controlled

macro porosity, by selecting the range of particles to be introduced in the system. Several SAP macropores revealed growing of products with non-standard shapes and composition. This subject, being out of scope, is to be studied further.

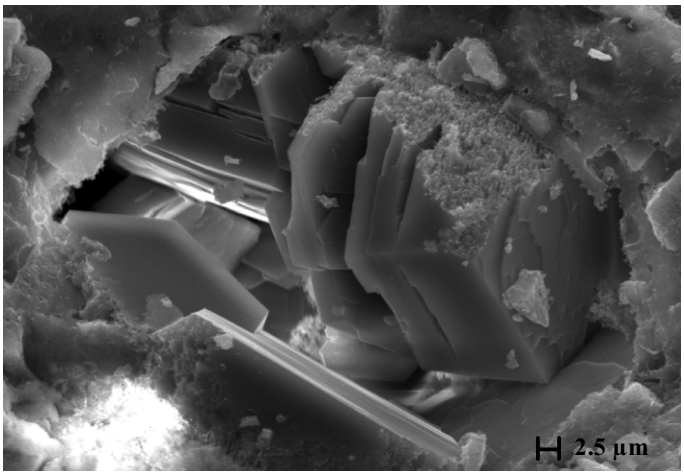

a)

Hexagonal crystals (CH) filling an air void or pore network system, enclosed by hydrated solid gel. It is seen that the crystal is well-connected through surrounding solid gel. Curing age is 24 hours.

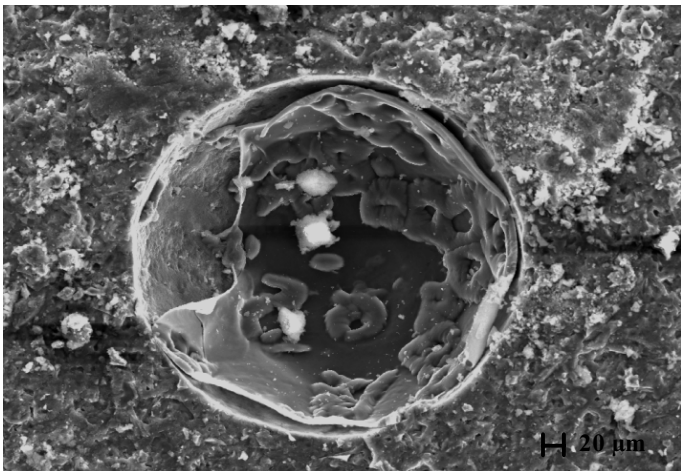

b)

Macro-inclusion left by superabsorbent polymer particle upon hardening, The diameter of the macro pore is of 300 µm. Curing age is 24 hours.

Figure 3.25

Crushed surface of water-entrained SF-modified cement paste with w/c=0.30 and s/c=0.15. The system is highly homogeneous material gel comprising SAP inclusions.

In Figure 3.26, crushed versus polished surface is shown for a plain cement paste. Despite the crack opening upon fracture, the systems show high homogeneity of phases at the microscopic scale. Therefore, only polished samples will be analysed further.

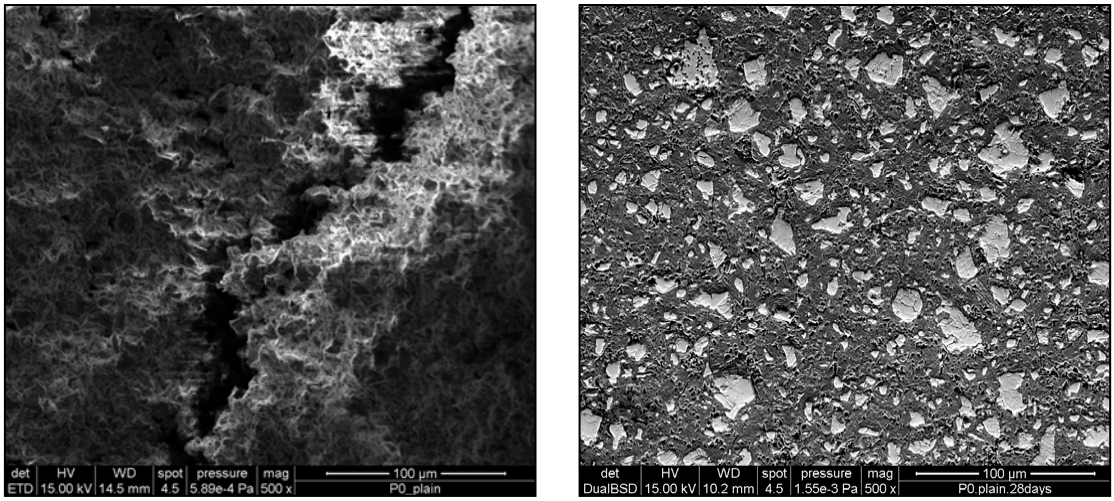

Figure 3.26

Crushed surface versus polished surface of plain cement paste with w/c=0.30. The system is highly homogeneous material gel, often showing entrapped air pores. The microcrack propagating in the paste at the left-bottom image is due to exposure to high-vacuum in SEM.

In the second set of images (Figure 3.27), comparison between plain cement paste and water-entrained SF-modified paste is made. At low magnification (first row) it is apparent the different pore structure of the water-entrained pastes, while differentiation at the higher magnification (last row) discloses the effect of the silica fume addition in the pore structure of SF-modified pastes, this being significantly denser in respect with the plain cement paste. At this ratio of water to cement, the systems are highly homogenous and do not show a well defined capillary pore network. Moreover, a quantitative approach to differentiate CSH and CH phases is extremely difficult, even tough different thresholds in the gray scale were applied. According to Karen Scrivener[167], different threshold values when grey scaling CSH and CH phases may be applied to differentiate these phases. This is not apparent in the present study, although slight changes in the grey scale appearing at higher magnifications indicate the present of multi-phase within the gel solid. Furthermore, as pointed out by Mouret et al[168], the non-hydrated cement grains may be easily quantified at medium magnifications, i.e. 200x, the number of fields being concomitant with well-known statistical laws. Thus, both qualitative and quantitative differentiation between non-hydrated cement particles, gel solid and macro porosity may be performed. However, in the present study, only qualitative information will be disseminated. Even in the absence of silica fume, the system shows poor connectivity in the pore structure. In the case of the water-entrained mixture, being micro-structurally equivalent to the SF-modified paste, the pores appear completely isolated, sustaining that the pore network is not connected at all. The pore volume, deduced from the darker areas is significantly higher in the absence of silica fume, leading to the conclusion of that the addition of both silica fume and superabsorbent polymers dramatically affects the pore structure of the cement paste, the silica fume reducing the capillary porosity and the superabsorbent affecting the magnitude of the macro porosity.

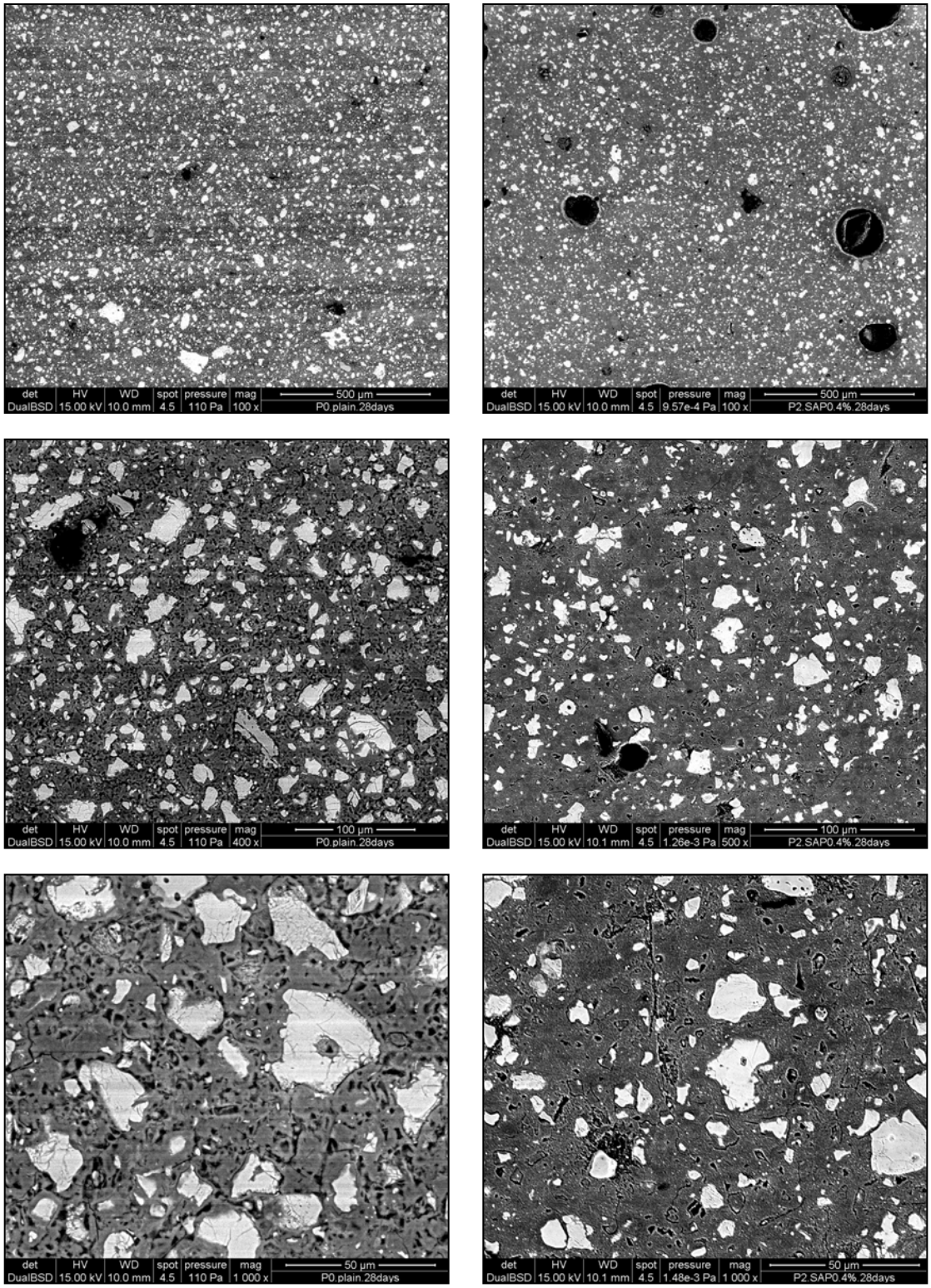

Figure 3.27

Polished surfaces of plain cement paste (system P0) versus water-entrained SF-modified paste (system P2) as taken by SEM.

Igarashi et al[169], by combining SEM analysis with the Powers model, were able to differentiate the macro from micro porosity. For a cement paste with w/c ratio of 0.40, the macro porosity, defined as the specific volume including pores bigger than 0.2 μm in diameter, is higher when silica fume is added to the system. Contradicting results are deduced from the observations performed in the cement pastes at higher magnifications, both micro and macro porosity being significantly reduced due to the presence of silica fume. This view is supported in references [170, 171], by using SEM and TEM techniques.

A third set of images is given in Figure 3.28, where the time parameter and the influence of the detector in the image acquisition are taken into account in the analysis. At 24 hours, the microstructure of SF-modified pastes is mainly constituted by non-hydrated cement cores and gel-like paste. It is also seen that porosity is mainly constituted by isolated pores with poor connectivity, suggesting that the system may be de-percolated at very early age (prior to the first day hydration). This view, although not well-recognised by the research community, is consistent with previous work by Dale P. Bentz[172, 132].

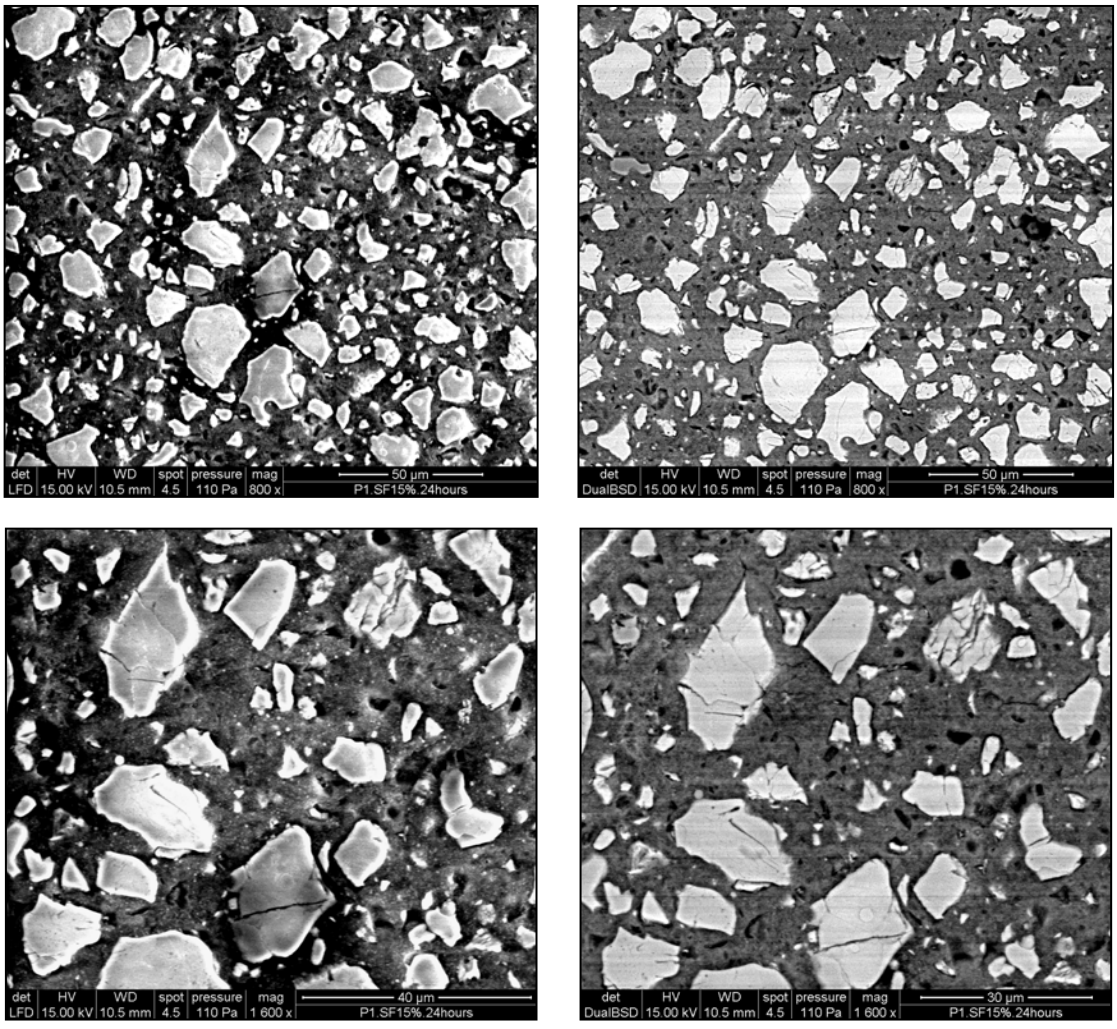

Figure 3.28

SF-modified cement paste as seen by SEM with two detectors. Bottom: left-images taken by LFD detector, using primary electrons; right. Image taken by BSD detector, using backscattered electrons.

Moreover, the variation in the detector used to capture the microstructure discloses an interesting observation. The regions surrounding the non-hydrated cement grains appear partially dark when LFD is used as detector. Inversely, when the image is capture via *backscattering*, the same regions appear in gray, resulting a reading of gel solid instead of a surface-depression, i.e. slit-pore. This may be producing measurement artefacts, resulting in systematic error in the real pore volume of the system. In either case, both the pore structure and transport properties of the systems require a more systematic investigation. In respect with the time parameter, it is appreciable the difference in the amount of non-hydrated cores in the course of hydration. There are clear differences between the second and third set of images when accessing the white-area fraction of the plain cement paste and SF-modified cement pastes.

3.2.5. Hydration model of cement-silica systems: including water-entrainment

Hydration is defined as the reaction of water and clinker minerals into hydrated phases. In the case of XRD, hydration degree of the clinker minerals is derived directly from the mineral consumption. However, this technique may be overestimating the quantities of minerals that have been effectively consumed, as the non-hydrated cores may be covered with CSH forming at the core-surface and thus, affecting the real reading of crystalline material. SEM technique may be also used to follow the development of the amount of non-hydrated cement. Despite the intrinsic measurement artefacts, the previous techniques have the advantage of following directly the existence of non-hydrated material. However, hydration of Portland cement is more often expressed by the ratio between the water of constitution at time t and an infinite value, which corresponds to the maximum value of water-reacted to complete the hydration of clinker compounds. The clinker compounds may achieve complete hydration when the chemically bound water, meaning that no hydrates may further be formed, equals the values presented in eq. (3.9), as taken from the literature[173, 148].

$$w_n = \begin{cases} C_3S = 0.24\,g/g \\ C_2S = 0.22\,g/g \\ C_3A = 0.40\,g/g \\ C_4AF = 0.16\,g/g \end{cases} \tag{3.9}$$

The later may be combined with the chemical formula of cement to derive the infinite value of water of constitution, as defined by eq. (3.10), where w_i represent the individual water-combined amounts, the clinker compounds appearing as weight percentage.

$$W_n = w_1(C_3S) + w_2(C_2S) + w_3(C_3A) + w_4(C_4AF) \tag{3.10}$$

By equating the values from Bogue analysis given in Table 3.3, a global maximum value of 0.224 g/g is found. The water-combined values in time may be easily determined by any of techniques referred previously.

In the case of blended cement-based systems comprising mineral additions, the previous equations need to be re-arranged to include the fraction resolving the pozzolanic activity, which requires the knowledge of the time-dependent amounts of both silica fume reacted and calcium hydroxide

formed. Thus, either SEM or XRD techniques may be not so straightforward to isolate the pozzolanic activity by silica fume as TG/DTA.

The activity of a pozzolan may be defined by the stoichiometry of the chemical reaction with $Ca(OH)_2$, which takes the general form translated by eq. (3.11).

$$x \cdot S + y \cdot CH + z \cdot H \rightarrow C_y S_x H_{y+z} \tag{3.11}$$

It arise a first problem in balancing the previous equation, which is to know the ratio C/S in the hydrated structure of the CSH_{SF} phase. According to El-Shimy[150], this ratio may be about the unit for low molar ratios between lime and silica. In this respect, it is further referred the work by Burkes[174], who showed by means of XRD that the main product of hydration between the pure substances consists mainly in CSH type I. It follows a second uncertainty, which is connected with the amount of water that is being consumed in the reaction. According to Sellevold[36] and also Papadakis[175], the amount of water bound in the CSH_{SF} is to be found the same as the water present in the CH phase. Figure 3.29 shows the calculation of water bound to CSH in the systems, as found by subtracting the water bound to CH in each system. It is found that the water bound per gram of cement is higher in the presence of SF, which means that additional water is to be bound to the CSH formed in the secondary reaction. This is also supported in experiments by Diamond[176] and also by Bentz et al[132]. Thus, both the effects of silica fume and superabsorbent polymer addition are clearly indicating an increase in the amount of water bound per gram of anhydrous cement. It is also clear the course of pozzolanic activity due to the presence of both SF and SAP. In the case of system P2, the pozzolanic activity seems to cease earlier in respect with the SF-modified cement paste. This is an indication of that the water of the superabsorbent is mainly active during the first three days in sealed conditions.

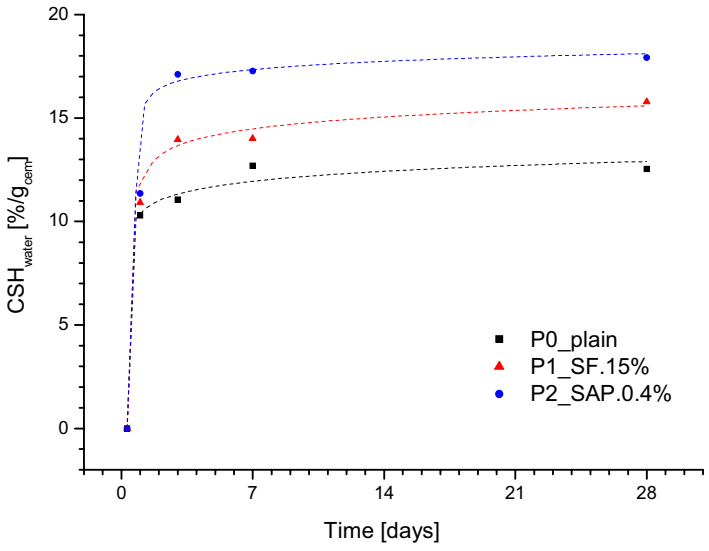

Figure 3.29.

CSH water in the studied systems, as found by TG method. The dashed lines corresponds a three-parameter approximation by a logarithmic function of the type $y = a - b \cdot \ln(x + c)$

The pozzolanic activity may be derived from the ratio between the rate of binding water occurring in the SF-modified systems and the rate of binding water in the plain cement paste, which may be obtained by derivation of each CSH_{water} content as function of time, according to eq. (3.12).

$$\alpha_{pozz} = \frac{\frac{dCSH_{water}^{Cem+SF}}{dt}}{\frac{dCSH_{water}^{Cem}}{dt}} \tag{3.12}$$

This is done in alternative to assume an ultimate value of water consumed by gram of silica fume, as shown in Figure 3.30. It may be seen that the pozzolanic activity of water-entrained system is significantly different from that of the SF-modified paste. The interpretation of the water-entrained curve is not simple, since the introduction of additional water may be promoting both first and secondary reactions. Therefore, the rate of addition bound-water may be not solely due to the activity of SF, but also due to hydration of clinker minerals. The term internal curing activity should be introduced in alternative to the term pozzolanic activity in this case.

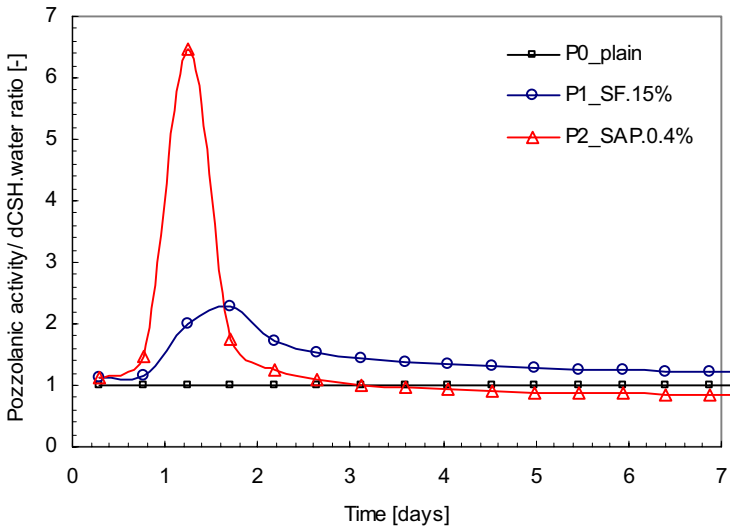

Figure 3.30.

Pozzolanic activity of SF-modified paste and internal curing activity of water-entrained SF-modified paste, based on the knowledge of bound-water from the correspondent cement paste, according to eq. (3.12).

In either case, the relative rate of reaction correspondent to the development of additional bind water in the water-entrained paste seems to happen very fast in respect with the SF-modified paste, the later appearing at a later time and taking a longer period, in relation with the plain cement paste. A factor of 6.5 is found for this acceleratory period in the water-entrained system within the second 48 hours. It may be that the internal curing activity is promoting the consumption of SF in the system, leading to additional hydrated material, and thus, affecting the diffusivity of the system with concomitant reduction in additional hydration beyond the third-day, but at the present, this is just a speculation that, not being well-supported, requires further evaluation. The introduction of 15% of SF also results in an increased relative rate of hydration with a factor of 2 in respect with the rate of hydration expressed by the plain cement paste. The de-acceleratory period may be indicating the onset of a diffusion-controlled reaction, which remains persistently during the whole period of hydration. This is consistent with the perception by Yogendran et al[151], even though silica fume is introduced as cement substitution and not as an addition, leading to a different w/c ratio. On the other hand, this approach leads systematically to lower values of chemical combined water.

The knowledge of the water-bound to hydrates may be use in addition with the purpose of characterising the full hydration of blended systems, by assuming that the stoichiometric parameters in eq. (3.11) are equal to the values presented in eq. (3.13), as taken from the literature.

$$\begin{cases} x = 1.1 \\ y = 1.0 \\ z = 2.8 \end{cases} \tag{3.13}$$

By computing the initial quantities of phases present in the system, it is possible to describe the consumption of silica fume and the development of CSH type one, as presented in Figure 3.31.

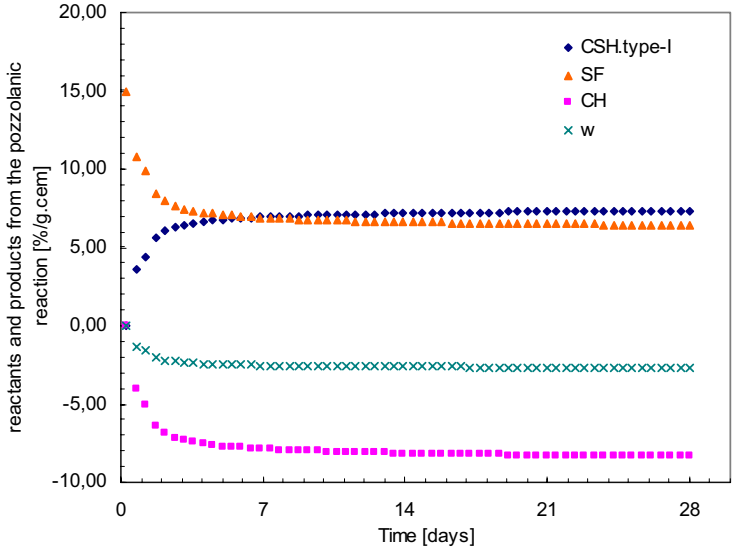

Figure 3.31.

Pozzolanic activity in SF-modified systems, described by SF-reacted, CH and water consumption and the development of CSH-type I (reaction product).

It may be seen that about 8% of the total silica fume is consumed in the production of about 7% calcium silicate hydrate (type I), the water being given by the difference in the bound water of SF-modified paste and the water bound in the plain cement paste. It is concluded that in low water and low porosity systems, the pozzolanic activity may not be completed at the 28th day of sealed hardening, and the full consumption of silica fume is physically impossible due to lack of water to sustain either the first reaction and especially the secondary reaction. This may be why the hydration is hampered as early as the 1st 24 hours and, in the case of the pozzolan, at the 3rd day of sealed hardening, the diffusivity of the system playing a major role.

This approach is obviously empirical-oriented and is based on the knowledge of the water bound per gram of cement in the systems. Pane and Hansen[177] have proposed a hydration model for blended systems, which is based on the knowledge of the ultimate value of non-evaporable water. For a SF-modified paste with s/c ratio of 0.10 and a w/c ratio of 0.385, the infinite value of non-evaporable water per gram of binder is of 0.256. However, it is noted that the basic assumptions are not physically meaningful to describe the pozzolanic activity. For example, the model predicts that only 20% of the silica fume reacted at the age of 4 days, which is in disagreement with the well-established idea of that most of the secondary reaction happens in the first three days. A more consistent and comprehensive approach is found in the work by Yajun and Cahyadi[178]. By assuming that the pozzolanic reaction of silica fume follows the equation based on the

stoichiometry of the reaction, as proposed by Bentz et al[132], they were able to describe theoretically the pozzolanic activity as a diffusion controlled reaction, being expressed by Jander equation, which in addition, is a well-known equation to describe the reaction of tri-calcium silicate C_3S, as referred by Ivan Odler[179]. A good theoretical review in chemical reaction engineering that may be used to approach this particular problem, is given by Octave Levenspiel[180]. Accordingly, in diffusion controlled reactions with changing core in the particle, the rate of reaction is governed by the particle size and the chemical potential of the medium, in this case, being the pore fluid. The basic assumption in the approach by Yajun and Cahyadi[178] is based in work by Bonen and Diamond[181], who have found that the penetration depth of pozzolanic CSH with 35 to 80 µm, due to the dissolution and subsequent reaction with dissolved cations from calcium hydroxide, is within 20 µm, with the C/S molar ratio decreasing towards the centre of the core (agglomeration of silica fume particles), which was seen to remain Ca-free after 1-year. However, one of the limitations of this approach is that the pozzolanic activity is mainly depending on the reaction rate constant and the existence of calcium hydroxide produced in the first reaction. This may not be the case in the system evaluated here, the existence of insufficient water, the pore structure and diffusivity of the system, playing a central role in the course of the pozzolanic reaction. Although an approach of this kind would be preferable, at the present it does not seems feasible to be applied further, due to lack in information of the above parameters. For the purpose of the present investigation, it seems sufficient to conclude about the effect of both silica fume addition and superabsorbent polymers in the course of hydration.

3.2.6. Method for evaluating SAP_{water} consumption

As seen in the preceding sections, the introduction of superabsorbent polymers had a significant effect on both rate and extent of hydration. At early-age, the additional water present in the superabsorbent was effective in enhancing both primary and secondary reactions. It is possible to calculate the SAP water content, by comparing the evaporable water in entrained and non-entrained systems. In Figure 3.32, it is exemplified the procedure to derive the water in the superabsorbent at each instant *t*, as taken from the thermogravimetry measurements. It is assumed that both the water present in the superabsorbent and physically-bound water leaves the system at 110 ºC.

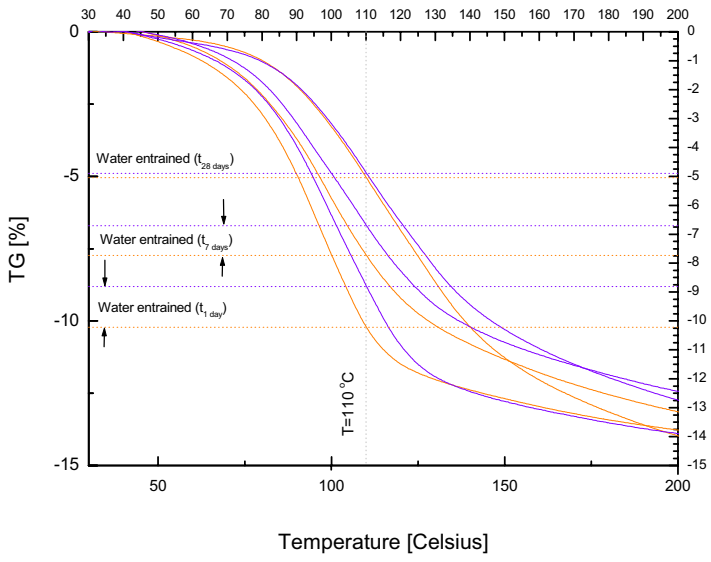

Figure 3.32.

Graphical solution for quantifying SAP_{water} as function of time (*t*).

It is apparent that as hydration proceeds, SAP_{water} is being consumed, by observing the decrease of the difference between the evaporable water in the water-entrained and SF-modified cement pastes.

Thus, by assuming that the initial state of the water complies with the predicted absorption proposed by Jensen[124], the full profile of the water that is effectively consumed in the hydration reactions may be obtained, as shown in Figure 3.33. It may be seen that the water present in the SAP particles is mostly used-up during the first 24 hours. This is not surprising, since it coincide with the primary reaction, and thus with the most part of the chemical shrinkage of the system. More than 50% of the water-entrained is consumed during this period and about 70% is registered at the end of the 7th day. The different rate of water desorption seems natural, since after the hardening period, the process of water transport should be diffusion-controlled, and, as stated previously, the additional hydrates may present increasingly difficulties translated by fewer connected water paths.

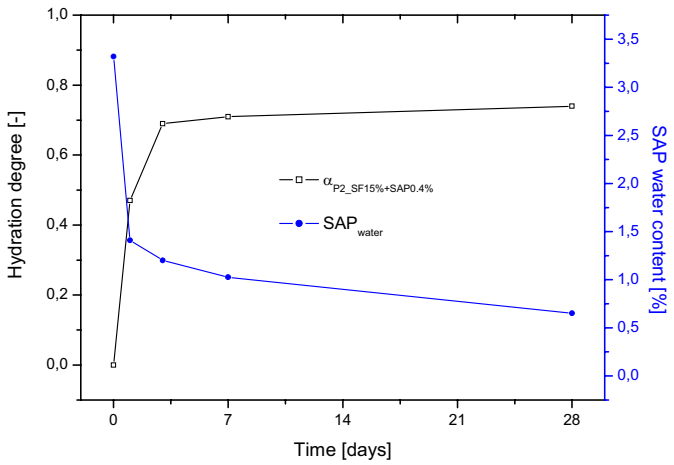

Figure 3.33.

Hydration degree of water-entrained system versus the water present in the superabsorbent as function of time. The water content at time 0 was taken directly from the formulation.

Nevertheless, is also observed that nearly the full amount of water is being used, by looking to the value of the twentieth eighth day. A remark should be made about this observation. It is apparent that the hydration degree is higher when additional water is present in the cross-linked structure of superabsorbent. It seems logic that the additional water should contribute to both primary and secondary reactions. On the other hand, the water consumption from the third day forward is not traduced in additional secondary reaction. It may be that the more stable nature of CSH with curing time corresponds to higher binding forces influencing the removal of additional water in the superabsorbent. Figure 3.33 is built on the basis of two reference temperatures, which are commonly used to differentiate evaporable water and non-evaporable water by different volatile behaviour. It may be that higher energy is needed to remove water with low-volatile capacity in more matured pastes. In fact, the selection of a constant temperature independently of the response from the system is a highly arbitrary simplification for highly complex systems, and thus should be corrected in future work.

3.2.7. Conclusions and Final remarks

Hydration of cement-silica systems comprises highly complex phenomena at the microscopic scale. An approach to isolate the pozzolanic activity by silica fume was tried, based on the differentiation of CH and CSH phases through thermogravimetric measurements. In the present study, only qualitative information was possible to take from the measurements of three pastes having distinct nature. However, some important conclusions may be outlined:

1. Techniques

Fours techniques were used to describe hydration of the studied systems. TG/DTA technique should be preferably applied to describe the pozzolanic activity of silica fume. In addition, it may be used to differentiate the consumption of SAP-water. A good correlation was obtained by TG and DTA methods on quantifying the CH present in the system. On the other hand, these show to be poorly correlated with the XRD technique, which may be underestimating the production of calcium hydroxide due to limitations in identifying poor or hindered crystalline phases. SEM technique may be preferably used to describe the pore structure of low water and low porosity systems. In addition, SEM showed poor potential in differentiating hydrated phases. This difficulty is connected with the physical structure of low water systems, which may be hindering sub-microscopic and poorly developed crystal phases. However, the preparation of the samples may be enhanced to overcome this problem, for example by sputtering techniques. A gold coating may provide higher conductibility of the electron beam, enabling differentiation analysis at higher magnifications and potentially amplifying the threshold values in the backscattering.

2. Hydration of clinker compounds

It is clear that the secondary reaction by adding silica fume into the system makes use of additional binding water. This was seen by three different techniques. The excess CSH forming is related to CH consumption within the pozzolanic activity by silica fume. The total consumption of CH can not be verified with the current results, although is not expectable that substantial pozzolanic reaction may occur in long-term hydration. Further tests are needed at long-term hydration-times to confirm the previous statement. The addition of superabsorbent increases both the formation of CH and rate of secondary reaction, especially during the 1st week of sealed hydration. From the third-day forward, activity of both silica fume and additional water in the superabsorbent polymers to sustain further hydration seems severely diminished. It is suggested that internal curing is mainly active during this period, rather then the whole hydration time.

3. Microstructure and Pore structure

The investigated systems are found to be highly homogeneous materials at the microscopic scale. Differences in morphology may only be found in sub-microscopic scale, where crystalline phases appear within voids or capillary space. Water-entrainment by superabsorbent polymers dramatically changes the pore structure of the system, which comprises isolated macro-inclusions and little capillary porosity. The later is also found in SF-modified cement paste in respect with the plain cement paste, which shows higher absolute porosity, although it seems poorly connected as well. Potentially, gel porosity in SF-modified cement pastes may be

significantly reduced as well, but a higher resolution is required to corroborate this suggestion. This is more evident in the water-entrained system, where additional water may have promoted hydration in pores, leading to the sublimation of fine porosity. It is further seen that superabsorbent polymer is well dispersed throughout the matrix. Furthermore, the evaluation of macro porosity on 2D sections may be hindering pore depressions or slit-pores, which may have source in measurement artefacts. A 3D approach would be of great interest to describe the pore network system in cement-based materials.

4. Hydration model

A simple approach based on the stoichiometry of the chemical reaction between silica fume and forming calcium hydroxide to model hydration of blended cement-silica systems was applied. However, it is seen that this modelling approach, which is solely based on the kinetics of the pozzolanic activity is not sufficient to describe hydration in low water and low porosity SF-modified systems. Information about the diffusivity and transport properties of each system seems vital to truly understand the extent of the pozzolanic activity. In order to study this, it is necessary to develop the physical knowledge on the pore structure of the system with time. However, for a cement paste with w/c=0.30 and at s/c=0.15, it is concluded that the system may not fully convert the calcium hydroxide into CSH via pozzolanic activity. The recognition of that the pozzolanic activity is not significant in the long term hydration is consistent with the experimental results, as the rate of pozzolanic activity is practically negligible after the third-day of sealed hydration. This effect is even more marked in the water-entrained SF-modified cement paste, suggesting that water movement is primarily dependent from the initial water to cement ratio and the amount of silica fume in the system, the physical properties governing the course of water release from the superabsorbent.

3.3. Early-age properties of Portland cement-silica systems versus water-entrained systems

This section deals with the basic properties of cement-based materials with silica fume addition and internal curing by superabsorbent polymers. The purpose of this study is to characterise fresh and hardened properties of low porosity and low water cement pastes with insight on the underlying mechanisms that may prove value in the modelling of autogenous deformation in cement-silica systems. Such a task involves a deep and wide knowledge of the early age properties of cement-based materials at the macroscopic scale. An integrated perspective emerges from the experimental framework, which is based on the correlation of the volume changes via autogenous deformation measurements with both chemical and thermodynamical-based phenomena, via heat of hydration and RH-change. This discussion is done taking into consideration the different physical properties of the system, referring to the addition of silica fume and the use of superabsorbent polymers.

3.3.1. Introduction

The major difficulties in explaining the source of the free movement in low water and low porosity systems are related with the poor knowledge of the material properties at a microscopic scale. However, it is extremely problematic to access or monitor the changes in the microstruture in autogenous conditions. For example, the use of SEM or even ESEM techniques will lead to the introduction of several artefacts in the system-physics, e.g. external pressures via SEM-chamber, affecting the volume-change of the system. A second difficulty is that of the perception of the third dimension, making the unit volume difficult to comprehend. Thus, there are still a great number of uncertainties in the micro properties of the composite material: density of the different hydrated compounds, developing pore structure and space available to accommodate highly heterogeneous hydration products, both in morphology and in stoichiometry. This forms a basis for a tremendous challenge towards the modelling of these phenomena at a macroscopic scale, as it is autogenous deformation or RH-change. However, the investigation at such small scale requires the knowledge of the material properties at macroscopic scale. The correlation between micro and macro material parameters is one of the major scientific tasks being offered by the material science.

In the present study, several material properties of cement-based materials are analysed at the macroscopic scale. An empirical approach though time is used to follow the volume change at early-age, with insight in correlating the autogenous deformation with chemical, physical and mechanical parameters with dynamic nature. It is concluded that chemical shrinkage is not feasible to characterize the bulk shrinkage of high performance composites in sealed conditions. Moreover, the isolated view of chemical and RH-change dependency of autogenous deformation may be of interested. An approach to differentiate such dependency is tried. Thus, a third dependency is fundamental, which is related with the mechanical properties of the system, which is again time-dependent. In this study, the hardened properties of cement-based systems are accessed and a correlation between chemical and thermodynamical-based phenomena with volume-changes is tried.

3.3.2. Materials

Three systems selected among a broader experimental framework are presented in this section: a plain cement paste, a cement-silica paste and a water-entrained cement-silica paste. The basic water to cement ratio was 0.30. Silica fume was added at a rate of 15% wt. of cement. To ensure adequate

workability, a naphthalene-based superplasticizer was added to the SF-modified cement pastes at a rate of 1% wt. of cement. Superabsorbent polymer was used at a rate of 0.4% wt. of cement, the internal curing being performed by adding additional water into the water-entrained mixture, which corresponds to an effective curing water to cement ratio of 0.05.

3.3.3. Methods

Chemical shrinkage

Chemical shrinkage was measured by the gravimetric method. For each system, about 8 g of cement paste were cast into cylindrical glass tubes with diameter of 25 mm and 60 mm height. The thickness of the cement paste specimen was approximately 10 mm. About 6% in water (by wt. of sample) was carefully introduced in the top of the fresh paste, corresponding to a layer of 1 mm in height. A metal vial encasing the system of specimen plus glass container was then submerged into a temperature controlled poliglycol bath at 20 ºC. Measurements started at about 30 minutes after mixing time and were performed during 7 days in isothermal conditions.

RH-change and AD measurements

Internal humidity change was determined in RH-stations according to procedure described in reference[182]. Autogenous strain was recorded once for each system in the paste dilatometer developed by Ole M. Jensen and P.F Hansen. The fully automated measuring device is described in detail in reference[104]. Corrugate tubes with diameter of 28 mm and length of 300 mm were used as casting moulds for the fresh cement pastes. Special end-closures assure that the cement paste is contained in the corrugated tube during an "unlimited" test period, performed in submerged temperature-controlled and isothermal condition. Measurements started at about 30 minutes after the mixing time. The deformations were zeroed at setting time.

Compressive Strength

Compressive strength and modulus of elasticity in compression were determined in a fully automated INSTRON testing machine with a load capacity of 250 KN. Early-age tests were done according to the hydration peaks of each system, as measured by temperature evolution in the cement pastes. In the case of cement-silica pastes, cylindrical specimens with diameter of 14 mm and length to diameter ratio of 2 were tested at the first 24 hours. The strength properties at 3, 7 and 28 days in sealed conditions were also examined. The tests were performed according to the procedures described in ASTM standard number C39-86.

Heat of Hydration

Hydration heat was deduced from temperature increase in a calorimeter developed in the LAB. Temperature to heat transformation was performed by calculating the thermal conductivity of the calorimeter by heat loss with water. It is found that the heat loss from the system can not be considered purely isothermal, since the rate of heat loss does not show a linear slope with temperature decrease. However, for the purpose of this investigation, it seems sufficiently relevant to know the rate of reaction taken from the temperature increase of each system, assuming a quasi-isothermal condition. About 100 g of cement paste were cast into cylindrical tubes with diameter of 40 mm. End-closures prevent any mass loss from the sample within a test duration of 7 days. The

measurements started after 30 minutes in respect with the mixing time. A more detailed description of the method is presented in 4.4.

3.3.4. Results and discussion

Chemical shrinkage

Chemical shrinkage of each system is presented in Figure 3.34. The plain cement paste absorbs not more than about 0.04 ml per gram of cement during the first 7 days. The introduction of mineral admixture as binder in 15% wt. of cement showed a similar value of the chemical shrinkage in relation with the plain cement paste. This result is considerably lower than the value found in the literature, whereas 22 ml/g has been reported[39, 30]. One of the difficulties of this test procedure is to control the amount of water that is able to penetrate in the sample. If a sample is submitted to saturation after hardening, the time that the system may take to achieve volumetric stability may be fare more beyond than the time of the chemical reaction, at hydrostatic pressure. Therefore, the diffusion rate that determines the time that water takes to penetrate in low porosity systems may be masking the real chemical shrinkage. However, it should be pointed out that the space to accommodate new hydration products is fundamentally depending on the initial water volume. If hydration is hampered due to lack of space, rather then insufficient water, then the chemical shrinkage may approximate the registered values. In addition and although it is not apparent, the rate of chemical shrinkage between the plain system and the SF-modified systems is slightly different. Because a secondary reaction is occurring due to the presence of silica fume, the lower rate shown by the curve representing the SF-modified system may be explained by the different diffusion rate from the external water source. The results taken for the SF-modified systems suggest that the test protocol for chemical shrinkage may not be applied so straightforward for low water and low porosity systems.

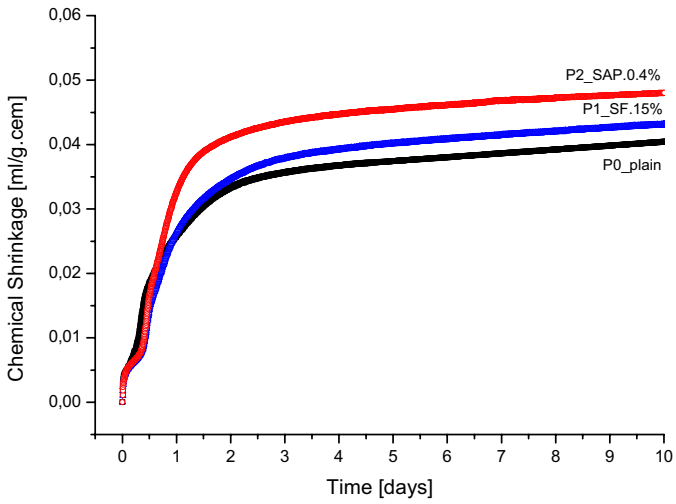

Figure 3.34.

Chemical shrinkage of plain cement paste versus SF-modified paste and water-entrained system. Basic water to cement ratio is of 0.30.

Surprisingly, the water-entrained paste seems to develop higher chemical shrinkage, in respect with the non-entrained systems. This is mostly observed within the initial 48 hours, as seen in Figure 3.34. It is interesting to note that the water absorption due to chemical shrinkage preferably occurred from an external source, rather than the internal source, viz curing agent. It would be expected that the internal water source could balance the chemical shrinkage of the system. The

physical forces embracing internal curing water sources may explain this behaviour, while any significant moisture gradient is being formed. Thus, it seems that in an open curing condition, the water-entrained system may be affected by the presence of superabsorbent. It is suggested that the higher moisture content in this particular system is favouring the water movement from external sources. It is interesting to note that the water absorption due to chemical shrinkage is not the only feasible explanation for this physico-chemical event, since only part of the water was uptake by the sample. This was confirmed by simple observation of the height of the water in the containers. Therefore, the internal curing water was partially used to enhance hydration, leading to a different extent of hydration and consequently to different amount of hydration products. This is an indication of additional hydration of cement compounds due to internal curing.

Independently from the real value of chemical shrinkage, it is registered that the low porosity and low water system is able to uptake an amount of water which is much less than 0.22 ml per gram of cement, as proposed in the literature. This is also valid for the plain cement paste, where a typical value of 0.06 ml/g is usually admitted. Similar effect is found in the case of systems comprising other mineral admixtures[51]. This is explained by the masking of a true value for the real chemical shrinkage, via depercolation of the system.

Temperature increase and reaction rate

Temperature evolution in the studied systems is presented in Figure 3.35. It is apparent that the introduction of silica fume in the system leads to a temperature decrease. The delay in hardening is explained by the absence of superplasticizer in the plain cement paste. By translating the curve SF.15% towards the curve SF.0%, it may be concluded that the rate of reaction is not significantly altered, as measured by temperature development. This is consistent with the data from the chemical shrinkage.

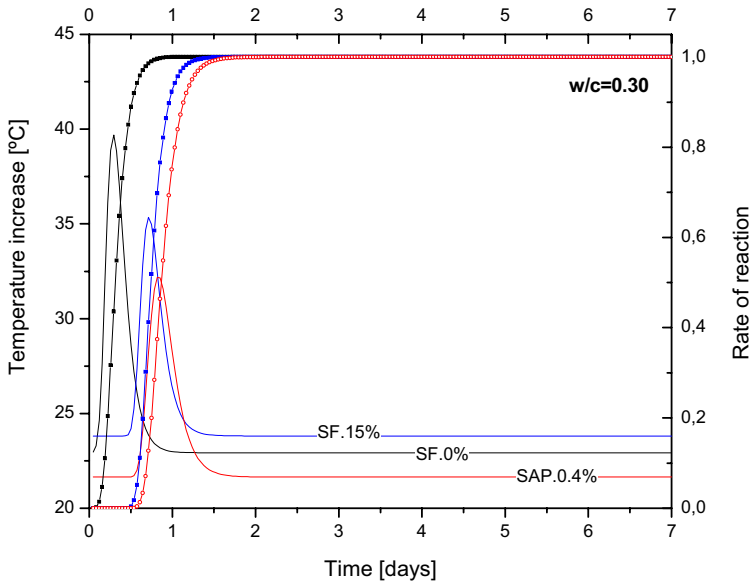

Figure 3.35.

Temperature development of cement paste versus SF-modified paste. Basic water to cement ratio is of 0.30.

The introduction of superabsorbent polymers and the corresponding curing water leads to a further decrease in the temperature of the system. This is explained due to the decrease in the specific volume of cement in the system, due to the inclusions. It is also noted that the half-width of the temperature-peak is slightly broader than the non-entrained SF-modified paste and occurs at a later time. This may be related with the diffusion rate of internal heat towards the equilibrium, which is function of the internal moisture of the system, the higher internal RH damping the heat flow.

Autogenous deformation and Internal RH-change

As shown in Figure 3.36, there is a remarkable difference in the RH-change between the studied systems. The plain cement paste desiccates till about 92%, whereas no further change is registered. Inversely, the SF-modified paste shows a different RH-profile, in respect with the plain cement paste, starting with a initial saturation plateau, which being the lowest, may be related with the different salt concentration in the pore fluid, motivated by both the presence of silica fume or the superplasticizer. Subsequently, the RH-drop appears faster, and after the first 48 hours, the system shows further desiccation, although at a slower rate.

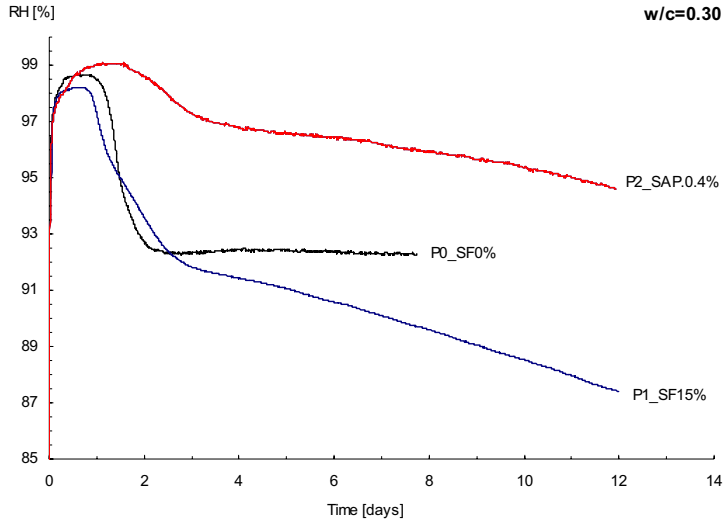

Figure 3.36.

Internal relative humidity of cement paste versus SF-modified paste and water-entrained paste. Basic water to cement ratio is of 0.30.

Furthermore, the introduction of superabsorbent polymers was effective in maintaining a high level of saturation in the system, the desiccation being about 95% at 7 days sealed hardening. It is interesting to note that, although the RH-level of the water-entrained paste show a higher absolute value in respect with the plain paste, the RH-change develops at a comparable rate in respect with the non-entrained silica fume mixture (system P1). Evidently, self-desiccation is occurring also in this system, mostly within the secondary reactions. However, it has been shown by Jensen and Hansen[124] that by increasing the amount of internal curing water in the superabsorbent polymers, the RH-change profile would show a steady curve during the whole curing period.

Figure 3.37 shows the linear autogenous strain measured in the studied systems, where important differences may be observed. The plain cement paste, designated by P0, shows an ultimate deformation of about 1000 microstrain. The addition of 15% of SF by weight of cement induces an early-age deformation of about 2500 μs, a factor of 1.5 in relation to the plain cement paste. The rate of deformation may be subdivided in three periods: the first 24 hours, the second 24 hours and

the subsequent period. The volumetric stability of the system is not achieved in less than 2 weeks, whereas the measured deformation rate is of about 0.95 microstrain per hour.

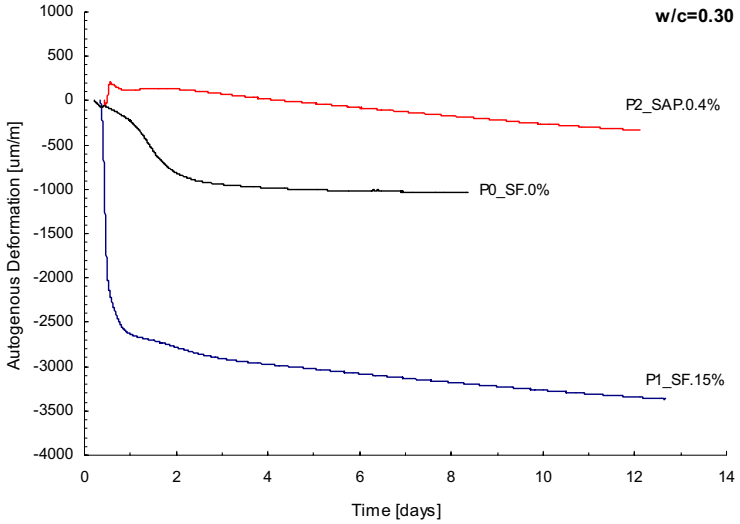

Figure 3.37.

Autogenous deformation of cement paste versus SF-modified paste and water-entrained paste. Basic water to cement ratio is of 0.30.

The data is consistent with previous work by Jensen[183], where stability of the system is found at the end of the first month at 20 ºC. The introduction of superabsorbent was effective in mitigating the initial deformation, but the curve P2_SAP.0.4% shows that the amount of internal curing water may not have been sufficient to fully offset the autogenous deformation. In fact, during the late period, as measured between 3 and 7 days, the measured rate of deformation is of about 1.90 microstrain (μm/m) per hour, about the double the rate shown by the non-entrained SF-modified paste (P1_SF.15%). This may be another evidence of additional hydration occurring in the system promoted by the presence of internal curing water and concomitant favourable condition towards mineral reaction.

Compressive strength

Results of strength development for the studied systems within the first month in sealed hydration are presented in Figure 3.38. It may be observed the effect of the introduction of silica fume and the water entrainment by superabsorbent polymers in a plain cement paste with w/c ratio of 0.30. In the former case, the addition of silica fume leads to a significant increase in the hardened properties. It should be mentioned that the introduction of silica particles was performed as function of the cement weight, the w/c ratio being constant. This method may be a source of criticism, since the relation between water and binder is changed. However, this approach enables one to see the direct influence of the introduction of silica fume, which ideally is not reacting within the initial hydration period, thus not playing a major role on the modification of the system within the first reaction. In fact, the one-day strength level is nearly equal for both plain and SF-modified systems.

In respect with the effect of the introduction of superabsorbent polymers on the strength properties, it is found that the addition of 0.4% (wt-% of cement) leads to a significant the decrease in the compressive strength, in relation with system P1. This may be related with the existent level of moisture in the system and the additional porosity inherent to the system-physics of this mixture. It is well know the effect of drying on the mechanical properties of cement-based materials[184].

Furthermore, it is interesting to note the variation in the rate of strength development. Apparently, the systems that include silica fume may have not achieved mechanical stability (or strength equilibrium) in the evaluated time length, by looking into the strength rates of the systems P1 and P2 in the third-quarter of the analysed period.

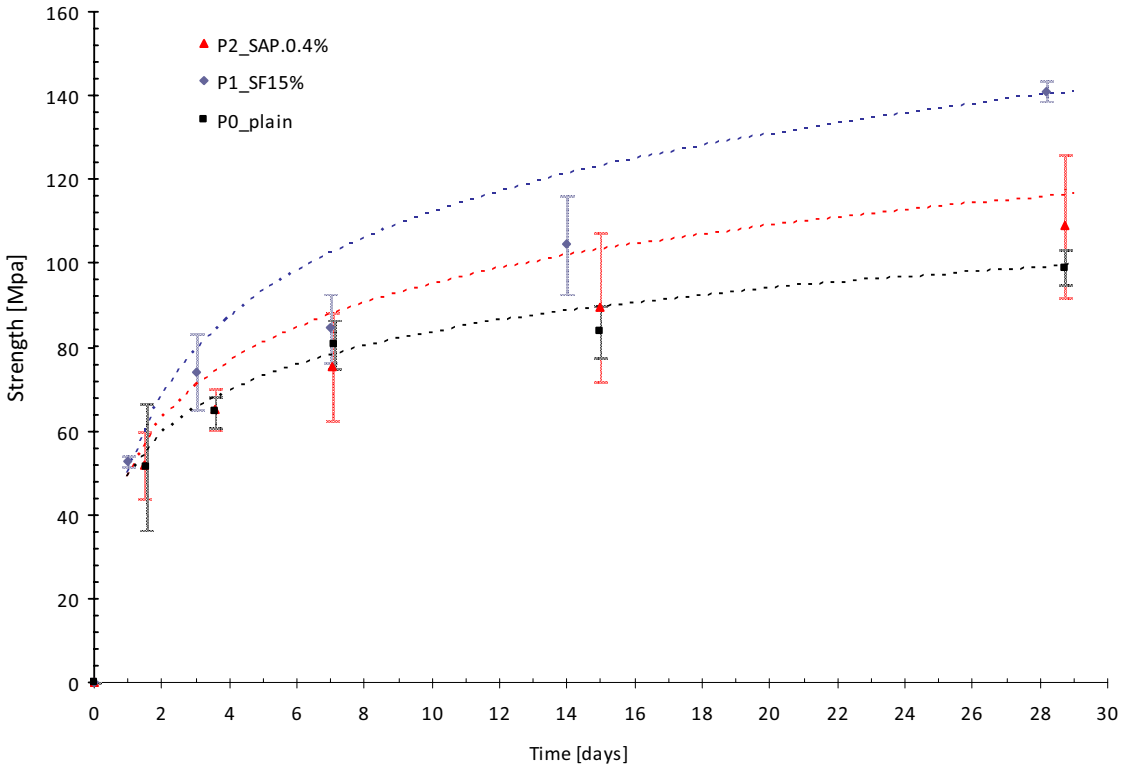

Figure 3.38.

Strength development of cement paste versus SF-modified paste and water-entrained paste. Basic water to cement ratio is of 0.30.

This observation is especially pertinent in the case of water-entrained systems, in connection with the variability of results taken at the age of 28 days, which may further indicate that the mechanical stability of water-entrained cement-based materials is achieved at longer curing times for a specific curing temperature. The variability of results may be seen by plotting the time and standard deviation between the samples of the same system. Moreover, this tendency is consistent with other companion tests.

It should be emphasised that is extremely difficult to access the strength of cement pastes without the presence of aggregate. This is mainly due to the fragile behaviour of cement paste considered alone, even though the standard deviation show reasonable values for non-entrained cement pastes at the 28th day. In the present series of tests, the coefficient of variation COV<5%, which is below the values presented in previous studies[185], where more interference during the sample preparation is noted. It is interesting to note that the test results show a comparable strength level despite the initial rotation of the samples, which was performed prior setting by Lura et al.[185]. In either case, the stress introduced during sample preparation is relevant to explain the drop in strength of the systems, as noted by testing samples prepared from cylindrical cores, which were

prepared from the same batches. It may be concluded that the gain in compaction due to rotation is lost due to the sample preparation procedure.

Furthermore, the very dense packing and high degree of desiccation of the systems, especially the non-cured specimens, may have given rise to cracking events resulting from the higher brittleness of the composite material. This was observed during testing of the materials at 7 and 28 days, as the first crack appeared systematically earlier than the samples tested at early-age. It is possible that cracking phenomena may be highly related with internal humidity or degree of desiccation that the system reaches during sealed curing.

3.3.5. Correlation between the chemical reaction, autogenous RH-change and autogenous strain

It is straightforward to correlate the analysed properties through time. After setting, where it may be considered that the pore structure is formed, the system is characterised by a solid porous material. Thus, a major part of the transition from the viscous-elastic state to solid state is undergone. This corresponds to about 3 to 4 hours in the plain cement pastes and 7 to 10 hours in the cement-silica paste, due to the introduction of superplasticizer.

Systems have developed a degree of rigidity/elasticity at this time, as shown by the strength/elasticity tests, indicating the appearance of the hardening stage. This period, which takes only a few hours, is characterised by a specific temperature evolution and the pastes undertake great part of the shrinkage strain. It is seen that the introduction of superabsorbent polymers may completely resolve this part of the strain. The temperature evolution in the system may be seen as a macroscopic measure of the reaction between the clinker minerals and water, the reaction being principally attributed to the chemical reaction between the calcium silicate phase, which is the main constituent of clinker, and water.

The first correlation which should be then evaluated is the possibility of considering that the rate of reaction may give an indication of the rate of volume change. Thus, the linear strain may by transform into rate of linear strain. Figure 3.39 shows the relation between the strain rate and the reaction rate of the systems. It is interesting to note the shift in the time of strain due to the presence of silica fume. It is observed that within the hardening stage, the SF-modified paste undergoes most of the strain, while in the case of the plain cement paste the rate of strain becomes important only at the late period of hardening. In the particular case of the SF-modified cement paste, there may be different mechanisms acting in the hardening stage.

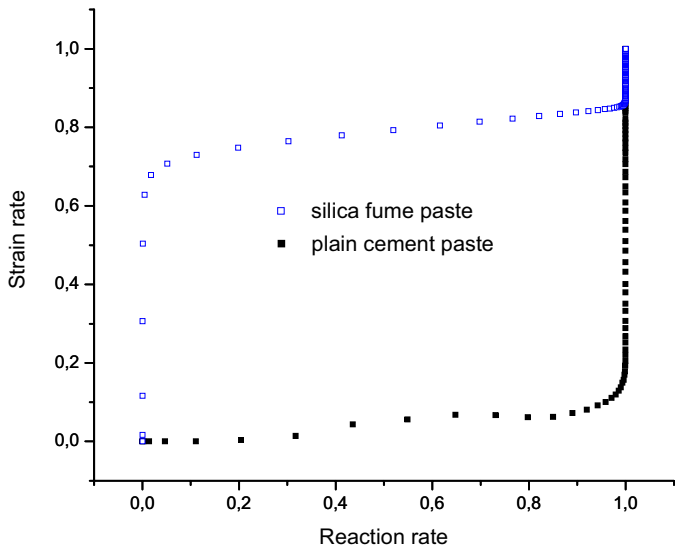

Figure 3.39.

Relation between the rate of linear strain and the rate of reaction, as taken from the temperature evolution measurements.

As seen in the isotherm, three strain stages may be identified. It transpires that the diffusion of species may be blocked at the middle period of hardening, in respect to the initial stage. Since at this time, the system is fully saturated, it is impossible that the RH-change is the sole mechanism acting on the system. It would be interesting to further analyse the effect of the rate of silica to cement with this respect.

It also transpires that this correlation is not physically meaningful, since the heat development of the system cannot translate the change in the relative humidity of the system or differentiate the secondary reaction from the first reaction. This is further proved by absurd logic, i.e. if a system with a higher w/c ratio is considered, the autogenous RH-change due to self-desiccation would be negligible, the heat of hydration not being significantly changed. Moreover, for the same amount of binder, it is seen that the heat of hydration is significantly diminished due to the presence of mineral addition, while the autogenous strain increases severely. Thus, it may be deduced that temperature-time-based functions as the maturity method may not apply in systems where autogenous deformation is active. This was first shown by Ole M. Jensen[186], in a more theoretical approach.

Another time-based correlation may be tried, by taking the data from the measurements of autogenous RH-change and autogenous strain. Both were transformed by differentiating the absolute values by a referenced change, which, in the present case was taken at the seventh day (see Figure 3.40). This approach permits to clarify some differences in the observed phenomena when silica fume is added to the system. In the case of SF-modified paste, a major part of the strain occurs without significant changes in the relative humidity. An opposite observation may be seen in the plain cement paste. These differences would be maintained even when the reference time is expanded, since the major part of the shrinkage occurs at very early-age. Thus, the major mechanism in controlling the initial strain may be other than the change in the relative humidity, and it may find ground on the volume-change due to chemical reactions.

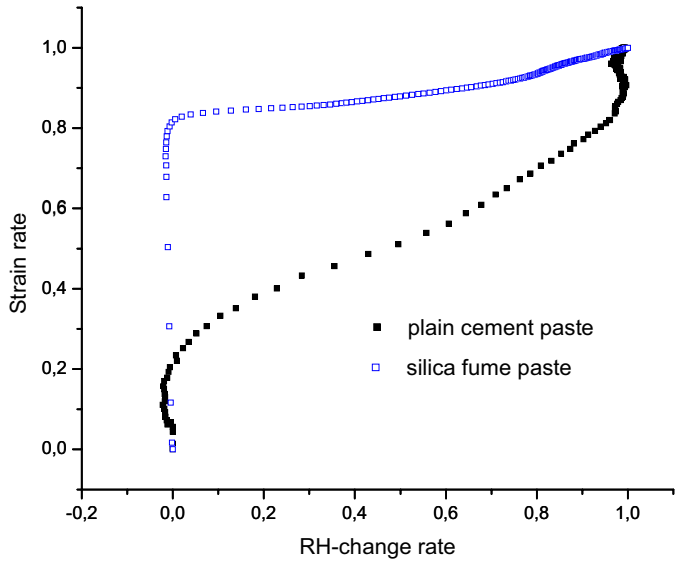

Figure 3.40.

Relation between the rate of linear strain and the rate of RH-change for plain cement paste and SF-modified paste.

The last statement is highly controversial, since it is generally accepted that the RH-change may explain autogenous deformation of cement-based materials. However, almost 80% of the measured strain seems to be highly correlated to chemical phenomena, rather than the RH-change of the system. It is interesting to note that the remaining 20% of the strain matches the observed rate of RH-change. In the case of the plain cement paste, the major macroscopic property influencing autogenous deformation may be the opposite, the RH-change rate being more feasible to explain the major part of the volume-change.

The previous exercise may also be applied to the case of water-entrained cement pastes. Thus, as shown in Figure 3.41, the introduction of superabsorbent polymers is in great extent independent from the chemical reaction and mainly dependent of the RH-change rate. However, it is interesting to note that the negative strain rate, which should be read as expansion rate, overpasses the total negative strain (shrinkage) of the system. The expansive behaviour cannot be explained either by the change in the relative humidity or by the hydration of cement. Thus, there should be other mechanism opposing the shrinkage verified in the non-entrained SF-modified cement paste.

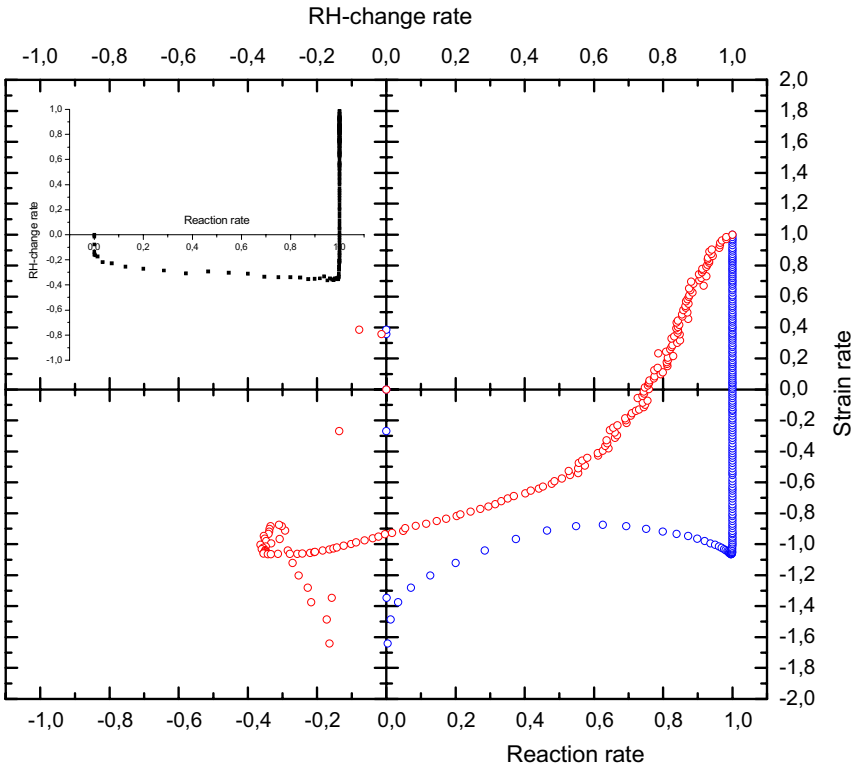

Figure 3.41.

Correlation between the rate of linear strain, the rate of RH-change and the rate of reaction in water-entrained SF-modified cement paste.

It is interesting to note the activity of the water present in the superabsorbent before hardening. Immediately after a short shrinkage, the water entrained SF-modified paste expands without significant change in the reaction rate, whereas heat evolves and shrinkage appears again. However, the non-linear shape of the curve indicates that within the hardening stage, internal curing is very active. Furthermore, when the exothermic reaction seems to cease, the system recovers the negative strain with a significant rate. The relation between the volume-change and the RH-change when internal curing is active seems complex. A major part of the expansion may not have cause in the RH-change. After a chaotic transition between negative and positive strain rates, the RH-change seems to be the governing mechanism affecting the strain rate, the relation being also non-linear. The strain rate per RH-change rate is increased by the double at the third-day without any change in the reaction rate. Thus, it is clear that a physical or mechanical mechanism is governing the volume-change at this point.

3.3.6. Conclusions

In this section, focus was given to the knowledge of material properties that may in light the perception of mechanisms in the base of autogenous phenomena and the consequences on the macroscopic material properties. The results of the tests suggest the following conclusions:

Chemical shrinkage versus self-desiccation

The chemical shrinkage measurements were inconclusive in respect with the deformation of the system. This is related with the uncertainty in the percolation/depercolation of the systems, which may be masking the real chemical shrinkage. On the other hand, it is suggested that the test results may be valid, within the hypothesis of that the hydration is hampered due to lack of space in the system to accommodate further hydration products.

The combined analysis of chemical and thermodynamic-based phenomena, viz. heat of hydration and RH-change, in respect with autogenous deformation pointed out that a great part of the volume-change in low water cement-based systems is based on the self-desiccation of the system. However, the same correlation may not be concluded in SF-modified systems, where chemical-based phenomena seem to govern the major part of the volume-change, occurring within the first 24 hours.

Compressive strength and modulus of elasticity in compression

The test results taken from mechanical testing are clear on perceiving the effect of adding silica fume and performing internal curing by superabsorbent polymers. The former leads to higher strength of the composite material and the later induce strength loss via porosity and different internal humidity at the time of test. However, the strength level of the water-entrained should be analysed at longer curing times and for the same level of internal RH, since the mechanical stability appears later in respect with non-entrained SF-modified system. It is expected that subsequent internal drying, running at very slow rate may give the water-entrained system more mechanical performance in terms of strength in compression.

It is also concluded that the sample preparation procedure may have significant influence on the strength level of the systems. The strength gain from rotation prior to setting may be lost in the core preparation during cutting. It is suggested that the system is highly sensible and brittle, as further self-desiccation develops.

3.4. Superabsorbent polymers: On the interaction with water and pore fluid

Superabsorbent polymers are hydrogels capable of absorbing considerable amounts of water without dissolving, and may have wide application in cement-based materials. They were initially used within concrete industry in high performance concrete to secure the drop in the relative humidity during hydration of cement. This assures the optimum development of cement-based materials properties avoiding self-desiccation and early-age deformations. Mechanisms about the kinetic change of the hydrogel with water or pore fluid within the cement-based system are not fully understood. This paper deals with the absorption kinetics of superabsorbent polymer in water and synthetic pore fluid mediums. The physical state of selected particles from 50 to 500 micrometers was examined by means of optical microscopy and subsequent image analysis. This showed an accurate technique for quantifying the absorption of water or fluid into the cross-linked structure of superabsorbent polymers. The results clearly show that the size of the polymers particles have a significant effect on the absorption kinetics of poliacrylate-based polymers. In addition, hydrostatic pressure seems to be the main mechanism contributing to the swelling rate. A model based on Fick's second law is found to accurately express the physical or volumetric change within the fluid medium, after a spontaneous fluid uptake at submersion. An extension to this model is proposed to calculate the kinetics of absorption for a given particle size distribution. The present work constitutes a first part of a wider scientific work. In the second part, a comprehensive study on desorption kinetics will be presented.

3.4.1. Theoretical

Superabsorbent polymers are hydrogels capable of absorbing considerable amounts of water without dissolving, and may have wide application in cement-based materials. The characterization of superabsorbent polymers referred in the literature is usually focused in other industrial applications rather than cement-based materials, e.g. personal care market, which involves by large the main commercial interest within the development of superabsorbent polymers. Their introduction in the construction materials technology may have been initially proposed by P.F Hansen and O.M. Jensen[135], referring to water-entrained cement-based materials, in patented work. Recently, RILEM established a Technical Committee, the TC-SAP, whose main concern is to study and potentially to widen the use of superabsorbent polymers in building materials.

This section deals with the absorption kinetics between superabsorbent polymers and both water and pore fluid. This is particularly important, since the absorption capacity parameter is a key aspect in the superabsorbent polymer technology within most of their practical applications. In the case of cement-based materials, key issues as the effective water to cement ratio within a water-entrained system and the initial porosity at early age may gain deeper perspective, since the fresh and hardened properties of such materials highly depend on the intrinsic properties of this component. Physical properties of superabsorbent alone may significantly alter the pore structure and thus affect the hardened properties of high performance concrete. Other characteristic that may be of first interest is the time elapsed from the original state of the polymer to reach the volumetric equilibrium, when submerged in a fluid medium as fresh cement paste. If the casting of concrete into the formwork is performed before this volumetric equilibrium is reached, the subsequent absorption may influence the amount of free water in the system and thus, induce rheology change. Therefore, undesirable fresh behaviour may be obtained. Furthermore, the knowledge developed

within the following sections may be of great interest in the application of superabsorbent polymers in the shotcrete market.

The definition of absorption capacity is based on the time equilibrium that a certain amount of polymer takes to achieve constant weight or a stable volumetric condition. The methods usually applied for determining the absorption capacity include gravimetric and volumetric measurements[187, 188]. In addition, rheology experiments were also used with the same objective[144]. The gravimetric techniques, while giving a fast response, have the drawback on the accuracy of the real absorption capacity. For example, the "tea-bag" technique is not capable of taking in consideration the interstitial liquid phase bonded by physical forces within the particles, even when associated with centrifugation. Brandt et al.[189] proposed a colorimetric procedure by means of spectrophotometer to isolate macromolecular dye in the swelling liquid as a solution excluding the interparticle liquid from the experimental results. However, this technique assumes that the dye is excluded from the swelling gel and that the chemistry of the swelling liquid is not modified by the introduction of extraneous elements. A more comprehensive description of the methods that can be applied to determine polymer absorption capacity and swelling time is given elsewhere[136]. In this paper, a new technique by means of the optical microscope is proposed to investigate "polyeletrolite polyacrylate-base polymers and fluid interaction with time. This technique has the advantage of taking into consideration only the liquid phase that can penetrate the cross-link structure of the polymer, leading to higher accuracy in the calculation of both maximum absorption capacity and the swelling time of unique size particles, which constitutes one of the fundamental parameters in the theoretical background[190]. In a way, the path between the theoretical and the experimental framework may have been shortened.

3.4.2. Materials and Methods

Spherical superabsorbent polymer particles, with sizes comprehended between 0 and 500 μm, were used in the experiments. Demineralised water and synthetic pore fluid were used as the liquid phase. The synthetic pore fluid is a reproduction of the liquid phase brought out from the dissolution of cement compounds in water, as determined by ion chromatographic analysis and, in the present work had the following composition (mmol/l): $[Na^+]$ =200, $[K^+]$ =200, $[Ca^{2+}]$ =1, $[SO_4^{2-}]$ =15, $[OH^-]$ =672.

A stereo optical microscope, equipped with a Nikon DN camera, was used to monitor the absorption process. Polymer particles are submerged in a micro swimming pool and digital images of 1280x960 pixels with 96 dpi are captured in time. Magnified depths of 40 and 50x shown to be compatible with the scale in examination. Because the scale in examination may change with time due to the particle movement in the fluid medium, the magnification required to monitor the particles may change during testing. Therefore, a scale is attached to the micro swimming pool, enabling to calibrate the magnified depth in real time. The monitoring procedure consisted in taking one frame within each minute up to the 10^{th} minute after water contact. Hereafter, the image capturing frequency was of 1 frame within every 10 minutes and up to 60 min. Image analysis was carried out with a software package IMAGE J, to determine the geometrical properties of particles with time. This essentially consists in calculating the area change of the polymer particles, by calibrating the unit of pixels to the real scale of the image. To this procedure, follow a simple numerical transformation to derive the volume change. The tests were performed at room temperature, which was of about 22 ºC.

3.4.3. Particle Size Distribution and diffraction analysis

Particle size distribution of superabsorbent polymer was analysed in dry state at room temperature (see section 3.1). Quantitative image analysis performed to the digital images showed that the average size of the polymer particles is about 90 μm. The sample is constituted by 180 of randomly selected particles from a batch with particle size ranging between 0 and 300 μm. More than 60% of the total amount of particles has size comprehended between 50 and 150 μm. It should be noted that the sample size should be at least 500 particles, which is probably a limitation of this approach. However, the chosen magnification permits to identify particles to the nearest of 10 μm. A lower magnification would enable to have more particles in the sample, but differentiation in the range of 0 to 100 μm would be extremely difficult.

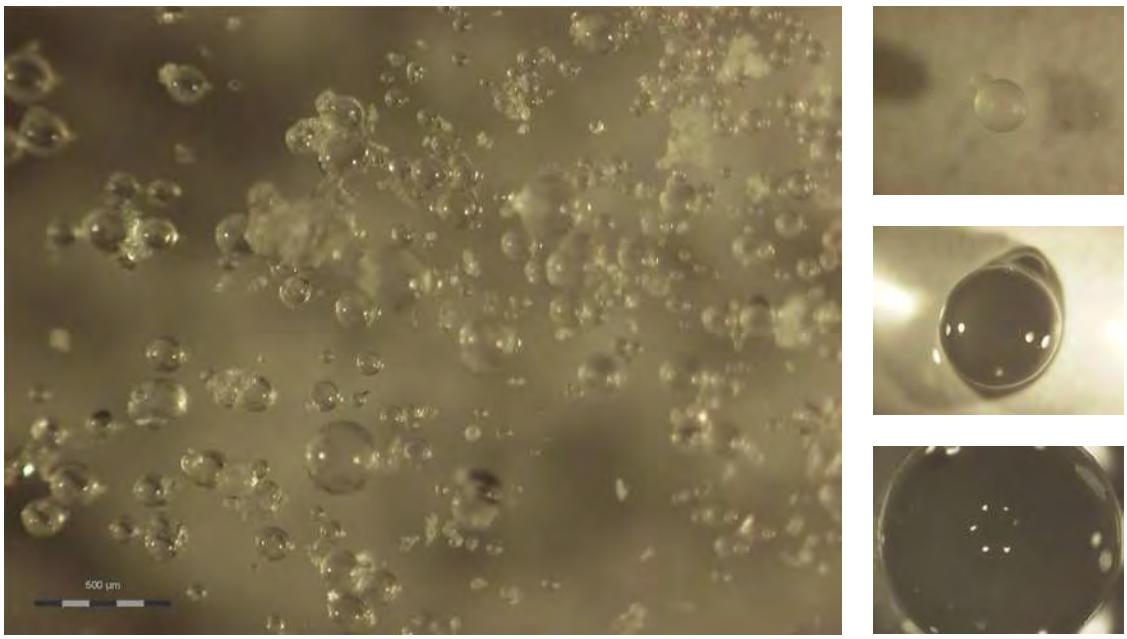

Figure 3.42.

Superabsorbent polymers at time zero, before water contact. The observed particle size is in the range of 0 to 300 μm. The morphology at both dry and swollen state is characterized by spherical particles. The physical change from dry to swollen state (right-middle and right-bottom) is characterized by a rapid solid to gel transition.

The frequency distribution of each particle diameter is shown in Figure 3.43. Different frequency plots could be drawn, by assuming an average size in each range of increasing steps of 1, 10, 20 and 50 μm, whereas the effect of choosing one step on the frequency plot can be foreseen. The cumulative particle size distribution seems to be independent of the step count. Thus, a probability density function based on Gauss or Rosin-Rammler equations, which are commonly used to express the distribution of granular matter, may apply to the present case.

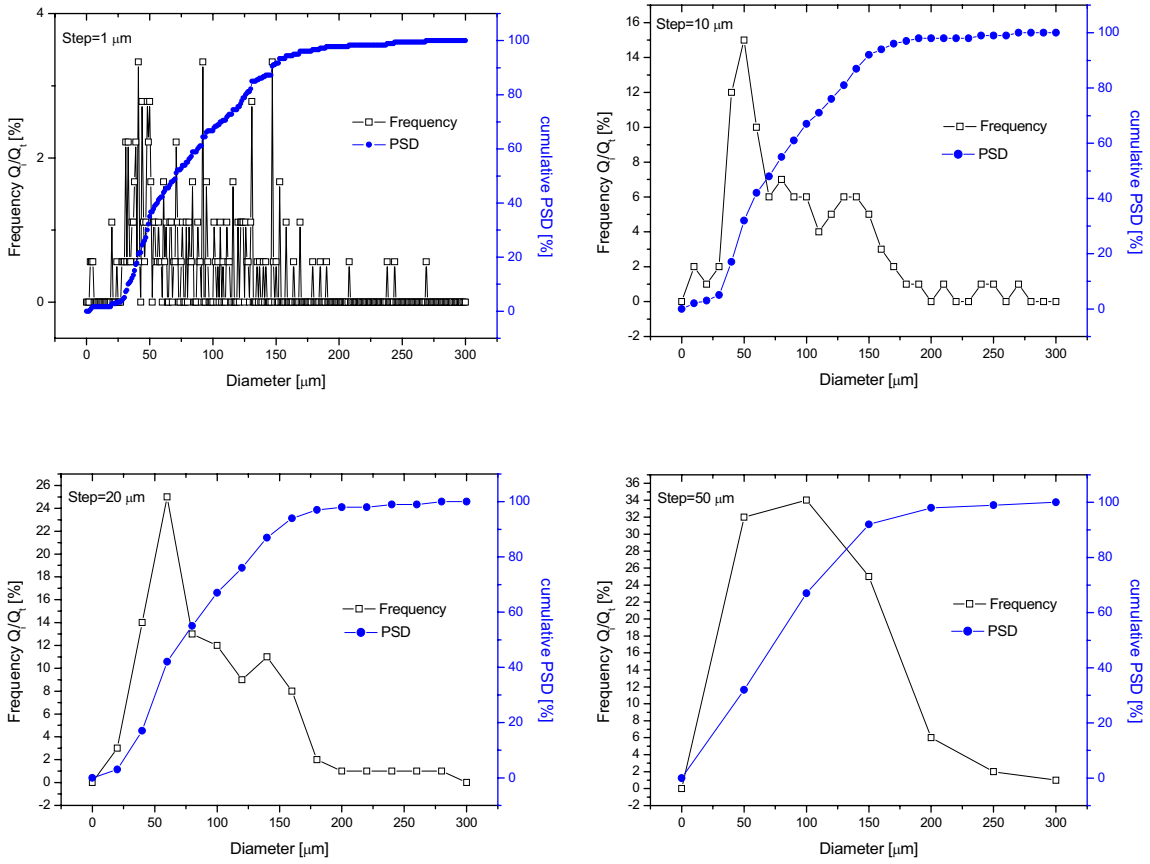

Figure 3.43.

Frequency charts showing the size distribution of particles of superabsorbent polymers with increasing step count.

On the other hand, in order to find a mathematical agreement in compliance with a physical attribute of the polymer particles, e.g., a physical dimension as diameter, area or volume in each cluster, it is necessary to properly define the scale and the target accuracy. An expression may be drawn to describe a specific physical attribute in respect with the dispersion of particles in the system:

$$f(\xi) = \frac{1}{s_c} \cdot \int_{\xi=0}^{\infty} Q_i \cdot \xi_i \cdot d\xi \tag{3.14}$$

Where ξ represents the physical attribute, Q_i is the quantity of particles of equal cluster and s_c is the step count. The error of evaluating a sum of diameters according to eq. (3.14) in a given universe of particles would increase in 30% by choosing the step count of 50 μm in respect with the step count of 1 μm. The previous value times the water absorption of each size would lead to an order of magnitude. Therefore, in order to establish a continuous function to describe a physical dimension within the particle size distribution of the polymer, a step count of 1 μm seems more reliable and it is preferred in relation with the previous approaches. This expression forms the basis

for the study of absorption kinetics. In the following, this expression will be combined to monitor the superabsorbent polymer expansion in time.

3.4.4. Absorption capacity versus swelling time

Absorption capacity refers to the maximum volume that a given universe of polymer particles can achieve when submerged in a fluid medium. In the case of cement-based materials, this corresponds to the uptake of pore fluid from the dry state, which may be considered metastable at 20 ºC and at a reduced vapour pressure. The time between the initial volume at dry state and the final volume at the swollen state constitutes the swelling time. It is fundamental to know the influence of each particle size on the absorption and desorption kinetics, as it may play a central role in the water movement during the early stages in the hydration of water-entrained cement-based materials. Figure 3.44 shows a moment in time within the discrete analysis on the growth of polymer particles while submerged in pore fluid, as taken by optical microscopy.

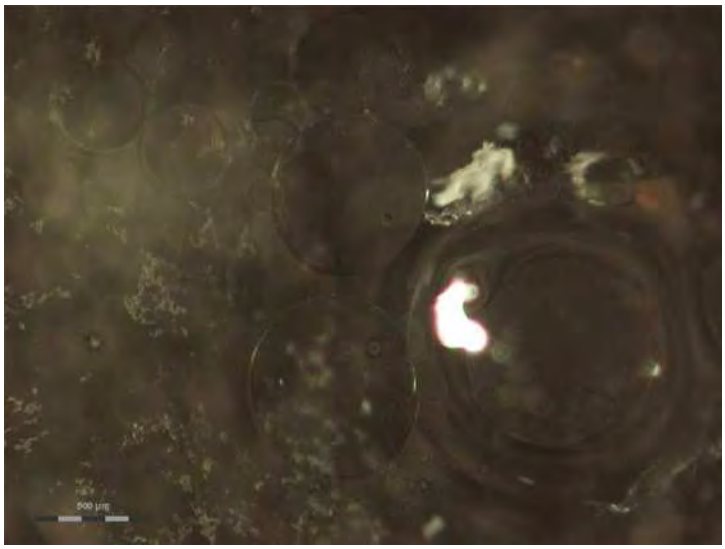

Figure 3.44.

Image acquisition of polymer particles with different size during absorption in synthetic pore fluid medium.

It is clear that is possible to identify different growing diameters with this technique. Therefore, different particles were selected to follow their volume change in time. From the image analysis, it was possible to follow the diameter change of different particle size, as presented in Figure 3.45.

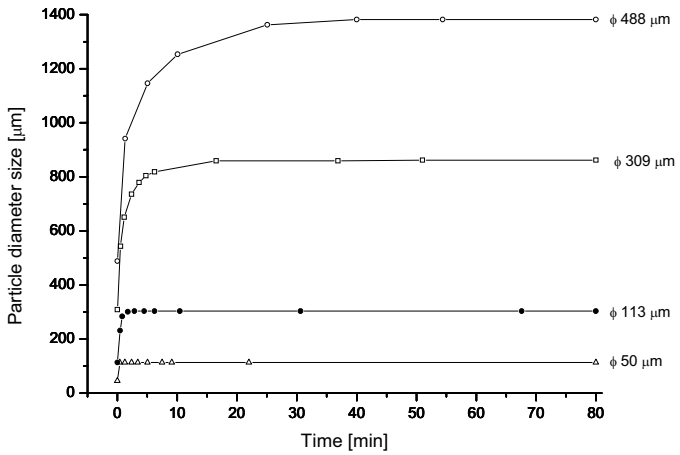

Figure 3.45.

Growth of individual polymer particles expressed by diameter change as function of time. The interaction medium is synthetic pore fluid.

Within the size range in study, the volumetric equilibrium is achieved in about 10 minutes after immersion in synthetic pore fluid. It is convenient to transform the previous data into a normalized volume, to facilitate the study of the absorption kinetics in the different particle-based systems. The volume change may be expressed according to eq. (3.15).

$$\Delta V(t) = \frac{V(t) - V(t_0)}{V(t_0)} \tag{3.15}$$

Where $\Delta V(t)$ expresses the change in volume with time [unit-vol./unit-vol.], $V(t)$ is the volume at the time t and $V(t_0)$ represent the volume at the time zero, corresponding to the volume of the particle at the dry state.

The absorption rate may be obtained by the quotient between the change in volume by the ultimate volume change, $\Delta V(t_\infty)$, that a particle can take in respect with the original volume. Rearranging the data sets to reflect the previous arguments, Figure 3.46 and Figure 3.47 may be drawn.

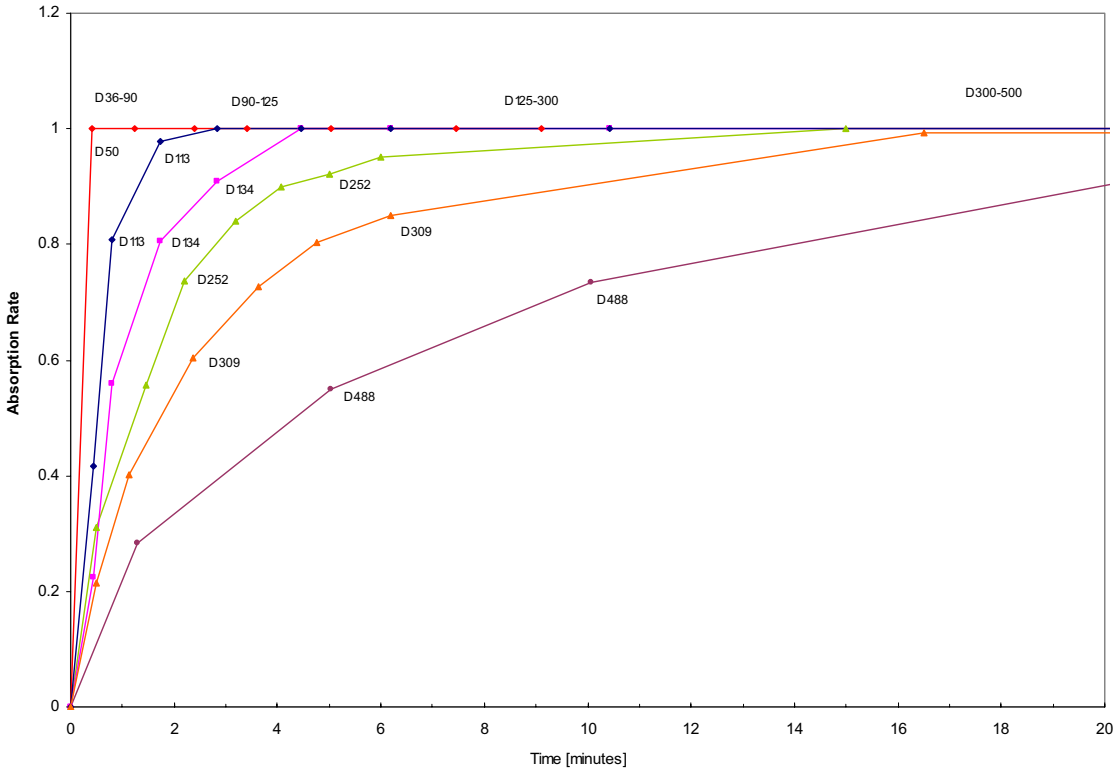

Figure 3.46.

Absorption rates of individual polymer particles with different particle size. The interaction medium is synthetic pore fluid. Numbers refer to µm.

It may be seen that the particle size of the polymer particles greatly interferes with the absorption rate of the fluid phase. The lower the particle size, the faster is the absorption process. Particle D50 achieves the volumetric equilibrium in less than one minute. For particles greater than 125 µm, the

full absorption process takes more than 5 minutes and may even be extended up to more than 20 minutes, in the case of particles greater than 300 micron.

Absorption capacity is shown in Figure 3.47, in ml of pore fluid per gram of dry polymer, by assuming that the density of the polymer is 1.4 g/cm^3. It can be observed that the particle size of the polymer particles influences the maximum amount of liquid phase absorbed. The absorption capacity varies from about 10 to 16 ml per gram of dry polymer, for particle sizes comprehended between 50 and 500 μm. In previous research work, while without isolating the particle size effect on the absorption capacity of this superabsorbent polymer, a value of 12.5 ml/g is registered[124]. This value fits well with the present experimental results.

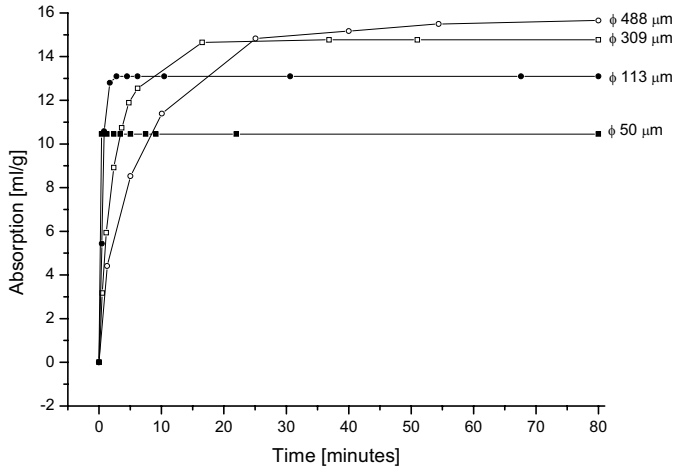

Figure 3.47.

Absorption capacity of individual polymer particles with different particle size, expressed in ml of pore fluid per gram of dry polymer. The interaction medium is synthetic pore fluid.

Thus, it is concluded that the absorption capacity is also diameter-dependent: the bigger the particle is the more pore fluid is absorbed into the cross-linked structure by original weight. This may suggest that the cross-linked structure is changing accordingly to the size of the particles. The particle size effect may be also manifested in the density of the polymer. In the present case, the density was taken as a constant. Nevertheless, the previous observations would not change by attending the last statement. Furthermore, the mechanism of absorption may be related with hydrostatic pressure exerted by the fluid phase on the surface zone of the particle. Since this test is performed in individual particles, the pressure exerted on the low-diameter particles should be lower than the hydrostatic pressure exerted at the surface of bigger particles. Further investigation is required to comprehend this parameter. The overall absorption capacity will mainly depend on the concentration of the different particle clusters. This issue is dealt in the following sections.

3.4.5. Mechanism of absorption: assumptions and modelling

The mechanisms of fluid absorption by superabsorbent polymers pointed out in the literature are usually focused on few parameters: the density of the cross-linked structure, the liquid phase in relation with the presence of salt in the solution, and hydrostatic pressure, constitute the usual variables in the problem. Although all these factors have a role, hydrostatic pressure and diffusion seems to be the principal factors governing the absorption rate. In addition, is important to express the measured data in a way that it is possible to predict the absorption rate of a specific universe of

particles. In the next statements, a model to translate the pore fluid absorption, typically found in cement-based materials is proposed. The following assumptions are made: the swelling process is controlled by a diffusion process, after a spontaneous up-take of the liquid phase. The governing factor affecting the absorption rate is the particle size of the polymer particles, thus, a physical dimension related with the cross-link structure of the different particles.

The swelling kinetics governed by diffusion may be studied by applying the first-order expression based on Fick's second law of diffusion, as given by eq. (3.16).

$$\frac{dQ}{dt} = k(Q_{\max} - Q) \tag{3.16}$$

Where Q_{max} and Q are the swelling capacities at equilibrium and at any time t, and k is the swelling constant rate, which depends on the particle size. Integrating between 0 and the maximum value Q_{max}, yields:

$$Q(t) = Q_{\max}(1 - e^{-kt}) \tag{3.17}$$

The parameter k, expressing the swelling rate constant is diameter-dependent and is governed by the diffusion coefficient. An empirical relation may be derived from the data sets of individual particles with varying diameter:

$$k = 2.76 \times 10^{3} \cdot \phi^{-1,567} \tag{3.18}$$

In eq. (3.18), ϕ represents the diameter of the particle [μm]. This expression may be applied within the geometrical interval of particles with size between 0 and 500 μm. In the case of upper diameters, this expression may be expanded by assuming that the absorption rate should probably tend to a k-asymptotic value between zero and 0.15. It is expectable that this asymptotic value may be considered constant in an order of magnitude. It is also interesting to argue that the shape of the curve may be approximated to an S-shape, which is often found to support other domains of phenomenological mathematics.

Figure 3.48 shows the simulation of eq. (3.17) on the measured data sets. The expression accurately translates the observations of pore fluid absorption, by varying the parameter k. The approximation seems more efficient for the upper range of the studied diameters. There is a slight deviation when approximating the expression on the lower diameters during the initial reaction. It should be noted that the experimental set up presents a limitation during the first seconds of the absorption process, due to imprecision on the time calibration at the instant where the particles enter in contact with the absorbing liquid. Nevertheless, Fick's law may be used to model the evolution of pore fluid absorption in water-entrained cement-based materials by superabsorbent polymers.

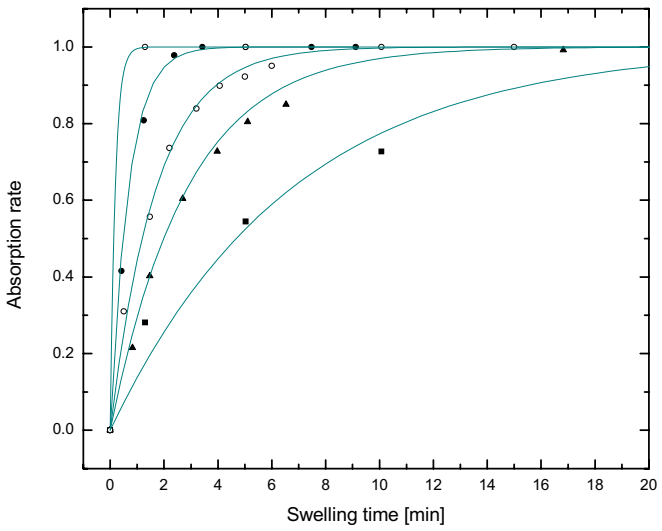

Figure 3.48.

On modelling absorption kinetics of hydrogels by Fick's law.

Dots represent the measured data and lines translate the model curves arising from the direct application of Eq. (3.17).

A remark should be made about the absorption medium. The expression derived for the swelling rate constant *k* is valid for synthetic pore fluid. The chemical properties of the fluid medium may govern the osmotic pressure, which is the driving force for the fluid uptake. The hydrostatic pressure acting on the polymer surface may also have a relevant effect on the absorption coefficient. In principle, the depth of the liquid-solid system should affect the swelling time, as the pressure increases, while not affecting significantly the absorption capacity. For the purpose of simplicity, the model was restricted from the previous parameters.

3.4.6. Mathematical derivation of superabsorbent volume in time

The purpose of this section is to establish a mathematical expression capable of predicting the volume generated by the hydrogel expansion with time, as function of the dispersion of the particle size of superabsorbent polymers. The initial state may be expressed by the sum of volumes calculated from the initial particle size distribution, which relates a given universe of particles with their geometrical properties, e.g., the volume or diameter. This is valid for a general set of particles with known size. Then, it seems feasible to relate each particle with a growth function, which is able to augment the volume for each instant of time *t*. Hence, a Taylor series may be use to compute continuous cycles of Eq. (3.17), in order to calculate the sum of volumes at a given dimension of time. Such expression should be therefore time-dependent and diameter-dependent. By combining the Fickean law with the pseudo volume distribution function arising from the PSD of the polymer, the expression may be written in the general form as:

$$F(t) = \int_0^{\infty} g(\phi, t) \cdot f(\phi) \cdot dt \tag{3.19}$$

The function *F(t)* defines the sum of volumes for a given particle size distribution, and thus, is dependent of the occurrence of each diameter of a universe, as given by eq. (3.14). The function g(x) translates the evolution of each volume as the pore fluid is absorbed as defined by eq. (3.16). Since $Q_{máx}$ is also diameter-dependent, a relation between the size of each particle and the maximum volume of fluid uptake needs to be found. According to the experimental data, it is possible to correlate the maximum growth with the particle diameter. Hence:

$$Q_{máx} = 13.462 \cdot \phi^{\,3.146} \tag{3.20}$$

The function *F(t)* can now be written in a form of Taylor series:

$$\begin{cases} t = 0 & V_0 = \int_0^{\infty} (Q_i \cdot v_i) \cdot dv \\ t > 0 & V(t) = \sum_{t=0}^{\infty} \left[\int_0^{\infty} (Q_i \cdot v_i) \cdot \left[Q_{máx} \cdot (1 - e^{-kt}) \right] \cdot dv \right] \end{cases} \tag{3.21}$$

At a given instant, the now designated *porosity model function* can be set up to determine the sum of the total volume that grows in the system. In the following, an example is given with the computations.

Let the universe be defined by a system of two diameters of 50 and 100 µm, occurring in equal frequencies. The total volume of this universe at the initial state is about 0.71 cm3. The resulting particle count leads to about 1,21x106 particles in the system. Figure 3.49 shows the results of the simulation of this system during the first 20 minutes. It can be seen the effect of the polymer concentration on the overall volume uptake in respect with the same system comprising unique particle clusters. The presence of 50% of particles with cluster D50 does not significantly affect the absorption kinetics of the system with cluster D100. If the concentration of D50 particles increases, the curve D50+D100 approaches the curve representing the cluster D50. This finding is particularly important, since the size of smaller particles may be of less significance if a low concentration of higher diameter particles exists in the system.

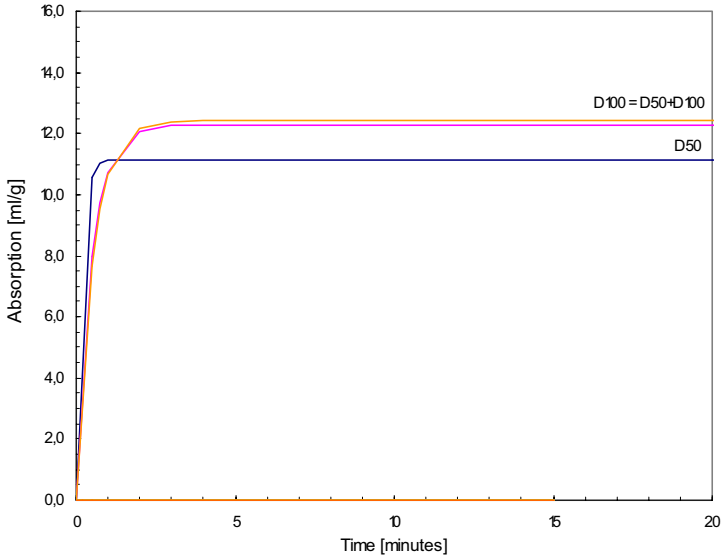

Figure 3.49.

Simulation of absorption kinetics for systems with particles of 50 and 100 micron.

Now, it is possible to predict the superabsorbent expansion, for specific particle size distributions and predict the initial porosity of each particular system on cement-based materials at early-age. In the following example, various PSD profiles, including the PSD presented in the first section, are plotted against time. In addition, a simulation on the absorption kinetics of two systems is

performed in augmented reality, which essentially consists in randomly placing of spheres in space despite of the real spacing of particles in a formal volume. This distortion enables the representation of individual particle and the tracking of the volume change within a reduced time scale.

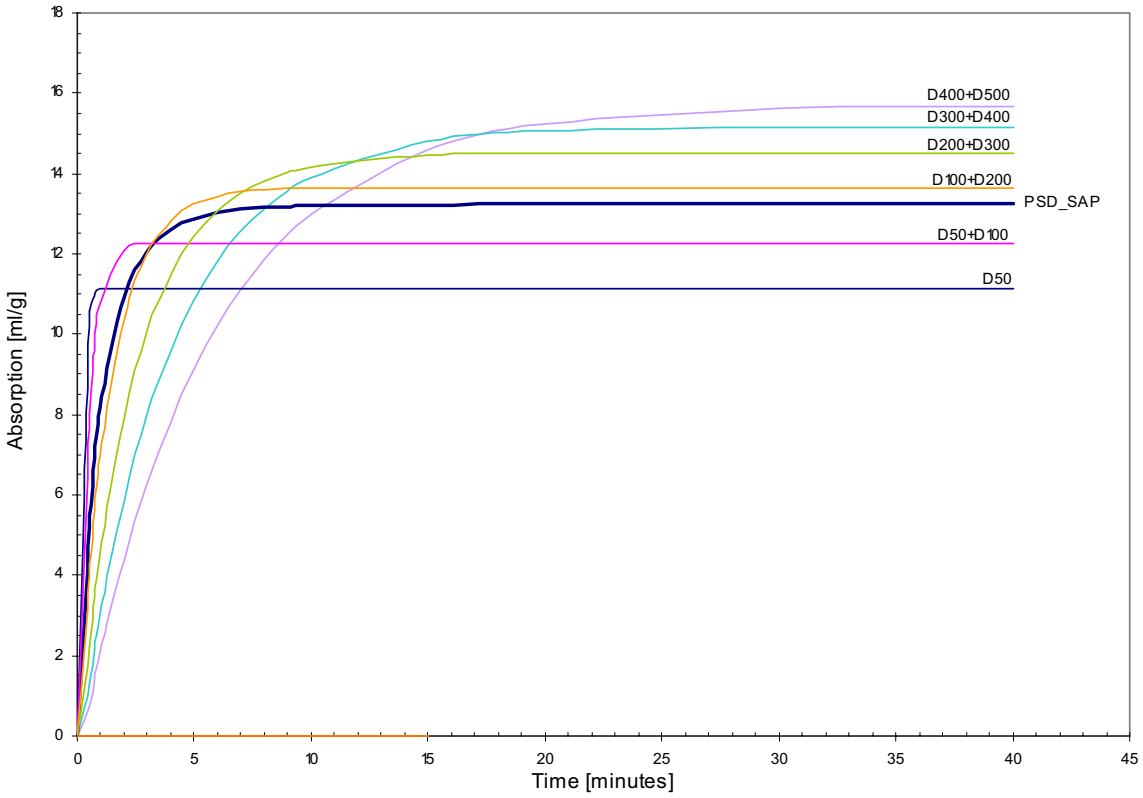

Figure 3.50.

Simulation of absorption kinetics for SAP systems with varying PSD, including the global PSD of the superabsorbent, as determined in section 1. The PSD profiles include unique particle clusters with equal frequency. A simulation on the absorption kinetics performed on different systems is shown below in augmented reality.

System: D50+D100

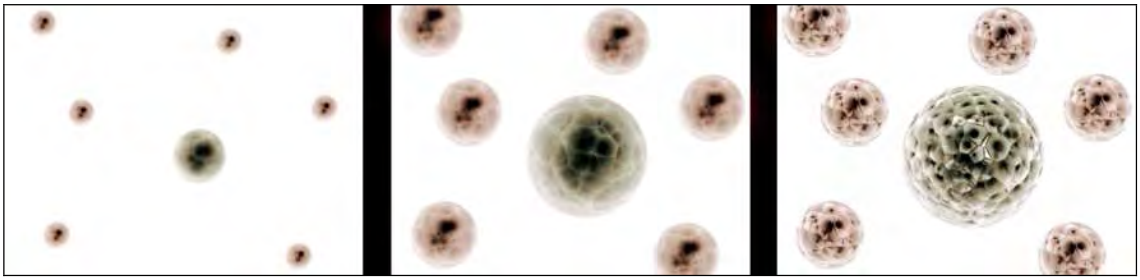

Time: 0 sec Time: 1 min Time: 5 min

System: D50+D100+D200

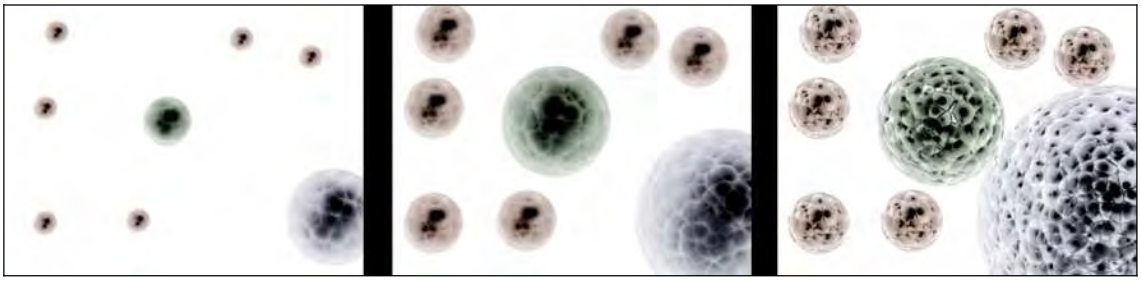

Time: 0 sec Time: 1 min Time: 5 min

3.4.7. Final remarks

The method proposed for the determination of superabsorbent polymer absorption may be used to quantify specific liquid phases into the cross-linked network of hydrogels. The measuring accuracy was improved in relation with former techniques used to describe the investigated parameters. Because gravimetric techniques may take into account the physical water at the particle interstitials, it may lead to higher inaccuracy of the real fluid absorption by the hydrogel. In addition, the lower the particle size of the polymer particles, the more surface zone will be laid open to Van der Waals forces, inducing higher uncertainty on the quantity of water absorbed, due to water fixation at the interstitials.

Fick´s law of diffusion may be applied to describe the kinetics of superabsorbent absorption. A remark should be made about the expressions derived for pore fluid. In the experiments, synthetic pore fluid was used to follow the volume change. The chemical formula of the real pore fluid is highly dependent on the cement-based system and especially on the dissolution of cement in the first few minutes after water addition. The amount of water added to the system will determine the concentration of the different ions for a given cement type. For example, in the case of high performance systems, where the water to cement ratio is typically below 0.36, the concentration of salts may increase, leading to lower absorption capacity.

From the findings, it is clear that the particle size influences the rate of absorption and the maximum absorption capacity, whose were shown to have a non-linear relationship with the particle diameter. The absorption capacity is higher for increasing particle diameters. A power relation gives a high correlation coefficient to the analysed data.

The desorption kinetics require further research. The preliminary tests indicate that volume stability of superabsorbent polymers is highly dependent on the range of the vapour pressure, showing slow kinetic change in respect with the absorption kinetics in fluid medium. This study is presently being carried out, and it is expected that in the fall of 2009 it may be concluded.

3.5. Water-entrained cement-based materials by superabsorbent polymers: On the fundamentals…

3.5.1. Abstract

The use of superabsorbent polymers in cement-based materials is focused in the mitigation of autogenous phenomena. Hence, by providing the necessary water to control the volume change occurring at early-age, the deformation of cement-silica paste is controlled, as measured by linear displacement methods. The mechanisms of internal curing in high performance cement-based materials are poorly understood. The present study will bring into perspective several aspects related with the water movement from superabsorbent polymer particles with varying diameter size to the surrounding cement paste, by examining the water state in water-entrained and non water-entrained cement-silica pastes. The effect of size of superabsorbent polymer particles on autogenous deformation is analysed by linear dilatometer measurements and the relation between expansion and shrinkage with the water state in time is discussed. The results indicate that superabsorbent polymers are able to imbibe the bulk paste, but the particle size may have significant effect on the subsequent deformation. It is proposed that mechanical effects such as self-restraint of the pore structure may play an important role as governing mechanism in the course of the early-age deformation, after capillary suction and internal curing. As a consequence, it may be that the internal curing water may be partially kept in the superabsorbent during longer periods while diffusion to the bulk cement paste is finalised.

3.5.2. Introduction

The use of superabsorbent polymers in cement-based materials is a fairly new technique in concrete technology and it may be used as mean to eliminate autogenous deformation. In the literature review, it was pointed out that the mechanisms of internal curing are poorly understood. Most of the knowledge about the functioning of superabsorbent in cement-based materials is based in the work by Ole Jensen and Hansen[123, 124]. The simple approach of adding internal curing water to equalise the chemical shrinkage of the system is, for practical purposes, a very straightforward mean to properly design the mix proportions of water-entrainment cement-based systems. However, adding to the uncertainty in the real chemical shrinkage occurring in the system, witch may be overestimated in low water and low porosity systems there is also the problem of the real distance that water paths can overcome in the course of hydration, especially when the hardened material has developed capillary discontinuity. According to Bentz and Snyder[129], the distance from the internal curing agent that is protected by internal curing water may be in the order of a few micrometers. Thus, the spatial network of the reservoirs is considered to play a relevant role in the process of water release or desorption. Accordingly, well dispersed and small particles spread out through the matrix may increase the efficiency of internal curing by increasing the protected volume. In addition, Østergaard[191] suggested that the protected distance may be of 300 μm, in his experiments with X-ray absorption technique, which was used in the validation of the water transportation distance modelled with the HCSS model. However, it is also recognised that the measuring accuracy in a given specimen may be within 100 μm. Lura et al.[192] have studied water transport from saturated pumice aggregates to hardening cement paste, concluding that the distance covered by the internal curing agents is at least of 4 mm during the first days, the time being omitted. Moreover, the author suggests that the amount of water released by the internal curing

agent, rather then the spatial distribution is the crucial factor to avoid early-age self-desiccation shrinkage.

This raises the problem related to the efficiency of superabsorbent in respect with the size of the particles, the later determining the water transportation distance. In this study, the effect of the particle size of superabsorbent on the autogenous deformation and RH-change is analysed. If the previous argumentation is valid, smaller diameter sizes of swollen SAP may improve the curing process, by increasing the protected volume paste. It is proposed that the amount of water and the spatial distribution are not the unique parameters governing the kinetics of desorption, the physical properties and the state of the matrix governing the deformation after internal curing.

3.5.3. Materials and methods

The systems analysed in this study comprehended a reference paste, which is a SF-modified at 15% SF-addition and three water-entrained pastes with varying superabsorbent particle size. The basic water to cement ratio was 0.30 for all mixtures. The entrained-water ratio was kept constant at 0.05. Superplasticizer was added at a rate of 1% by wt-% of cement to all mixtures, to ensure adequate workability.

Autogenous deformation and RH-change measurements were performed to all mixtures, according to the same procedures reported in the previous section.

3.5.4. Results

Autogenous deformation

Figure 3.51 shows the autogenous deformation of the studied hardening SF-modified pastes with varying size of superabsorbent polymer particles up to two weeks in sealed and isothermal conditions. At no superabsorbent addition, a significant autogenous strain is observed during hardening and subsequent secondary reactions. After 2 weeks, the measured autogenous strain of the non water-entrained system is approximately of 3400 microstrain. The water entrainment based on superabsorbent addition seems to be effectively counteracting the shrinkage development during early-age, which is seen to have an inverse relationship with the particle size of superabsorbent. However, the variation of the polymer particle size has a considerable effect on the measured deformations. As expected, for the studied amount of water entrainment, the water-entrained systems showed an early-expansion, which will be dealt in more detail further on discussion.

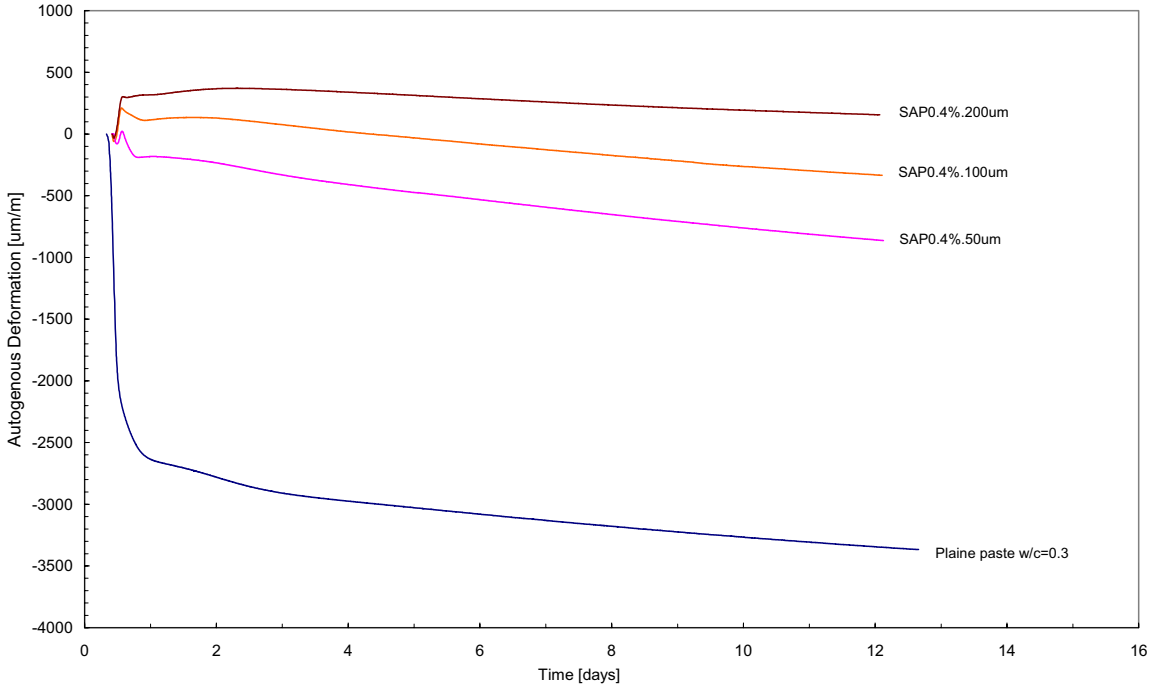

Figure 3.51.

Autogenous deformation of SF-modified pastes with different size of superabsorbent polymer particles. The internal curing water was added to the system according to an absorption capacity of 12.5 ml/g of dry gel. Basic water to cement ratio was of 0.30. Temperature: 20 ˚C.

After this short expansion, the water-entrained systems experience different degrees of shrinkage. For the particle size of 200 µm, it is observed that the deformation rate is lower than the measured rate for the lower diameters. At 2 weeks sealed hardening, the measured strain is of about 900 µs, for the system with polymer particles of 50 µm. The absolute difference in respect with the system with particle size of 200 µm is of about 1000 µs.

Internal RH-change

Figure 3.52 shows the autogenous RH-change of hardening SF-modified pastes with water-entrainment with varying size of superabsorbent polymer particles. At no superabsorbent addition, a significant drop in the RH is observed during hardening. Internal curing by superabsorbent could efficiently maintain the level of internal relative humidity at more than 95%, up to 1 week sealed hardening. The variation of the size of the polymer particles does not affect the RH-change of the water-entrained mixtures, from where it should be concluded that the particle size of the polymer is independent from the RH-change.

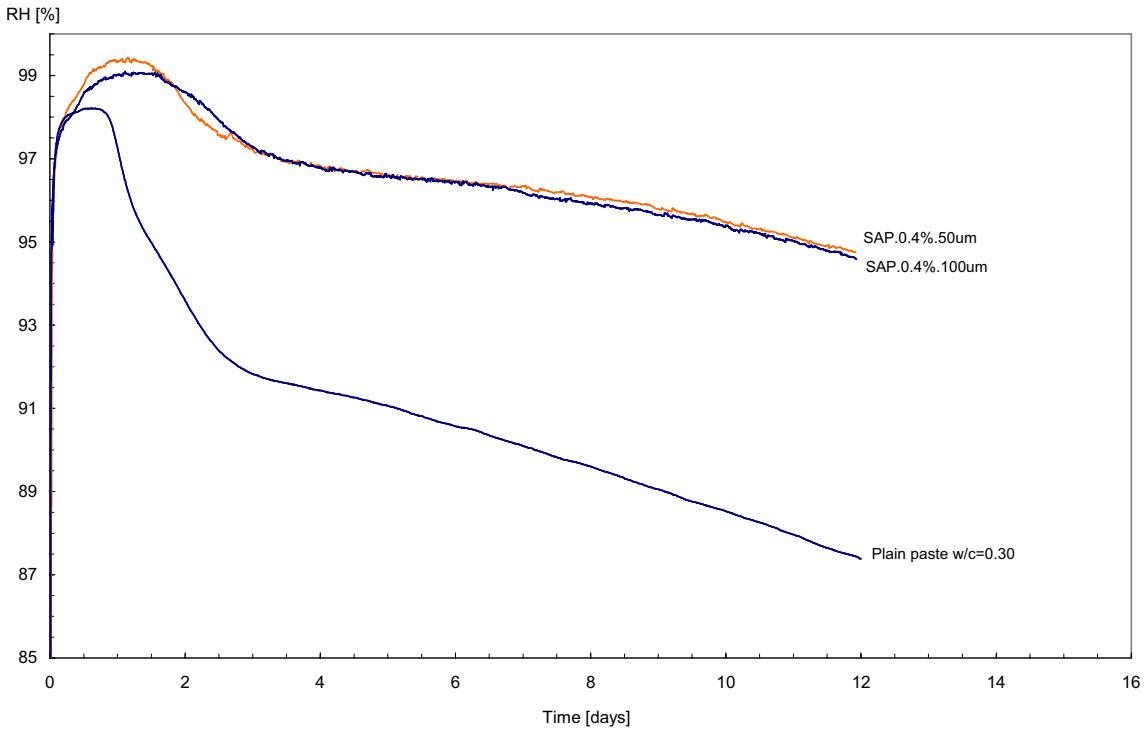

Figure 3.52.

Autogenous RH-change of SF-modified pastes with different size of superabsorbent polymer particles. The internal curing water was added to the system according an absorption capacity of 12.5 ml/g of dry gel. Basic water to cement ratio was of 0.30. Temperature: 20 ˚C.

After 2 weeks of sealed curing, the measured RH is approximately 94%. The water-entrained system with an average size-fraction of 50 micron desiccates to RH-values near of 90% at 28 days in sealed hardening. At the same age, system P1, with 15% added-silica fume self-desiccates to a RH-value near of 75%. Reproducibility for the experimental results may be found elsewhere in the literature[186].

3.5.5. Discussion

The rate of deformation decreases systematically as the particle size of the superabsorbent polymer particles increases. This observation suggests that the pore system of water-entrained pastes may be inducing different degrees of restraint in the system, brought out from the different changing microstructures. The data sets of the water-entrained pastes were normalized by the last measurement, which occurred about 2 weeks after mixing (see Figure 3.53). It is clear that the lower SAP particles show less efficiency in “controlling” the autogenous negative strain. It is also interesting to note that apparently, the time of the secondary reaction governing the strains is postponed to a later period, as the particle size of superabsorbent increases.

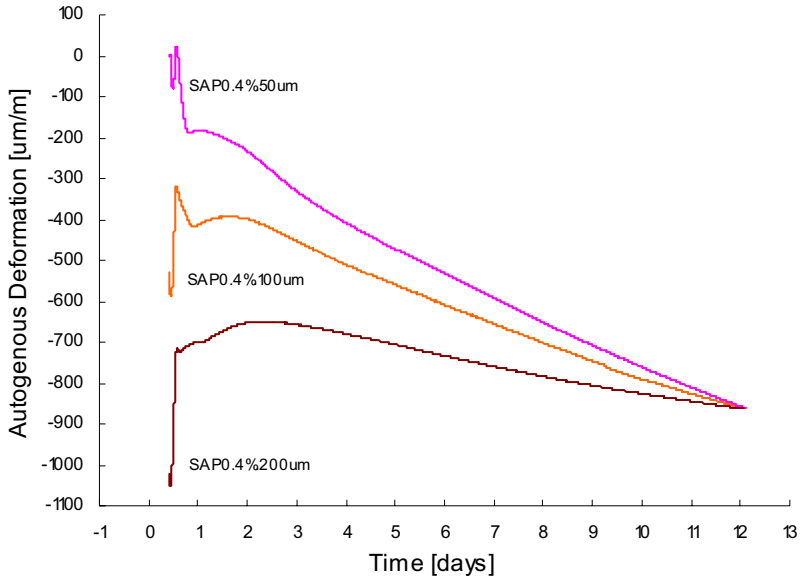

Figure 3.53.

Normalized data sets of the autogenous deformation measurements of water-entrained SF-modified pastes.

This suggests that self-restraint of the bulk paste may be occurring and that is diameter-dependent (or pore structure dependent). In addition, the early expansion is also significantly different for the studied SAP particle sizes. The higher expansion is noted in the water-entrained paste with SAP particles of about 200 micron. After setting, it is denoted a slight negative strain preceding the early-expansion. It is possible that the mechanism at this point may be capillary suction which is the driving force for the water movement from the hydrogel, thus, activating the internal curing process within the curing agent. It would also constitute a possibility that a higher number of water sites might potentially enhance hydration of the bulk paste, according to the surface area effect. However, this should not be the case, since it would result in a higher deformation rate, when compared with the reference system. Lura et al[138] have also studied the effect of the particle size of superabsorbent on the autogenous deformation of cement paste with w/c of 0.30 and 20% of silica fume. The results, while being consistent with the present work, don't lead to such deviation in terms of absolute difference in the measured deformation. It is possible that the selection of time zero in this particular case may be on the base of the given explanation for this phenomenon, which is in contradiction with the previous arguments.

Furthermore, the growth of superabsorbent polymers in synthetic pore fluid was recently studied by means of optical microscopy (see section 3.4), being concluded that both absorption rate and absorption capacity of the superabsorbent polymer particles are size-dependent. Thus, the lower absorption denoted by SAP particles with 100 and 50 µm in respect to the diameter size of 200 µm, may partially explain the lower expansion experienced by the water-entrained pastes, since lower particles may have less internal curing water within the cross linked structure. On the other hand, desorption of water or pore fluid from the SAP particles should be faster for the lower diameters. It is not obvious from the results that the expansion rates are significantly different. Nevertheless, it seems that internal curing is closely related with the measured expansion. Subsequently, the hydrated paste may have sufficient capacity to self-restraint. It is suggested that superabsorbent particle size may affect the volume change of SF-modified cement paste within the secondary reaction via pore structure. However, another mechanism may play an important role: the rate of desorption in the diffusion mode versus capillary suction. This idea is equivalent to sustain that while the rate of water diffusion is higher than the rate of pozzolanic activity from the silica fume,

the strains in the system may be equilibrating. The diffusion rate may be harshly diminished if the percolation of the system is broken. This may be within the first 24 hours of sealed hydration, as supported by D.P. Bentz.

If the previous discussion is true, then an air-entrained SF-modified paste should be able to "control" autogenous deformation as well. If the pore volume created by the superabsorbent through the macro inclusions could be simulated without water, then a system without curing water can be created to simulate the behaviour of superabsorbent pastes without water movement, which is the base-assumption for existing self-restraint by SAP-pores at early-age. In order to investigate this phenomenon, a system with air-entrained mixture was performed. The results are shown in Figure 3.54.

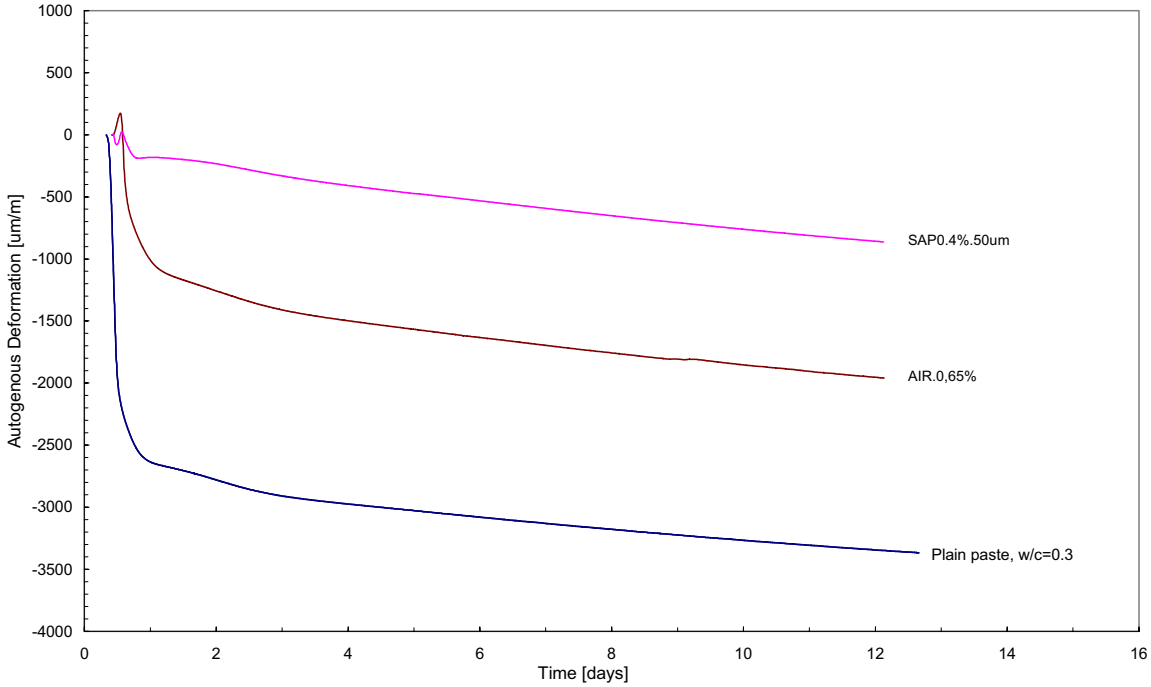

Figure 3.54.

Autogenous deformation of SF-modified pastes with superabsorbent polymer and air-entraining admixture. The internal curing water was added to the system according an absorption capacity of 12.5 ml/g of dry gel. Air-entrainment was performed by wt.-% of cement. Basic water to cement ratio was of 0.30. Temperature: 20 °C.

It can be observed that air-entrainment was able to partially "control" self-desiccation by self-restraint from the macro pore structure. This is noted even in the first reaction, as seen by the first slope of the SF-modified air-cured curve. The measured negative strain is higher in the air-entrained mixture in respect with the water-entrained paste. This may be due to (air bubbles blowing up: find scientific terminology). It should be pointed out that the air pore volume is different from that of the SAP pore volume. The air bubbles generated may consist in a substantially lower diameter in comparison with the partially swollen superabsorbent polymers. Nevertheless, after the third day sealed hardening, there is no major difference on the strain development, by comparing it to the system with the lower SAP particles, in this case of about 50 micron at dry state. Thus, it seems that self-restraint of the system may be the governing factor at this point.

Furthermore, imaging by means of SEM was performed for a water-entrained and an air entrained system, as shown in Figure 3.55. It may be seen that the resultant macro inclusions in the water-entrained system is significantly bigger from that of air entrainment. The later, consists in fine spherical dispersed air-volume throughout the section, with an average size comprehended between 10 and 100 μm, although pores up to 200 μm may also be found. In relation to the microstructure of the water-entrained system, the macro porosity is ranging between 100 and 200 μm. The microstructure of the air-entrained mixture should then approximate the microstructure of the lower size-range of superabsorbent, which was of 50 micron.

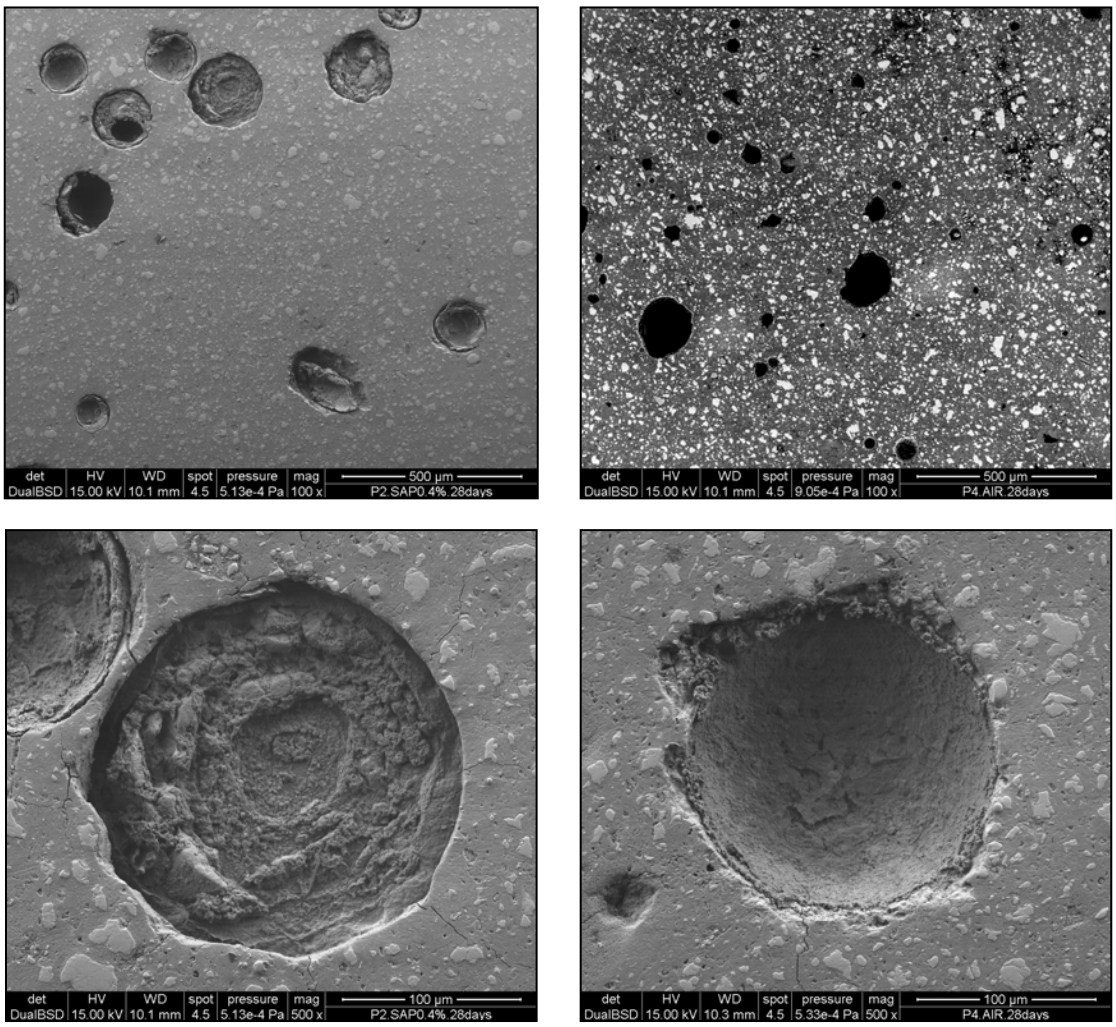

Figure 3.55.

SEM images of water and air-entrained mixtures. The macro inclusions refer to the system SAP.0.4%.100.

3.5.6. Final remarks

Autogenous deformation of water-entrained pastes was analysed in terms of dependency from the particle size of superabsorbent polymer particles. It is concluded that the size of the polymer particles may have strong effect on the courses of autogenous strain. At least three mechanisms are most probably interacting during hardening of water-entrained pastes: capillary suction and diffusion mode within internal curing, and self-restraint of the bulk paste, expressed by the macro

pore structure of water or air-entrained systems. The following sketch is proposed to integrate the referred mechanisms in the course of autogenous deformation of water-entrained SF-modified pastes:

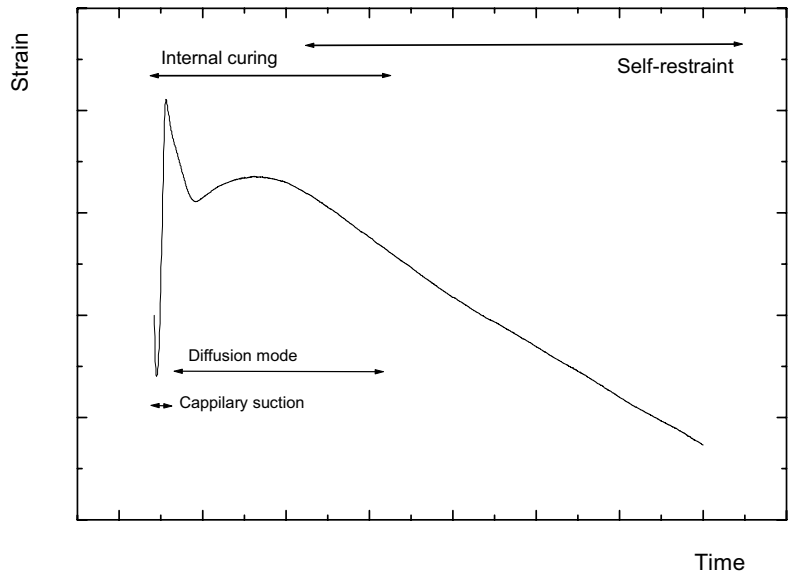

Figure 3.56.

Proposed mechanisms for water-entrained cement-based materials by superabsorbent polymers.

The mitigation of autogenous deformation in SF-modified cement-based materials is a complex phenomenon. The extent of internal curing may not be not fully related with the autogenous relative humidity change, as seen by the RH-change of water-entrained pastes with different diameters. The more internal curing is provided to the system, the more macro inclusions may be inducing self-restraint on the paste by pore structure. This will be surely governed by the diffusivity of the bulk paste, which fundamentally depends from the amount of silica fume introduced in the system.

Furthermore, an obvious consequence of a larger macro pore structure is most probably the loss of strength of the material. In principle, the bigger the macro porosity is, the higher is risk to micro cracks develop through the system, being preferential held by the macro inclusions. On the other hand, if the diameter is kept below 100 μm, the strength potential of water-entrained cement-based materials should be most prominent. Moreover, in respect with the microcracking, the smaller macro inclusions should held higher concentration of tension due to the smaller radius, which, on the other hand, will be localised at more discrete points due to relation with the specific surface area. For the same density, smaller diameters will result in shorter distances between macro inclusions, leading to reduced stresses at each site. This aspect, together with the study of microcracking in SF-modified cement pastes is required in further investigation. It is suggested that a smaller pore structure should result in less cracking events, since it induces multi-point stresses upon the bulk paste, leading to a different stress concentration if a lower number of pores exist, as in the case of bigger SAP particles being used.

The fact that the paste is self-restraining is not negative, if the stress generated in the mesostructure of the system does not induce risk of microcracking. This is still to be determined. The water located at the inclusions may take many months to diffuse, especially if a diffusion mode

coefficient is assumed. For example, this can favour growth of new products towards the SAP pores, by inverse matter transport, which may function as nucleation sites. Eventually, if the SAP-pores are little enough further hydration may even close the pore at later ages. It is well known that the micro porosity may have changes in a long term.

Finally, and for practical purposes, the specific target when designing the material under the predicted service conditions should determine the strategy for prescribing a range of superabsorbent. As an example, if freeze-thaw resistance is required, it may be that the higher size fraction of superabsorbent may be preferable. When the target design is strength, smaller particles should be use to internally cure high performance cement-based materials.

4. Internal Curing by Fine Aggregate Particles

4.1. Internal curing by fine aggregate particles. I - Principles and theoretical background.

This section describes a new concept for partial prevention of self-desiccation in hardening cement-based materials. The concept consists in the use of fine aggregate particles, as a vehicle to "water fixation" at interfacial transition zone (ITZ), which consists in regions with higher water to cement ratio in respect with the bulk regions within the paste volume. The power relation in respect with the change in the specific volume that arises from the variation of fine aggregate particle size is associated to the formation of correspondent ITZ regions that may actively contribute to control self-desiccation and autogenous deformation at early-age. This section uses Powers' model as basis for the development of a simplified paste-mortar hydration model in cement-based systems, forming the first part of a series. In a second part, experimental observations will be presented.

4.1.1. Introduction

Recent research focused in the comprehension and mitigation of self-desiccation phenomenon in high performance concrete[87, 6]. For cement-based materials with low water to cement ratio, in the range of 0.19 and 0.36 and with addition of silica fume, internal curing may be required to control the early-age deformations occurring in the bulk paste. This essentially consists in water reservoirs, whose fundamental purpose is maintaining internal relative humidity at high levels and consequently prevent self-desiccation. The main strategies available to internal cure concrete and thus, avoid cracking are known: by the addition of lightweight aggregate, LWA[122] or by introducing superabsorbent polymers, SAP[123]. However, some macro and micro structural consequences arise from these techniques. For example, in the case of LWA addition, it is well known the practical difficulties in controlling consistency and a significant reduction on the strength of the material and in the elastic modulus may be found. By other hand, water-entrainment by superabsorbent may have microstructural consequences, since the introduction of macropores in the system can be a potential source of loss in strength of the composite material, referring to the water-entrained cement paste.

This section describes a new strategy for partial prevention of self-desiccation, taking advantage of the high surface area resultant from the selection and introduction of fine aggregate particles in the formulation. The specific design of the diameter size integrating the aggregate phase in a three component cement paste may lead to the formation of pre-designed quantity of ITZ regions, which essentially consists in higher water to cement ratio in respect to bulk cement paste. The hydrating bulk cement paste will require water from the ITZ volumes as soon as the water at the bulk volume is used up, and thus, further maintaining the requirement of higher relative humidity. This method may be then combined with other strategies for internal curing of cement-based materials for full prevention of self-desiccation. A brief introduction of the physical properties of ITZ is presented in the following section. Literature can give more comprehensive information about these aspects[193-198].

4.1.2. Physical properties of fine aggregate particles and Interfacial Transition Zone in cement-based materials

Fine aggregate particles are added to cement-based materials in specific amounts, usually within a size distribution comprehended between 75 and 4000 μm. In high performance cement-based

materials, the aggregate phase may be at the order of 50% by volume, from which the fine aggregate may be of about the half. The theoretical density of fine aggregate typically used in cement and concrete composite materials is of about 2.65 g/cm^3, geometry and shape of aggregate particles being highly heterogeneous. While crystals may vary upon the specific growth conditions within the nano and micro meter scale, in an order of magnitude higher, the geometry of fine aggregate may be considered to have "nearly" spherical shape (Figure 4.1).

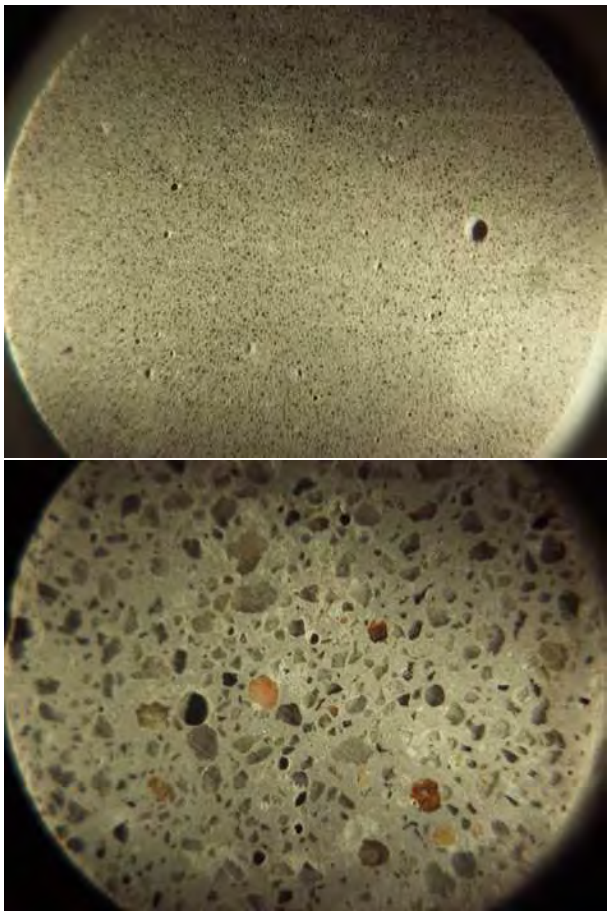

Figure 4.1.

Optical microscopy polished sections with aggregate particles within the range of 75 and 4000 μm, in cement paste bed. Image length is approximately 14 mm.

Up frame: aggregate particles of about 90 μm.

Low frame: aggregate particles in the range of 500 and 1000 μm.

Packing of cement-based materials with fine aggregate particles may be compared to randomly filling of a box with spheres of different sizes. At a given aggregate to paste ratio, the paste volume should be sufficient to involve the aggregate, in order to assure appropriate binding of the composite material. For the same volume fraction, the finer is the diameter of the particle, the more specific area will interact with bulk cement paste by unit volume (see Figure 4.2). The fundamental consequence of this geometrical feature is that the number of ITZ regions, defined as the volume or area of paste interacting with the aggregate surface areas, will accompany the number of particles in the system. In the literature, interfacial transition zone is defined as the region of the cement paste around the surface of the aggregate particles[195]. In a mono-sized aggregate system, by lowering the particle size from 500 to 125 micron is equivalent to increase 4 times the specific surface area of the aggregate. For an aggregate to paste ratio of 1 by volume, this is equivalent to create 125 times more ITZ regions, if these are assume to match the surface area of aggregate particles.

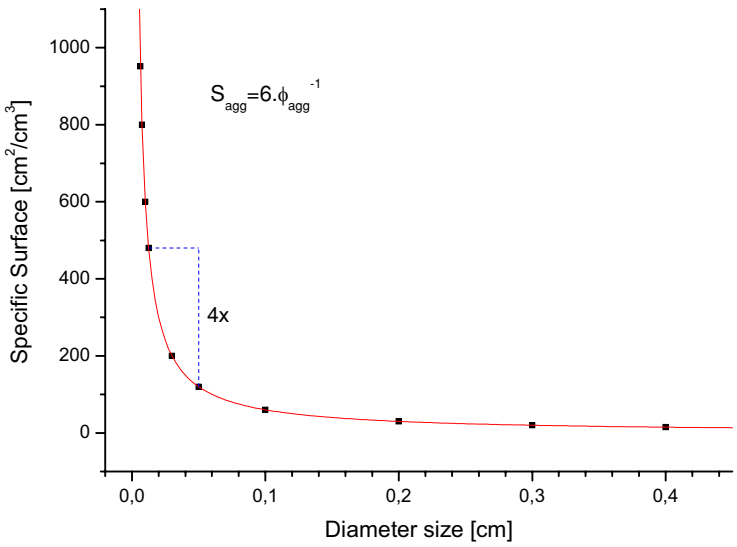

Figure 4.2.

Relation between particle size and the specific area of aggregate in the system.

Microstructure of interfacial transition zone is of major importance when modelling the basic characteristics of cement-based materials. The physical properties of aggregates and cement, together with the chemistry of admixtures and particularly the water to cement ratio, form the principal factors when analyzing ITZ[199, 195]. From a microstructural point of view, the ITZ region is highly heterogeneous material with random porosity and packing. Microstructure analysis by backscattered electron images of polish concrete samples show that ITZ reveals higher porosity regions, decreasing towards the bulk cement paste[167]. A. Delagrave et al.[193] measured the double of porosity by mercury intrusion, in a cement-based mortar with 50% of aggregate and low water to cement ratio (0.25), in respect with the equivalent cement paste. On the other hand, this region of increased porosity may be significantly diminished by the migration of ions in the course of hydration of clinker minerals. Although literature can not accurately define the limits of ITZ, previous work indicates that the depth of ITZ can be on the order of size of the largest cement grain (up to 100 μm), as supported by K.L. Srivener and K.M. Nemati[200, 196]. However, work by D.P. Bentz et al[201, 202] indicates that the thickness of ITZ may be as low as 10 to 20 micron. In addition, P.J.M. Monteiro et al[203] supports that the thickness of the mortar-aggregate transition is larger in the presence of bigger aggregate particles and decreases with the lowering of water in the system.

Furthermore the presence of silica fume in high performance cement-based materials with low water to cement ratio may lead to the refinement of the paste-aggregate transition and therefore, a pronounced reduction in both depth and porosity of the ITZ is expected[200]. However, systematic work on the physical characteristics of ITZ in cement-silica systems with fine aggregate particles and particularly at early-age cannot be found in the literature.

From the perspective of strength design of cement-based materials, it is often claimed that ITZ represents the weaker link in concrete[198]. On the other hand, ITZ may be used as mean for transport of matter[193], making ITZ a valuable “natural” and “independent” material for concrete design with different target performances. Thus, the key aspect of ITZ is that it comprises a “unique” porous medium from that of the bulk cement paste. This is mostly due to the so called

"wall effect", as illustrated by K. Srivener[195]. Aggregate particles may represent several orders of magnitude the size of an average cement grain, which in turn typically ranges from less than a micron up to 100 micron in size. Only by chance, perfect packing of cement particles around an aggregate particle as represented in Figure 4.3 could occur. Thus, an important consequence of the existence of a transition zone is that water to cement ratio in bulk paste may be affected by the increased porosity at these regions. Therefore, it is possible that the water to cement ratio at ITZ is higher in relation with the bulk cement paste, the porosity being initially occupied with water.

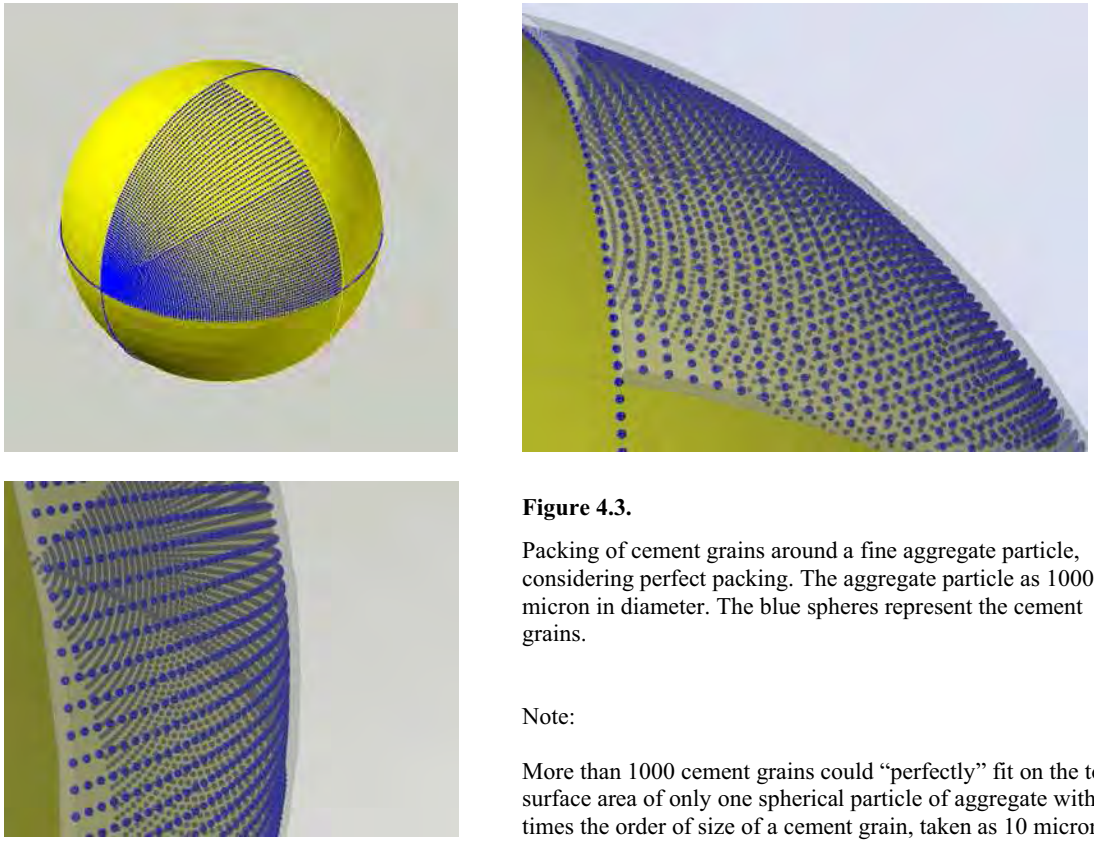

Figure 4.3.

Packing of cement grains around a fine aggregate particle, considering perfect packing. The aggregate particle as 1000 micron in diameter. The blue spheres represent the cement grains.

Note:

More than 1000 cement grains could "perfectly" fit on the total surface area of only one spherical particle of aggregate with 100 times the order of size of a cement grain, taken as 10 micron.

"Perfect packing", or closest packing as postulated by Kepler, stands on the idea of the natural hexagonal configuration in the infinite Euclidean space that leads to the highest density, or in the case of cement-based materials, the most effective way of positioning both aggregate and cement grains in space. The idea of that cement grains may assume an ordered spatial position around any aggregate particle is far away from the real packing of particles in cement-based materials, but yet, if the former packing configuration could occur and the depth of ITZ is assumed as the average size of a cement grain, then the volume of water at ITZ sites can be foreseen. This is done in accordance with Eq. (4.1), from where Figure 4.4 is developed. Full derivation of Eq. (4.1) is presented in appendix to this thesis (Appendix A).

$$V_{w,ITZ} = V_{agg} \cdot \left(6\chi + 12\chi^2 + 8\chi^3\right) - \frac{\pi^2}{6}\phi_{cem}{}^2 \cdot \left(\phi_{agg} + \phi_{cem}\right) \tag{4.1}$$

To calculate the ITZ volume, a mono-sized cement grain with spherical shape is assumed to be ordered around the aggregate particles according to the hexagonal configuration and by considering

that the average cement grain is in the order of size of the ITZ. It is interesting to note that the ITZ volume, created according the number of aggregate particles in the system overrides the total volume of the composite material at the diameter of 75μm, for an aggregate concentration of 30% by volume. The physical meaning in this hypothetical scenario is that the ITZ volumes are overlapping below a threshold value corresponding to a particle size diameter of 75μm, resulting that the total volume of paste could be ITZ volume, and that no bulk paste may form. In fact, computer simulations show that the maximum random packing density obtained in a granular material is not greater than 64%[204]. Yet, in the case of cement-based mortars, which are subjected to high-speed mixing and vibration, where the initial state of the composite is characterized by solid and "liquid" phases, accordingly, the aggregate and the paste volume fraction, the packing density may be substantially higher in respect with the random packing density of a mono-sized granular material. In Figure 4.4, it is further seen that the variation of the average particle-diameter of cement results in an increment of the ITZ volume at each aggregate particle and consequently, ITZ water. A threshold value, or the lower limit for the particle size of the aggregate phase which makes possible the existence of both ITZ and bulk paste, is noted to be strongly dependent from the ITZ depth.

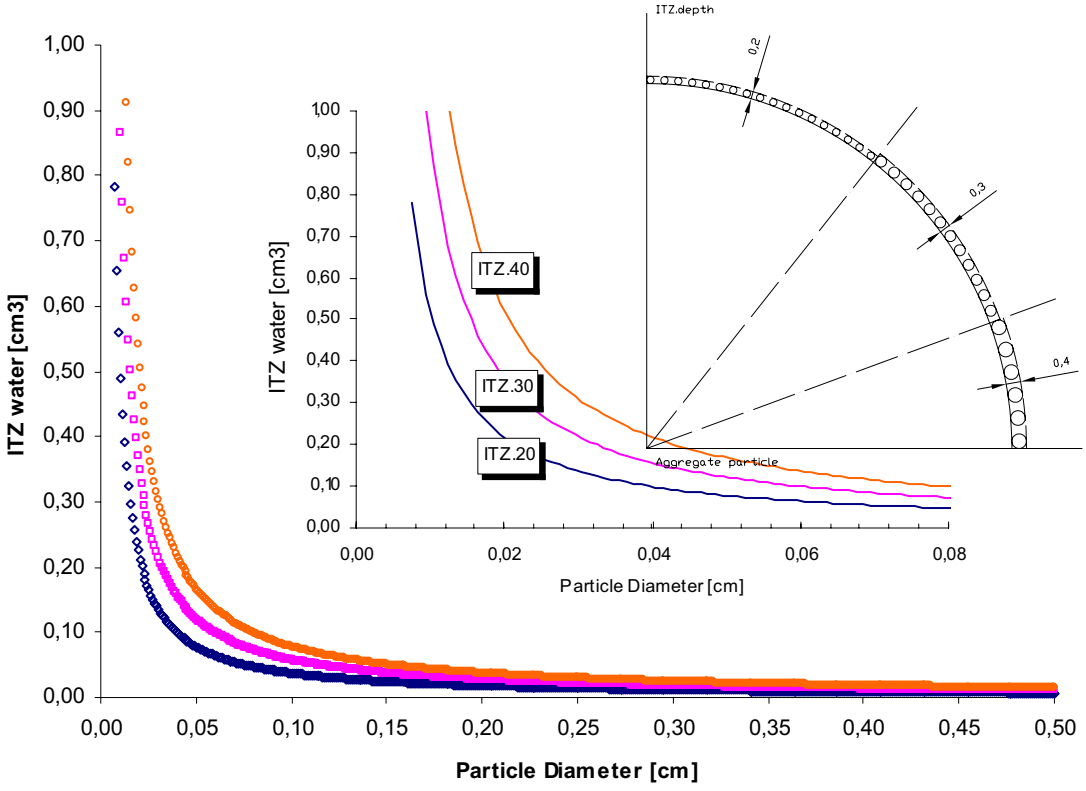

Figure 4.4.

Relation between particle size of aggregate particles and the volume-water at ITZ regions, according Eq. (4.1).

System physics:

V_{agg}=30 vol.-%, (w/c)=0.30

Model assumptions:

ITZ depth=ϕ_{cem}=20 μm, ITZ depth=ϕ_{cem}=30 μm, ITZ depth=ϕ_{cem}=40 μm

Furthermore, the proximity of aggregate particles is not being taken into consideration. However, the probability of nearest aggregates depends, among other parameters, of the aggregate concentration throughout the volume, which in this case was idealised to be of 30%. Nevertheless, the main point from the previous introductory statements is that a divergent modelling approach is required. In the following, a framework for the definition of ITZ volumes and the calculation of free water at ITZ regions is developed.

4.1.3. Definition of ITZ regions and derivation of free water volume brought out by wall effect

The previous discussion gave physical meaning to the idea of that lower aggregate particles can easily lead to increase the number of ITZ regions in the system, holding an higher w/c ratio in respect with the bulk cement paste. A 3-component model of mono-sized particles may be set up in order to define the ITZ volume, so that the knowledge of the water present at ITZ may be derived. The following assumptions are made: 1) the ITZ depth is defined as the average size of a cement grain, 2) the water to cement ratio at ITZ is dependent on the wall effect, which will be assume to be within 0.4 and 0.5 by mass, and 3) there is no overlapping ITZ regions in the range of 0 to 30% concentration of aggregate by volume.

To calculate the free volume of water at ITZ regions, it is necessary to determine the relation between water and cement at bulk paste and at ITZ regions. Thus, let $(w/c)_{bulk}$ and $(w/c)_{ITZ}$, be respectively the water to cement ratios of bulk cement paste and ITZ volumes, within the global water to cement ratio of the system. The volume of water at ITZ is governed by the depth of the transition phase d_{ITZ}, morphologically different from those at bulk because of a second parameter, the wall effect, W_{eff} and the size of the aggregate particles ϕ_{agg}, as expressed in Eq. (4.2).

$$V_{w,ITZ} = f\left(\phi_{agg}, d_{ITZ}, W_{eff}\right) \tag{4.2}$$

The constitutive volumetric equation that translates the volume phases in this tri-component mortar system is given by Eq. (4.3), where the V_i indices *w*, *c* and *agg* stand for the phase-volumes of water, cement and aggregate, the first two components comprising the paste volume.

$$V_t = V_{paste} + V_{agg} = V_w + V_c + V_{agg} \tag{4.3}$$

The existence of interfacial regions with a specific paste volume will be designated by ITZ volume paste, viz. V_{itz}. The ITZ-dependence from the particle diameter may be analysed by Eq. (4.4), where V_{itz} is seen to be function of the aggregate particle diameter ϕ_{agg}, the depth of the ITZ region, which is being defined as the average diameter of cement grains ϕ_{cem}, and the number of ITZ regions, n_{agg} which is given in units per volume [un./cm^3], and corresponds to the number of aggregate particles in the system. At a given concentration, this expression is derived with the same principle as shown in Appendix A.

$$V_{itz} = \frac{\pi}{6} \cdot n_{agg} \cdot \left[\left(\phi_{agg} + 2 \cdot \phi_{cem}\right)^3 - {\phi_{agg}}^3\right] \tag{4.4}$$

The total volume fraction correspondent to the cement paste may be now differentiated into two specific volumes, being namely the bulk paste, V_{bulk} and the ITZ paste volume, both comprising water and cement volumes, as shown in Eq. (4.5):

$$V_{paste} = V_{itz} + V_{bulk} = V_{w,itz} + V_{c,itz} + V_{w,bulk} + V_{c,bulk} \tag{4.5}$$

The next step in the calculation of the water volume at ITZ regions needs to take in consideration the wall effect, which is physically equivalent to assume a value for the water to cement ratio at ITZ regions, hence:

$$V_{w,itz} = V_{itz} - V_{c,itz} \tag{4.6}$$

$$\left(\frac{w}{c}\right)_{ITZ} \propto W_{eff} \tag{4.7}$$

In Eq. (4.7), W_{eff} represents the wall effect. For example, if the wall effect produces a loss in packing of 50%, the w/c ratio at ITZ is considered to be of 0.5, which is equivalent to have 50% water at ITZ regions (by weight). The knowledge of the bulk paste volume is now possible to derive by the simple mass transformation of the volumetric water to cement ratio, taken from the total volume that includes each constitutive volume-phase as defined by Eq. (4.5), hence:

$$\left(\frac{w}{c}\right)_{bulk} = \frac{V_{w,bulk} \cdot \rho_w}{V_{c,bulk} \cdot \rho_c} \tag{4.8}$$

As an example, let the system be defined by a unitary mass fraction between the aggregate and cement phases, the value for the particle diameter of the aggregate phase being attributed of 125 and 500 micron. The total mass of the system is 2.3 grams for an elementary volume of 1 cm^3. If a value of 0.3 is assumed for the water to cement ratio, the paste fraction is of 0.62 cm^3.

Table 4.1. Calculation of free water in a composite system of mono-sized aggregate and cement paste

Particle Average diameter		Number of particles	Volume Phases							
ϕ_{cem}	ϕ_{agg}	n_{agg}	V_{itz}	$V_{w,itz}$	$V_{c,itz}$	V_{bulk}	$V_{w,bulk}$	$V_{c,bulk}$	$\left(\frac{w}{c}\right)_{ITZ}$	$\left(\frac{w}{c}\right)_{bulk}$
[cm]		[un/ cm^3]	[cm^3/cm^3]						[wt-%]	
0,0020	0,0075	2,82E+06	0,64	0,38	0,27	-0,14	-0,08	0,05	0.45	-0,47
0,0020	0,0100	1,19E+06	0,45	0,27	0,19	0,04	0,03	0,13	0.45	0,08
0,0020	0,0125	6,09E+05	0,35	0,20	0,14	0,15	0,04	0,11	0.45	0,11
0,0020	0,0200	1,49E+05	0,21	0,12	0,09	0,29	0,18	0,23	0.45	0,24
0,0020	0,0350	2,77E+04	0,11	0,07	0,05	0,38	0,23	0,27	0.45	0,27
0,0020	0,0500	9,51E+03	0,08	0,05	0,03	0,42	0,25	0,29	0.45	0,28
0,0020	0,0750	2,82E+03	0,05	0,03	0,02	0,45	0,27	0,30	0.45	0,29

0,0020	0,1000	1,19E+03	0,04	0,02	0,02	0,46	0,28	0,30	0.45	0,29

According to Table 4.1, if W_{eff} is taken as 0.45, a system with aggregate particle size within the range of 125 µm will generate an ITZ volume of 0.35 cm^3, from which 0.20 is water. On the other hand, if the particle size of fine aggregate introduced in the formulation is of 500 µm, the resultant ITZ volume will decrease to 0.08 cm^3, from which 0.05 is water. The free water may be only part of the total water volume at ITZ regions, since physically adsorbed water and chemical bound water also exists in the paste at ITZ volumes. In addition, by analyzing further the results from Table 4.1, it is seen that for this system, the particle size that should be used to create substantial ITZ volumes is about 125 micron. Below 100 micron, the system is not able to simultaneous generate ITZ and bulk regions, from where the bulk volume holds a negative value. On the other hand, if the selection on the size of the aggregate particles is of 1 mm, it is not expected that substantial ITZ volumes may be generated.

In Figure 4.5., it can be seen the influence of the particle size on the resultant water volume at ITZ regions, by considering different values for the wall effect parameter, within two ITZ thicknesses.

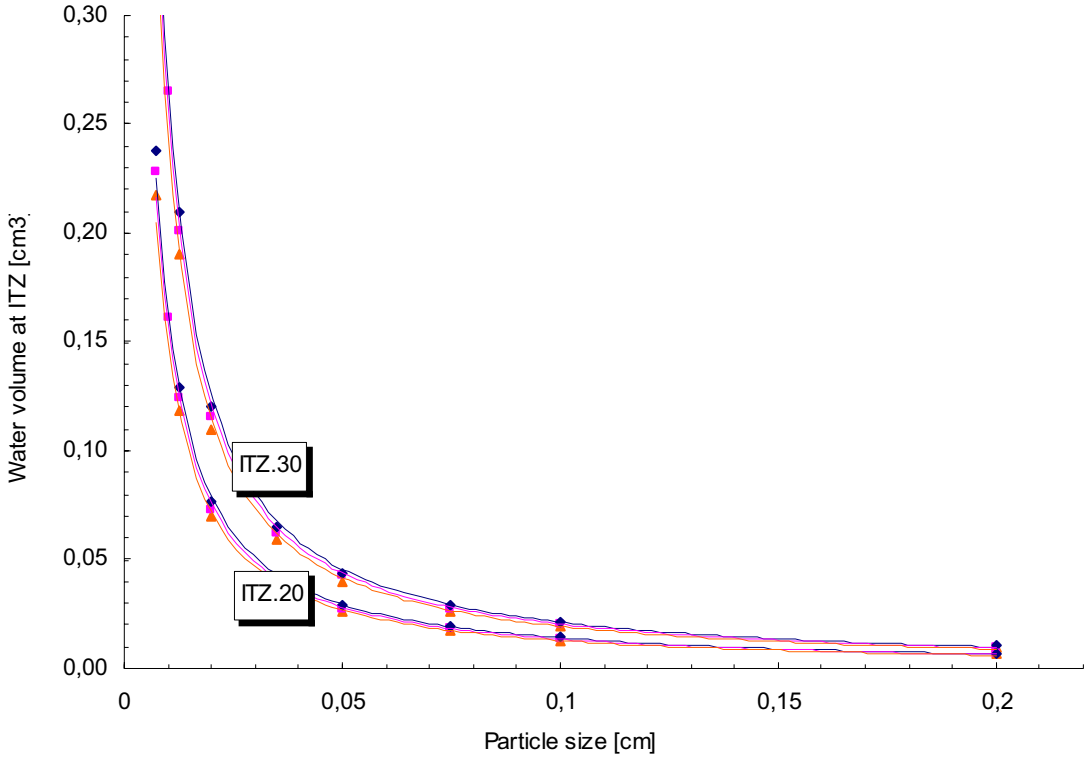

Figure 4.5.

Theoretical water volume at ITZ sites as function of the particle size considering different values for the wall effect ($W_{eff} \in [0.40 - 0.50]$).

System physics:

V_{agg}=30%, (w/c)=0.30

Model assumptions:

ITZ depth=ϕ_{cem}=20 µm, ITZ depth=ϕ_{cem}=30 µm

Some conclusions can be drawn from Figure 4.5.. The wall effect variation only slightly affects the water volume at ITZ regions, being practically independent from the volume-water at ITZ sites. The dimensional range of fine aggregate that may be used to produce substantial ITZ regions is limited up to 1 mm. On the other hand, a lower threshold value for the formation of both ITZ and bulk regions is noted at the aggregate size of about 100 μm, being possible to shift according to the ITZ depth. As mentioned previously, below this threshold value there is no available space to accommodate the quantity of aggregate particles plus ITZ volumes. An equation may be easily set up to account for different combinations of aggregate particles in the system, but such consideration will be not evaluated here, since it is out of the main scope of the present work. In the following, the requirement of internal curing for cement-based materials with fine aggregate particles is derived.

4.1.4. Internal curing by fine aggregate particles

A water-entrained cement paste is a cement paste that in the freshly mixed state has predesigned, water-filled cavities[123]. In the present case, the water-filled cavities will considered to be water volumes at ITZ regions, and the macro inclusions are “aggregate inclusions”. Figure 4.6 shows the basic principle of internal curing by fine aggregate particles. The bulk regions, at some point of hydration, will show extreme shortness of water. At the same instant the free water at ITZ regions will start diffusing into the bulk phase.

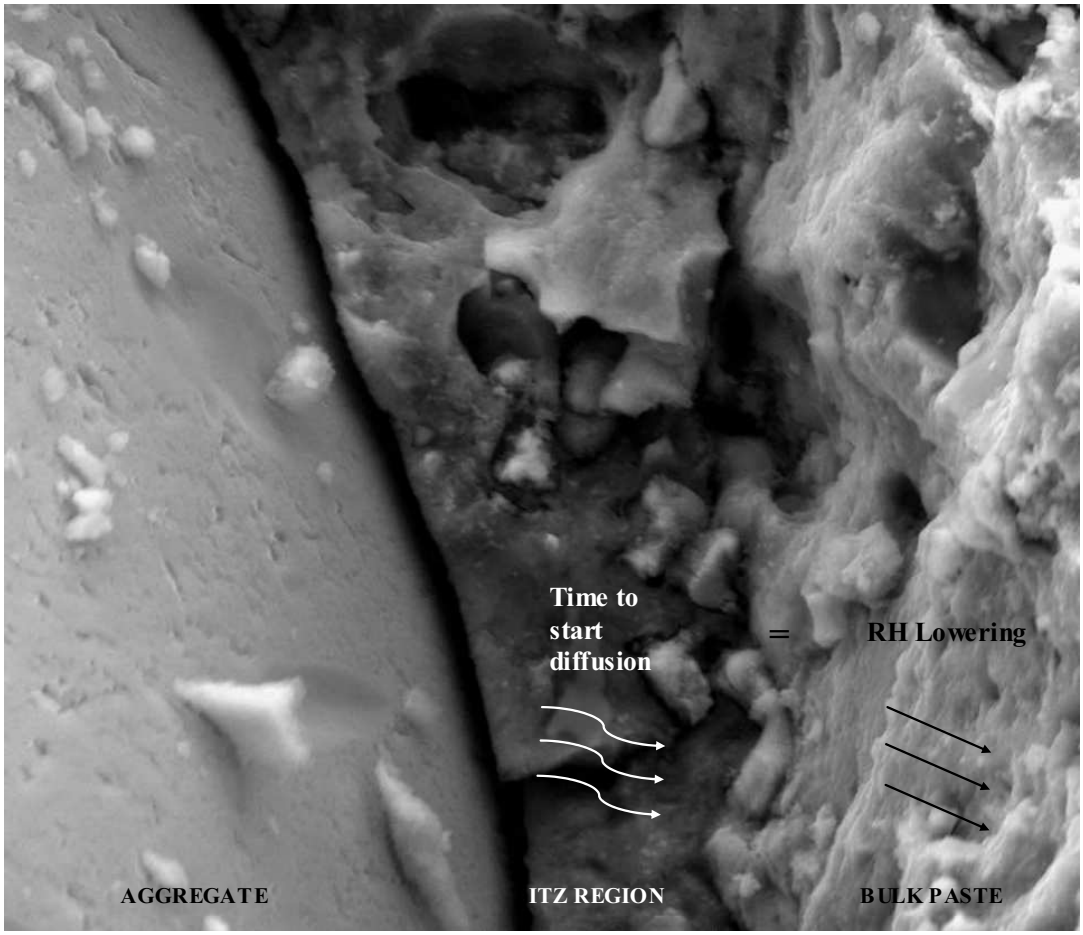

Figure 4.6.

Schematically representation of internal curing by fine aggregate particles

A remarkable part of modern research on cement hydration modelling is based on the work of T.C. Powers, which may be still, after more than half a century, the most widely applied model to quantitatively describe a hydrating cement system. Detailed information on this classical approach can be found elsewhere in the literature[205, 20]. According to Power's model-equations, Eq. (4.9) to (4.13), the maximum hydration degree for a system with water to cement ratio below 0.36 can be obtained when the free water volume, defined as the capillary water, reduces to zero ($V_{cw} = 0$).

chemical shrinkage $$V_{cs} = 0.20(1-p)\alpha \quad (4.9)$$

capillary water $$V_{cw} = p - 1.32(1-p)\alpha \quad (4.10)$$

gel water $$V_{gw} = 0.60(1-p)\alpha \quad (4.11)$$

gel solid $$V_{gs} = 1.52(1-p)\alpha \quad (4.12)$$

unhydrated cement $$V_{uc} = (1-p)(1-\alpha) \quad (4.13)$$

In the previous set of equations, V_i stands for the relative volume fraction [m^3/m^3 cement paste], α is the degree of hydration [kg cement reacted/ kg initial cement], $\rho_c = 3150$ kg/m^3 the cement density, $\rho_w = 1000$ kg/m^3 the water density, p the initial porosity being given by $p = V_{cw,0} = \dfrac{w/c}{w/c + \rho_w/\rho_c}$, where w/c is the water to cement ratio [kg/kg].

Figure 4.7 is developed by adapting the Powers model to describe the phase distribution of a hydrating cement paste with low water to cement ratio that is "freely" supplied with water during hydration from the ITZ regions. It should be mentioned that the ITZ water will be influenced by the aggregate phase through physical forces resultant from the water link. However, such influence will be considered negligible in the following ($V_{aw,agg} = 0$). The figures x and y account for the volume phase of bulk paste and volume phase of ITZ regions respectively. These depend fundamentally from the the z volume and the aggregate particle size ($x = V_{bulk}$; $y = V_{ITZ}$; $z = V_{agg}$).

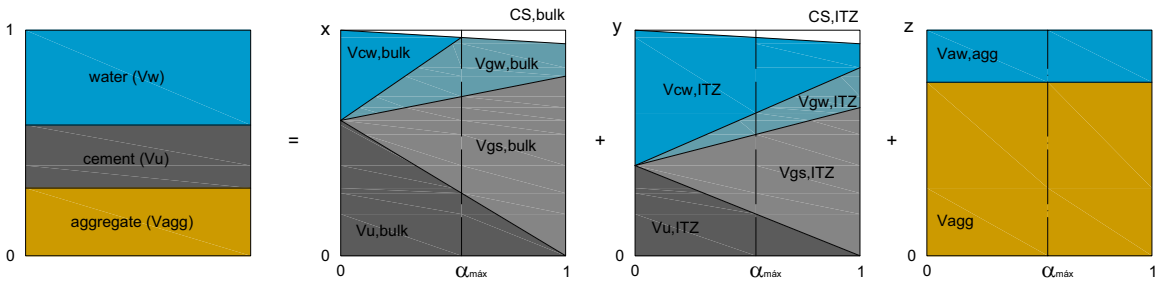

Figure 4.7.

Power's model revised to account the ITZ effect upon aggregate introduction.

The bulk volume paste will require water at the moment correspondent to achieve $\alpha_{máx}$, which occurs at the *x*-fraction since internal relative humidity starts to decrease due to lower water content. Water diffusion from the ITZ regions may then start, since free water is still available within pores produced by imperfect packing and particle arrangement. Thus, internal curing by means of water at ITZ regions will be active when $\alpha_{máx}$ at bulk paste is reached, corresponding to the point where the phase $V_{cw,bulk}$ equals zero, hence:

$$\left\{\alpha = \alpha_{máx} \Rightarrow V_{cs,bulk} + V_{gw,bulk} + V_{gs,bulk} + V_{uc,bulk} = 1\right\}$$

$$\Rightarrow 0{,}60(1 - p_{bulk})\alpha_{máx} + 1{,}52(1 - p_{bulk})\alpha_{máx} + (1 - p_{bulk})(1 - \alpha_{máx}) = 1$$

From where it is retrieved Eq. (4.14):

$$\alpha_{máx} = \frac{p_{bulk}}{1{,}1 \cdot (1 - p_{bulk})} \tag{4.14}$$

The volume water present at the ITZ, $V_{cw,itz}$ at the same moment in the hydration process, viz hydration time *t* can be calculated according Eq. (4.15):

$$V_{cw,itz} = p_{itz} - 1.32 \cdot (1 - p_{itz}) \cdot \alpha_{máx} \tag{4.15}$$

The mitigation of self-desiccation shrinkage was recently theorised by assuming that the volume of entrained water should equal the chemical shrinkage to be attained by the system of water plus cement with a given ratio between water and cement[123]. It follows that the volume of free water at ITZ regions may not be sufficient to balance the self-desiccation at the bulk regions. On the other hand, the requirement of additional water in the bulk cement paste may ascend at the maximum, up to the volume created by the chemical shrinkage at the bulk. Accordingly, for an open system with low w/c, the amount of water to be added to the system is given by Eq. (4.16):

$$V_{ew,0} + V_{cw,itz} = 0.20 \cdot (1 - p_{bulk}) \cdot \alpha_{máx} \tag{4.16}$$

Only the modification of the system, which is related with the presence of fine aggregate particles, significantly influences the internal curing requirement within the bulk paste volume. This is mostly due to the extremely low w/c ratio, which results in less space to be occupied by hydration products, which in turn is reducing the chemical shrinkage and consequently, the requirement internal curing water. Since the initial porosity is equal to the initial water volume in the system ($p_{bulk} = V_{cw,0,bulk}$), insertion of (4.14) and (4.15) in (4.16) holds Eq. (4.17).

$$V_{ew,0} = 0.18 \cdot V_{cw.o,bulk} - V_{cw,itz} \tag{4.17}$$

In principle, the water content at the ITZ regions is sufficient to fully hydrate the cement at the ITZ fraction. However, the volume of free water that is to be transferred to the bulk regions may be diminished, as physical forces appear within the structure. Therefore, and for simplicity of the model, the term $V_{cw,itz}$ will be neglected in the following. Thus, on a mass basis, the expression (4.16) may be transformed in Eq. (4.19), considering a simple volumetric to mass relation, as expressed by (4.18):

$$\left(\frac{w}{c}\right)_e = \frac{V_{ew.0} \cdot \rho_w}{V_{c.0} \cdot \rho_c}; \left(\frac{w}{c}\right) = \frac{V_{cw.0} \cdot \rho_w}{V_{c.0} \cdot \rho_c} \tag{4.18}$$

$$\left(\frac{w}{c}\right)_e = 0.18 \cdot \left(\frac{w}{c}\right)_{bulk} \tag{4.19}$$

Eq. (4.19) is only relevant for $\left(\frac{w}{c}\right) \leq 0.36$, in this case for a water cement ratio at the bulk paste. For w/c ratios at bulk above this value, complete hydration can be achieved and the requirement for extra curing water is diminished. For cement pastes with water to cement ratio between 0.36 and 0.42, the full hydration of cement is possible if:

$$\left(\frac{w}{c}\right)_e = 0.42 - \left(\frac{w}{c}\right)_{bulk} \tag{4.20}$$

Let the example from the previous section be taken to examine the validity of the previous theoretical framework. The calculated water to cement ratio at bulk is 0.11. From Eq. (4.14), the maximum hydration degree would equal 0.30. Conversely, the free water volume in ITZ sites at the same moment *t* would be 0.20 cm^3/cm^3, from which 0.15 consists in free water, thus potentially being available to be transferred to bulk regions. It should be emphasized that the later quantity may not be sufficient to entirely balance the autogenous deformation. At the moment that ITZ regions overpass the spatial threshold, the bulk cement paste loses binding capacity due to the extremely low water to cement ratio at bulk, as in any other cement paste considered independently without the presence of aggregate particles.

Eq. (4.19) shows that a cement mortar with a particle size of 125 μm requires $0.18 \cdot 0.11 = 0.02$ g entrained water per gram of cement. This only takes into account the consequence of the physical change, which is in the safe side.

Figure 4.8 is built from the application of Eq. (4.19) and (4.20) for several running cycles of particle diameters. Accordingly, it shows the requirement of entrained water for different internally cured pastes by fine aggregate particles.

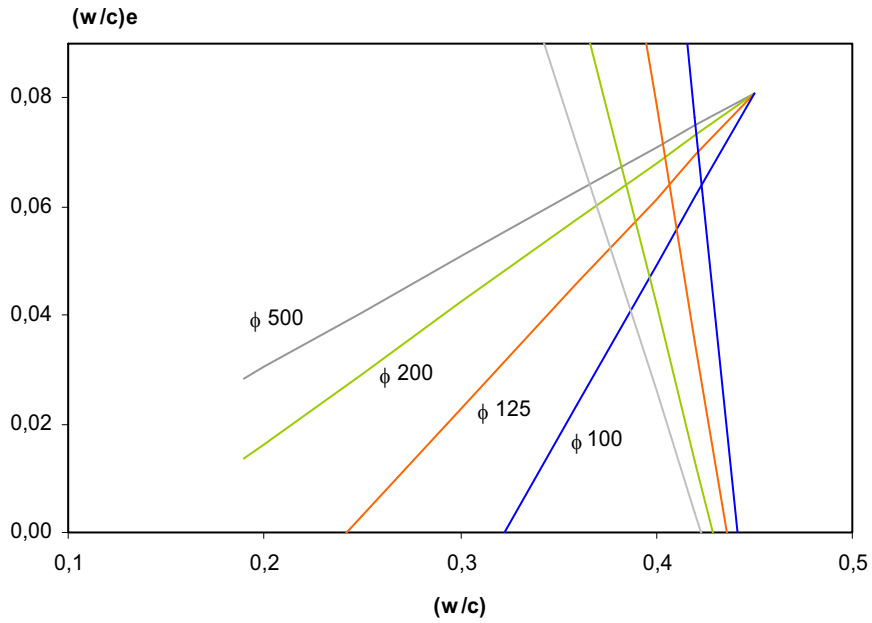

Figure 4.8.

Requirement of entrained water needed at bulk cement paste to obtain $\alpha_{máx}$ in order to prevent self-desiccation taking in consideration the effect of ITZ regions on cement-based systems.

4.1.5. Final remarks: Consequences of internal curing by ITZ

In the previous sections the potential application of ITZ concept for internal curing of cement-based materials was described as mean to actively counteract part of the self-desiccation occurring at bulk paste. It is also concluded that very fine particles may generate severe difficulties to bulk cement hydration, by taking-out water from the bulk regions, and accentuating the requirement for additional water to compensate the lack of rheology performance. This should be an initial consequence of using internal curing by fine aggregate particles. On the other hand, the rate of superplasticizer may be increased to improve the fresh behaviour of the system. This issue is developed in section 4.3.

It is also seen that the aggregate particle-diameters which would likely result in substantial internal curing through ITZ formation are in the range between 75 and 250 micron. For upper diameters, the effect should be negligible, as only few ITZ volumes are being created. The lower bound may be also of interest to address additional comments. There is a lower diameter at which the ITZ formation may not longer be applicable. For example, in the case of some non-reactable silica-based powders, where the diameter of the particles may be in the order of size of cement particles, the ITZ formed between cement grains and powder particles will result in an inverse targeted system-physics, meaning that cement grains will be involved by powder particles and not cement

grains be involving aggregate particles. Moreover, nucleation sites may appear at the surface of ultra fine materials, and other phenomena may be more relevant rather than internal curing.

Furthermore, the free water at ITZ regions may not be sufficient to fully hydrate the bulk paste and simultaneously counteract self-desiccation. As shown in Figure 4.8, referring to a system with 35% of aggregate (volume-%), the requirement of additional entrained water should be negligible at the intersection of each diameter-line with the abscissa. This corresponds to a system without bulk phase, and this point may be very difficult, if not impossible to obtain. Nevertheless, the water requirement to fully cure a mixable system should be lower than an equivalent cement paste considered alone. It is then preferable to combine the physical limitations of using this internal curing method with other means of internal curing.

Another aspect that should be emphasised is the effect of the increased ITZ formation over the pore structure of the system, as brought out from the wall effect. It is possible that a different pore structure is obtained when considering a significantly higher amount of ITZ regions, with higher porosity than the bulk regions. Primarily, the resultant pore size distribution is affected, higher porosity with random shapes being encountered within ITZ regions in respect with the bulk. Alias, this should be the major reason for a smaller desiccation of the system, as the biggest empty pore will in principle take more time to be emptied, due to the capillary tension forming at the interface pore-wall-pore-fluid, the menisci comprising higher diameters and thus lower tension.

The micro-strength of the material should be also affected. On one hand, there are bulk regions with superior strength properties, due to a lower water to cement ratio, resulting a higher bulk density in respect with the global system-density when considering the global water to cement ratio. By other hand, there are substantially more regions with higher porosity, which are increasing as internal curing potential increases. From this assumption, it is possible to consider two different effects on strength: the higher the ITZ regions, the more volume of free water is available to the bulk paste surroundings, and the higher is the volume of sites with high water to cement ratio through wall effect. The later, will obviously conduce to a loss of strength, since weaker connections between aggregate particles and the bulk paste are to be created.

The durability of systems formulated with the present internal curing concept should be also enhanced. This is related with the transport properties within the composite system, which may also be affected due to the existence of ITZ regions. In principle, the higher volume of ITZ regions may result in increased porosity in the system. On the other hand, this effect may be balanced with the higher density at the bulk regions. The bulk regions, comprising lower water in respect with the global water to cement ratio will provide additional protection, being increasingly more resistant to the diffusion of species throughout the system, as lower the w/c ratio at bulk is attained. However, if the system approaches the physical form of zero bulk paste volume, the performance in the permeability of the system will be negatively affected. In fact, if the paste volume is fully constituted by ITZ types, no protection to diffusion is to be expected, since the resultant paste volume will comprise a relatively high ratio between water and cement. Further work on these particular aspects is surely needed, having in mind that the design-based on this concept may be also an opportunity to create specific-targeted high performance systems with internal curing by fine aggregate particles.

4.2. Internal curing by fine aggregate particles. II – Experimental observations.

This section deals with a new concept for the partial mitigation of self-desiccation in hardening cement-based materials. The concept is based on the use of fine aggregate particles, as a vehicle to "water fixation" via ITZ volume, which comprises higher water content in respect with the bulk paste volume. The power relation in respect with the change in the specific volume arising from the variation of particle size of fine aggregate is associated with the formation of correspondent ITZ regions that can actively contribute to control self-desiccation and autogenous deformation in early-age. In this section, experimental observations are described and discussed. The results show that, although self-desiccation may be partially controlled by higher volume of water in the ITZ regions which surrounds fine aggregate particles, the significance of the internal curing effect may be limited by several parameters. This section follows the theoretical background presented in the previous section.

4.2.1. Introduction

Since the development of high performance concrete in early 1980s, its industrial application was hampered by the problem of early-age cracking. Considerable efforts were done in research during the 1990s in order to find solutions to mitigate shrinkage ensuing from self-desiccation. Scientific community developed strategies that can effectively counteract this phenomenon. These internal curing strategies have been published and thorough explanation on their application can be found elsewhere[124, 122].

This study suggests another approach to the problem, by the use of fine aggregate particles to partially mitigate self-desiccation and autogenous deformation. This is similar to water-entrainment methodology, but is done via ITZ regions, taking advantage from the high specific surface of very fine aggregate particles, which can prevent in some extent the self-desiccation shrinkage of hardening concrete. The principles and theoretical background were described in the previous section. The present work reports the experimental observations with focus on autogenous strain, relative humidity change and microstructure of mortars systems with fine aggregate particles. An examination of other important properties, especially mechanical properties of cement-silica pastes and concrete, is presently being carried out.

4.2.2. Materials and Methods

Materials

A low-alkali Danish white Portland cement with Blaine fineness 420 m^2/kg was used. The density of the cement is 3150 kg/m^3. The Bogue-calculated phase composition (in wt.-%) is: C_3S: 66.1, C_2S: 21.2, C_3A: 4.3, C_4AF: 1.1, $C\bar{S}$: 3.5, free CaO: 1.96, Na_2O eq.: 0.17. Silica fume (SF) was added as a dry powder at a rate of 15 to 20% of the wt. of cement. The specific surface of the silica fume is 17.5 m^2/g (BET method). The chemical composition (in wt.-%) is: SiO_2: 94.1, Fe_2O_3: 1.00, Al_2O_3: 0.13, MgO: 0.71, SO_3: 0.43, and Na_2O eq.: 1.09. A naphthalene-based dry powder superplasticizer (SP) was added at a rate of 1.0 wt.-% of cement. Narrow-sized quartz aggregate particles were used in the mixtures, keeping constant the aggregate to cement ratio at about 30% by volume. Demineralised water was used in all mixtures. The basic w/c ratio is 0.30 in all experiments.

Mixing and sample preparation

Cement-silica mortars were mixed in a 5 litre epicycle mixer. The procedure started by mixing dry cement and silica fume with water during the first 2 minutes at low speed (speed level 1). Mortar was left stand for 1 minute and again mixed at high speed (speed level 2). Room temperature was approximately 20 ºC. All samples were prepared from the same batch.

Measuring Techniques

Autogenous RH-change of cement-silica mortars was measured by a Rotronic Hygroscope DT equipped with WA-14TH and WA-40TH measuring cells (see Figure 4.9), which are kept in a thermostatically controlled box (± 0.1 ºC). Calibration of each measurement cell was performed prior and after each set of experiments, by using saturated salt solutions within the range of 75 to 100%: K_2SO_4, KNO_3, KCl and NaCl. A more thorough description of the set up and calibration procedure is publish in reference[142].

Figure 4.9.

Rotronic station for RH-change measurements. The image shows the measuring cell, the measuring chamber and the lifting system.

Autogenous deformation was measured by means of a dilatometer, which was developed by O.M Jensen and P.F. Hansen[104]. The cement mortars are encapsulated in a thin corrugated polyethylene mould with approximately 300 mm length and diameter of 30 mm. This tube has an insignificant influence in the system, since it does not induce external restraint but the force of the spring when cement paste stiffens. Both digital (manual) and fully automatic dilatometers were used in the experiments. Only the measurements performed at the fully automatic dilatometer are presented in this section. The dilatometer is equipped with a datalogger and electronic linear displacement transducers TRANS-TEK series-350, for high precision measurements. The standard deviation of two samples was less than 5 microstrain (μm/m). Measurements started just after setting of cement, as measured by VICAT needle, which, in the case of the actual systems, was about 8 hours after water addition. Figure 4.10 shows the main components of this apparatus. A more detailed description of this apparatus can be found in the reference[104].

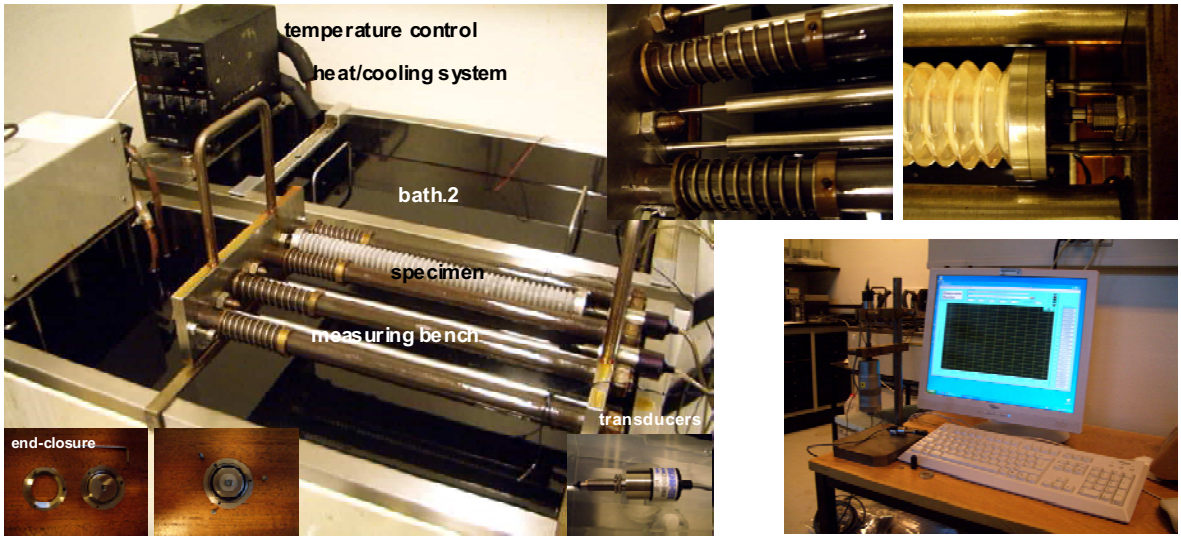

Figure 4.10.

Autogenous deformation measurement system.

Scanning Electron Microscope, SEM and *Electron Probe Micro analysis, EPMA* were also used in the experimental work. The preparation of specimens followed the procedure described in section 3.2. Prior to the resin impregnation procedure, 24 hour-specimens were let in high purity ethanol-based medium during night. This was done to ensure that the free water at this age is effectively removed by exchange with the non-hydrating medium. However, subsequent drying unavoidably affects the system-physics. In either case, this technique may be used to study the dispersion of the aggregate phase in the systems, which was the primary objective of this experimental framework.

4.2.3. Results and discussion

Figure 4.11 shows the autogenous *RH-change* of the investigated cement-silica mortars, with varying particle size of aggregate. Despite the presence of different-size aggregate particles, a significant autogenous RH-lowering is observed. After autogenous curing for about 2 weeks, the RH of the SF-modified paste is approximately 87%, whereas the RH level of systems with fine aggregate range from 87 and 88%. In a general view, the particle size does not seem to significantly affect the RH-change of the reference mixture, and consequently the self-desiccation of the system, although slight differences may be observed. The maximum in the absolute difference is found in the system with particle size within 125 and 300 μm, being able to keep the RH level about 1% higher in relation to the paste.

A closer examination into the first 48 hours profile of the internal relative humidity change during sealed curing discloses a striking moisture event. As shown in the Figure 4.11 (insert plot), the system with particle size ranging 75 and 125 micron approximates the RH-behaviour of the cement-silica paste up to about 36 hours, from where RH level is maintained above the RH level found for system P1. However, the drop of RH occurs earlier for mortars P3 and P4, being faster for the mortar with lower particle size, and attains a maximum difference at the end of first 24 hours, which is in the order of about 2%. This clearly indicates that the hydration of this system may be accelerating in the presence of finer aggregate particles, due to reduced water content at the bulk paste volume. This is consistent to the model approach.

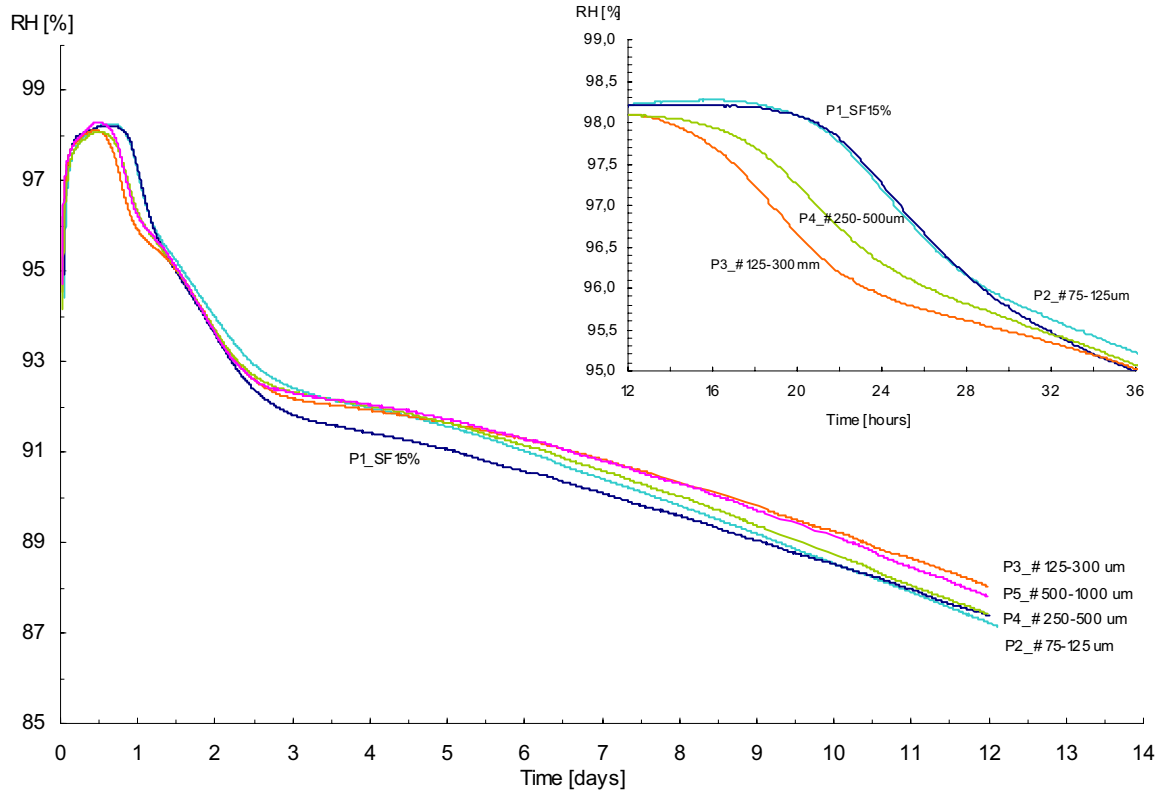

Figure 4.11.

Autogenous relative humidity change of cement-silica pastes with different aggregate particle size. Basic w/c is 0.30. Aggregate is added in 35% by volume. Insert shows the first 36 hours in more detail.

As registered by O.M. Jensen[206], the water to cement ratio affects both the initial drop and rate of RH-change in SF-modified pastes. In his work, it is found that a reduction of the water to cement ratio from 0.30 to 0.25 results in an increase rate in the initial drop of RH from 0.22%/hour to 0.36%/hour (an increase factor of about 1.6). However, these tests were performed at a curing temperature of 30 ˚C. Therefore, the previous rates should be only seen as a qualitative indication of this behaviour, since the increase of hydration rates at a higher temperature is most prominent leading to different degrees of maturity in the pastes, which makes a quantitative comparison of the experimental values erroneous. In the present case, it is sufficient to conclude that the ITZ formation via fine aggregate particles may play an important role on the activation of the first reaction, due to the existence of bulk paste regions with lower water to cement ratio in respect with the water to cement ratio of the correspondent SF-modified paste.

According to the modelling approach presented in section 4.1, the time for water movement from the ITZ sources should be equal to the moment of maximum hydration degree at the bulk paste. Accordingly, this should be within the first 24 hours of sealed hydration. The results clearly indicate that a moisture balance, viz. internal curing may be occurring within this diameter particle interval, by analysing the subsequent RH-profile of the systems (second 24 hours). Thus, it is observed two marked breaks between the paste and mortar curves, both occurring within the first 48 hours. The first break takes place during the hardening period, from about 12 hours, where it seems that the self-desiccation phenomenon is exacerbating due to the presence of fine aggregate particles, and the second break, where the RH-change rate is reduced, approximating the RH-

change behaviour of the SF-modified paste. At this stage, the RH-change of the systems with fine aggregate particles is favourably limiting the self-desiccation. The larger difference can be found at 22 hours, where the absolute difference in the internal relative humidity in respect with the SF-modified cement paste is of about 1.62 % and 1.07%, respectively for the mortar with particle size starting at 125 and 250 micron. However, the same conclusion cannot be made in respect with the system with particle size of 75 micron, which in the same interval, follows the RH-change behaviour of the SF-modified paste. As noted by O.M Jensen and P.F. Hansen[142], the filler effect of silica fume should not play a major role on the RH-change of SF-modified cement pastes. In their experiments, the silica fume was replaced by inert filler, being concluded that the RH-change of the filler-modified paste does not show significant change in respect to a plain Portland cement paste. However, the combined effect of the silica fume and fine aggregate particles may be stronger in this case due to a higher addition-ratio. In this case, it is noted one curve break occurring after the first 24 hours, from where the RH-change rate turns lower in relation to the SF-modified paste. Furthermore, from 48 hours up to 5 days, the RH-change of the SF-modified mortars shows a steadier RH-curve, in respect with the SF-modified paste.

The previous discussion suggests that the presence of fine aggregate particles does influence the RH-change of the system, but the significance of this effect may not be relevant to sustain that internal curing is an important mechanism as theoretically proposed. The significance of such mechanism is to be found in the answer to the following questions:

(a) What is the physical meaning of the global RH-change of the system during early-age at bulk and ITZ paste volumes?

(b) What is the significance of a 1% RH-change in the autogenous phenomena and how does such variation affects the mechanical properties of bulk and ITZ volumes?

Moreover, other phenomena may influence the acceleration of the first reaction. For example, if the fine particles act as nucleation surfaces for silica fume particles, the production rate of the hydrates should result higher, and the RH-change would turn faster. However this should not be probable, since the surface area of the fine aggregate particles is in an order of magnitude higher than the powder materials. In the present case, the rate of RH drop is steeper in the cement paste, even in the presence of powder-near aggregate phase, viz. fine aggregate particles with 75 μm. Thus, the delay of the second RH-drop in the systems with fine aggregate particles suggests that the bulk cement paste has increased water availability, extending the RH-change to a later period in respect with the plain cement-silica paste.

Autogenous deformation measurements performed to cement-silica systems with fine aggregate particles is shown in Figure 4.12. It can be observed that the particle size as a considerable effect on the early-age autogenous strain. The decrease of the grading within the aggregate particles from 2000 to 125 μm results in an increase in the AD of about 1000 μm/m. This suggests that a restraint effect is present by comparing the strain obtained with the autogenous deformation of the cement paste alone, and that it is highly dependent of the size of fine aggregate. Further decrease of the particle size to about 75 μm resulted in a significant reduction of the measured autogenous strain. As suggested in the theoretical background, a higher number of particles in the system should be able to "produce" enough quantities of ITZ volumes so that bulk paste would cease to exist. Thus, this phenomenon cannot be seen as restraint from aggregate, which should be governed by the size

of aggregate. It should be seen as internal curing by fine aggregate particles. The higher water to cement ratio present at the ITZ volumes was able, to a certain extent, to internally cure the bulk cement paste. This resulted in the reduction of self-desiccation and consequently, in the reduction of the autogenous strain.

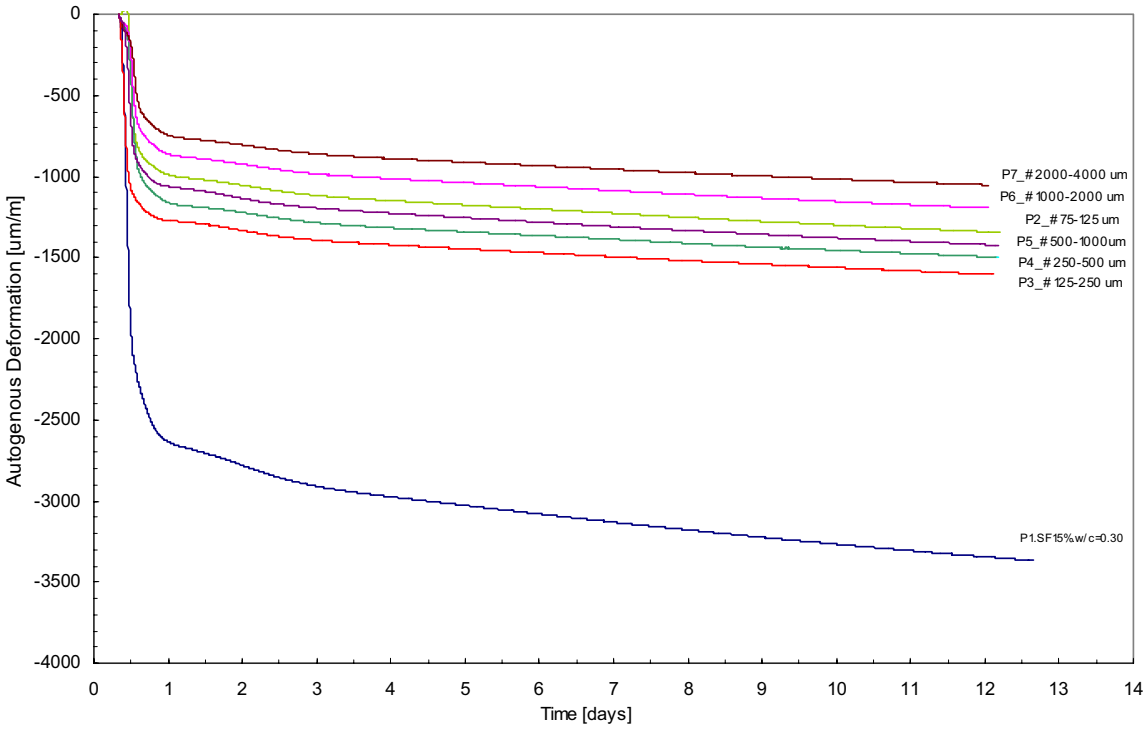

Figure 4.12.

Autogenous deformation of cement-silica mortars with different particle size of fine quartz aggregate, and consequently different ITZ regions. Basic w/c was 0.30.

However, the combined view of AD and RH-change through the systems is rather complex, the difference in the deformation found within the variation of the aggregate particle size in the system not consistently following the RH-change. For example, although the RH-level of the SF-modified mortar with fine aggregate particles of 125 μm appears higher, the measured ultimate deformation does not appear lower in respect with the system with particles of 75 μm. Moreover, it is not denoted any significant difference in the rate of deformation within the secondary reaction, when self-desiccation is still developing within the system. It may be that two mechanisms are overlapping, viz. internal curing and a restraint effect. Both effects will tend to push the position of each curve to an upper position in Figure 4.12. This synergy may be represented schematically by Figure 4.13. With this respect, it should be mentioned that, the regions of particle diameters where internal curing is enhanced should correspond a less significant restraint over the system.

A more fundamental discussion is that if the AD of SF-modified paste is comparable with the AD of the equivalent cement mortar. The presence of about 35% less cement in the system may be relevant to reduce the reading of the global autogenous deformation, as this volume is not influencing self-desiccation since any hydration in this fraction is occurring. As supported in early work by Pickett[207], the increase in the aggregate phase concentration progressively results in the reduction of the absolute shrinkage during drying.

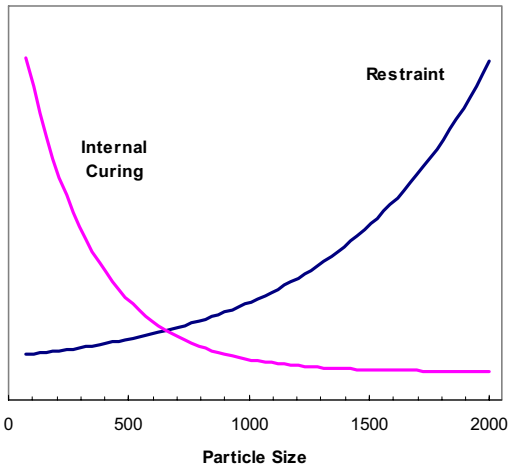

Figure 4.13.

Schematically representation of the mechanisms that may be interacting in the strain development of cement-based materials with fine aggregate particles.

Moreover, the AD of the cement-silica paste system is composed by two main courses of simultaneous chemical and physical changes. It should exist a moment in time where the non-reacted cement grains exert a degree of restraint over the bulk paste volume, when the stiffness of the hydrated compounds is sufficient to impose stresses back to the non-hydrated grain-cores. A question arises from the previous discussion: Is the presence of powders during the transition from viscous to solid state exerting self-restraint over the developing pore volume? If this is true, the measured strain will be obviously smaller than the cement-silica paste, explaining the AD development of the system with particle size with 75 μm. Because there is a transition interface between SF-modified paste and the fine aggregate particles, the restraining effects should be only minor.

4.2.4. Internal curing by fine aggregate particles

In front of the previous results, it may be concluded that fine aggregate particles may have a significant effect on the measured linear strain. However, the combined view of the RH and AD data indicates that overlapping mechanisms may be hindering the perspective of the real deformations in the system. A number of factors may be the cause for this:

1. Internal curing by fine aggregate particles govern

   (a) Experimental fact: the finer aggregate particles comprehended from 125 and 500 μm are able to accelerate the first reaction, by lowering the water to cement ratio at the bulk.

   (b) Uncertainty: The ITZ formation was not sufficient to maintain substantial internal curing of the system in the subsequent second reaction.

2. Restraint from the aggregate particles govern

   (a) Experimental fact: The finer aggregate particles comprehended from 125 and 500 μm are able to reduce restraint effects, leading to a higher deformation in respect with the other fractions of aggregate particles.

(b) Uncertainty: Microcracking occurred in the systems with particle size above 500 micron, leading to a lower measured deformation.

In two series of experiments, the volume of fine aggregate particles was increased in order to potentiate the internal curing effect. For the same water to cement ratio of 0.3, a 10% increase in the volume of aggregate was used. In another system, the water to cement ratio was changed to 0.36 and the autogenous deformation was determined in a plain paste and an aggregate volume replacement of 45% and 55%. The results for the first case study are present in Figure 4.14.

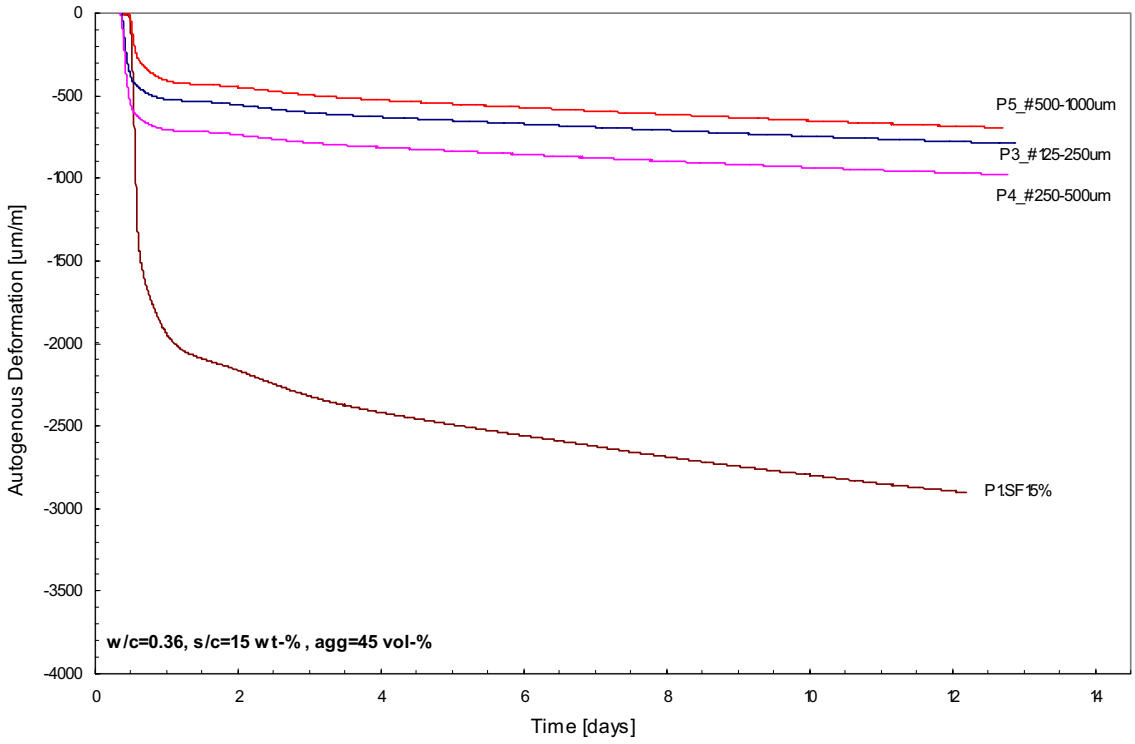

Figure 4.14.

Autogenous deformation of cement-silica mortars with different particle size of fine quartz aggregate, and consequently, different ITZ regions. Basic w/c was 0.36.

The results of the tests indicate that there is an AD turning-point, which corresponds to the inversion of behaviour in the measured AD. This occurred systematically in both systems with aggregate volume fraction of 35% and 45%, and with water to cement ratios of 0.3 and 0.36, respectively, for the particle size starting at 125 µm.

The following strain behaviour is proposed for high performance SF-modified cement-based mortars. Figure 4.15 shows that the particle size where internal curing is overcoming the restraint effect should be observed at particle diameters from 75 to about 200 µm, the curve suffering a translation over the x-axe as function of the water to cement ratio of the system. However, the restraint effect should be independent from the ability of the system being internally cured by it self. Thus, restraint should tend to an asymptotic value, which would result in a concomitant broader curve, as the ratio between cement and water is decreased in the system.

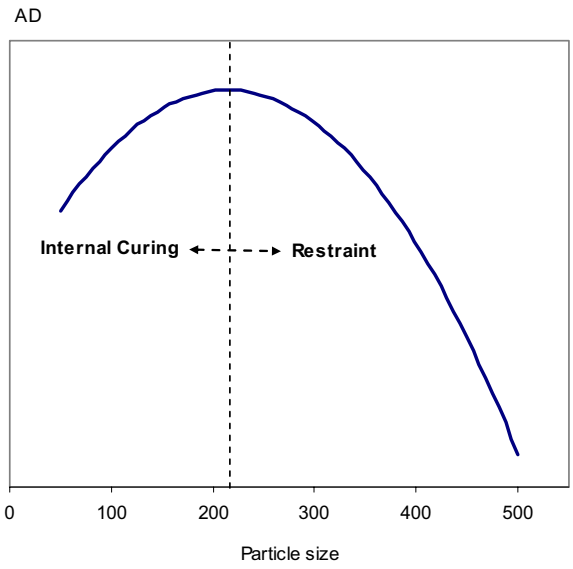

Figure 4.15.

Schematically representation of the internal curing and restraint mechanisms in cement-based materials with fine aggregate particles.

In the section dedicated to results, it is argued about the significance of the internal curing effect in the autogenous deformation of SF-modified cement-based materials. Pietro Lura et al.[41], based on the capillary tension approach, have proposed that the compressive stress in the pore fluid and the resultant tensile stress over the saturated paste fraction could be related with the RH-level of the system. In their modelling approach, a variation in the RH of 2% results in an increase tensile stress with factor of 2 MPa. As an example, the change from 96 to 94% results in a tensile stress from 3 to 6 MPa, which is a level o stress that, at this age, may be considerably above from the tensile strength of the cementitious system. From this perspective, the measured absolute difference in the RH-level between the SF-modified cement paste and the correspondent cement-based mortar with fine aggregate particles may be significant in maintaining a better curing condition of bulk regions. Moreover, the bulk paste is prone to have a lower requirement of additional water than the correspondent SF-modified paste. From the previous discussion, it transpires that the mechanical properties of both bulk and ITZ regions are required in order to have the perception of the effect of the autogenous deformation on the risk of cracking of these systems. With this respect, it seems fundamental to know the relation between the material properties, essentially mechanical, in pure tension and compression as function of the relative humidity change. In face with the present results, it seems that the initial drop in the RH level of the internally cured systems does not seem as harmful to the system, since it is occurring at very early-age, where the RH-level may allow higher deformation, but further research on this topic is surely required to validate the previous arguments. Nano-indentation and ESEM techniques may be applied with this purpose.

In the following, two model parameters are studied: the dispersion of aggregate particles within the paste matrix and the influence of silica fume on the thickness of ITZ.

4.2.5. Dispersion of fine aggregate particles

To prove the validity of the model proposed, it is essential that the assumptions can be clearly demonstrated. One of the assumptions made in the modelling approach was to consider that the total quantity of aggregate particles is surrounded by paste fraction. Thus, the concentration of fine aggregate particles in the system is therefore of fundamental importance. The dispersion of aggregate particles throughout the paste matrix in two formulations is shown in Figure 4.16. It may be concluded that at an aggregate concentration of 35% by volume, the system physics performs as expected, the aggregate particles being involved by the paste volume, making the assumption valid at this concentration.

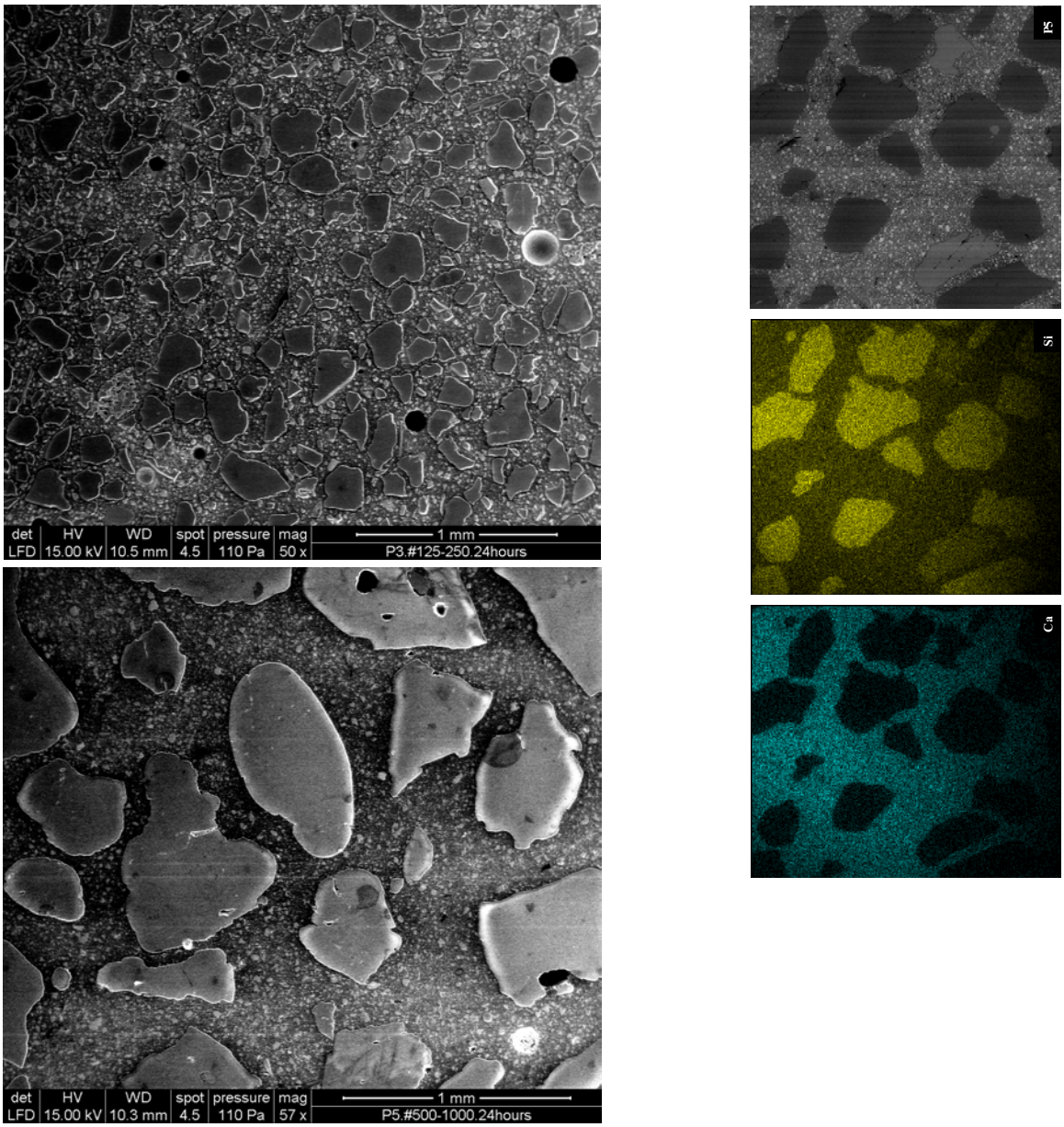

Figure 4.16.

ESEM and EPMA (colour) images of SF-modified cement mortars with fine aggregate particles. Aggregate concentration is of of 35 vol.-%.

In principle, each system should have an "exact" match of fine aggregate particles to take advantage from the internal curing by ITZ concept. Thus, it is expected that systems with higher water to cement ratio may comprise higher number of ITZ entities, viz higher concentration of aggregate phase.

4.2.6. Effect of silica fume on internal curing by fine aggregate particles

Internal curing by fine aggregate particles is also based on the existence of an ITZ thickness, which comprises higher availability of water in respect to the bulk cement paste. According to Cwirzen and Penttala[200], the ITZ is strongly influenced by the amount of silica fume in the system. In Figure 4.17, it may be systematically seen that the addition of fine aggregate at a rate of 45% by volume results in a higher RH level in respect with the correspondent reference system (cement pastes). The variation of silica fume content results systematically in a drop in the RH level of both pastes and mortars. As expected, and considering the cement pastes alone, the rate of RH-change decreases monotonically with the increase of silica fume content, which clearly shows that an increasing pozzolanic activity is occurring in the system.

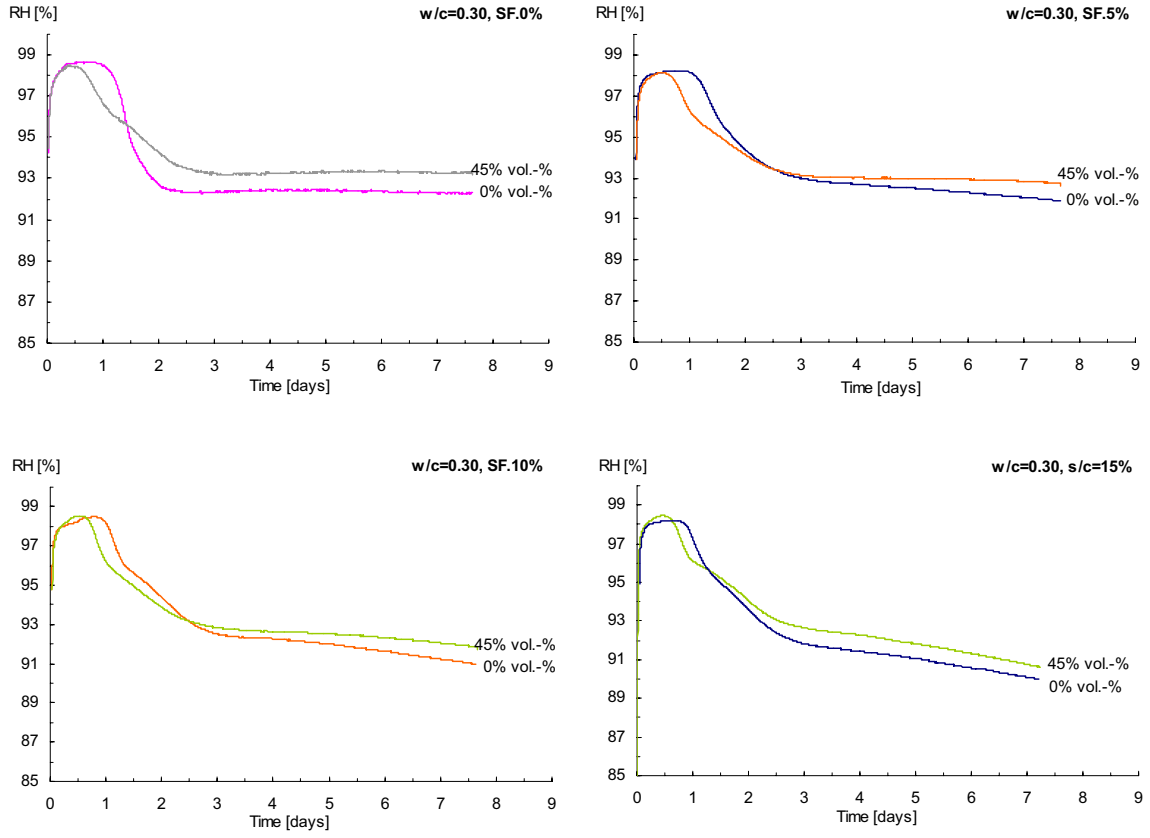

Figure 4.17.

RH-change of SF-modified paste and mortar comprising aggregate particles with size of 125-250 μm.

The absolute RH-difference between each pair of curves in Figure 4.17 is also decreasing, which suggests that internal curing by fine aggregate particles is being limited as higher the amount of silica fume is. This indirectly shows the close relation between the amount of silica fume and the consequent physical property, viz. ITZ thickness. Nevertheless, it seems that internal curing by fine

aggregate particles is particular effective during the initial period of the secondary reaction, as shown in the RH-profiles during the second 24 hours, the RH-change occurring at a significantly slower rate in all systems. Internal curing is noted in all systems, by observing the rate of RH-change that occurs after the initial 24 hours, the significance amplifying with the decrease of silica fume.

4.2.7. Conclusions and final remarks

Fine aggregate particles may be used as partial mitigation of autogenous deformation. The test results indicate that several mechanisms are overlapping, potentially masking the real deformation of the bulk paste. Microcracking phenomena requires further investigation in order to properly model the restraint effect in SF-modified cement-based mortars. With this respect, the results of the tests suggest that microcracking may develop faster when the particle size of the aggregate is higher then 500 micron. Internal curing by fine aggregate particles should be used for aggregate sizes below this value and down to about 75 micron, where filler effect may be governing the development of autogenous deformation and RH-change. Eventually, this fraction may be used to minimise stresses forming during the first reaction, mainly by micro-restraining the system. If the particle size of the aggregate is of the same order of magnitude than the cement grains, the restraint from the aggregate particles may be the same order of size as self-restraint within transition of hydrated products and the non-hydrated cores. In addition, an ultra-high surface area of the aggregate particles may provide base for nucleation of cement clinker products, likely different in nature in respect with nucleation of normal calcium silicate.

To achieve maximum internal curing potential by fine aggregate particles, the volume fraction of aggregate may be unique for a given water to cement ratio and silica fume addition. It is clear from the experiments that silica fume influences the internal curing effect, being more efficient at lower ratios of silica fume and cement. This should be related with diffusion of species within the pore system, but mainly with the refinement of the ITZ thickness, stretching as silica fume content increases.

Further investigation on the mechanical properties of these systems is required, as the significance of the internal curing effect is still not sufficiently clear. It is especially relevant to understand the relation between the RH-change and the material properties, essentially mechanical, in tension and in compression. The potential negative effects of the increase of the volume fraction of fine aggregate particles include the rheology change and the acceleration of the first reaction of clinker minerals. In the later case, calorimetry studies were performed with this purpose (see section 4.4). The presence of fine aggregate particles did not show significant changes in the temperature development, suggesting that only the activation of the first reaction is affected.

The balance between bulk and ITZ regions may be achieved by the modelling approach proposed in section 4.1. Further tests are recommended prior to practical applications. However, complete mitigation of autogenous shrinkage may not be necessary.

4.3. Effect of fine aggregate on the rheology properties of high performance cement-silica systems

This section deals with the effect of fine aggregate particles on the rheological properties of high performance cement-based materials with silica fume addition and low water to cement ratio. The study on the effect of narrow-fractions of fine aggregate particles on rheology of cement-based materials was performed in a rheometer. Yield stress and plastic viscosity were derived for time intervals between 10 and up to 150 minutes after water addition. It was concluded that the fine aggregate particles act as water fixation points in the range of 75 to 1000 μm, via surface area, whereas for upper diameters the governing factor in terms of the resistance to flow may be related to other mechanism as the particle dimension and resultant friction forces. Moreover, the water requirement in order to give each system the same workability is calculated for cement-silica fume systems with fine aggregate. Furthermore, a quantitative model is proposed to describe the characteristic initial torque peak and initial resistance to flow of high performance concrete, as function of the particle size of aggregate. The combined effect of silica fume and fine aggregate particles on the rheology parameters is discussed.

4.3.1. Theoretical introduction

Rheology is the science that studies the flow of matter and deformation of materials, and it is concerned with the interaction between shear stresses, shear strains and time[208]. The rheology of fresh cement, mortar and concrete can be influenced by a considerable number of parameters. There is a variety of measurement instruments to describe rheological properties of cement-based materials. It can be found in literature a comprehensive study of both flow characterization and modelling of high performance concrete [209, 210].

Mortars can be considered to be fresh concrete without coarse aggregate, and can be used as base-model to concrete rheology. Liquids and solids in suspension can behave differently when subjected to velocity gradients. Cement-based materials are classified within the non-Newtonians liquids, where a two-point measurement is sufficient to characterise the rheological parameters, based on the Bingham plastic model [211].

Cement pastes undergo structural breakdown and measured data is sensible to previous shear history [212, 208]. Composition effects are similar to those observed in fresh concrete, enabling mortar test to be used as small scale prediction of concrete rheology [213, 214].

Previous research showed that mortar made with coarse sand is less sensitive to water content than mortar with fine sand. P.F. Banfill [215] studied the influence of different aggregate fineness on the rheological properties of mortars, but on the investigated sand a criterion based on the "percentage of contamination" was applied, referring to the total weight of fine sand passing the 63 μm sieve. This criterion introduces a limitation for quantitative analysis on the influence of particle size on the flow properties of cement-quartz systems, since the effect of fewer quantities within the filler-range diameters can rapidly change the intrinsic characteristics of the solid system, through water fixation near the filler-type cluster. Adding to these quantitative uncertainties in the rheological properties of cement-based materials with time, there is also another parameter with considerable importance: the mixing process. The energy and the time spent on the mechanical action that blend water and powder into a fluid paste are of particular importance in the properties of either cement pastes or mortars. A homogenous cement mix can be obtained by a mixing process that provides sufficient stress to break the agglomerates [216]. This results in a well dispersed blend, where every solid phase is involved by water. High performance mixtures are usually made with very fine

materials such as silica fume at low water contents. As silica fume often exists in the agglomerate state, due to difficulties on stabilizing very fine particles independently, higher mixing time may be needed, in respect to ordinary cement-based materials. It has been shown the effect of replacement of silica fume on the rheological parameters, namely on promoting the drop of the plastic viscosity, despite of a marked increase of the yield stress [212, 208]. Systematic work on this subject can be found elsewhere [217]. However, the combined effect of mineral additions and fine aggregate particles is not clearly understood. One of the consequences of using fine particles as aggregate is the loss of workability, as the system requires more water to achieve the same rheological performance. Previous research has shown that the fineness of sand favours water demand, as the rheological parameters (yield stress and plastic viscosity) increase with decreasing particle size distributions [215]. This could only qualitatively describe the behaviour of fresh concrete in the presence of finer fractions of aggregate.

This study aims to analyse the effect of fine aggregate particles on the rheological parameters: yield stress and plastic viscosity. Narrow size fractions of fine aggregate should affect the flow properties similarly to the intrinsic relation of the specific area that arises from the variation of the particle size distribution of very fine aggregate particles, when evaluating the grading from 75 to 1000 μm. Thus, by analysing sharp spectrum aggregate grading, it should be possible to isolate the size effect of individual particle on rheological parameters and derive quantitative data to predict the rheology of high performance concrete. In addition, the water requirement to achieve the same workability is determined.

4.3.2. Materials

Ordinary Portland white cement, type II was used in the experiments, with nominal strength of 52.5 MPa and specific surface of 460 m^2/kg, as measured by Blaine. Density of this cement is of 3040 kg/m^3. The chemical analysis is presented in Table 4.2.

Table 4.2: Chemical analysis of powders

Powder description	SiO_2	Al_2O_3	Fe_2O_3	CaO	MgO	SO_3	Na_2O eq.
	[wt.-%]						
CEM II/ A-L 52.5N	19.67	2.41	0.16	66.45	0.36	2.25	-
SF.SIKACRETE P	95.80	0.10	0.13	-	0.19	1.55	0.19

Silica fume (SIKACRETE P), provided by SIKA S.A. was added as a dry powder at a rate of 15% (wt.-% of cement). The specific surface of the silica fume is 17.5 m2/g (BET method). The chemical composition is also shown in Table 4.2. The particle size is comprehended between 2 and 20 μm, from where 75% is below than 10 μm.

A wide range water reducer was added at a rate of 1.0 wt.-% of cement. This third generation superplasticizer VISCOCRETE3006, is a polymer-based modified-policarboxilic in suspension, with density of 1.05 g/cm^3.

Narrow size fractions of quartz aggregate particles were used in the mixtures, keeping constant the aggregate to paste volumetric ratio at about 0.55, which corresponds to an aggregate concentration of about 35% (vol.-%). The standard mixtures were performed with the basic w/c ratio of 0.30. The water to solid mass ratio was kept constant for paste and mortar mixtures at 0.30 and 0.14, respectively. The composition of each system is shown in Table 4.3. The water requirement for each particular system was introduced in the system keeping constant the mass fraction of aggregate and binder.

Table 4.3: Cement paste and mortar formulations

Mixture	Agg/paste ratio	Water	Cement	SF	Sand	SP
Standard mixtures	vol.-%	wt.-% of cement				
P1_plain	0.55	0.30	1	0.15	0	0.01
P2_#75_150um	0.55	0.30	1	0.15	1	0.01
P3_#150-250um						
P4_#300-425um						
P5_#600-1000um						
Water requirement mixtures						
P3*_#150-250um	0.47	0.40	1	0.15	1	0.01
P4*_#300-425um	0.51	0.35	1	0.15	1	0.01

* indicates the mixtures with additional water.

4.3.3. Methods

Rheology measurements were done by a specific mortar rheometer Viskomat NT (see Figure 4.18). The rotation speed, time and torque data are sampled by a data acquisition system.

Figure 4.18.

Mortar rheometer (Viskomat NT)

Cement paste and mortars were mixed in 5-1 epicycle mixer. All the components were mixed in dry state, and water was added during the first 2 minutes at low speed (speed level 1). The mortar was left stand for 1 minute and again mixed for 2 minutes at high speed (speed level 2). The mixtures were first tested in the flow table, according to ASTM C230 and then poured into the rheometer cylindrical container. Rheology tests were performed according to the speed profile presented in Figure 4.19. This apparatus is internally limited to a maximum torque value of 300 N.mm.

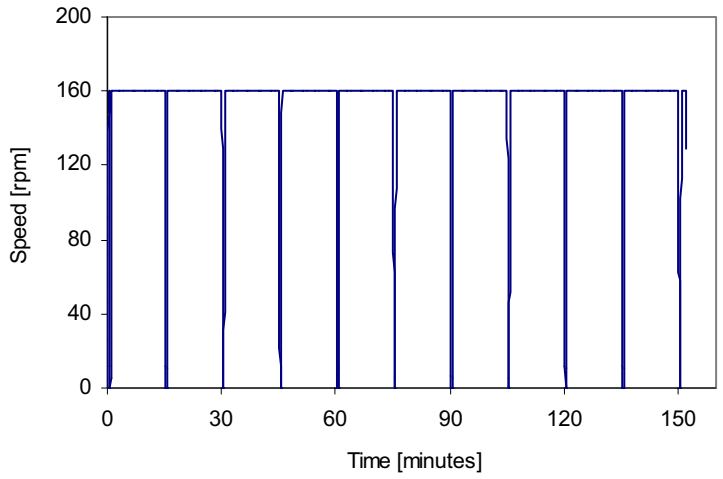

Figure 4.19

Dwell speed profile set in the Viskomat.

Measurements were done at constant speed (160 rpm). Rheological parameters are taken at 15 minutes intervals during 150 minutes.

In this work, the test consisted of a speed loop starting from rest and going up to a rotation speed of 160 rpm. The speed is then gradually reduced to zero at each 15 minutes interval, where a total of 17 measurements of speed and torque are recorded in approximately 20 seconds, followed by a waiting period of about 13 seconds in each stop. The sampling frequency during speed variation is adequate to construct the flow curves with time. Test duration was 150 minutes, a compromise between the initial setting time and the rheology change in the system.

From the data taken, it is possible to characterize the rheological parameters of each mixture, assuming the Bingham behaviour for the material, as expressed by eq. (4.21).

$$T = g + h \cdot N \tag{4.21}$$

Where g and h are directly proportional to yield stress and to plastic viscosity, respectively. These values can be determined with an experimental precision typically of ±5% [208].

Penetration tests were performed in each mixture in the VICAT apparatus, by procedure described in ASTM C 191 [146]. All tests were performed at room temperature at 20±2 ºC.

4.3.4. Results and discussion

Effect of particle size on the rheological properties of cement-silica systems

Figure 4.20 shows the variation of torque with time of the studied mixtures. It can be seen that the particle size of fine aggregate fractions has a considerable effect on the rheology of cement paste. This effect has a threshold, somewhere below 1000 μm, where the specific surface may govern the process of deformation and flow. The presence of very fine particles of about 150 to 250 μm, results in higher torque values, as observed by the curve of the mixture P3. This may be explained by the water fixation and particle interaction arising from the high surface area produced by this particle size distribution. In fact, the variation of aggregate size from 1000 to 100 μm results in increasing by a factor of 10 the surface area of aggregate per unit volume and consequently the particle interaction with the cement paste. In this case, the use of a narrow diameter fraction within 150 and 250 micrometers induced a magnified effect of 4 times on the initial torque value by comparing with the plain cement paste (system P1). The water fixation is so severe, that the system lost the flow capacity before the end of test, by observing the curve instability after 120 minutes.

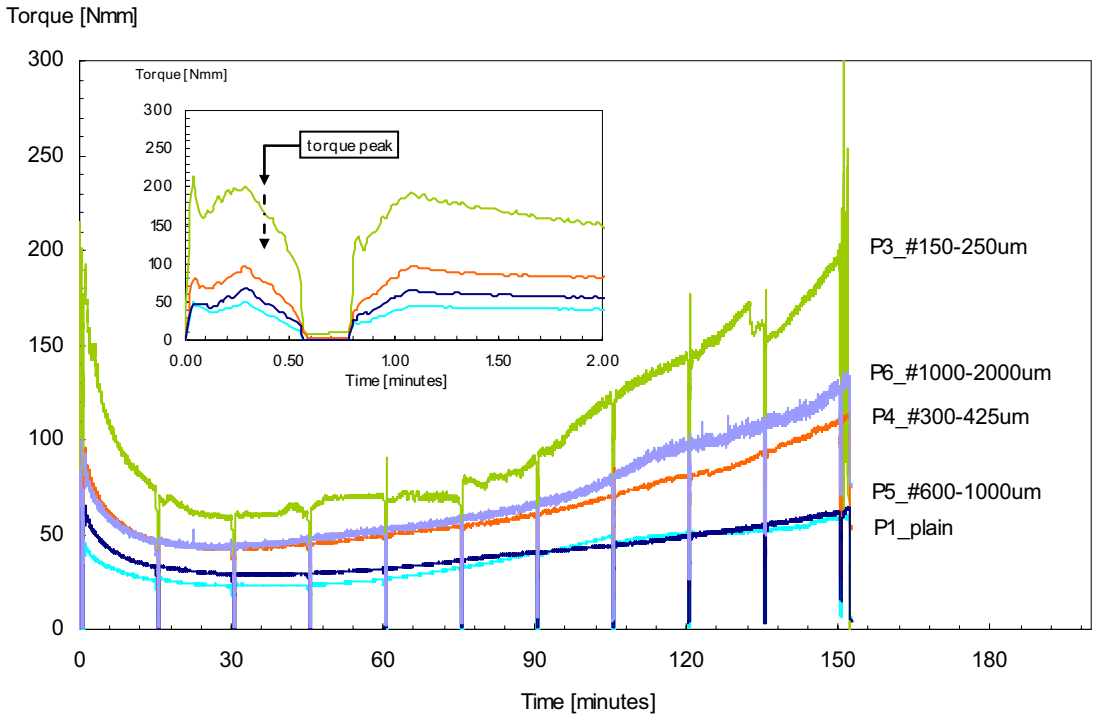

Figure 4.20.

Torque variation with time at constant speed in a dwell profile.

The addition of 35% aggregate (by volume) with particle size ranging between 600 and 1000 µm does not have a significant impact on the torque values in respect to the plain cement paste, despite the different water to solid ratio between both mixtures. This may be explained by the low resistance that individual particles within this size span impose to flow in the global cement paste media. By other hand, increasing the average diameter of particles to the range of 1000 and 2000µm, leads to increasing values of torque as observed by the curve of the system P6. This may be explained by other phenomena, where gravity and resistance to flow may govern the process. Thus, if the mass of individual particles is increasing, the work required to impose movement into one particle considered individually is proportional to the mass of the particle. Since the velocity is constant, the ratio of the buoyancy and gravitational force results in higher frictional forces, if exerted by bigger particles. Therefore, the cement paste media is subjected to different friction forces (drag forces), which are function of the size of the particles. Higher diameters would probably promote segregation phenomena or sedimentation, if the finer fractions were not present, as the terminal force of the system is reached.

From the previous discussion, the following rheological behaviour is proposed for cement-based materials with water to solid ratio of 0.14. Figure 4.21 shows the initial torque peak as function of the particle size of aggregate particles. The torque peak was taken as a characteristic value from Figure 4.20. A threshold value at the particle diameter of about 600 micron is found for the minimum torque peak. For decreasing particle diameters, the torque peak grows exponentially, accompanying the number of particles in the system.

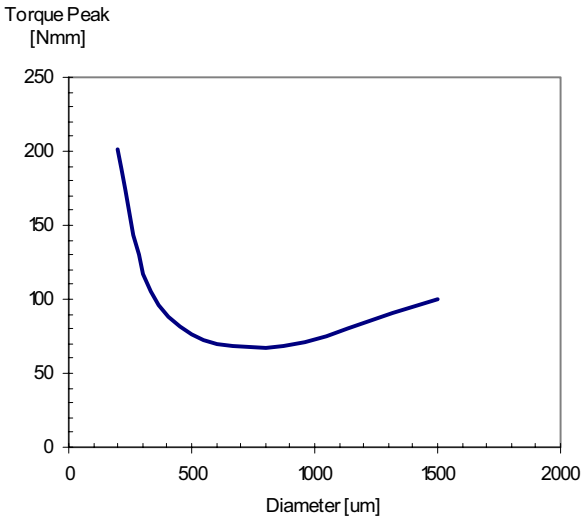

Figure 4.21

Rheological behaviour of cement-based materials with fine aggregate, expressed by the initial torque peak.

The fact that the surface area may induce such variations on the cement-silica pastes is of importance on the understanding of the fluid mechanics of a certain composition. This explanation may be amplified to further consider this effect for varying volumetric ratios or aggregate concentrations. It is expectable that a higher number of interfaces between paste and fine aggregate particles lead to higher values of initial torque peak, as found in the system P2. If the volume fraction of aggregate is increased, the consequence on the previous figure would be a vertical translation with similar behaviour. A similar shift should also occur in the presence of less water in the system, corresponding to increasing the aggregate to paste volumetric ratio. Inversely, the lowering in the quantity of the liquid phase corresponds to the water requirement of each particular system to achieve equal flow resistance. This issue is dealt with more detail in section 3.2.

Flow curves (T vs. N) were built at the starting of rotation, according to the speed profile presented in Figure 4.22. Up-down (1+2) and down-up (2+3) flow curves are shown in Figure 4.22.a and 4.16.b, respectively.

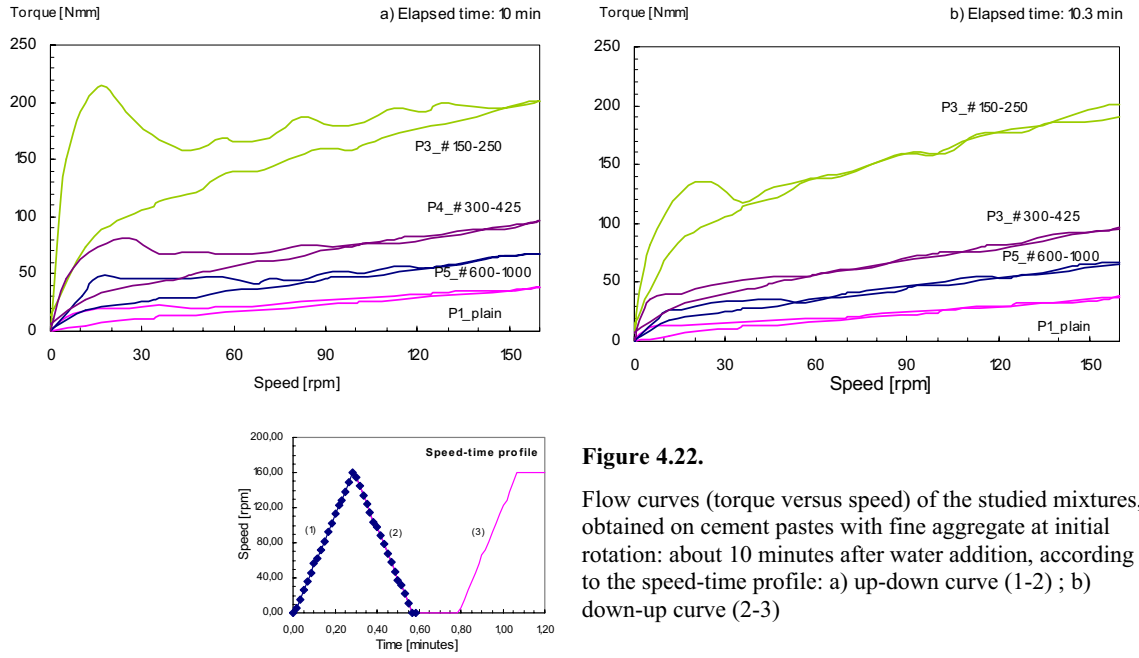

Figure 4.22.

Flow curves (torque versus speed) of the studied mixtures, obtained on cement pastes with fine aggregate at initial rotation: about 10 minutes after water addition, according to the speed-time profile: a) up-down curve (1-2) ; b) down-up curve (2-3)

The formation of a hysteretic area can be observed in several formulations, but is especially significant in the system P3 (Figure 4.22.a). This may be attributed to insufficient structural breakdown during mixing procedure. However, the rotation at 160 rpm during the first up-down step was able to significantly reduce the hysteretic behaviour (compare with Figure 4.22.b), which seems systematically more relevant as finer the narrow size fractions are used.

From the analysis of the torque and speed data in each measuring instant, yield stress and plastic viscosity may be plotted against time, as shown in Figure 4.23.. The rheological parameters were obtained according to Eq. (4.21). From a general perspective over Figure 4.23., it can be observed the separate effects of the diameter change on the rheological parameters. Yield stress presents an approximately parabolic development with time. The extremes, corresponding to initial and final yield stresses are higher for smaller particle sizes. The plastic viscosity shows a different development with time, as it decreases progressively until the end of the test. The initial peak is also related with the aggregate size, which corresponds to the initial value of torque for each particular system: the lower the diameter of fine aggregate particles, the higher the initial plastic viscosity is observed.

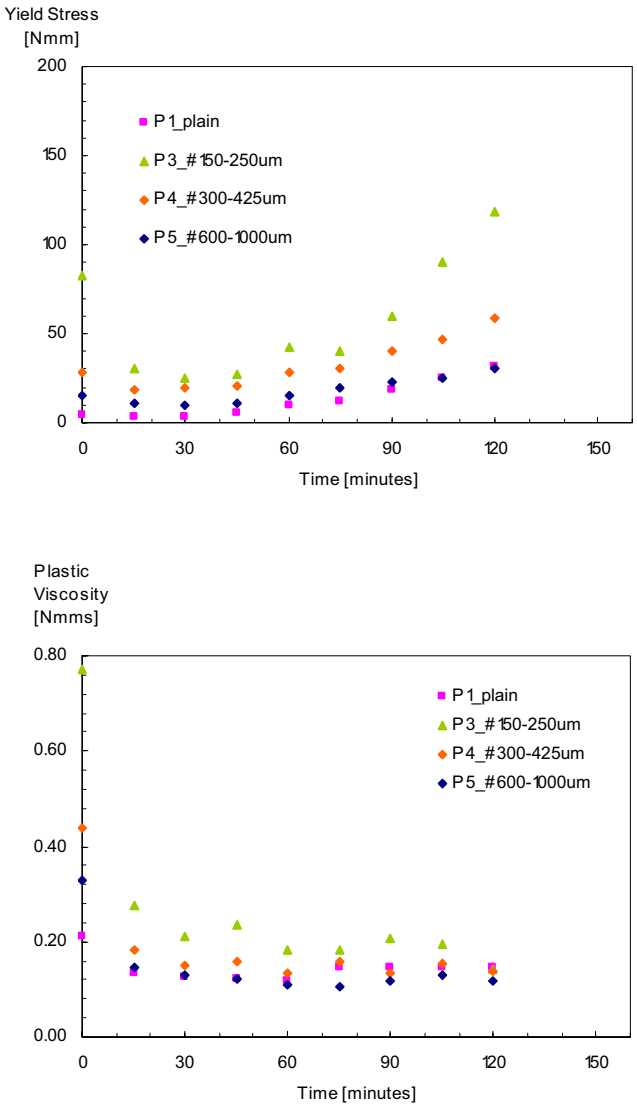

Figure 4.23.

Variation of rheological parameters: yield stress and plastic viscosity, with time.

The effect of the average diameter of fine aggregate particles on the rheological parameter relationship, yield stress and plastic viscosity can be seen in Figure 4.24.

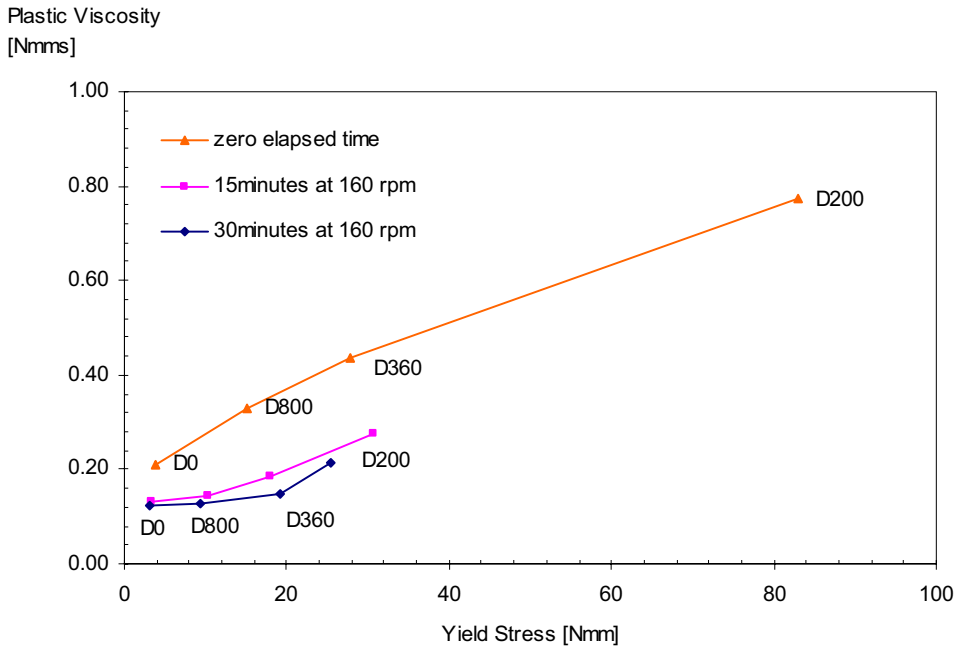

Figure 4.24.

Effect of the average diameter of fine quartz particles on the relationship between yield stress and plastic viscosity. Aggregate to paste ratio is 0.55 by volume. "zero elapsed time" corresponds to 10 minutes after water addition. D0 translates a plain cement paste system. Di represents the average particle size of each fraction tested.

For a volumetric aggregate to paste ratio of about 0.55, the closest geometrical size of aggregate is about 1 mm, in order to maintain the rheological properties of cement paste. This finding is particularly interesting to produce high performance cement-based materials with improved workability. It is interesting to observe the convexity type shape between both curves, which may be related to previous mixing history. The inversion on the concavity seen between 15 and 30 minutes in continuous rotation at 160 rpm suggests that higher mixing time is required for decreasing size of fine aggregate particles in relation with the plain cement paste (D0). Further research is needed to study both cement and mineral addition agglomerate index in mortar systems.

Table 4.4 resumes the rheological properties of the studied mixtures, including the data taken from the measurements of the spread, taken from the flow table test (mini-slump). The slump value can qualitatively describe the workability of the system, by the observation of the intrinsic ability that a sample shows in terms of cohesiveness and spreading. However, it is not able to distinguish the effect of the yield stress and plastic viscosity. From the analysis of Table 4.4, it is possible to conclude that all mixtures showed sufficient cohesion to stand alone without spreading, by looking to the initial slump values. On the other hand, torque peak, yield stress and plastic viscosity may be related to the final slump value, as shown in Figure 4.25.

Several attempts were made to find a relation between the slump value and the rheology parameters. Y. Tanigawa et. al [218, 219] have supported the idea of that the slump value is more sensitive to the yield stress than to plastic viscosity. Subsequent work by other authors focused on the packing density and the virtual packing density from a particular particle size distribution, resulting a number of equations to express both rheological parameters and consequent correlation

with the slump value [220, 221]. However, the correlation factor obtained by this approach show lack in accuracy. As an example, in reference [222], a correlation factor between yield stress and the slump value of 0.86 is found and plastic viscosity is not taken into account, since it is found to be poorly correlated with the slump value.

Table 4.4: Rheological parameters and slump values

Mixture	Slump values		Torque	Rheology parameters	
	Initial	Final	Initial Peak	Yield stress	Plastic viscosity
P3_#150-250 µm	100	125	201,11	82,90	0,77
P4_#300-425 µm	100	140	96,41	27,91	0,44
P5_#600-1000 µm	110	175	67,40	15,17	0,33
P6_#1000-2000µm	110	160	99.66	22.10	0.47
P1_plain	110	175	48,49	3,91	0,21

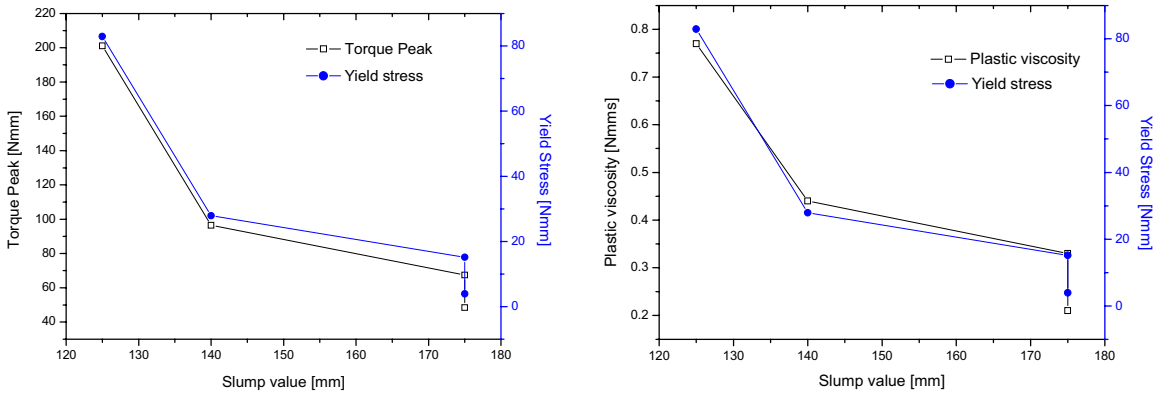

Figure 4.25.

Relation between final slump value, torque peak and yield stress.

In the left-plot, the double y-axe shows the synergy between initial torque peak, characteristic of each system and the measured yield stress. At the right, the same correlation is attempted with plastic viscosity and yield stress.

Figure 4.25 shows that both plastic viscosity and yield stress are influenced in the same proportion with varying values of the intrinsic surface area on the same type of cement and at the same packing density. This is not surprising, as if the rheological parameters are linearly related within the Bingham equation, and therefore the variation of both parameters in respect with slump should result similar. But the bottom line is that the packing density approach cannot explain the previous results, since theoretically speaking, the same packing density should result in similar rheological behaviour, which is not the case of the investigated mixtures.

Other researchers have studied the effect of ultra-fine fillers on the rheological parameters of cement-based materials [223, 224]. M. Nehdi et al [225] have conducted comprehensive work on this topic. Some important observations are taken from his work, referring to the requirement of the superplasticizer used to attain the same workability, being higher for silica fume added systems than for plain cement systems. In the present work, the silica fume replacement ratio was kept constant and therefore is not a parameter in observation. On the other hand, the combined effect of fine aggregate particles and silica fume may be of interest to address in the following.

The use of ultra-fine particles as silica fume should be favourable towards the improvement of the rheological parameters in a mortar system. This should be brought out by the break of interlocking forces occurring when cement and aggregate particles act alone within the flow process. In fact, the shape and size of the micro-fillers may act as lubrifying elements similar to rolling-element bearing systems. While these micro-ball bearings have sufficient water adsorbed at their surface, the aggregate particles should flow more easily within the cement paste matrix. An opposite effect is found in the case of plain cement-silica pastes, as observed for plain cement pastes without the presence of microsilica. In this case, the geometrical scale factor between cement grains and microsilica particles may limit the mechanism mentioned above. The affinity with surfactant molecules (SP) and multilayer adsorption forces at the ultra-fine material surface were pointed out to explain the rheology-change induce by the addition of silica fume [225]. In addition, the dissolution of silica fume, due to the growing alkaline medium which forms at the wetting of cement, may also support such rheology-change [217]. However, higher contents of silica fume may favour the rheological properties of the cement paste, provided that these are sufficiently small in respect with the cement grains and stable within the dormant period of the hydration process. Further examination of these aspects is required to have a deeper comprehension of the silica fume effects on the rheology of cement pastes.

4.3.5. Water requirement of cement-silica-quartz systems

The previous section gave ground to the idea of that the fine aggregate particles greatly interfere with the rheology of high performance cement-based materials. In the following, water is added to system P3 and P4. Different particle diameters may require different quantities of water to achieve equal rheological performance. This is particularly important to sustain the idea of that the surface area is governing the flow behaviour within the low diameter sizes and to confirm the empirical relation proposed here. Figure 4.26 shows the rheology-change of the previous samples when this specific amount of water is added to the system.

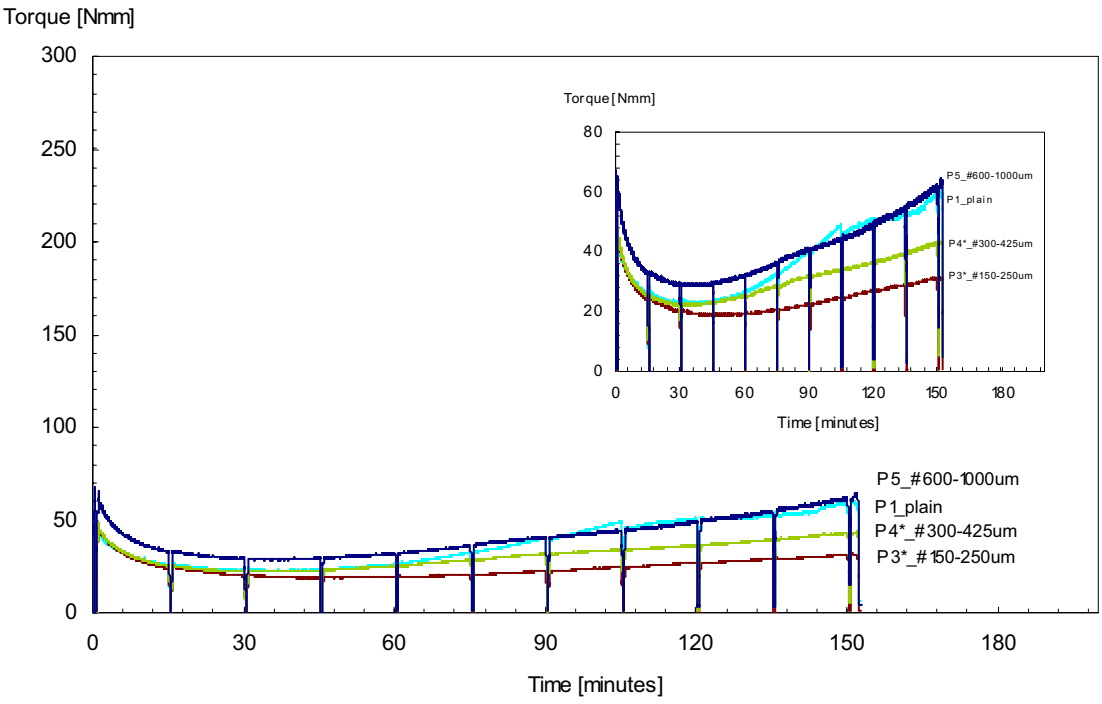

Figure 4.26.

Torque variation with time at constant speed in a dwell profile for water-added specimens

It can be seen that the water addition performed according to Table 4.3 results in similar rheological behaviour in respect with the plain cement paste, especially for the initial torque values and the subsequent drop. After 15 minutes of continuous mixing at 160 rpm, the mixtures with additional water (system P3 and P4) show a less pronounced increase in torque, as the water to solid ratio increases. Thus, the rheology-change may be occurring at a slower rate, indicating that the transition from viscous-elastic to solid state is extended. This observation is supported by the penetration tests performed to the same mixtures. The VICAT value (final setting time) found for the system P3 and P3* is of respectively 10 and 14 hours. It is noted that the transition from viscous to solid state occurs at a faster rate in the system with less water, by analysing the penetration profiles.

The water quantity in each particular system automatically defines the volume fraction of water and solids. As the water is added to the system, this ratio decreases and thus, in high performance systems, this is often on the brink of the cohesiveness loss. Figure 4.27 shows the effect of different water quantities in the studied systems in respect with the torque peak. It can be observed that a given quantity of water and thus, a similar volumetric aggregate to paste ratio, the torque peak is different for varying particle size of aggregate. This sustains the theory of that the surface area is governing the flow properties of cement-silica-quartz systems. The system with particle size of 150 to 250 µm requires higher amount of water than the system with particle size of 300 to 425 µm to achieve the same rheological performance.

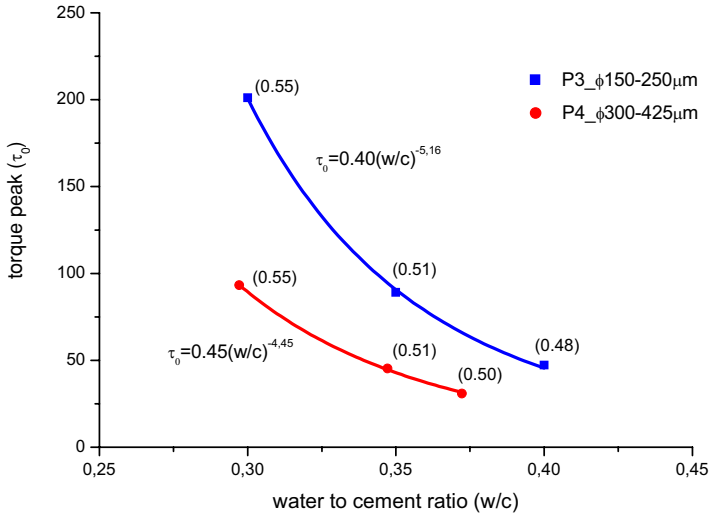

Figure 4.27.

Influence of the water to cement ratio on the rheological properties of cement-silica pastes with fine aggregate particles.

Values of the volumetric aggregate to paste ratio are indicated between parentheses.

The following empirical expressions were obtained from the previous results:

$$\tau_0 = 0{,}40(w/c)^{-5.16}, \text{ for particle size between 150 and 250 µm} \quad (4.22)$$

$$\tau_0 = 0{,}45(w/c)^{-4.45}, \text{ for particle le size between 300 and 425 µm} \quad (4.23)$$

These equations can be used to express the torque peak as function of the water to cement ratio in a given system. Mixture P5 was not considered in the previous, since it does not dramatically interfere with the flow properties of the cement-silica paste considered alone.

The requirement of water to achieve a similar rheological behaviour may affect the hardened properties of each system, as the water to solid ratio increases. However, the superplasticizer dosage is kept constant in this work. The use of higher dosages of SP might reduce the water requirement and may sustain the hardened properties of each particular system.

4.3.6. On modeling rheology of cement-silica-quartz systems

According to data, the change of the diameter range between 75 and 1000 μm influence in great extent the flow resistance with time and thus, the rheological parameters. The initial period is of major importance for describing each system in relation with the characteristic yield stress and plastic viscosity. In addition, the rheology studies are restricted by the limitations of the rheometer used in the experiments: for example, the maximum diameter of the aggregate (2 mm) and the maximum torque (300 N.mm) supported by the apparatus. Modelling rheology is therefore required both to predict the fresh behaviour of high performance cement-based materials with low water to cement ratios and to overcome the intrinsic limitations of this particular rheometer.

From the results obtained in the experiments, several tests were made to mathematically express the behaviour of mortars in the initial period of the flow measurement.

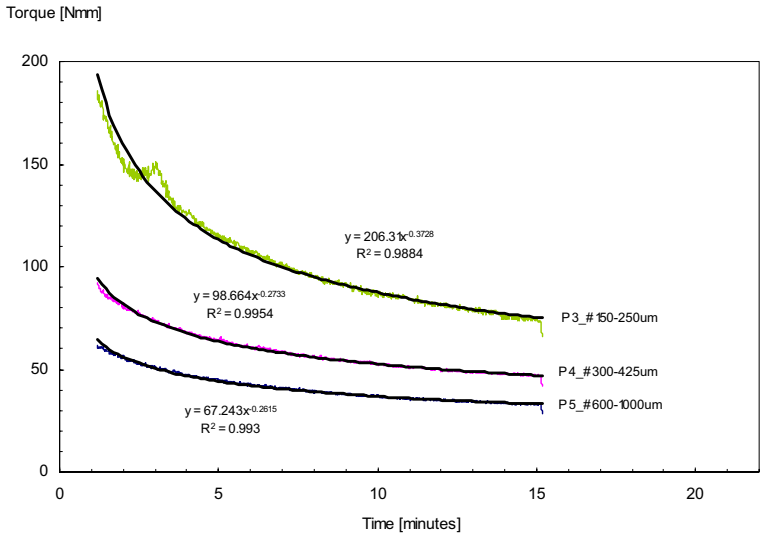

Figure 4.28.

Torque variation in the first 15 minutes at 160 rpm

A power expression was applied to translate the drop in torque presented by both paste and mortars in the first 15 minutes at 160 rpm.

$$y = Ax^{-B} \tag{4.24}$$

Where A and B are constants that depend on the average particle size extracted from the sharp or narrow fraction of aggregate. This applies only to this particular cement-silica paste with basic water to cement ratio of 0.30. The curve fitting accurately translates the influence of the selected

particle size distribution on the measured torque. From the assumption that *A* and *B* depend on the average diameter of aggregate, it is possible to obtain the independent constants as function of the diameter, as follows:

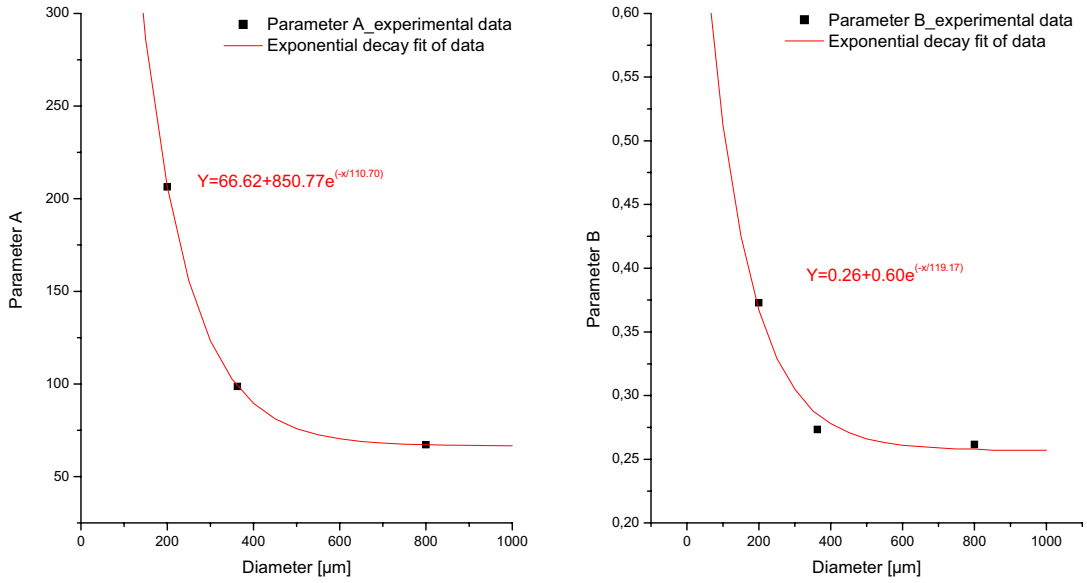

Figure 4.29.

Curve fitting for A and B parameters as function of average diameter

Three approximations were performed in order to find the best fitting curve for each parameter of the function f(x). The polynomial expression cannot be directly applied, since, although a high correlation factor is found, it does not provide the proper physical background. In fact, the second order quadratic expression predicts a lowering within the intermediate diameter range, which does not conform to the reality. The power relation gives more physical background, since it best describes the specific surface area of particles, but the correlation factors are very weak and do not provide the required confidence level. A third approximation, based on the exponential decay in the form of eq. (4.25), was adopted to express the variation of the average particle size with the parameters A and B.

$$y = y_0 + A_1 \cdot e^{\left(-\phi / t_1\right)} \tag{4.25}$$

Where y_0 is the infinite value of each parameter A and B, ϕ is the particle diameter, A_1 and t_1 are constants that depend on the growth behaviour of each parameter with the particle size of aggregate particles.

From the previous assumption, it should be possible to plot the effect of lower aggregate fractions on the initial resistance to flow. Eq.(4.26) and (4.27) were derived from the data and may be used to calculate the yield stress and plastic viscosity of an individual system. An example is given in

Figure 4.30 for the system with particle size between 75 and 125 µm. This system was impossible to test within the intrinsic limitations of the rheometer.

$$A = 66.62 + 850.77 \cdot e^{\left(-\phi/110.70\right)} \tag{4.26}$$

$$B = 0.26 + 0.60 \cdot e^{\left(-\phi/119.17\right)} \tag{4.27}$$

A remark should be made about these expressions. The parameters A and B can be directly related to yield stress and plastic viscosity within the time interval from about 1 to 15 minutes. The later (15 min) is more sensible to parameter B than parameter A. In fact, at this period, the paste has been subjected to continuous structural breakdown. When the flow velocity is taken from 160 to 0 rpm, the system tends to recover and rebuild. At this point, plastic viscosity may be the governing factor on the rheology, rather then the yield stress. Since hydration is now at the dormant period only a few products are formed. If the stationary time interval is stretched, the yield stress would probably further increase, recovering up to the initial values. This idea is also supported by N. Roussel [226, 227]. Accordingly, this recovering stage is expressed by structuration at rest, meaning that, more time or energy is required to achieve the steady state of flow.

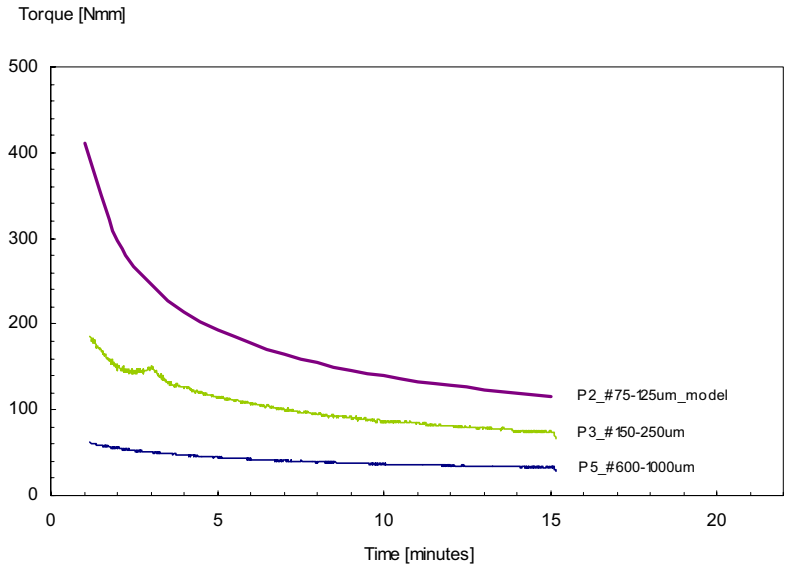

Figure 4.30.

Model for system with aggregate size below 150 microns and basic w/c ratio of 0.30.

From the direct observation of Figure 4.30, the model presented is able to translate the initial rheological behaviour of system P2 (75-125µm), unperformed due to the rheometer limitations and due to the low water content. This model can be further developed to account other parameters. For example, the effect of combined narrow sized clusters in the characteristic torque and slump value can be easily derived from the expressions 7 and 8, by simple proportioning.

In order to validate the model assumptions, a combined analysis between the model prediction and the experimental results is performed in the system P2, as shown in Figure 4.31. It should be emphasized that this particular system was subjected, in the experimental procedure, to higher mixing time at higher speed, and a slight increase of water was required to overcome the torque peak limitation.

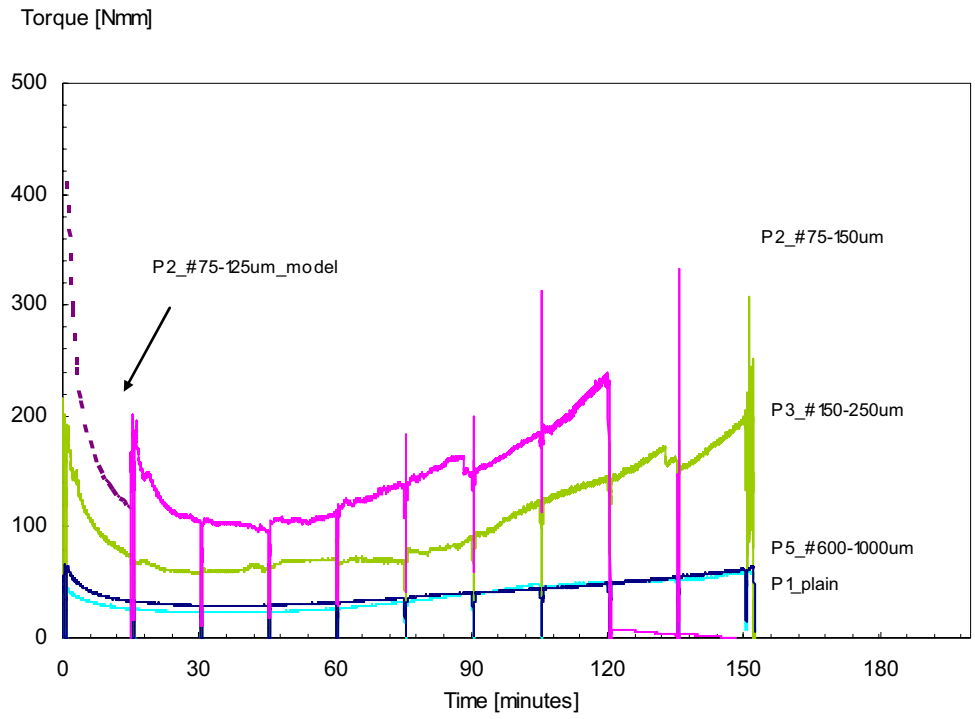

Figure 4.31.

Flow resistance of system P2 combined with the previous model

There is a clear miss-fit at the time instant of 15 minutes in the torque value considering the model value versus the experimental value. This can be explained by different shear history that the mixture P2 experienced in respect to the continuous breakdown that the standard mixtures were subjected. It is noted that the torque value assumes the model value by shifting of the mixture P2 from 30 to 15 minutes, which would bring additional 15 minutes at 160 rpm to the same torque value of the model value. Further research is required to develop the modelling of such complex phenomenon, where numerous parameters interact.

4.3.7. Conclusions

The effect of narrow size fractions of fine aggregate particles on the rheological parameters was analysed. This allowed the development of an empirical model to predict the torque of high performance cement-based mortars with time. Some conclusions may be drawn from the experimental observations:

(1) Rheology of high performance cement-based materials can be strongly affected by the addition of fine aggregate.
(2) Particle size of aggregate particles governs the flow in the range of 75 and 1000 micrometers, via specific surface and water fixation mechanisms. Above this range, resultant friction forces from the equilibrium between gravitational and buoyancy forces, together with intrinsic measuring system parameters (gap in the paddle) seem to be to governing factors influencing the rheological parameters.

(3) The water requirement was performed for varying particle diameters and expressions were obtained in order to achieve the same workability. These expressions may be extended to account different fractions of aggregate and to predict the initial torque peak. Further examination on the superplasticizer requirement is needed.
(4) The modelling approach proposed in the manuscript to characterize the initial drop of torque may be used to express the behaviour of mortars with low water to cement ratio and the addition of silica fume. A comprehensive set of equations were brought out from this approach and may be applied to translate both yield stress and plastic viscosity for a given system.
(5) The viscous-elastic to solid transition measured by VICAT needle is faster, as finer the aggregate particles are used. The use of superplasticizer (SP) could efficiently delay this transition by stretching the dormant period up to 4 to 6 hours after the water addition. Although this transition cannot be seen by the rheometer, the increasing values of torque at about 2 to 4 hours, suggests that a degree of structural build-up occurred in the system, which, at this instant, may be at the onset of setting.

4.4. Early-age properties of Portland cement-silica mortars

This section deals with the basic macroscopic properties of cement-based materials with silica fume addition and fine aggregate particles. The purpose of this study is to characterise fresh and hardened properties of low porosity and low water cement mortars with focus on the underlying mechanisms that may influence the autogenous deformation occurring in the paste sub-system. This is done with two main objectives. Primarily, it seems important to know the influence of fine aggregate particles on the first reaction of clinker minerals. This may be studied by means of isothermal calorimetry. Secondly, it is fundamental to study the basic hardened properties, namely the mechanical properties, which knowledge may prove of value in separating the restraint effect from other phenomena such as internal curing by fine aggregate particles in high performance cement-based materials.

4.4.1. Introduction

The use of silica fume in cement-based materials has shown to be of value in improving the fresh and hardened properties of SF-modified systems. The fresh behaviour was analysed in section 4.3. There are contradicting ideas about the effect of silica fume on the mechanical properties of high performance concrete. This is mostly related to the mechanical effects that arise from self-desiccation and autogenous deformation phenomena. The effect of silica fume on plain cement pastes was analysed in section 3.3, where it is seen that silica fume may significantly increase the mechanical performance of the system. With this concern, autogenous deformation turns out beneficial. However, the introduction of aggregate particles may limit the potential for strength enhancement, due to a restraining effect that cleaves the free movement of the paste fraction. The anchoring of such movement by the aggregate phase may give rise to internal build-up stresses, that may have has a consequence generalised microcracking of the system. Little work is found at a microscopic level with this respect. This is mostly due to the difficulties in analysing this problem without creating new cracks caused by sample preparation procedures. However, Lura et al[228], in their experiments with gallium intrusion were able to observe microcracking in SF-modified systems subjected to restraint by steel rods. A linear elastic analysis of the stresses generated by autogenous shrinkage is proposed by Jason Weiss[229], on the base of the previous experimental framework. In either case, no microcracking was ever observed in systems were the restraint develops mainly by the aggregate phase.

Furthermore, it is suggested that internal curing may be active in cement-based systems due to the presence of fine aggregate particles. It follows that it is of vital importance to understand the effect of the fine aggregate particles on the mechanical properties of the system. In this work, the compressive strength of SF-modified cement mortars is studied. The influence of the size of aggregate particles on the compressive strength of the composite material is analysed.

4.4.2. Materials

The systems in analysis comprised a SF-modified paste by an addition rate of 15% wt. of cement and a basic w/c ratio of 0.30. The mortar systems were prepared by adding fine aggregate particles in fractions starting in diameter of 125, 250, 500 and 1000 μm at a volume concentration of about 35%. To ensure adequate workability, a naphthalene-based superplasticizer was added to the SF-modified cement-based systems at a rate of 1% wt. of cement.

4.4.3. Methods

Heat of Hydration

Hydration heat was deduced from temperature increase in a calorimeter developed in the LAB. The set-up of this apparatus is shown in Figure 4.32. The calorimeter consists in four cylindrical units which are polyvinyl-based. Semi-adiabatic conditions are assured by insulating the internal cylinders with liner similar to the used in furnaces. Each cell has two thermocouples type K. An external sensor is placed at the surface of the polyurethane box that accommodates the cells can monitor the exchange of temperature with the surroundings. The four cells can operate continuously during the desired curing age. Tests were performed at room temperature and readings were sampled every 5 min by a Compact Fieldpoint CFP-2100 datalogger, provided by NI Instruments.

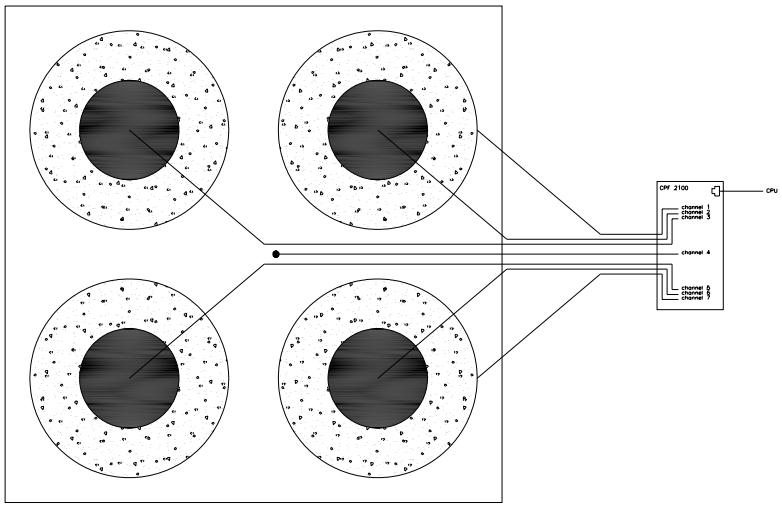

Figure 4.32.

Kalorimeter set-up scheme. Solid area corresponds to hydrating cement paste. Dashed area represents the foam insulation and white area constitutes the polyurethane box.

The equipment was thoroughly tested and calibrated before and after each experiment, by measuring the heat loss with water. According to the calibration and testing procedure, the maximum measurement error of the temperature sensors is less than 2 degrees Celsius, corresponding to a variation not higher than 1%, within the operating temperatures taken from seven samples of plain cement paste. It is found that the heat loss from the system can not be considered purely isothermal, since the rate of heat loss does not show a linear slope with temperature decrease. However, for the purpose of this investigation, it seems sufficiently relevant to know the rate of reaction taken from the temperature increase of each system, assuming a quasi-isothermal condition.
About 100 g of cement paste were cast into cylindrical tubes with diameter of 40 mm. End-closures prevent any mass loss from the sample within a test duration of 7 days. The measurements started after 30 minutes in respect with the mixing time.

Compressive Strength and Modulus of Elasticity in compression

Compressive strength and modulus of elasticity in compression were determined in a fully automated INSTRON testing machine with a load capacity of 250 KN. Early-age tests were done according to the hydration peaks of each system, as measured by temperature evolution in the cement pastes. In the case of cement-silica systems, cylindrical specimens with diameter of 14 mm

and length to diameter ratio of 2 were tested at the first 24 hours. The strength properties at 3, 7 and 28 days in sealed conditions were also examined. The tests were performed according procedures described in ASTM standards number C39-86.

4.4.4. Results and discussion

Temperature increase and reaction rate

Temperature evolution in the studied systems is presented in Figure 4.33. The different absolute temperature is due to the different specific volume of cement in the paste and mortar systems. As expected, it may be seen that the first reaction occurs earlier for the system with smaller aggregate particles. There is no substantial variation in both peak intensity and width at half-height when comparing the systems with different aggregate size, which is indicating that the main clinker reaction is independent from the particle size of aggregate, viz the aggregate may not be influencing the heat transfer rate from the system. Although it is not clear in Figure 4.33, the peak position decreases systematically when decreasing the particle size of fine aggregate, as observed for the intermediate range of aggregate particle size (#250-500 μm).

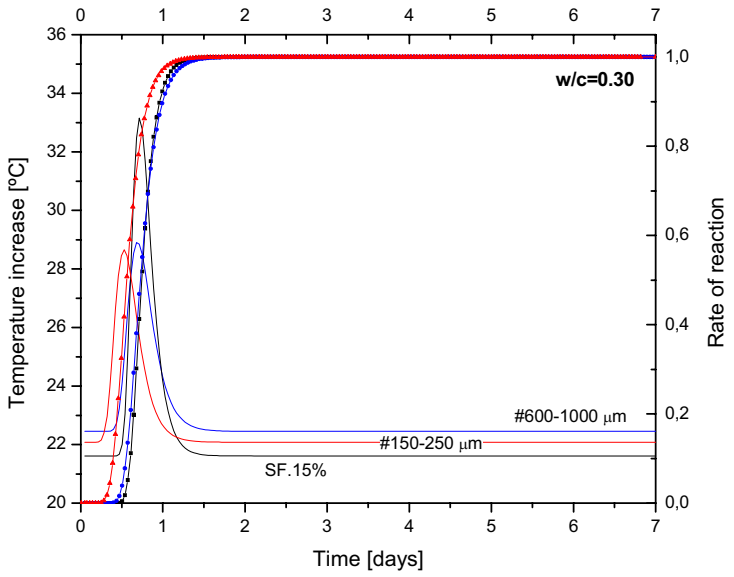

Figure 4.33.

Temperature development of cement mortars with varying fine aggregate particle size versus cement paste.

Furthermore, VICAT needle tests are consistent with the previous argument, the time for first reaction decreasing monotonically with the particle size of fine aggregate particles, within the range from about 1 mm down to 125 micron.

Compressive strength and modulus of elasticity in compression

Test results of the strength development on the studied systems, as taken within the first month in sealed hydration are presented in Figure 4.34. It is seen that the strength of the system is inverse-related with the particle size of fine aggregate, the strength increasing as finer the aggregate is used. A relevant strength loss is noted in the system M4 when compared with the system M1, which ascends to 30%, no segregation being noted. It is also registered that the introduction of aggregate at a concentration of 35% by volume leads to a relevant decrease in strength, when comparing the

mortar systems with the plain cement-silica paste. At the age of 28 days, the system with particle size within 1000 and 2000 has less than 50% of the strength of the correspondent SF-modified paste. This may be explained either by the poor mechanical properties of the aggregate in relation with the pure cement paste or by the combined effect from the existence of weaker regions, ITZ, which comprises a higher water to cement ratio, thus higher porosity, and the occurrence of cracking events due to restraint during shrinkage of the paste fraction causing weakening of the system. In other words, the weaker link is the aggregate phase, rather than the cement paste, or the cement paste structure looses density, the later event being due to ITZ formation or due to microcracking, viz. physical or/and mechanical.

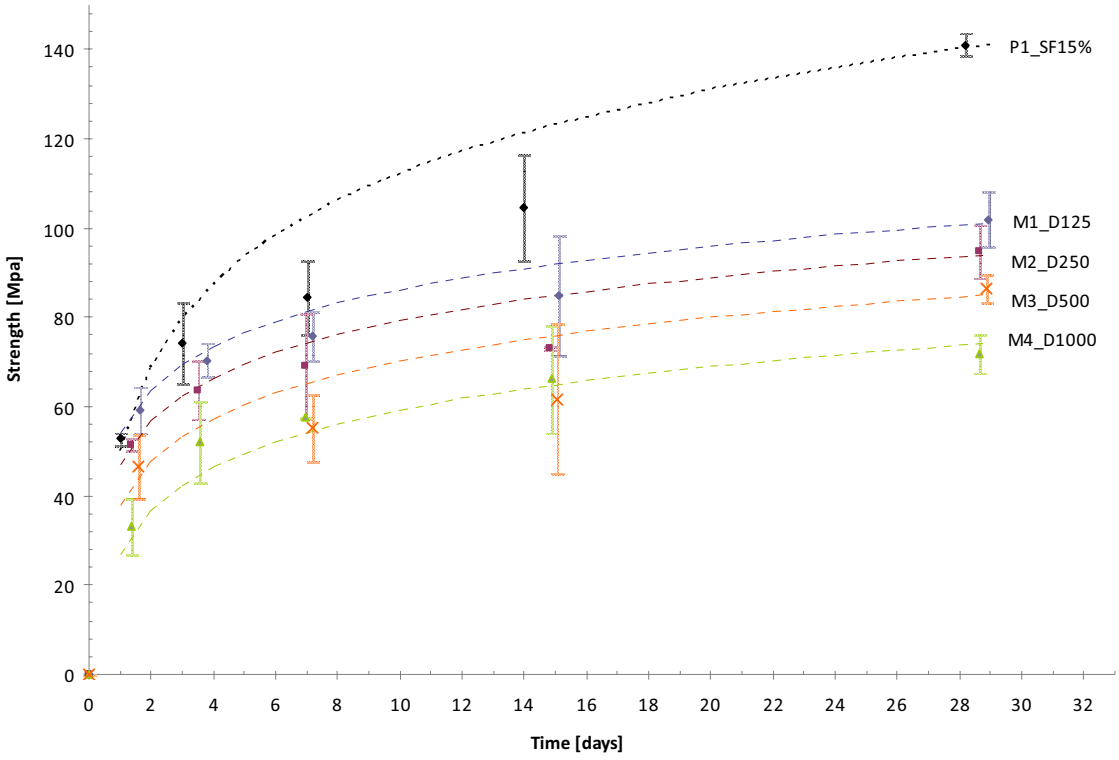

Figure 4.34.

Compressive strength of high performance cement-based mortars with varying size of fine aggregate particles. Basic water to cement ratio is of 0.30. Curing was performed in autogenous conditions and at the temperature of 20 ºC.

In the later case (system M4), it seems feasible to assume that, in the absent of substantial ITZ regions, which was seen in section 4.1 to be related with the particle size of the aggregate, microcracking did developed due to restrained shrinkage, causing weakening of the paste fraction.

In relation with the effect of the variation of the particle size of aggregate on the strength properties of mortar systems, the following hypotheses may apply in front of the experimental observations. Either the system suffered from restraint effects and microcracking has concomitant developed with the increase of the restraint size or the strength of the aggregate particles affected the strength of the composite material, and mechanical properties of the phase constituents are governing the strength development. Internal curing promoted in systems M1 and M2 may be also influencing the strength development in these systems.

With this respect, it seems fundamental to consider the degree of desiccation of the systems and study the relation between internal relative humidity and strength level. In section 4.2, it is seen that the introduction of this concentration of aggregate particles only slightly affects the internal relative humidity, the significance being only relevant during the initial period of hydration (first 3-days). In either case, it is difficult to separate the three effects with the present results, because all explanations are viable to explain the strength decrease. Primarily, it seems feasible to assume that microcracking has developed more severely in the present of bigger aggregate particles, due to increased degree of restraint. This may have support in the poor stability shown by the systems M3 to M4. In addition, all systems showed poor stability at the end of two weeks in sealed conditions, by observing the dispersion in the strength-values obtained in the compressive tests. Secondly, it is also possible that the higher the size of the aggregate particles, the lower is the strength of the material, since it may show more defects. It is well known that the degree of fracture may be related with the size of the aggregate particles subjected to crushing. If the finer particles included fewer defects upon fracture, this would also explain the difference found when accessing the strength of the composite material. Finally, internal curing may also have played its role, since a lower desiccation rate will, in principle, subject the system to a lower build up-stress. A simultaneous action of these aspects finds space in logic, but it seems that the most probable cause for the previous events is that microcracking did developed, weakening both the transition zone and the cement paste fraction.

4.4.5. Conclusions and further research

Fine aggregate particles may significantly affect the hydration and hardened properties of SF-modified cement-based systems at the macroscopic scale. The autogenous phenomena in cement-based mortars must include mechanical effects in the evaluation of such properties, as microcracking seems to appear in the course of autogenous shrinkage. However, the degree of fracture by fine aggregate particles must be studied to clarify any interference with the observed phenomena. From the results taken, the following conclusion may be outlined:

(1) Hydration of mortar systems

Hydration of SF-modified cement-based materials is significantly influenced by the presence of fine aggregate. The time for first reaction decreases systematically, when the particle size of the aggregate is decreased, as observed by rheology (section 4.3), calorimetry and penetration (VICAT) measurements. The kinetics in the first and second reaction should be further analysed in the first 48 hours. This is presently being done.

(2) Compressive strength and modulus of elasticity in compression

The particle size of aggregate dramatically influences the mechanical behaviour of cement-silica systems. The lower particle size in the range of 125 to 250 micron leads to increased stability of the system and higher strength at the age of 28 days. Particles in the range of 500 and 1000 micron registered the lower strength. Three mechanisms were pointed out to explain such behaviour: internal curing, restraint effect and degree of fracture in aggregate, with the obvious consequence in the degree of microcracking, the flaws increasing with the particle diameter. The test results are consistent with the discussion performed in section 4.2, which refers to the autogenous deformation of the same systems.

The preliminary testing on modulus of elasticity in compression showed that the particle size of aggregate also influences the stress-strain curves of cement-based systems with fine aggregate particles. However, further studies on the relation between the material properties, essentially mechanical, in pure tension and compression, seem fundamental to comprehend the build-up stresses arising at ITZ regions. From this knowledge, it should be feasible to predict the cracking behaviour in face of autogenous deformation

(3) Restraint, Internal Curing and Microcracking

Further research is needed in relation with microcracking in SF-modified systems. Only few isolated references may be found about this topic. This is because it is not easy to study a cement-based system in autogenous conditions without inducing microcracking events, which advents from the sample preparation procedures or from interferences with the system-conditions. However, some experiments with *Gallium* intrusion combined with ESEM/EPMA analysis may be used with this purpose. This is presently being done.

5. Conclusions and future research

This section describes the principal findings which are resultant from the framework that was taken during the course of the PhD work. It seems logic to separate the main conclusions in the same manner as the parts that integrate this thesis, namely theoretical and experimental. Furthermore, integration between the parts is performed.

In relation with the theoretical overview, it should be emphasised that autogenous deformation and internal curing may not be solely characterised by macroscopic material-analysis. The underlying mechanisms require a more fundamental approach in questioning the sources of deformation. The evolution of the system-physics within the viscous-elastic to solid transition remains uncertain. It should be also noted that the mechanical dependency of autogenous deformation is poorly developed. The relation between the elastic behaviour of the composite material at early-age is extremely difficult to describe, adding the difficulty in characterising the elastic properties of cement paste individually. The fragile behaviour of pure cement paste, especially when hardening is considered makes any interference with the system a potential source of damage. The knowledge of the pore structure is essential to clearly identify which mechanism is governing the volume-changes at any point. This knowledge is poorly developed in low water and low porosity systems. A time-dependent micro-mechanical approach may be of interest in understanding the self-restraint of the system. It is concluded that an isolated approach of taking a governing mechanism to explain the deformation occurring in the system can not explain the whole phenomena, referring to both autogenous deformation and internal curing.

In section 3.3, the autogenous deformation was analysed in respect with the dependency from purely chemical and thermodynamic phenomena. It is seen that a major part of autogenous shrinkage occurring in plain cement pastes is due to RH-change, rather than chemical-based phenomena. However, the addition of silica fume into the hydrating system corresponds to an increased dependency from chemically-based phenomena, such as first reaction of clinker minerals, which is seen to be empowered by the presence of silica fume. It is also seen that pozzolanic activity may be mostly prominent at very early-age, essentially in the first three days in sealed curing, as concluded in section 3.2. A more fundamental characterisation of such reactions may be of interest in pointing out the underlying mechanisms that result in volume-change of the material, since it is not clear that RH-change during the middle period (considering the time needed to achieved strain stability) always is accompanied by a marked deformation. Some questions are then left open with this respect.

In section 3.1, the effect of w/c ratio and silica fume content on autogenous deformation was analysed. The results are consistent with the experimental background registered in previous research. It is seen that the pozzolanic activity of silica fume may be limited at early-age, which is consistent with the micro-analysis performed in section 3.2. In sufficient content, this turns even beneficial in “controlling” the strain development, but is not clear if the restraining effect may damage the system. Furthermore, it is seen that the mitigation of autogenous deformation by superabsorbent polymers is not as straightforward as the present state of knowledge indicates. The physical and chemical nature of superabsorbent may significantly affect the course of autogenous deformation. For practical applications, it is suggested that preliminary tests on the polymer response with water, and especially with pore fluid may be done, followed by autogenous

deformations measurements. The basic formula proposed by Ole Jensen may be used for prescribing the amount of internal curing water to be used in counteracting autogenous deformation, in the case of plain cement-based materials. Such application in the case of SF-modified systems may be more critical, since the system easily develops capillary discontinuity. Any excess-water that may be beyond this threshold may be of little importance, since the time that water-diffusion takes at this point may overpass the required curing time over a certain under-curing fraction. This is sustained by the results in section 3.2, where internal curing activity is analysed. In conjunction with this aspect, it should be clearly demystified that self-desiccation may be beneficial in protecting the system from water-dependent long-term reactions, as alkali-silica reaction and other long-term phenomena. In addition, the strength properties of the material are also improved as the bulk density is a function of the water to cement ratio of the system and consequently, of the space available for hydration products. Thus, self-desiccation is, within the mechanical stability of a particular system, beneficial.

Furthermore, in section 3.4, fundamental research on the absorption kinetics of superabsorbent polymers revealed the importance of the superabsorbent particle size in influencing the absorption capacity and absorption rate. In fact, the findings brought out from this framework may give new direction when predicting fresh and hardened properties of water-entrained cement-based materials. Some applications are presently being developed.

Other important results are described in section 3.5, which dealt with the mechanisms of internal curing. Beside the process of internal curing, which should be activated by chemical shrinkage of the system, a third mechanism is proposed. This is mechanical-based and is related with restraining effects determined by the macropore-structure of the system, which being a consequence of the use of superabsorbent polymers, is controlled by the diameter size of the polymer particles. However, some open questions result from the previous statement, which are related with the time required for internal curing. This is why it is fundamental to study the risk of microcracking associated with the stability of the system. For a cement-based system, the strain stability may be obtained only a few days after the activation of hydration process. In the case of SF-modified systems, the strain stability may take the whole month, for a system cured at 20 ºC. If the curing temperature is increased to the double, the time required so that the system achieves stability in strains may be shortened by approximately 2 weeks.

Section 4 dealt with the possibility of using very fine aggregate particles as a new method for internal curing of cement-based materials. It is concluded that the model approach was feasible to explain the proposed phenomena, but the effectiveness of such preposition is not clear from the experimental framework, especially in respect with the significance of the internal curing when compared with the restraining effect. It is systematically seen that special-size and concentration of fine aggregate particles may lead to a reduction in the autogenous deformation, as measured by the linear technique. However, this reduction do not encounters a “significant” correspondence when analysing the same variation in the RH-change profiles. However, a significant change in the RH-change within the first 48 hours is noted. It follows that the use of special-size aggregate affects the first reaction at the bulk regions. Subsequently, the desiccation at the ITZ regions is controlled.

In either case, a “significant” restraining effect is also operating, the particle size being primarily important in restraining the free movement of the paste. Again, mechanical-based mechanisms require further understanding. Efforts should be done to answer the following questions:

(a) Is the change in internal humidity registered in SF-modified systems internally cured by fine aggregate particles significant in terms of build-up stress?

(b) When does the restraint effect become significant for a particular cement-based mortar?

As seen in the section dedicated to rheology of high performance cement-based materials, the particle size of fine aggregate significantly affects the rheology parameters yield stress and plastic viscosity. Although a direct relation between internal stresses and the rheological parameters may not be easily established, the conclusions about the fresh state of SF-modified mortars support some considerations made about the systems in respect with the internal curing possibility. The rheology-modification of a system may be also used as an indication of poor deformability during hardening. A model to control such deformability is suggested. To correlate the rheology parameters with the deformation upon setting in autogenous conditions may be an interesting topic to be developed in further work.

The final section of this thesis was dedicated to early-age properties of SF-modified cement-based mortars. This may give ground to the development of a framework for modeling the restraint effect arising from the aggregate phase in cement-based materials. A more consistent perception of the elastic properties of both cement paste and mortars is essential with this respect. This is presently being done. Microcracking was pointed out as a potential cause in the decreased compressive strength in the material, being governed by restraint effect for the higher diameter range of fine aggregate particles. However, the use of finer particles leads systematically to higher strength at the end of 28 days. A framework in order to observe microcracking in SF-modified systems with fine aggregate particles was initiated. The upcoming results will appear in a short come. In either case, there is a marked increase in the strength properties of SF-modified mortars when the same size of aggregate particles is used to develop internal curing.

The pre-assumption of that only one strategy to eliminate autogenous deformation may be overseen to be of close-minded nature. Thus, several combine strategies can and should be tried, which may bring significant advantages within the design target for each application. A first example that may be idealised is the combine approach of ITZ/SAP, which would return the results shown in Figure 5.1.

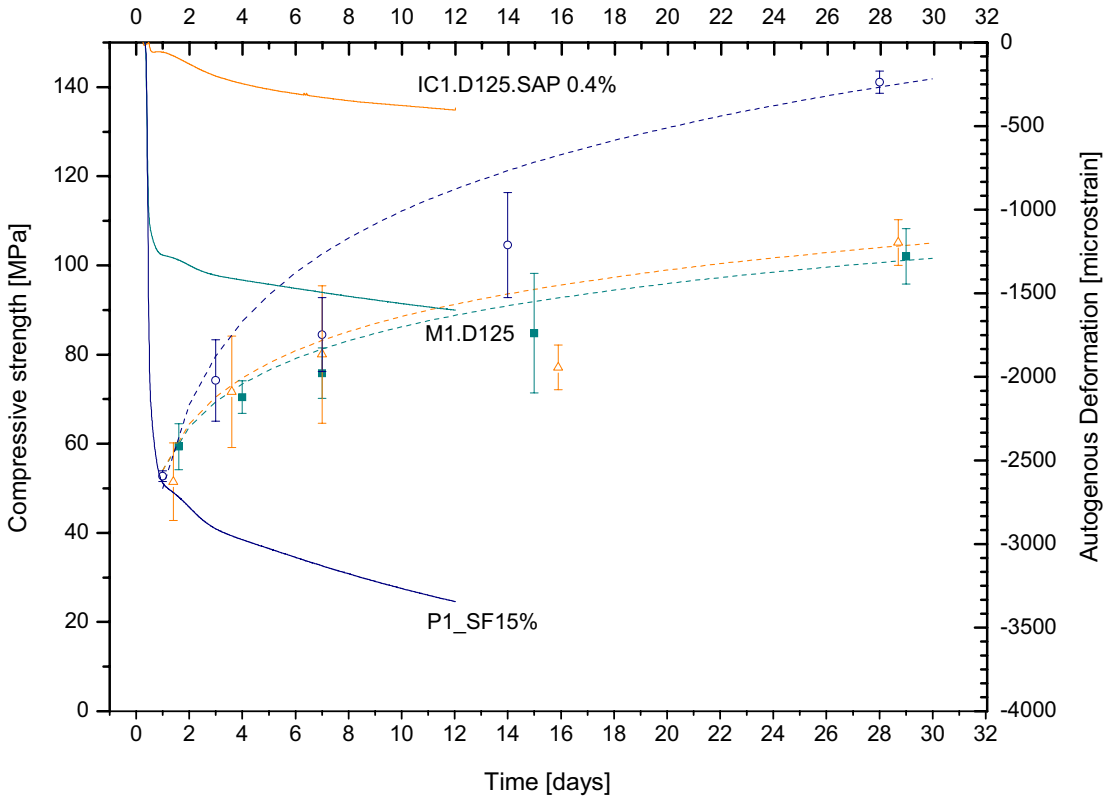

Figure 5.1.

Combined view of strength and strain development of SF-modified systems with internal curing.

The combined approach of using fine aggregate particles and superabsorbent polymers may be simultaneously used for mitigating autogenous deformation and increasing strength of the system, with reduced probability for microcracking of the system.

A second approach may be tried, which is based on the integration of a minimum-restraint combined with the ITZ concept. The result, obtained by non-natural selection of powder materials would appear as shown in Figure 5.2.

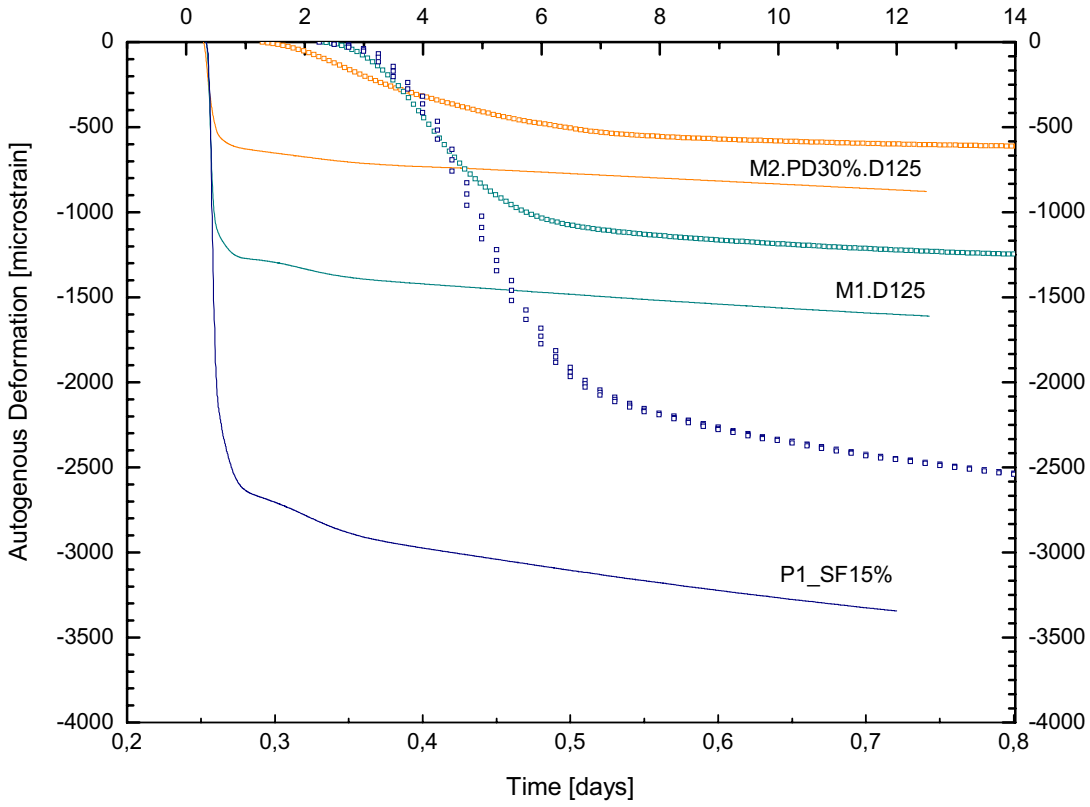

Figure 5.2.

Combined view of strain development of SF-modified systems with internal curing.

The combined approach of using powder and fine aggregate particles may be simultaneously used for reducing the potential for microcracking within the first and secondary reaction of clinker minerals and silica fume, and as partial mitigation of autogenous deformation.

Again, full mitigation of autogenous deformation may not be needed.

The result may be micro-concrete with nanocracking, rather then micro.

References

1. Esteves, L.P., P. Cachim, and V. Ferreira, *Mechanical Properties of Cement Mortars with Supersabsorbent Polymers*, in *Advances in Construction Materials 2007*, C.U. Grosse, Editor. 2007, Springer Publ.
2. Esteves, L.P., et al., *Effect of curing conditions on the mechanical properties of mortars with superabsorbent particles.* Materiales de Construcción. **(in press)**.
3. Paiva, H., et al., *Rheology and hardened properties of single-coat render mortars with different types of water retaining agents.* Construction and Building Materials, 2009. **23**(2): p. 1141-1146.
4. Aïtcin, P.-C., *High-performance concrete*: Taylor & Francis, 1998, 591pp.
5. Meeks, K.W. and N.J. Carino, *Curing of High-Performance Concrete: Report of the State-of-the-Art*. 1999, National Institute of Standards and Technology.
6. Jensen, O.M. and P.F. Hansen, *Autogenous deformation and RH-change in perspective.* Cement and Concrete Research, 2001. **31**: p. 1859-1865.
7. Bentz, D.P., *Capillary Porosity Depercolation/Repercolation in Hydrating Cement Pastes Via Low-Temperature Calorimetry Measurements and CEMHYD3D Modeling.* Journal of American Ceramic Society, 2006. **89**(8): p. 2606–2611.
8. *ACI Committee 308: Guide to Curing Concrete*, ACI, Editor. 1999.
9. Lerch, W., *Plastic Shrinkage.* ACI Materials Journal, 1957. **53**(2): p. 797-802.
10. Cohen, M.D., J. Olek, and W.L. Dolch, *Mechanism of plastic shrinkage cracking in portland cement and portland cement-silica fume paste and mortar*, in *Cement and Concrete Research*. 1990. p. 103-119.
11. Aïtcin, P.C., *The durability characteristics of high performance concrete: a review.* Cement and Concrete Composites, 2003. **25**: p. 409-420.
12. Bentur, A., *Introduction: Overview of early age cracking*, in *Early Age Cracking in Cementitious Systems*, A. Bentur, Editor. 2000, RILEM.
13. Tazawa, E.-i. and S. Miyazawa. *Autogenous shrinkage of concrete and its importance in concrete*. in *5th International RILEM Symposium on Creep and Shrinkage in Concrete*, Z.P. Bazant and I. Carol, Editors. London, 1993. E&FN Spoon.
14. Jensen, O.M., *Autogenous Phenomena in Cement-based Materials*: Nyt Teknisk Forlag, Ingerslevsgade 44, 1705 Kobenhavn V, Denmark, 2005.
15. Neville, A.M., *Properties of Concrete*. 4th ed: Longman Group Limited, 1995.
16. Aroni, S. and M. Polivka. *Effect of expanded shale aggregate on properties of expansive-cement concrete*. in *Proceedings of RILEM Symposium On Testing and Design Methods of Lightweight Aggregate Concretes*, J. Ujhelyi, Editor. Budapest, Hungary, 1967.
17. Holm, T.A. *Performance of Structural Lightweight Concrete in a Marine Environment*. in *Proceedings of International Symposium On Performance of Concrete in Marine Environments, ACI SP65*, V.M. Malhotra, Editor. St. Andrew By-The-Sea, Canada, 1980. American Concrete Institute.
18. Dhir, R.K., et al., *Investigation into the feasibility of formulating 'self-cure' concrete*, in *Materials and Structures/Materiaux et Constructions*. 1994, Chapman & Hall Ltd. p. 606-615.
19. Dhir, R.K., P.C. Hewlett, and T.D. Dyer, *Durability of 'self-cure' concrete.* Cement and Concrete Research, 1995. **25**(6): p. 1153-1158.
20. Powers, T.C. and T.L. Brownyard, *Studies of the physical properties of hardened Portland cement paste, Bulletin 22.* Research Laboratories of the Portland Cement Association, 1948.
21. Hewlett, P., *Lea's Chemistry of Cement and Concrete*. 4th edition ed: Butterworth-Heinemann, 2003.
22. Taylor, H.F.W., *Cement chemistry*. 2nd. ed: Telford, London, 1997.

23. Jennings, H.M., B.J. Dalgleish, and P.L.Pratt, *Morphological development of hydrating tricalcium silicate as examined by electron microscope techniques.* Journal of American Ceramic Society, 1981. **64**(10): p. 567-572.
24. Dubinin, M.M., *The Potential Theory of Adsorption of Gases and Vapors for Adsorbents with Energetically Nonuniform Surfaces.* Chemical Reviews, 1960. **60**: p. 235-241.
25. Everett, D.H., *Manual of Symbols and Terminology for Physicochemical Quantities and Units, Appendix II: Definitions, Terminology and Symbols in Colloid and Surface Chemistry.* Pure and applied chemistry, 1971. **Vol. 31**(4).
26. Aligizaki, K.K., *Pore Structure of Cement-Based Materials: Testing Interpretation and Requirement*: Taylor & Francis, 2005.
27. Bažant, Z.P. and F.H. Wittmann, *Creep and shrinkage in concrete structures*: John Wiley & Sons, New York, 1982.
28. Andersson, K., et al., *Chemical composition of cement pore solutions*, in *Cement and Concrete Research*. 1989. p. 327-332.
29. Page, C.L. and Ø. Vennesland, *Pore Solution Composition and Chloride Binding Capacity of Silica-Fume Cement Pastes.* Materials and Structures, 1983. **16**(91): p. 19-25.
30. Jensen, O.M., *Autogenous deformation and RH-change - self-desiccation and self-dessication shrinkage*, Building Materials Laboratory, Technical University of Denmark, 1993, **PhD**.
31. Bentz, D.P. and P.E. Stutzman, *Evolution of porosity and calcium hydroxide in laboratory concretes containing silica fume*, in *Cement and Concrete Research*. 1994. p. 1044-1050.
32. Feldman, R.F., *The effect of sand/cement ratio and silica fume on the microstructure of mortars*, in *Cement and Concrete Research*. 1986. p. 31-39.
33. Mehta, P.K. and O.E. Gjørv, *Properties of portland cement concrete containing fly ash and condensed silica-fume*, in *Cement and Concrete Research*. 1982. p. 587-595.
34. Bentur, A. and M.D. Cohen, *Effect of Condensed Silica Fume on the Microstructure of the Interfacial Zone in Portland Cement Mortars.* Journal of the American Ceramic Society, 1987. **70**(10): p. 738-743.
35. Bentz, D.P., P.E. Stutzman, and E.J. Garboczi, *Experimental and simulation studies of the interfacial zone in concrete*, in *Cement and Concrete Research*. 1992. p. 891-902.
36. Sellevold, E.J., et al., *Silica fume-cement pastes: hydration and pore structure*, in *Condensed silica fume in concrete, Report BML 82.610*, O.E. Gjorv and K.E. Loland, Editors. 1982, Norwegian Institute of Technology: Trondheim. p. 19-50.
37. Jensen, O.M. and P.F. Hansen, *Autogenous deformation and change of the relative humidity in silica fume-modified cement paste.* ACI Materials Journal, 1996. **93**(6): p. 539-543.
38. Pallière, A.M., M. Buil, and J. Serrano. *Durability of very high performance concrete:effect of hydration shrinkage on early age cracking*. in *1st International RILEM congress on durability of construction materials*, J.C. Maso, Editor. Versailles, 1987. Chapman and Hall.
39. Geiker, M.R., *Studies of Portland Cement Hydration*, Institute of Mineral Industry, Technical University of Denmark, 1983, **PhD**.
40. Tazawa, E.-i., S. Miyazawa, and T. Kasai, *Chemical shrinkage and autogenous shrinkage of hydrating cement paste*, in *Cement and Concrete Research*. 1995. p. 288-292.
41. Lura, P., *Autogenous Deformation and Internal Curing of Concrete,* PhD thesis, Technische Universiteit Delft, 2003, **PhD**: p. 169.
42. Hagymassy, J., Jr., S. Brunauer, and R.S. Mikhail, *Pore structure analysis by water vapor adsorption - I. t-Curves for water vapor*, in *Journal of Colloid and Interface Science*. 1969. p. 485-491.
43. Lynam, *Growth and movement in Portland cement concrete*. 1934, Oxford University Press: London. p. 26-27.
44. Powers, T.C., *Thermodynamics of volume change and creep*, in *Materiaux et Constructions, Materials and Structures*. 1968. p. 487-507.
45. Wittmann, F., *Surface tension shrinkage and strength of hardened cement paste.* Materials and Structures, 1968. **1**(6): p. 547-552.
46. Shuttleworth, R., *The surface tension of solids*, in *Proceedings of the Physical Society. Section A*. 1950. p. 444-457.

47. Polzer, E., *Diplomarbeit angefertigt am Lehrstuhl für Baustoffkunde und Werkstoffprüfung der T. H. München.* 1967.
48. Bangham, D.H. and N. Fakhoury, *The Swelling of Charcoal. Part I. Preliminary Experiments with Water Vapour, Carbon Dioxide, Ammonia, and Sulphur Dioxide.* Proceedings of the Royal Society of London. Series A, 1931. **130**(812).
49. Setzer, M.J., *A method for description of mechanical behaviour of hardened cement paste by evaluating adsorption data*, in *Cement and Concrete Research*. 1976. p. 37-47.
50. Feldman, R.F. and P.J. Sereda, *A model for hydrated Portland cement paste as deduced from sorption-length change and mechanical properties.* Materials and Structures, 1968. **1**(6): p. 509.
51. Lura, P., O.M. Jensen, and K.v. Breugel, *Autogenous shrinkage in high-performance cement paste: An evaluation of basic mechanisms.* Cement and Concrete Research, 2003. **33**: p. 223–232.
52. Jensen, O.M., *Thermodynamic limitation of self-desiccation.* Cement and Concrete Research, 1995. **25**(1): p. 157-164.
53. Bentz, D.P., M.R. Geiker, and K.K. Hansen, *Shrinkage-reducing admixtures and early-age desiccation in cement pastes and mortars*, in *Cement and Concrete Research*. 2001. p. 1075-1085.
54. Folliard, K.J. and N.S. Berke, *Properties of high-performance concrete containing shrinkage-reducing admixture*, in *Cement and Concrete Research*. 1997. p. 1357-1364.
55. Rongbing, B. and S. Jian, *Synthesis and evaluation of shrinkage-reducing admixture for cementitious materials*, in *Cement and Concrete Research*. 2005. p. 445-448.
56. Beltzung, F. and F.H. Wittmann, *Role of disjoining pressure in cement based materials.* Cement and Concrete Research, 2005. **35**: p. 2364 –2370.
57. Splittgerber, H., *Spaltdruck zwischen festkorpern und auswirkungen auf probleme in der technik*, in *Cement and Concrete Research*. 1976. p. 29-35.
58. Ferraris, C.F. and F.H. Wittmann, *Shrinkage mechanisms of hardened cement paste*, in *Cement and Concrete Research*. 1987. p. 453-464.
59. Völkl, J.J., R.E. Beddoe, and M.J. Setzer, *The specific surface of hardened cement paste by small-angle X-ray scattering effect of moisture content and chlorides*, in *Cement and Concrete Research*. 1987. p. 81-88.
60. Stockhausen, N., et al., *Untersuchung von gefriervorgǎngen in zementstein mit hilfe der DTA*, in *Cement and Concrete Research*. 1979. p. 783-794.
61. Odler, I., et al., *Pore structure analysis by water vapor adsorption. IV. Analysis of hydrated portland cement pastes of low porosity*, in *Journal of Colloid and Interface Science*. 1972. p. 265-276.
62. Pashley, R.M., *DLVO and hydration forces between mica surfaces in Li+, Na+, K+, and Cs+ electrolyte solutions: A correlation of double-layer and hydration forces with surface cation exchange properties*, in *Journal of Colloid and Interface Science*. 1981. p. 531-546.
63. Hua, C., P. Acker, and A. Ehrlacher, *Analyses and models of the autogenous shrinkage of hardening cement paste - I. Modelling at macroscopic scale*, in *Cement and Concrete Research*. 1995. p. 1457-1468.
64. Fisher, L.R., *Forces due to capillary-condensed liquids: Limits of calculations from thermodynamics*, in *Advances in Colloid and Interface Science*. 1982. p. 117-125.
65. Crassous, J., et al., *Experimental Study of a Nanometric Liquid Bridge with a Surface Force Apparatus*, in *Langmuir*. 1993. p. 1995.
66. Hansen, T.C., *Drying shrinkage of concrete due to capillary action.* Materials and Structures, 1968. **2**(1): p. 7-9.
67. Churaev, N.V., G. Starke, and J. Adolphs, *Isotherms of Capillary Condensation Influenced by Formation of Adsorption Films - 1. Calculation for Model Cylindrical and Slit Pores*, in *Journal of Colloid and Interface Science*. 2000. p. 246-253.
68. Starov, V.M. and N.V. Churaev, *Thickness and stability of liquid films on nonplanar surfaces*, in *Colloid Journal of the USSR*. 1978. p. 757-761.
69. Glasser, L.S.D., *Osmotic pressure and the swelling of gels*, in *Cement and Concrete Research*. 1979. p. 515-517.
70. Kalousek, G.L. and E.J.Benton, *MECHANISM OF SEAWATER ATTACK ON CEMENT PASTES*, in *J Amer Concrete Inst*. 1970. p. 187-92.

71. Mehta, P.K., *Mechanism of expansion associated with ettringite formation*, in *Cement and Concrete Research*. 1973. p. 1-6.
72. Mehta, P.K. and A. Klein, *Investigations on hydration products in system 4CaO.3Al2O 3.SO3-CaSO4-CaO-H2O*, in *National Research Council -- Highway Research Board -- Special Reports*. 1966, National Research Council. p. 328-352.
73. Nagataki, S. and H. Gomi, *Expansive admixtures (mainly ettringite)*, in *Cement and Concrete Composites*. 1998. p. 163-170.
74. Bentur, A., *Properties of type K expansive cement of pure components I. Hydration of unrestrained paste of expansive component - Results*, in *Cement and Concrete Research*. 1974. p. 519-532.
75. Correns, C.W., *Growth and dissolution of crystals under linear pressure*, in *Discussions of the Faraday Society*. 1949. p. 267-271.
76. Scherer, G.W., *Crystallization in pores*, in *Cement and Concrete Research*. 1999. p. 1347-1358.
77. Weiss, J. and N. Berke, *Admixtures for Reduction of Shrinkage and Cracking*, in *Early Age Cracking in Cementitious Systems*, A. Bentur, Editor. 2000, RILEM.
78. Hori, A., et al. *Influence of expansive additives on autogenous shrinkage*. in *Autoshrink'98, Proceedings of the International Workshop on Autogenous Shrinkage of Concrete*, E. Tazawa, Editor. Hiroshima, Japan, 1998.
79. Bentz, D.P. and O.M. Jensen, *Mitigation strategies for autogenous shrinkage cracking*, in *Cement and Concrete Composites*. 2004. p. 677-685.
80. Bjøntegaard, Ø., T.A. Hammer, and E.J. Sellevold, *On the measurement of free deformation of early age cement paste and concrete.* Cement and Concrete Composites, 2004. **26** p. 427–435.
81. Garrault-Gauffinet, S. and A. Nonat, *Experimental investigation of calcium silicate hydrate (C-S-H) nucleation.* Journal of Crystal Growth, 1999. **200**: p. 565-574.
82. Garrault, S., et al., *Study of C-S-H growth on C_3S surface during its early hydration.* Materials and Structures, 2005. **38**: p. 435-442.
83. Bentz, D.P., et al., *Influence of cement particle-size distribution on early age autogenous strains and stresses in cement-based materials*, in *Journal of the American Ceramic Society*. 2001, American Ceramic Society. p. 129-135.
84. Setter, N. and D.M. Roy, *Mechanical features of chemical shrinkage of cement paste*, in *Cement and Concrete Research*. 1978. p. 623-634.
85. Lawrence, F.V., J.F. Young, and R.L. Berger, *Hydration and Properties of Calcium Silicate Pastes.* Cement and Concrete Research, 1977. **7**: p. 369-378.
86. de Haas, G.D., et al., *The shrinkage of hardening cement paste and mortar*, in *Cement and Concrete Research*. 1975. p. 295-319.
87. Hansen, P.F. and O.M. Jensen, *Self-desiccation shrinkage in low porosity cement-silica mortar.* Nordic Concrete Research, 1989. **8**: p. 89-102.
88. Knudsen, T., *The dispersion model for hydration of portland cement I. General concepts*, in *Cement and Concrete Research*. 1984. p. 622-630.
89. Charron, J.P., et al., *Microstructural models*, in *Early Age Cracking in Cementitious Systems*. 2000, RILEM.
90. Diamond, S., *A critical comparison of mercury porosimetry and capillary condensation pore size distributions of portland cement pastes*, in *Cement and Concrete Research*. 1971. p. 531-545.
91. Diamond, S., *Mercury porosimetry - An inappropriate method for the measurement of pore size distributions in cement-based materials*, in *Cement and Concrete Research*. 2000. p. 1517-1525.
92. Bentz, D.P., E.J. Garboczi, and D.A. Quenard, *Modelling drying shrinkage in reconstructed porous materials: application to porous Vycor glass.* Modelling and Simulation in Materials Science and Engineering, 1998. **6**: p. 211-236
93. van Breugel, K., *Numerical simulation of hydration and microstructural development in hardening cement-based materials (I) theory*, in *Cement and Concrete Research*. 1995. p. 319-331.
94. van Breugel, K., *Numerical simulation of hydration and microstructural development in hardening cement-based materials (II) Applications*, in *Cement and Concrete Research*. 1995. p. 522-530.
95. Koenders, E.A.B. and K. van Breugel, *Numerical modelling of autogenous shrinkage of hardening cement paste*, in *Cement and Concrete Research*. 1997. p. 1489-1499.
96. Bentz, D.P., *A Three-Dimensional Cement Hydration and Microstructure Program. I. Hydration Rate, Heat of Hydration, and Chemical Shrinkage*, in *NIST 6265*. 1995.

97. Bentz, D.P., *Three-dimensionnal computer simulation of portland cement hydration and microstructure development.* Journal of the American Ceramic Society, 1997. **80**(1): p. 3-21.
98. Bentz, D.P. and E.J. Garboczi, *A hard core/soft shell microstructural model for studying percolation and transport in three-dimensional composite media*, in *NIST 6265*. 1999.
99. Maekawa, K., R. Chaube, and T. Kishi, *Modelling of concrete performance*: E & FN Spon, 1999.
100. Zhutovsky, S., *Modelling of Autogenous Shrinkage*, in *Early Age Cracking in Cementitious Systems*. 2000, RILEM.
101. Ishida, T., et al., *Micro-physical approach to coupled autogenous and drying shrinkage of concrete*, in *Proceedings of International Workshop on Autogenous Shrinkage of Concrete*, E.Tazawa, Editor. 1998: Hiroshima, Japan. p. 301-312.
102. Boivin, S., et al., *Experimental assessment of chemical shrinkage of hydrating cement paste*, in *Autogenous Shrinkage of Concrete*, E. Tazawa, Editor. 1999, London: E&FN Spon. p. 81-92.
103. Hu, C. and L. Barcelo, *Investigation on the Shrinkage of Self-compacting Concrete for Building Construction.* Concrete Engineering Series, 1999. **30**: p. 228-242.
104. Jensen, O.M. and P.F. Hansen, *A dilatometer for measuring autogenous deformation in hardening Portland cement paste.* Materials and Structures, 1995. **181**(28): p. 406-409.
105. Justnes, H., B. Reyniers, and E.J. Sellevold, *An evaluation of methods for measuring chemical shrinkage of cementitious pastes.* Nordic Concrete Research, 1994. **25**(2): p. 45-61.
106. Barcelo, L., et al. *Linear vs. volumetric autogenous shrinkage measurement: Material behaviour or experimental artefact?* in *Self-desiccation and its importance in concrete technology*, B. Persson and G. Fagerlund, Editors. Lund, Sweden, 1999.
107. Hammer, T.A., *Test methods for linear measurement of autogenous shrinkage before setting*, in *Proceedings of the International Workshop: Autogenous Shrinkage of Concrete*, T. E-I, Editor. 1999, E & FN Spon. p. 143–154.
108. Hammer, T.A., Ø. Bjøntegaard, and E.J. Sellevold. *Measurement methods for testing of early age autogenous strain*. in *Proceedings of the RILEM International Conference on Early Age Cracking in Cementitious Systems*, K. Kovler and A. Bentur, Editors. Haifa, Israel, 2001.
109. Ø. Bjøntegaard, T.A.H., ErikJ. Sellevold, *On the measurement of free deformation of early age cement paste and concrete.* Cement and Concrete Composites, 2004. **26**: p. 427-435.
110. Lura, P. and O.M. Jensen, *Discussion: On the measurement of free deformation of early age cement paste and concrete [Bjøntegaard Ø, Hammer TA, Sellevold EJ. Cement & Concrete Composites 2004;26:427–435].* Cement and Concrete Composites, 2005. **27**: p. 854-856.
111. Sant, G., P. Lura, and J. Weiss, *Measurement of Volume Change in Cementitious Materials at Early Ages: Review of Testing Protocols and Interpretation of Results.* Journal of the Transportation Research Board. **Concrete Materials 2006**: p. 21-29.
112. Aïtcin, P.C. *Autogenous shrinkage measurement*. in *AUTOSHRINK International Workshop on Autogenous Shrinkage of Concrete*, E.-i. Tazawa, Editor. Hiroshima, Japan 1998.
113. Jia-ping, L., et al. *Study on the self-desiccation effect in early-age concrete and the determination of "time-zero" of self-desiccation shrinkage*. in *International RILEM Conference on Volume Changes of Hardening Concrete: Testing and Mitigation*, O.M. Jensen, P. Lura, and K. Kovler, Editors. Technical University of Denmark, Lyngby, Denmark, 2006. RILEM.
114. Han, N., A.v. Beek, and E.A.B. Koenders, *Electric methods*, in *Advanced Testing of Cement-Based Materials during Setting and Hardening - Final Report of RILEM TC 185-ATC*, H.W. Reinhardt and C.U. Grosse, Editors. 2005, RILEM. p. 35-79.
115. Reinhardt, H.-W., C. Grosse, and A. Herb, *Ultrasonic monitoring of setting and hardening of cement mortar - A new device.* Materials and Structures, 2000. **33**: p. 580-583.
116. Tian, Q. and O.M. Jensen, *Measuring Autogenous Strain of Concrete: Technical report*. 2007, Department of Civil Engineering, Technical University of Denmark.
117. Hammer, T.A., *Deformations, strain capacity and cracking of concrete in plastic and early hardening phases*, Faculty of Engineering Science and Technology, Norwegian University of Science and Technology, 2007, **Ph.D.**
118. Sellevold, E.J. and Ø. Bjøntegaard. *Thermal expansion coefficient (CTE) of cement paste and concrete: effect of moisture content*. in *Advances in Cement and Concrete*, D.A. Lange, K.L. Scrivener, and J. Marchand, Editors. Copper Mountain, Colorado, USA, 2003. Engineering Conferences International.

119. Bentz, D.P., *A review of early-age properties of cement-based materials.* Cement and Concrete Research, 2008. **38**: p. 196-204.
120. Bjøntegaard, Ø. and T.A. Hammer. *RILEM TC 195-DTD: Motive and Technical content*. in *International RILEM Conference on Volume Changes of Hardening Concrete: Testing and Mitigation*, O.M. Jensen, P. Lura, and K. Kovler, Editors. Technical University of Denmark, Lyngby, Denmark, 2006. RILEM.
121. *RILEM Technical Committee TC 196-ICC: Internal Curing of Concrete. Chapter 2 - Definitions*, RILEM, Editor. 2003: Bagneux.
122. Weber, S. and H.W. Reinhardt, *A New Generation of High Performance Concrete: Concrete with Autogenous Curing.* Advanced Cement Based Materials, 1997. **6**: p. 59-68.
123. Jensen, O.M. and P.F. Hansen, *Water-entrained cement-based materials. I. Principles and theoretical background.* Cement and Concrete Research, 2001. **31**: p. 647-654.
124. Jensen, O.M. and P.F. Hansen, *Water-entrained cement-based materials. II. Experimental observations.* Cement and Concrete Research, 2002. **32**: p. 973–978.
125. Philleo, R.E., *Concrete science and reality*, in *Materials Science of Concrete II*, J.P. Skalny and S. Mindess, Editors. 1991, American Ceramic Society: Westerville, OH.
126. Zhang, M.H. and O.E. Gjørv, *Characteristics of lightweight aggregates for high performance concrete.* ACI Materials Journal, 1991. **88**(2): p. 150-158.
127. Zhutovsky, S., K. Kovler, and A. Bentur. *Autogenous curing of high-strength concrete using pre-soaked pumice and perlite sand*. in *Proceedings of the Third International Research Seminar: Self-desiccation and its importance in concrete technology*, B. Persson and G. Fagerlund, Editors. Lund, Sweden, 2002.
128. Zhutovsky, S., K. Kovler, and A. Bentur, *Influence of cement paste matrix properties on the autogenous curing of high performance concrete.* Cement and Concrete Composites, 2004. **26**: p. 499-507.
129. Bentz, D.P. and K.A. Knyder, *Protected paste volume in concrete. Extension to internal curing using saturated ligthweight fine aggregate.* Cement and Concrete Research, 1999. **29**: p. 1863-1867.
130. ASTM, *C33 Standard Specification for Concrete Aggregates*.
131. Geiker, M., D.P. Bentz, and O.M. Jensen, *Mitigating autogenous shrinkage by internal curing*, in *High Performance Sructural Ligthweight Concrete*, J.P. Ries and T.A. Holm, Editors. 2004, American Concrete Institute. p. 143-154.
132. Bentz, D.P., et al., *Influence of silica fume on diffusivity in cement-based materials. I. Experimental and computer modeling studies on cement pastes.* Cement and Concrete Research, 2000. **30**: p. 953-962.
133. Christensen, B.J., T.O. Mason, and H.M. Jennings, *Influence of Silica Fume on the Early Hydration of Portland Cements Using Impedance Spectroscopy.* Journal of the American Ceramic Society, 1992. **75**(4): p. 939-945.
134. El-Enein, S.A.A., et al., *Electrical conductivity of concrete containing silica fume.* Cement and Concrete Research, 1995. **25**(8): p. 1615-1620.
135. Hansen, P.F. and O.M. Jensen, *Water-entrained cement-based materials.* Patent V.P.A.S. Plougmann, Version Number, Densit A/S [DK/DK]
136. Buchholz, F.L. and A.T. Graham, eds. *Modern superabsorbent polymer technology*. 1998, WILEY-VCH: New York.
137. Igarashi, S.-i. and A. Watanable. *Experimental study on prevention of autogenous deformation by internal curing using superabsorbent polymer particles*. in *International RILEM Conference on Volume Changes of Hardening Concrete: Testing and Mitigation*, O.M. Jensen, P. Lura, and K. Kovler, Editors. Technical University of Denmark, Lyngby, Denmark, 2006. RILEM.
138. Lura, P., F. Durand, and O.M. Jensen. *Autogenous strain of cement pastes with superabsorbent polymers*. in *International RILEM Conference on Volume Changes of Hardening Concrete: Testing and Mitigation*, O.M. Jensen, P. Lura, and K. Kovler, Editors. Technical University of Denmark, Lyngby, Denmark, 2006. RILEM.
139. Mechtcherine, V., et al. *Internal curing by superabsorbent polymers (SAP) - Effects on material properties of self-compacting fibre-reinforced high performance concrete*. in *International RILEM Conference on Volume Changes of Hardening Concrete: Testing and Mitigation*, O.M. Jensen, P. Lura, and K. Kovler, Editors. Technical University of Denmark, Lyngby, Denmark, 2006. RILEM.

140. Mönnig, S. and H.W. Reinhardt. *Results of a comparative study of the shrinkage behaviour of concrete and mortar mixtures with different internal water sources*. in *International RILEM Conference on Volume Changes of Hardening Concrete: Testing and Mitigation*, O.M. Jensen, P. Lura, and K. Kovler, Editors. Technical University of Denmark, Lyngby, Denmark, 2006. RILEM.
141. Piérard, J., V. Pollet, and N. Cauberg. *Mitigating autogenous shrinkage in HPC by internal curing using superabsorbent polymers*. in *International RILEM Conference on Volume Changes of Hardening Concrete: Testing and Mitigation*, O.M. Jensen, P. Lura, and K. Kovler, Editors. Technical University of Denmark, Lyngby, Denmark, 2006. RILEM.
142. Jensen, O.M. and P.F. Hansen, *Autogenous relative humidity change in silica fume-modified cement paste.* Advances in Cement Research, 1995. **25**(7): p. 33-38.
143. *EN 13263-1:2005. Silica fume for Concrete. Definitions, requirements and conformity criteria.*
144. Reinhardt, H.W. and S. Mönnig, *Basic concepts for a model of different internal water sources*, in *International RILEM-JCI Seminar on Concrete Durability and Service Life Planning*, K. Kovler, Editor. 2006: Dead Sea, Israel p. 235-244.
145. *ASTM C XXXX-XX. PROPOSED DRAFT: Standard Test Method for Autogenous Strain of Cement Paste and Mortar*.
146. ASTM, *C 191 Test Method for Time of Setting of Hydraulic Cement by Vicat Needle*.
147. Powers, T.C., *The Nonevaporable Water Content of Hardened Portland-Cement Paste: Its Significance for Concrete Research and Its Method of Determination*. 1949, ASTM - American Society for Testing Materials: Philadelphia. p. 68-76.
148. Jensen, O.M., et al., *Clinker mineral hydration at reduced relative humidities.* Cement and Concrete Research, 1999. **29**(9): p. 1505-1512.
149. Holt, E. *Very Early Age Autogenous Shrinkage: Governed by Chemical Shrinkage or Self-Desiccation?* in *Proceedings of the Third International Research Seminar: Self-desiccation and its importance in concrete technology*, B. Persson and G. Fagerlund, Editors. Lund, Sweden, 1999.
150. El-Shimy, E., et al., *Physico-chemical and thermal characteristics of lime-silica fume pastes.* Journal of Thermal Analysis and Calorimetry, 2000. **60**: p. 549-556.
151. Yogendran, V., B.W. Langan, and M.A. Ward, *Hydration of Cement and Silica Fume Paste.* Cement and Concrete Research, 1991. **21**: p. 691-708.
152. Abdelrazig, B.E.I., S.D. Main, and D.V. Nowell, *Hydration studies of modified OPC pastes by differential scanning calorimetry and thermogravimetry*, in *Journal of thermal analysis*. 1992. p. 495-504.
153. Sha, W., E.A. O'Neill, and Z. Guo, *Differential scanning calorimetry study of ordinary Portland cement*, in *Cement and Concrete Research*. 1999. p. 1487-1489.
154. Bhatty, J.I., et al., *Estimation of calcium hydroxide in OPC, OPC/PFA and OPC/PFA/polymer modified systems.* Thermochimica Acta, 1986. **106**(115).
155. Vedalakshmi, R., et al., *Quantification of hydrated cement products of blended cements in low and medium strength concrete using TG and DTA technique.* Thermochimica Acta, 2003. **407**: p. 49–60.
156. Scrivener, K.L., A. Bentur, and P.L. Pratt, *Quantitative Characterization of the Transition Zone in High Strength Concretes.* Advances in Cement Research, 1988. **1**(4): p. 230-237.
157. Parrott, L.J., et al., *Monitoring Portland cement hydration: Comparison of methods*, in *Cement and Concrete Research*. 1990. p. 919-926.
158. Ono, K., K. Asaga, and M. Daimon, *Hydration in the System of Cement and Silica Fume*, in *Review of the 39th General Meeting - Technical Session*. 1985, Cement Association of Japan: Tokyo. p. 40-43.
159. *ACI Committee 234: Guide for the Use of Silica Fume in Concrete*, ACI, Editor. 2000.
160. Klug, H.P. and L.E. Alexander, *X-Ray Diffraction Procedures for Polycristalline and Amorphous Materials*: Wiley, New York, 1974.
161. Midgley, H.G., *The determination of calcium hydroxide in set Portland cements.* Cement and Concrete Research, 1979. **9**: p. 77-82.
162. Aldridge, L.P., *Accuracy and precision of phase analysis in Portland cement by Bogue, Microscopy and X-Ray diffraction methods.* Cement and Concrete Research, 1982. **12**: p. 381-398.
163. Gutteridge, W.A., *Quantitative X-Ray Powder Diffraction in the study of some cementive materials*, in *British Ceramic Proceedings*. 1984, British Ceramic Soc. p. 11-23.

164. Cheng-yi, H. and R.F. Feldman, *Hydration reactions in portland cement-silica fume blends*, in *Cement and Concrete Research*. 1985. p. 585-592.
165. Escalante-Garcia, J.I., *Nonevaporable water from neat OPC and replacement materials in composite cements hydrated at different temperatures.* Cement and Concrete Research, 2003. **33**: p. 1883–1888.
166. Abo-El-Enein, S.A., et al., *Characteristics of lime-silica fume mixtures.* Journal of Thermal Analysis, 1996. **46**: p. 275-284.
167. Scrivener, K.L., *Backscattered electron imaging of cementitious microstructures: understanding and quantification.* Cement and Concrete Composites, 2004. **26**: p. 935-945.
168. Mouret, M., E. Ringot, and A. Bascoul, *Image analysis: a tool for the characterisation of hydration of cement in concrete - metrological aspects of magnification on measurement*, in *Cement and Concrete Composites*, C. Prof Jean-Louis, Editor. 2001. p. 201-206.
169. Igarashi, S., M. Kawamura, and A. Watanabe, *Analysis of cement pastes and mortars by a combination of backscatter-based SEM image analysis and calculations based on the Powers model*, in *Cement and Concrete Composites*, S. Diamond, Editor. 2004. p. 977-985.
170. Sinclair, W. and G.W. Groves, *The microstructure of Portland cement-silica fume pastes*, in *Journal of Materials Science Letters*. 1986. p. 101-102.
171. Yajun, J. and J.H. Cahyadi, *Investigation on microstructure of silica fume cement pastes*, in *High Performance Structures and Materials*, C.A. Brebbia, et al., Editors. 2002, WITPress. p. 221-229.
172. Bentz, D.P., *Influence of silica fume on diffusivity in cement-based materials - II. Multi-scale modeling of concrete diffusivity*, in *Cement and Concrete Research*. 2000. p. 1121-1129.
173. Breugel, K.V., *Simulation of hydration and formation of structure in hardening cement-based materials,* PhD thesis, Technical University Delft, 1991, **PhD**.
174. Duck, A.D. and J.P. Burkes. in *3rd International Conference on Cement Microscopy*. Houston, 1981.
175. Papadakis, V.G., *Experimental investigation and theoretical modeling of silica fume activity in concrete*, in *Cement and Concrete Research*. 1999. p. 79-86.
176. Diamond, S., *Effects of Microsilica (Silica Fume) on Pore-Solution Chemistry of Cement Pastes.* Journal of the American Ceramic Society, 1983. **66**(5): p. C-82-C-84.
177. Pane, I. and W. Hansen, *Investigation of blended cement hydration by isothermal calorimetry and thermal analysis.* Cement and Concrete Research, 2005. **35**: p. 1155– 1164.
178. Yajun, J. and J.H. Cahyadi, *Simulation of silica fume blended cement hydration.* Materials and Structures, 2004. **37**: p. 397-404.
179. Odler, I. and J. SchUppstuhl, *Combined hydration of tricalcium silicate and B-dicalcium silicate.* Cement and Concrete Research, 1982. **12**: p. 13-20.
180. Levenspiel, O., *Chemical Reaction Engineering. An introduction to the design of chemical reactors.*: John Wiley and Sons, Inc., New York, 1962.
181. Bonen, D. and S. Diamond, *Occurrence of large silica fume-derived paticles in hydrated cement paste*, in *Cement and Concrete Research*. 1992. p. 1059-1066.
182. Jensen, O.M., *Rotronic Hygroskop DT. Fugtmåleudstyr - kalibrering og afprøvning*. 1993, Technical Uniervsity of Denmark.
183. Jensen, O.M., *Influence of temperature on autogenous deformation and RH-change in hardening cement paste*. 1998, Technical University of Denmark: Lyngby.
184. Bartlett, F.M. and J.G. MacGregor, *Effect of moisture condition on concrete core strengths.* ACI Materials Journal, 1994. **91**(3): p. 227-236.
185. Lura, P., et al. *Compressive Strenght of Cement Pastes and Mortars with Superabsorbent Polymers*. in *International RILEM Conference on Volume Changes of Hardening Concrete: Testing and Mitigation*, O.M. Jensen, P. Lura, and K. Kovler, Editors. Technical University of Denmark, Lyngby, Denmark, 2006. RILEM.
186. Jensen, O.M. and P.F. Hansen, *Influence of temperature on autogenous deformation and relative humidity change in hardening cement paste.* Cement and Concrete Research, 1999. **29**: p. 567–575.
187. Chatterjee, P.K. and H.V. Nguyen, in *Absorbency*, P.K. Chatterjee, Editor. 1985, Elsevier Science Publishers: Amsterdam.
188. Yin, Y.-L., *Swelling behavior of Polyelectrolyte Gels,* Ph.D. Thesis, Princeton University, 1993.
189. Brandt, K.A., S.A. Goldman, and T.A. Inglin, *Hydrogel-forming polymer compositions for use in absorbent structures.* Patent Version Number, The Procter & Gamble Company (Cincinnati, OH)

190. Mark, J.E. and B. Erman, *Rubberlike Elasticity: A Molecular Primer*: John Wiley & Sons, New York, 1988.
191. Østergaard, T., *Measurements on water-entrained cement paste at NIST*, in *Newsletter GNI*. 2001.
192. Lura, P., et al. *Measurement of Water Transport from Saturated Pumice Aggregates to Hardening Cement Paste*. in *Advances in Cement and Concrete. Engineering Conferences International.* Copper Mountain, 2003.
193. Delagrave, A., et al., *Influence of the Interfacial Zone on the Chloride Diffusivity of Mortars*, in *Advanced Cement Based Materials*. 1997. p. 86-92.
194. Diamond, S., *Considerations in image analysis as applied to investigations of the ITZ in concrete*, in *Cement and Concrete Composites*, C. Prof Jean-Louis, Editor. 2001. p. 171-178.
195. Scrivener, K., A.K. Crumbie, and P. Laugesen, *The Interfacial Transition Zone (ITZ) Between Cement Paste and Aggregate in Concrete.* Interface Science, 2004. **12**: p. 411–421.
196. Scrivener, K.L. and K.M. Nemati, *The percolation of pore space in the cement paste/aggregate interfacial zone of concrete*, in *Cement and Concrete Research*. 1996. p. 35-40.
197. Stroeven, P. and J. Hu, *ITZ's structural evolution during hydration in model concrete*, in *Magazine of Concrete Research*. 2009. p. 371.
198. Zheng, J.J., C.Q. Li, and X.Z. Zhou, *Characterization of Microstructure of Interfacial Transition Zone in Concre te*, in *ACI Materials Journal - American Concrete Institute*. 2005. p. 265.
199. Akcaoglu, T., M. Tokyay, and T. Celik, *Assessing the ITZ microcracking via scanning electron microscope and its effect on the failure behavior of concrete.* Cement and Concrete Research, 2005. **35**(2): p. 358-363.
200. Cwirzen, A. and V. Penttala, *Aggregate-cement paste transition zone properties affecting the salt-frost damage of high-performance concretes*, in *Cement and Concrete Research*. 2005. p. 671-679.
201. Bentz, D.P. and E.J. Garboczi, *Computer modelling of Interfacial Transition Zone: Microstructure and Properties*, in *Engineering and Transport Properties of the Interfacial Transition Zone in Cementitious Composites*, M.G. Alexander, et al., Editors. 1999, RILEM. p. 349-385.
202. Bentz, D.P., et al., *Interfacial zone percolation in concrete: Effects of interfacial zone thickness and aggregate shape*, in *Microstructure of Cement-Based Systems/Bonding and Interfaces in Cementitious Materials* S. Diamond and et.al, Editors. 1995: Pittsburgh. p. 437-442.
203. Monteiro, P.J.M., J.C. Maso, and J.P. Ollivier, *The aggregate-mortar interface.* Cement and Concrete Research, 1985. **15**: p. 953-958.
204. Baker, G.C., *Computer simulations of granular materials*, in *Granular Matter. An Interdisciplinary Approach.*, A. Metha, Editor. 1994, Springer-Verlag: New York. p. 35-83.
205. Hansen, T.C., *Physical structure of hardened cement paste. A classical approach.* Materials and Structures, 1986. **19**(114): p. 423-436.
206. Jensen, O.M., *Bilag: målinger og notater*. 1993, Technical University of Denmark.
207. Pickett, G., *Effect of aggregate on shrinkage of concrete and a hypothesis concerning shrinkage.* ACI Materials Journal, 1956. **52**(5): p. 581-590.
208. Tattersall, G. and P. Banfill, *The rheology of fresh concrete*: Pitman, 1983, 356.
209. Ferraris, C.F., *Measurement of the Rheological Properties of High Performance Concrete:State of the Art Report.* Journal of Research of the National Institute of Standards and Technology, 1999. **104**(5).
210. Ferraris, C.F. and F.d. Larrard, *Testing and modelling of fresh concrete rheology*. 1998, National Institute of Standards and Technology.
211. Tattersall, G.H., *The workability of concrete, A viewpoint Publication*. 1976, Portland Cement Association.
212. Banfill, P., *Rheological methods for assessing the flow properties of mortar and related materials.* Construction and Building Materials, 1994. **8**: p. 43-50.
213. Banfill, P. *The rheology of fresh cement and concrete - A Review*. in *11th Internation Cement Chemistry Congress*. Durban, 2003.
214. Jin, J., *Properties of mortar for self-compacting concrete*, University of London, 2002, **PhD**: p. 398.
215. Banfill, P. *The influence of fine materials in sand on the rheology of fresh mortar*. in *Utilizing ready-mix concrete and mortar*, R.K. Dhir and M.C. Limbachiya, Editors. University of Dundee, Scotland, UK, 1999. Thomas Telford.

216. Yang, M. and H.M. Jennings, *Influences of Mixing Methods on the Microstructure and Rheological Behavior of Cement Paste.* Advanced Cement Based Materials, 1995. **2**: p. 70-78.
217. Wallevik, O.H., *The Rheology of Fresh Concrete and its Application on Concrete with and without Silica Fume,* Dr.ing. thesis, Norwegian Institute of Technology, 1990.
218. Tanigawa, Y. and H. Mori, *Analytical study on deformation of fresh concrete.* Journal of Engineering Mechanics, 1989. **115**(3): p. 493-508.
219. Tanigawa, Y., H. Mori, and K. Watanabe. *Computer simulation of consistency and rheology tests of fresh concrete by viscoplastic finite element method*. in *Properties of Fresh Concrete, Proceedings of the RILEM Colloquium*. Cambridge, Great Britain, 1990. University Press.
220. Francois de Larrard, T.S., *Mixture-proportioning of high-performance concrete.* Cement and Concrete Research, 2002. **32**: p. 1699–1704.
221. Hu, C., et al., *Validation of BTRHEOM, the new rheometer for soft-to-fluid concrete.* Materials and Structures, 1996. **29**(194): p. 620-631.
222. Wallevik, J.E., *Relationship between the Bingham parameters and slump.* Cement and Concrete Research, 2006. **36**: p. 1214–1221.
223. Ferraris, C.F., K.H. Obla, and R. Hill, *The influence of mineral admixtures on the rheology of cement paste and concrete.* Cement and Concrete Research, 2001. **31**(2): p. 245-255.
224. Wallevik, O.H., A. Saasen, and O.E. Gjorv, *Efffect of filler materials on the rheological properties of fresh concrete.* ACI Materials Journal, 1995. **92**
225. Nehdi, M., S. Mindess, and P.C. Aïtcin, *Rheology of high performance concrete: effect of ultrafine particles.* Cement and Concrete Research, 1998. **28**: p. 687-697.
226. Roussel, N., *Steady and transient flow behaviour of fresh cement pastes.* Cement and Concrete Research, 2005. **35**: p. 1656-1664.
227. Roussel, N., *A thixotropy model for fresh fluid concretes: Theory, validation and applications.* Cement and Concrete Research, 2006. **36**: p. 1797-1806.
228. Lura, P., et al. *Identification of microcracks caused by autogenous shrinkage*. in *Proceedings of the International Workshop on Material Science in 21st Century for the Construction Industry - Durability, Repair and Recycling of Concrete Structures*. Sapporo, Japan, 2005.
229. Lura, P., J. Weiss, and O.M. Jensen, *Detection and analysis of microcracks in high-performance cementitious materials*, in *Advances in Construction Materials 2007*, C.U. Grosse, Editor. 2007, Springer Berlin Heidelberg.

Appendix

Appendix A. Calculation of free water space at ITZ regions brought out considering the closest packing approach

Let the average diameter of cement and aggregate particles be respectively designated by ϕ_{cem} and ϕ_{agg}, the later being assumed to be constant within a narrow particle size distribution. By combining the aggregate particle size and the specific volume of aggregate, V_{agg} in a system with unitary volume, it is possible to write Eq. (0.1), which may be use to derive the number of aggregate particles, η_{agg} [un./cm^3].

$$\eta_{agg} = V_{agg} \cdot \left[\frac{\pi}{6} \cdot \phi_{agg}{}^3 \right]^{-1} \tag{0.1}$$

In a system where every aggregate particle is involved by cement paste, the ITZ volume, V_{ITZ} may be calculated by Eq. (0.2), the ITZ-thickness being defined equal to the average particle-diameter of a cement grain, ϕ_{cem}.

$$V_{ITZ} = \eta_{agg} \cdot \frac{4}{3}\pi \cdot \left[\left(\phi_{agg} + 2\phi_{cem} \right)^3 - \left(\frac{\phi_{agg}}{2} \right)^3 \right] \tag{0.2}$$

Inserting Eq. (0.1) in (0.2), it follows Eq. (0.3):

$$V_{ITZ} = V_{agg} \cdot \left(6\frac{\phi_{cem}}{\phi_{agg}} + 12\frac{\phi_{cem}{}^2}{\phi_{agg}{}^2} + 8\frac{\phi_{cem}{}^3}{\phi_{agg}{}^3} \right) \tag{0.3}$$

By making χ to translate the relation between the particle-diameters, the previous equation reduces to Eq. (0.4):

$$V_{ITZ} = V_{agg} \cdot \left(6\chi + 12\chi^2 + 8\chi^3 \right) \tag{0.4}$$

To calculate the volume-water comprised within the ITZ-volume, it is necessary to deduce the volume occupied by the solid part, viz the cement grains. This may be done by assuming the cement grains closest-placed around the perimeter of the aggregate particle, equal to the average of the sum between the diameter of the aggregate particle and the diameter of the cement particle. The mathematical equation that translates the previous argument may be written in the form of Eq. (0.5):

$$V_{cem} = \frac{2\pi}{\phi_{cem}} \cdot \left(\frac{\phi_{agg} + \phi_{cem}}{2} \right) \cdot \frac{4}{3}\pi \cdot \left(\frac{\phi_{cem}}{2} \right)^3 \tag{0.5}$$

The water volume at ITZ may be now derived by subtracting Eq. (0.4) of (0.5), to hold Eq. (0.6).

$$V_{w,ITZ} = V_{ITZ} - V_{cem}$$
$$V_{w,ITZ} = V_{agg} \cdot \left(6\chi + 12\chi^2 + 8\chi^3\right) - \frac{\pi^2}{6}\phi_{cem}{}^2 \cdot \left(\phi_{agg} + \phi_{cem}\right) \quad (0.6)$$

By plotting Eq. (0.6) **as function of the aggregate particle-diameter, it retrieves Figure 0.1.:**

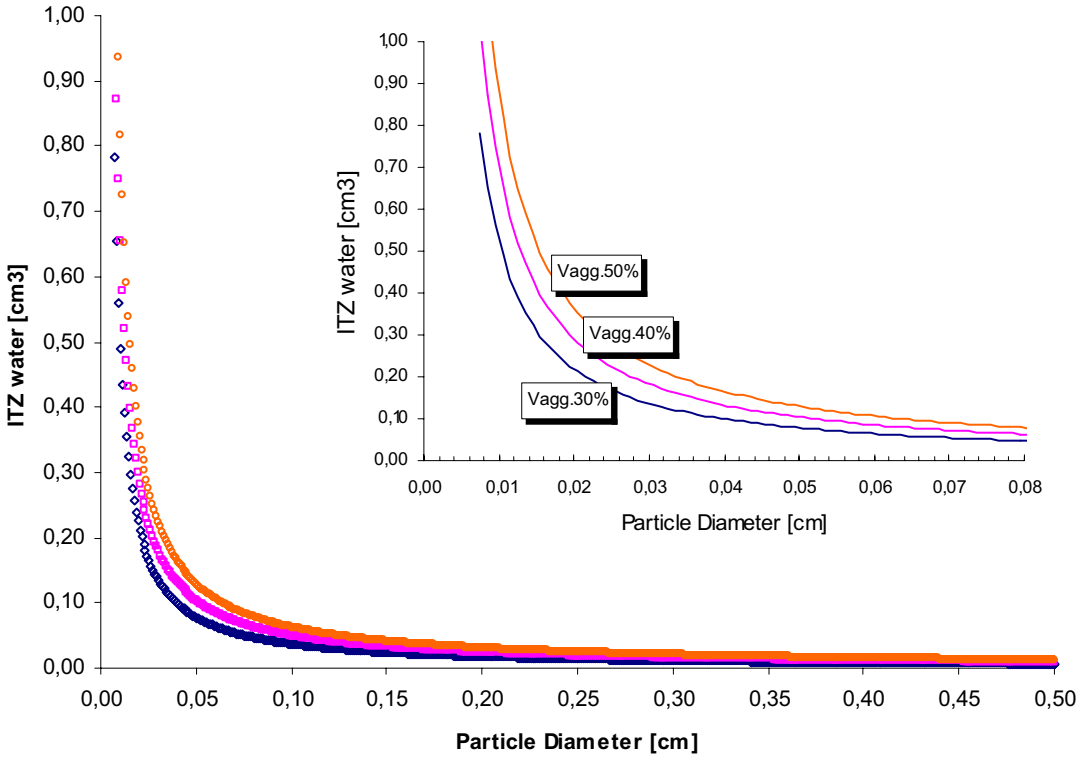

Figure 0.1.

Relation between the volume of water at ITZ regions and the particle size of the aggregate, according Eq. (0.6).

System physics:

(w/c)=0.30, V_{agg}=30%, V_{agg}=40%, V_{agg}=50%

Model assumptions:

ITZ depth=ϕ_{cem}=30 μm